



McGruer, Fiona (2017) Basic prediction mechanisms as a precursor for schizophrenia studies. PhD thesis.

<http://theses.gla.ac.uk/8236/>

Copyright and moral rights for this work are retained by the author

A copy can be downloaded for personal non-commercial research or study, without prior permission or charge

This work cannot be reproduced or quoted extensively from without first obtaining permission in writing from the author

The content must not be changed in any way or sold commercially in any format or medium without the formal permission of the author

When referring to this work, full bibliographic details including the author, title, awarding institution and date of the thesis must be given

Enlighten:Theses
<http://theses.gla.ac.uk/>
theses@gla.ac.uk



University
of Glasgow



BASIC PREDICTION MECHANISMS AS A PRECURSOR FOR SCHIZOPHRENIA STUDIES

Fiona McGruer (MSc, CertHE, MA)

THESIS SUBMITTED TO THE UNIVERSITY OF GLASGOW IN
FULLFILLMENT OF THE REQUIREMENTS FOR THE DEGREE OF DOCTOR
OF PHILOSOPHY

April 2017

Containing studies performed at the Centre for Cognitive Neuroimaging, Institute of Neuroscience and Psychology, University of Glasgow, Glasgow G12 8QB.

This work was supported by an Advanced Quantitative Methods grant from the Economic and Social Research Council [grant number 1247475].

© Fiona McGruer, 2017

SUMMARY

Traditionally, early visual cortex (V1-3) was thought of as merely a relay centre for feedforward retinal input, providing entry to the cortical visual processing stream. However, in addition to feedforward retinal input, V1 receives a large amount of intracortical information through feedback and lateral connections. Human visual perception is constructed from combining feedforward inputs with these feedback and lateral contributions. Feedback connections allow the visual cortical response to feedforward information to be affected by expectation, knowledge, and context; even at the level of early visual cortex. In **Chapter 1** we discuss the feedforward and feedback visual processing streams. We consider historical philosophical and scientific propositions about constructive vision. We introduce modern theories of constructive vision, which suggest that vision is an active process that aims to infer or predict the cause of sensory inputs. We discuss how V1 therefore represents not only retinal input but also high-level effects related to constructive predictive perception.

Visual illusions are a ‘side effect’ of constructive and inferential visual perception. For the vast majority of stimulus inputs, integration with context and knowledge facilitates clearer, more veridical perception. In illusion these constructive mechanisms produce incorrect percepts. Illusory effects can be observed in early visual cortex, even when there is no change in the feedforward visual input. We suggest that illusions therefore provide us with a tool to probe feedforward and feedback integration, as they exploit the difference between retinal stimulation and resulting perception. Thus, illusions allow us to see the changes in activation and perception induced only by feedback without changes in feedforward input. We discuss a few specific examples of illusion generation through feedback and the accompanying effects on V1 processing.

In Schizophrenia, the integration of feedback and feedforward information is thought to be dysfunctional, with unbalanced contributions of the two sources. This is evidenced by disrupted contextual binding in visual perception and corresponding deficits in contextual illusion perception. We propose that illusions can provide a

window into constructive and inferential visual perception in Schizophrenia. Use of illusion paradigms could help elucidate the deficits existing within feedback and feedforward integration. If we can establish clear effects of illusory feedback to V1 in a typical population, we can apply this knowledge to clinical subjects to observe the differences in feedback and feedforward information.

Chapter 2 describes a behavioural study of the rubber hand illusion. We probe how multimodal illusory experience arises under varying reliabilities of visuotactile feedforward input. We recorded Likert ratings of illusion experience from subjects, after their hidden hand was stimulated either synchronously or asynchronously with a visible rubber hand (200, 300, 400, or 600ms visuotactile asynchronicity). We used two groups, assessed by a questionnaire measuring a subject's risk of developing Schizophrenia - moderate/high scorers and a control group of zero-scorers. We therefore consider how schizotypal symptoms contribute to rubber hand illusory experience and interact with visuotactile reliability. Our results reveal that the impact of feedforward information on higher level illusory body schema is modulated by its reliability. Less reliable feedforward inputs (increasing asynchronicity) reduce illusion perception. Our data suggests that some illusions may not be affected on a spectrum of schizotypal traits but only in the full schizophrenic disorder, as we found no effect of group on illusion perception.

In **Chapter 3** we present an fMRI investigation of the rubber hand illusion in typical participants. Cortical feedback allows information about other modalities and about cognitive states to be represented at the level of V1. Using a multimodal illusion, we investigated whether crossmodal and illusory states could be represented in early visual cortex in the absence of differential visual input. We found increased BOLD activity in motion area V5 and global V1 when the feedforward tactile information and the illusory outcome were incoherent (for example when the subject was experiencing the illusion during asynchronous stimulation). This is suggestive of increased predictive error, supporting predictive coding models of cognitive function. Additionally, we reveal that early visual cortex contains pattern representations specific to the illusory state, irrespective of tactile stimulation and under identical feedforward visual input.

In **Chapter 4** we use the motion-induced blindness illusion to demonstrate that feedback modulates stimulus representations in V1 during illusory disappearance. We recorded fMRI data from subjects viewing a 2D cross array rotating around a central axis, passing over an oriented Gabor patch target ($45^\circ/135^\circ$). We attempted to decode the target orientation from V1 when the target was either visible or invisible to subjects. Target information could be decoded during target visibility but not during motion-induced blindness. This demonstrates that the target representation in V1 is distorted or destroyed when the target is perceptually invisible. This illusion therefore has effects not only at higher cortical levels, as previously shown, but also in early sensory areas. The representation of the stimulus in V1 is related to perceptual awareness. Importantly, **Chapter 4** demonstrated that intracortical processing can disturb constant feedforward information and overwrite feedforward representations. We suggest that the distortion observed occurs through feedback from V5 about the cross array in motion, overwriting feedforward orientation information.

The flashed face distortion illusion is a relatively newly discovered illusion in which quickly presented faces become monstrously distorted. The neural underpinnings of the illusion remain unclear; however it has been hypothesised to be a face-specific effect. In **Chapter 5** we challenged this account by exploiting two hallmarks of face-specific processing - the other-race effect and left visual field superiority. In two experiments, two ethnic groups of subjects viewed faces presented bilaterally in the visual periphery. We varied the race of the faces presented (same or different than subject), the visual field that the faces were presented in, and the duration of successive presentations (250, 500, 750 or 1000ms per face before replacement). We found that perceived distortion was not affected by stimulus race, visual field, or duration of successive presentations (measured by forced choice in experiment 1 and Likert scale in experiment 2). We therefore provide convincing evidence that FFD is not face-specific and instead suggest that it is an object-general effect created by comparisons between successive stimuli. These comparisons are underlined by a feedback higher level model which dictates that objects cannot immediately replace one another in the same retinotopic space without movement.

In **Chapter 6** we unify these findings. We discuss how our data show feedback effects on perception to produce visual illusion; effects which cannot be explained

through purely feedforward activity processing. We deliberate how lateral connections and attention effects may contribute to our results. We describe known neural mechanisms which allow for the integration of feedback and feedforward information. We discuss how this integration allows V1 to represent the content of visual awareness, including during some of the illusions presented in this thesis. We suggest that a unifying theory of brain computation, Predictive Coding, may explain why feedback exerts top-down effects on feedforward processing. Lastly we discuss how our findings, and others that demonstrate feedback and prediction effects, could help develop the study and understanding of schizophrenia, including our understanding of the underlying neurological pathologies.

TABLE of CONTENTS

SUMMARY	1
List of Figures	9
List of Tables	11
List of Publications	13
Acknowledgements	15
Author's Declaration	16
Definitions/Abbreviations	17
1. INTRODUCTION	19
1.1. The Human Eye and the Feedforward Visual System	19
1.2. Feedback in the Visual Hierarchy	22
1.3. Historical Theories of Constructive Visual Perception	27
1.4. The Bayesian Brain	30
1.5. Cortical Prediction	33
1.6. Illusions Dissociate Perception from Stimulation	35
1.6.1. Illusory Contours	37
1.6.2. Apparent Motion	39
1.6.3. Motion Silencing	43
1.6.4. Crossmodal Illusions	44
1.7. Illusion, Hallucination, and Delusion	45
1.7.1. Hallucinations and Delusions	47
1.7.2. Visual Illusions in Schizophrenia	48
1.8. Summary and Thesis Purpose	50

2. CROSSMODAL BOUNDARIES OF THE RUBBER HAND ILLUSION IN SCHIZOTYPY	53
2.1. Abstract	54
2.2. Introduction	54
2.3. Method	57
2.3.1. Participants	57
2.3.2. Apparatus	58
2.3.3. Design and Procedure	60
2.3.4. Analysis	60
2.4. Results	61
2.5. Discussion	65
2.6. Conclusion	70
3. VISUOTACTILE ILLUSION PERCEPTION IN EARLY VISUAL CORTEX	71
3.1. Abstract	73
3.2. Introduction	73
3.3. Method	75
3.3.1. Participants	75
3.3.2. Apparatus	75
3.3.3. Procedure	76
3.3.4. MRI Parameters	77
3.3.5. fMRI Pre-Processing	77
3.3.6. Behavioural Analysis	78
3.3.7. fMRI Analysis: Region of interest (ROI)	78
3.3.8. fMRI Analysis: Univariate	79
3.3.9. fMRI Analysis: Representational Similarity	79
3.3.10. fMRI Analysis: Representational Similarity across Time	80

3.4. Results	81
3.4.1. Behaviour	81
3.4.2. fMRI: Univariate Effects of Stimulation & Illusion Perception	82
3.4.3. fMRI: Multivariate Representation of Illusory Perception	84
3.4.4. fMRI: Multivariate Representation across Time	86
3.5. Discussion	87
3.6. Conclusion	92
4. STIMULUS REPRESENTATIONS IN V1 FLUCTUATE WITH PERCEPTUAL VISIBILITY DURING MOTION-INDUCED BLINDNESS	94
4.1. EXPLORING THE PARAMETERS OF MOTION-INDUCED BLINDNESS USING ORIENTED GABOR PATCHES AS TARGETS	94
4.1.1. Abstract	95
4.1.2. Introduction	95
4.1.3. Method	97
4.1.3.1. Participants	97
4.1.3.2. Design and Procedure	97
4.1.3.3. Analysis	99
4.1.4. Results	99
4.1.5. Discussion	102
4.1.6. Conclusion	106
4.2. STIMULUS REPRESENTATIONS IN V1 FLUCTUATE WITH PERCEPTUAL VISIBILITY DURING MOTION-INDUCED BLINDNESS	107
4.2.1. Abstract	108
4.2.2. Introduction	108
4.2.3. Method	111
4.2.3.1. Participants	111
4.2.3.2. Stimuli	111

4.2.3.3. Procedure	112
4.2.3.4. fMRI Parameters	114
4.2.3.5. fMRI Pre-Processing	114
4.2.3.6. Behavioural Analysis	115
4.2.3.7. fMRI Analysis	116
4.2.4. Results	120
4.2.4.1. Behavioural Analysis	120
4.2.4.2. ROI GLM Analysis	122
4.2.4.3. Multivariate Pattern Classification	124
4.2.5. Discussion	129
4.2.6. Conclusion	133
5. OF MONSTERS AND MEN- THE FLASHED FACE DISTORTION ILLUSION AS A DEMONSTRATION OF OBJECT-GENERAL VISUAL PREDICTIVE CODING	135
5.1. Abstract	136
5.2. Introduction	136
5.3. Method	141
5.3.1. Participants	141
5.3.2. Stimuli	141
5.3.3. Procedure	142
5.3.4. Analysis	144
5.4. Results	144
5.5. Discussion	147
5.6. Conclusions	153
6. DISCUSSION	154
6.1. Chapter Summaries	154

6.2. Vision is Constructive	159
6.3. Illusory Effects are Observed at the Lowest Levels of the Traditional Cortical Hierarchy	160
6.4. The Influence of Lateral Connectivity	163
6.5. Attention in Illusory Paradigms	165
6.6. Layer Specificity and Neurobiology	167
6.7. Does Early Visual Cortex Represent Visual Awareness?	172
6.8. Illusions May be an Effect of Cortical Prediction	176
6.9. Illusion Studies may Elucidate Deficits in Schizophrenia	185
6.10. Conclusions	189
7. REFERENCES	192
8. APPENDICES	215
Appendix 2.	215
Appendix 3.	218
Appendix 4.2.	224

List of Figures

1. INTRODUCTION

Figure 1.1. Feedback and feedforward connectivity.	24
Figure 1.2. Amodal and modal completion.	38
Figure 1.3. Apparent motion.	42
Figure 1.4. Motion illusions.	44

2. CROSSMODAL BOUNDARIES OF THE RUBBER HAND ILLUSION IN SCHIZOTYPY

Figure 2.1. Stimulus set up.	58
Figure 2.2. Long stimulation period.	62
Figure 2.3. Short stimulation periods.	63
Figure 2.4. Button press responses to ‘perceptual change’.	65

3. VISUOTACTILE ILLUSION PERCEPTION IN EARLY VISUAL CORTEX

Figure 3.1. Rubber hand apparatus in the MRI scanner.	76
Figure 3.2. Behavioural responses.	82
Figure 3.3. ROI definitions and Factorial GLMs in our regions of interest.	84
Figure 3.4. Representational similarity of stimulation and illusion condition pairings in each ROI.	85
Figure 3.5. Single trial RSMs across time.	87

4. STIMULUS REPRESENTATIONS IN V1 FLUCTUATE WITH PERCEPTUAL VISIBILITY DURING MOTION-INDUCED BLINDNESS

4.1. EXPLORING THE PARAMETERS OF MOTION-INDUCED BLINDNESS USING ORIENTED GABOR TARGETS

Figure 4.1.1. Motion-induced blindness stimuli.	98
Figure 4.1.2. Results per run and block in Experiment 1.	100
Figure 4.1.3. Results per eccentricity and block in Experiment 2.	101

4.2. STIMULUS REPRESENTATIONS IN V1 FLUCTUATE WITH PERCEPTUAL VISIBILITY DURING MOTION-INDUCED BLINDNESS

Figure 4.2.1. Stimulus, retinotopic mapping and target mapping.	112
Figure 4.2.2. Behavioural results.	122
Figure 4.2.3. GLM results in our ROIs.	124
Figure 4.2.4. Multivariate classification results decoding 45° vs 135° Gabor patch orientation for Experiment 1.	126
Figure 4.2.5. Multivariate classification results decoding 45° vs 135° Gabor orientation for Experiment 2.	127
Figure 4.2.6. Control analysis equating volumes.	128

5. OF MONSTERS AND MEN- THE FLASHED FACE DISTORTION ILLUSION AS A DEMONSTRATION OF OBJECT-GENERAL VISUAL PREDICTIVE CODING

Figure 5.1. Experimental procedure and expected results.	142
Figure 5.2. Proportional distortion difference between own- & other-race faces.	145
Figure 5.3. Proportional own-race choice as a function of stimulus and subject race, visual field, and presentation timing.	147

6. DISCUSSION

Figure 6.1. Layer specificity of feedback.	168
--	-----

Permission has been granted for use of all figures replicated or adapted from other works.

List of Tables

2. CROSSMODAL BOUNDARIES OF THE RUBBER HAND ILLUSION IN SCHIZOTYPY

Table 2.1. Likert statements.	59
-------------------------------	----

4. STIMULUS REPRESENTATIONS IN V1 FLUCTUATE WITH PERCEPTUAL VISIBILITY DURING MOTION-INDUCED BLINDNESS

Table 4.1.1. Behavioural outcomes.	100
------------------------------------	-----

5. OF MONSTERS AND MEN- THE FLASHED FACE DISTORTION ILLUSION AS A DEMONSTRATION OF OBJECT-GENERAL VISUAL PREDICTIVE CODING

Table 5.1. Distortion rating by stimulus race (SR) and presentation timing.	145
---	-----

Table 5.2. Proportional own-race choice as a function of stimulus and subject race, visual field, and presentation timing.	146
--	-----

8. APPENDICES

Table A.2.1. Comparisons between Likert responses: visuotactile	215
---	-----

Table A.2.2. Comparisons between Likert responses for Likert statements.	216
--	-----

Table A.2.3. 95% Confidence intervals for Likert responses for the interaction between visuotactile asynchronicities and Likert statements.	217
---	-----

Table A.3.1. Mean TAL coordinates, TAL coordinate standard deviations, and number of voxels for the V1 ROI of each subject.	218
---	-----

Table A.3.2. Mean TAL coordinates, TAL coordinate standard deviations, and number of voxels for the left V5 ROI of each subject.	219
--	-----

Table A.3.3. Mean TAL coordinates, TAL coordinate standard deviations, and number of voxels for the right V5 ROI of each subject.	220
Table A.3.4. Mean TAL coordinates, TAL coordinate standard deviations, and number of voxels for the LOC ROI of each subject.	221
Table A.3.5. Mean TAL coordinates, TAL coordinate standard deviations, and number of voxels for the VHand ROI of each subject.	222
Table A.3.6. Mean TAL coordinates, TAL coordinate standard deviations, and number of voxels for the VHand ROI of each subject.	223

List of Publications

Journal Articles

McGruer, F., L., Petro, Vizioli, L.S., Lao, J. & Muckli, L. (*In Preparation*). Predictive Coding of Body Representation in Primary Visual Cortex.

McGruer, F., Petro, L.S. & Muckli, L. (*In Preparation*). Stimulus Representations in V1 Fluctuate with Perceptual Visibility during Motion-Induced Blindness.

McGruer, F., Ramon, M. & Muckli, L. (*In Preparation*). Of Monsters and Men- The Flashed Face Distortion Illusion as a Demonstration of Object-General Visual Predictive Coding.

Edwards, G., Vetter, P., **McGruer, F.**, Petro, L.S. & Muckli, L. (*Under review*). Predictive feedback to V1 dynamically updates with sensory input.

Conference Abstracts

Petro, L.S., **McGruer, F.** & Muckli, L. (2016). Orientation Decoding in V1 during Motion-Induced Blindness. Poster presented at the Organisation for Human Brain Mapping, Geneva, Switzerland.

McGruer, F., Petro, L.S. & Muckli, L. (2015). Orientation Decoding in V1 during Motion-Induced Blindness. Poster presented at the European Conference for Visual Perception, Liverpool, UK.

McGruer, F., Petro, L.S. & Muckli, L. (2015). Orientation Decoding in V1 During Motion-Induced Blindness. Oral presentation at PsyPAG, Glasgow, UK.

McGruer, F., Murray, J., Uhlhaas, P. & Muckli, L. (2014). Visuotactile Synchronicity of the Rubber Hand Illusion in Prodromal Subjects. Poster presented at the Glasgow Neuroscience Day, Glasgow, UK.

McGruer, F., Vizioli, L., Hohwy, J., Smith, F.W.S. & Muckli, L. (2014). Investigating the Representation of Crossmodal Illusory States in Early Visual Cortex Using fMRI. Poster presented at the Organisation for Human Brain Mapping, Hamburg, Germany.

McGruer, F., Vizioli, L., Hohwy, J., Smith, F.W.S. & Muckli, L. (2014). Investigating the Representation of Crossmodal Illusory States in Early Visual Cortex Using fMRI. Poster presented at the Scottish Neuroscience Group meeting, Glasgow, UK.

McGruer, F., Murray, J., Uhlhaas, P. & Muckli, L. (2013). Visuotactile Synchronicity of the Rubber Hand Illusion in Prodromal Subjects. Poster presented at the Glasgow Psychosis Research Network, Glasgow, UK.

McGruer, F., Petro, L.S., Vizioli, L., Hohwy, J., Smith, F.W.S. & Muckli, L. (2013). Investigating the Representation of Crossmodal Illusory States in Early Visual Cortex Using fMRI. Poster presented at the Organisation for Human Brain Mapping, Seattle, WA, USA.

F McGruer, F., Petro, L.S., Vizioli, L., Hohwy, J., Smith, F.W.S. & Muckli, L. (2013). Investigating the Representation of Crossmodal Illusory States in Early Visual Cortex Using fMRI. Poster presented at the Glasgow Neuroscience Day, Glasgow, UK.

Acknowledgements

I would like to acknowledge the financial support of the Economic and Social Research Council Advanced Quantitative Methods 3+ Scholarship.

My warm thanks to Lars Muckli for his supervision. It has been truly amazing to have been touched by your enthusiasm for science, inspirational work, and sense of humour. My endless appreciation goes to Lucy Petro for her guidance and support in matters of research and in matters of life. Thank you to Meike Ramon and Luca Vizioli for their encouragement and research collaboration. I am indebted to Frances Crabbe for the time she spent assisting with data collection and teaching me how to safely operate in the world of fMRI.

I would like to highlight my gratitude to Tyler Morgan for his wit, quoting abilities, and endless willingness to go get a coffee; and to Matthew Bennett for reminding me I cannot hide in the coats forever, and for re-introducing me to the regenerative powers of a decent cuppa. I am also hugely thankful to the other brilliant minds of the Muckli lab- Grace, Hanna, Yulia, Angus, and Johanna- for their friendship, assistance, and all that they have taught me. I cannot imagine working in a better lab, or with better people.

I will never be able to repay my amazing friends and family; who have fed me, forced me to exercise, didn't laugh when I fell asleep on their sofas, and who have lovingly tolerated so many missed events, irregular communications, and stressed phone calls. I promise to attend your parties now!

Lastly, I would like to wholeheartedly thank Neal Robb; who has never let his complete lack of understanding of any of this research stuff get in the way of his full and unwavering belief in me.

Author's Declaration

I declare that, except where explicit reference is made to the contribution of others, this thesis is the result of my own work and has not been submitted for any other degree at the University of Glasgow or any other institution.

Fiona McGruer

Definitions and Abbreviations

ANOVA	Analysis of variance- a statistical test used to examine the differences among group means, including across multiple conditions.
BOLD	Blood-oxygen-level dependent; signal measured in fMRI.
CI	Confidence Interval. A range statistically defined so that it is highly likely that a single specific parameter falls within it. Likelihood is defined as a specific probability.
DCM	Dynamic causal modelling. A method used to infer the influence of the activity of one cortical area over the activity of another based on the BOLD response.
FA	Flip Angle.
FFD	Flashed face distortion.
fMRI	Functional magnetic resonance imaging. Brain imaging technique measuring blood flow as a proxy for changes in brain activity.
FOV	Field of View.
GLM	General Linear Model. A form of t-test implemented in fMRI data, as there are typically multiple independent variables on which to model the continuous outcome data (the BOLD signal). Mathematically identical to a multiple regression analysis. Can be easily extended into ANOVA.
LGN	Lateral Geniculate Nucleus; relays information from the retina to early visual cortex.
LOC	Lateral occipital complex, an object specific region in the extrastriate dorsal visual stream.
MIB	Motion-induced blindness.
MRI	Magnetic resonance imaging. Brain imaging technique imaging anatomy and certain physiological processes.
MVPA	Multivariate pattern analysis. A group of techniques which allow us to study the pattern of activity in an area as opposed to the overall univariate activation.
PQ	Prodromal Questionnaire (Loewy, Pearson, Vinogradov, Bearden, & Cannon, 2011).
RHI	Rubber hand illusion.

ROI	Region of interest. Defined as a subsection of cortex based on anatomical landmarks or functional mapping.
TE	Time to echo.
TMS	Transcranial magnetic stimulation. Method which uses magnetic fields to produce electric currents which provoke activation in brain regions. Can be used to facilitate or disrupt neural processing in stimulated regions.
TR	Repetition time.
T1	Structural fMRI image created using short TE and TR. Specialised to demonstrate grey matter white matter boundaries in the cortex.
vPMC	Ventral premotor cortex. An area of premotor cortex specifically implicated in illusory experience during the rubber hand illusion.
V1	Primary visual cortical area; on the posterior pole of occipital cortex around the calcarine sulcus. Entry site for cortical visual processing.
V5	Motion sensitive region in extrastriate visual cortex. Also known as hMT+/MT, in reference to its position on the medial temporal lobe.

1. INTRODUCTION

In this introductory chapter we will firstly describe the feedforward pathway of visual sensory input from the eye to the brain. Secondly, we describe the feedback pathways which pass information from various intracortical sources back down to the early visual cortex. To produce visual perception, the brain integrates feedforward sensory input from the eyes with fed back context and knowledge. We will consider how this integration affects visual processing at the lowest sensory levels of the traditional cortical hierarchy. We will use philosophical and historical ideas to clarify why feedforward vision alone is insufficient for visual perception, and will comment on more modern adaptations of these theories which describe vision as a constructive and inferential process. We will then consider how the inference inherent to visual perception can produce illusion. We describe the conceptualisation of visual illusions as incorrect percepts, resulting from inferences made in the integrative process between feedforward and feedback visual processing. Under most stimulus and contextual conditions these inferences would lead to optimal perception. As illusions arise from this integration, we may gain insight into feedforward and feedback integration by studying illusions. Lastly, we will consider how elucidating the integration involved in visual illusions can provide a view into errant cortical processing in neuropsychological disorder, specifically in Schizophrenia.

1.1. The Human Eye and the Feedforward Visual System

Visual sensory input entering the human eye is converted from photons to neural signals to be processed by the brain. Photons of various wavelengths provide the sole sensory input to the eye. This input originates in the human visual field, which extends from each eye 60° inwards towards the nose, past the vertical meridian, to 107° outwards from the vertical meridian. Vertically it extends 70° above to 80° below the horizontal meridian. In each eye, photons enter the cornea and are refracted through the pupil into the lens. Pupillary size controls how much light enters the eye, through dilation and contraction. Refraction from the lens focuses the inverted image of light onto the retinal photoreceptors.

Retinal photoreceptors are divided into rod and cone varieties, depending on the type of protein each contains. Rod photoreceptors are largely peripherally located and respond under low lighting conditions, whilst cone photoreceptors are foveated and are specialised for daylight. Cone photoreceptors form the beginning of colour vision, as the three varieties of cone photoreceptor absorb different wavelengths of light (short, middle, or long wavelength; by ‘S’, ‘M’, or ‘L’ photoreceptors; resulting in blue, green, or red light respectively). These photoreceptors link into five different types of ganglion cell, which transduce photons into electrical neural action potentials. Different ganglion cell types have different sized centre-surround receptive fields (RFs; the area of the visual field to which the cell will respond) and demonstrate specific sensitivities to depth, shape, and colour. As the system is already demonstrating selective response properties and filtering input to the brain, visual processing begins in these retinal ganglion cells (Wässle, 2004).

The electrical action potentials from ganglion cells are transmitted along the optic nerve, divided by their spatial origin in the visual field and by ganglion cell type. Optic nerves from each eye meet at the optic chiasm and, with the exception of fibres representing the inward/medial 60 degrees of each eye’s visual field, cross to the opposite hemisphere. This unites signals corresponding to a particular half of the total visual field and results in signals from each half being sent to the contralateral brain hemisphere (i.e. all signals from the left of the visual field are all sent to the right hemisphere). Optic nerve fibres terminate in various layers of the Lateral Geniculate Nucleus (LGN) in the thalamus, depending on the ganglion cell type they originated from. Signals are then fed forward to layer 4 of the primary visual cortex, ‘V1’ (for discussion about V1 cortical layers see **Chapter 6.6**).

V1 is the ‘earliest’ cortical stage of visual processing as it receives ~90% of feedforward retinal input. In each cortical hemisphere, visual field information is mapped onto V1, retaining the spatial relationships of the original input (Brewer, Liu, Wade, & Wandell, 2005; Sereno, Dale, Reppas, & Kwong, 1995; Wandell, 1999; Wandell, Dumoulin, & Brewer, 2007). Each neuron in V1 has a classic receptive field, a subsection of the viewed visual field that it will preferentially respond to (Hubel & Wiesel, 1959). As this spatial representation arose from retinal projection and passed through the optic chiasm, the image printed on the primary visual cortex of each hemisphere is vertically flipped, and represents the contralateral visual field.

The calcarine sulcus, an anatomical feature which is positioned in the centre of V1, roughly corresponds to the horizontal midline of the visual field. The lower half of the visual field image is represented above the calcarine sulcus, and the higher half of the image below. Areas V2 and V3 wrap around V1 at the occipital pole. The dorsal V1 (V1d) pattern of representation (of the lower visual field) is reflected into V2d, and then again into V3d. The same occurs for ventral V1 (V1v) representation (of the upper visual field) in V2v and V3v. Additionally, in all three early visual areas, information originating in the fovea is given greater cortical space at the occipital pole through cortical magnification, whilst more anterior representations of peripheral and far peripheral information cover increasingly less cortical space (Duncan & Boynton, 2003). This retinal topography (retinotopy) can be mapped in fMRI, as carried out in **Chapters 3** and **4.2**. In retinotopic mapping, phase encoded checkerboard stimuli move in a wedge, radially around the visual field (polar angle mapping) or as an annulus outwards from the centre with increasing diameter (eccentricity mapping; DeYoe et al., 1996; Engel, Glover, & Wandell, 1997; Engel et al., 1994; Sereno et al., 1995). By correlating the peak responses in the time course of each voxel's activation to a particular stimulus phase, we can determine which area of the visual field map the voxel most responds to (its receptive field). When all voxels in V1 are examined, we can construct a visual field map particular to the individual subject.

Whilst the retinotopy is represented laterally, V1 neurons are also vertically clustered through cortical layers in columns, which demonstrate selective responses for orientation (Hubel & Wiesel, 1974; Victor, Purpura, Katz, & Mao, 1994; Yacoub, Harel, & Uğurbil, 2008). Furthermore, different neuronal populations in V1 are selective for colour (Engel, Zhang, & Wandell, 1997; Victor et al., 1994; Wachtler, Sejnowski, & Albright, 2003), and spatial frequency (Mazer, Vinje, McDermott, Schiller, & Gallant, 2002; Victor et al., 1994). These, and other, neuronal preferences mean that activity in early visual cortex often correlates with low level visual features and the perception of low level visual features. From these properties, V1 is traditionally conceptualised as a low level sensory processor with a classic columnar arrangement and orientation-selective response properties; as measured by neuronal spiking and by fMRI (Hubel & Wiesel, 1959; Menon, Ogawa, Strupp, & Uğurbil, 1997; Sereno et al., 1995; Yacoub et al., 2008).

Neuronal activity in V1 in response to low level features is fed forwards up a cortical visual hierarchy (DeYoe & Van Essen, 1988; Grill-Spector & Malach, 2004). This information ascends to V2 and V3, then to assumedly more complex higher visual areas. Information is

fed forwards in two separate processing streams - the dorsal stream, which processes object representations, and ventral stream, which processes object's spatial locations and movement (Goodale & Milner, 1991; Mishkin, Ungerleider, & Macko, 1983). A purely hierarchical view assumes that information becomes more complex, abstract, and non-modal as it ascends the hierarchy (Grill-Spector & Malach, 2004). Some higher areas do appear to have functional specialisations, such as V5 a dorsal stream area which primarily processes motion stimuli (Rees, Friston, & Koch, 2000; Tootell, Reppas, Dale, & Look, 1995). In the ventral stream, object processing regions like LOC (Malach et al., 1995) respond for shapes, irrespective of their differing low-level features (Andrews, Schluppeck, Homfray, Matthews, & Blakemore, 2002; Grill-Spector, Kourtzi, & Kanwisher, 2001; Grill-Spector & Malach, 2004; Hasson, Hendler, Bashat, & Malach, 2001; Kourtzi & Kanwisher, 2000). Retinotopic field maps of visual field spatial location and eccentricity continue into higher regions, and can be mapped using more complex stimulus sets (Grill-Spector et al., 1998; Grill-Spector & Malach, 2004; Hasson, Harel, Levy, & Malach, 2003).

1.2. Feedback in the Visual Hierarchy

The brain feeds information forward: from retinal input, up the visual cortical hierarchy, to higher sensory areas which allow for complex processing. However, this is not the sole direction of communication in or to the visual cortex. In addition to feedforward input, any given area of cortex also receives feedback connections from around 66% of all brain areas; composed of local reciprocal links, long range connections, thalamic and other subcortical connections (Larkum, 2013; Markov et al., 2013). Only 5% of excitatory input to V1 cells corresponds to feedforward thalamocortical retinal input. The majority of input to V1 is instead received through feedback and lateral connections (Budd, 1998; Kayser, Kim, Ugurbil, Kim, & König, 2004). Recent work by Michalareas et al. (2016) demonstrated that feedback connectivity permeates the visual cortical hierarchy, showing feedback and feedforward influences between over 26 human cortical areas using MEG. This data compliments and extends their laminar recording data demonstrating this feedforward and feedback connection hierarchy in the macaque visual cortex (Bastos et al., 2015; Markov et al., 2014). It is critically important to understand the contribution of feedback processing to visual cortical activity. Despite complex modelling of the V1 response to feedforward input, full processing variance is not yet explained (Douglas & Martin, 2007; Muckli et al., 2015). Additionally internally generated activity, including feedback, accounts for roughly 90% of

cortical energy consumption (Raichle, 2011; Raichle & Mintun, 2006). This internal computation is not necessarily in response to stimuli but nonetheless has an impact on the response to and processing of future stimuli. Feedback begins very swiftly after the feedforward visual stream - as soon as activation is fed forward from V1, recurrent interactions begin between this early visual area and higher visual areas (Bullier, 2001; Lamme, 2004). These feedback projections can take as little as 10ms to transfer information between extrastriate visual cortex and V1 (Hupe et al., 2001).

The feedforward processing cascade captures only a small fragment of V1's processing capability and models of V1 must be adapted to include the wide response variance allowed by cortical feedback, permitting research to, 'reach beyond the classical receptive field' (Angelucci & Bullier, 2003). In addition to high-resolution retinal input in a particular receptive field, V1 neurons are capable of integrating abstracted top-down and lateral inputs, and these inputs can additionally modulate classical receptive fields (Muckli & Petro, 2013). Feedback contributes to V1's ability to demonstrate subtle centre and surround receptive field properties traditionally associated with higher areas (Angelucci & Bressloff, 2006). We can differentiate between three resulting receptive field qualities for each V1 neuron. The classic receptive field of a V1 neuron is the area of the visual field to which the cell responds to a stimulus, inducing spiking activity with a peak centre response. The receptive field surround is the area around the receptive field. The cell will not fire in response to stimulation to the surround; however stimulation to this area can modulate effects in the centre receptive field through feedback and long range horizontal connections. Finally, the perceptual receptive field refers to the area for which the cell has *potential* to respond to a stimulus given top-down feedback modulations (Das & Gilbert, 1995; Fitzpatrick, 2000; Kapadia, Westheimer, & Gilbert, 1998). The perceptual receptive field can differ from the classical receptive field in many parameters such as size, acuity, and feature preferences (Das & Gilbert, 1995; Kapadia et al., 1998). For example, Sharpee and Victor (2009) demonstrated that when viewing images with matched low level features, changes in the spatial response of the receptive field of V1 neurons occurred due to surrounding context, and as an effect of the strength of intra-cortical feedback modulation.

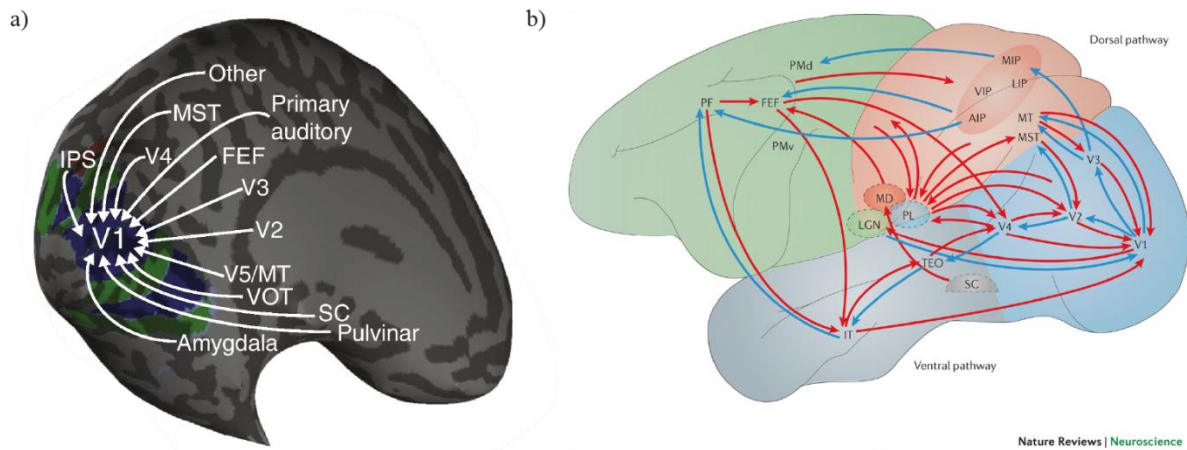


Figure 1.1. Feedback and feedforward connectivity. a) Image from Muckli and Petro (2013) showing areas which send cortical feedback to V1 including other primary sensory cortices and higher visual areas. b) Image from Gilbert and Li (2013) demonstrating the visual feedforward connectivity (blue) and feedback (red) pathways in the macaque.

The impact of cortical feedback on and within visual cortex is substantial. An impressively diverse assortment of areas send information to V1 through feedback (see Figure 1.1.a and b); including other sensory areas, higher visual areas, and emotion regions such as the amygdala (Felleman & Van Essen, 1991; Gilbert & Li, 2013; Shipp, 2007). Higher visual areas have a top-down influence on the activity of lower areas (Bar, 2007; Beck & Kastner, 2009; Bressler, Tang, Sylvester, Shulman, & Corbetta, 2008) all the way to V1 (Muckli, Kohler, Kriegeskorte, & Singer, 2005; Silvano, Cowey, Lavie, & Walsh, 2005; Ungerleider & Kastner, 2000) and even LGN (Gilbert & Sigman, 2007). This influence can be observed at all levels of the visual hierarchy, but is most clearly observed in V1, due to its well-documented mapped response to feedforward visual stimulation. Thus it can be clearly demonstrated that V1 reacts to and distinguishes between stimulation far outside its classic receptive field and response properties (Angelucci et al., 2002; Grill-Spector & Malach, 2004; Harrison, Stephan, Rees, & Friston, 2007).

Feedback allows V1 neurons to respond in the *absence* of feedforward retinal input, for example during occlusion (Lee, Mumford, Romero, & Lamme, 1998; Muckli et al., 2015; Sugita, 1999), and even in the blind (Amedi, Floel, Knecht, Zohary, & Cohen, 2004). Some of this feedback information is contextual- Smith and Muckli (2010) presented natural scenes with a quadrant occluded, and found that the non-feedforward-stimulated quadrant in V1 nonetheless carried a neural representation of the surrounding scene. They could successfully

decode individual scene representations from activity within the occluded quadrant. This result cannot be explained by low level feedforward visual properties- the quadrant receives no meaningful feedforward input and is sufficiently isolated from its feedforward surround as to discount contributions from lateral connections at the level of V1.

In V1 both working memory and imagery are represented in a ‘perception-like’ fashion, supporting suggestions that perception is not as disparate from knowledge about the perceptual world as previously assumed (see **Chapters 1.3-1.5**). Visual mental imagery elicits activation in V1 without any feedforward visual stimulus (Amedi, Malach, & Pascual-Leone, 2005; Slotnick, Thompson, & Kosslyn, 2005). Category-specific imagery representations in V1 can be elicited by auditory stimuli (Vetter, Smith, & Muckli, 2014), showing that non-visual stimuli are nonetheless represented in V1 activity patterns. V1 has also been shown to represent expected or remembered colour when presented with only grayscale images, despite no perception of colour in the image (Bannert & Bartels, 2013). Furthermore, Albers, Kok, Toni, Dijkerman, and de Lange (2013) showed that mental imagery decoded from V1 activity represents the world in a similar fashion to both representations of working memory and of actual feedforward visual stimulation. These properties demonstrate that the visual brain can be driven primarily by cortical feedback, and can create diverse perception with or without interaction with feedforward sensory input.

As stated, recurrent feedback and feedforward interactions start almost immediately after the feedforward cascade. This recurrence serves an important function for visual awareness. Feedback mediates both visual attention and visual awareness (Flevaris & Murray, 2015; Li, Piëch, & Gilbert, 2006; Maunsell & Treue, 2006). Whilst we think of a stimulus that is attended as similar to a stimulus we are aware of, neurophysiological findings suggest the two can be distinguished. However, they are difficult to separate in practice. Attention is the manner in which the brain selects which sensory inputs to prioritise in terms of processing speed and level of detail (Driver & Frackowiak, 2001; Lamme, 2003). Visual attention typically increases neural activation in the cortical space dedicated to that stimulus (Desimone & Duncan, 1995). Visual attention can be top-down, driven by feedback regarding context, aims and interests in the visual environment (endogenous attention, Lamme, 2003). Alternatively, salient features of stimuli (for example bright colours) can drive increased attention (exogenous attention). This selectivity is based on how memory and

learned responses shape sensory processing, and thus is also a feedback influence (Lamme, 2003).

Neural activation or attention do not necessarily translate to visual awareness of a stimulus (Lamme, 2003). Lamme (2003) posits that awareness is reliant on recurrent processing between higher and lower areas of the cortical hierarchy (see also Lamme, 2004). Critically for understanding experimental outcomes, awareness does not necessarily increase activation in the cortex (Watanabe et al., 2011). Recurrent interactions typically begin as soon as the feedforward activity related to a stimulus has started to ascend the cortical hierarchy. If backwards masking is applied ~40ms after the initial stimulus to interrupt recurrence, the initial stimulus is not perceived (Enns & Di Lollo, 2000). TMS can disrupt this awareness (Walsh & Cowey, 1998) if applied at the correct time point so as to interrupt recurrence. Pascual-Leone and Walsh (2001) found that if feedback from V5 is reduced using TMS, subjects cannot perceive moving phosphenes. A different group used TMS to show that recurrent feedback and feedforward interactions are required to complete a very simple scene categorisation task (Koivisto, Railo, Revonsuo, Vanni, & Salminen-Vaparanta, 2011; subjects were required to state whether or not there was an animal in the image). Feedback required for conscious perception may occur at very short distance ranges in the cortical hierarchy - information originating in foveal V1 is fed back in order to discriminate objects in the visual periphery (Chambers, Allen, Maizey, & Williams, 2013).

Lamme (2003; 2004) distinguishes fully conscious and attended awareness from general phenomenological awareness (for example the awareness of stimuli in the peripheral visual field, which are nonetheless not being processed). Phenomenological awareness occurs when recurrent interactions are present between visual cortical regions. This can occur for many aspects that make up a scene, as the cortical regions involved have retinotopic maps which separate the stimuli. When recurrent interactions involve higher frontal and temporal cortical areas, then the stimulus are considered in terms of cognition (goals, memory) and are fully conscious. Full awareness is therefore only present for some items in the visual input, with feedback and recurrent interactions from 'cognitive' areas of the brain.

These top-down influences of cortical feedback on perception, and many others such as expectation (Kok, Failing, & de Lange, 2014; Kok, Jehee, & de Lange, 2012), scene category (Morgan, Petro, Vizioli, & Muckli, 2015), object versus scene information (Bennett, Petro, &

Muckli, 2016; Kravitz, Saleem, Baker, Ungerleider, & Mishkin, 2013; Williams et al., 2008), and reward (Serences & Saproo, 2010; Shuler & Bear, 2006; Sirotin & Das, 2009) demonstrate high level effects at the traditionally lowest sensory levels. Two information streams- feedback and feedforward- interact to produce visual cortical activation and ultimately perception (Petro, Vizioli, & Muckli, 2015).

1.3. Historical Theories of Constructive Visual Perception

The properties of light, the retina, optic nerves, primary visual cortex, and feedforward processing streams demonstrate how visual inputs reach the brain. Through intracortical feedback connections, we see how early and later visual cortical regions can also receive higher level and non-visual information. However, these functional properties do not fully elucidate why this kind of interactivity in the cortex is required to produce visual perception. For this we turn to philosophical and historical theories of visual perception.

Visual perception is *the psychological perception of vision*, which does not precisely correspond to photon input to the retina. The correspondence between the external world and resulting visual perception has been a topic of philosophical debate for centuries. Philosophical ideas about perception vary between *externalist* views, in which perceptions are reflective of real world aspects, and *internalist* accounts, in which perceptions are reflective of the mind of the perceiver. We know that a purely externalist or realistic view cannot be accurate, as researchers observe perceptual effects that are reliant on the perceiver, and many individuals experience illusion and hallucination. Early internalist philosophical ideas of Plato, Plotinus, and Augustine of Hippo proposed that the reality of matter (in this case light input to the retina) is inferior to ideas and conceptualisation (Plato's Theory of Forms and Theory of Ideas; Plato; Plato). Later philosophical battles arose between *nativist* theories - the suggestion that concepts, mental capacities, and mental structures are innate rather than acquired by learning (Kant, 1781) - and *philosophical empiricism* - which promoted that knowledge and ideas are not innate and are derived from the senses (Berkeley, 1709).

In his *Critique of Pure Reason* (Kant, 1781), Kant argued that the mind, not external input, is the origin of human experience. He therefore suggested that our mental perception of the world does not mirror reality; instead the mind shapes what we perceive. In contrast, whilst Berkeley believed that we derive knowledge from the senses, he also proposed that nothing truly exists as a material substance (*immaterialism*). Predating modern knowledge of how the feedforward visual system operates, he suggested that vision is not truly of objects but arises from light and colour (Berkeley, 1709). He theorised that the environment and objects exist only within the mind of a perceiver, with their reality dependent on being perceived. His theory stressed repeated associations as the basis for this reasoning, and therefore as the basis of perception. These ideas gained further traction through philosophical movements such as *perspectivism*, the idea that each world is viewed through an individual's particular conceptual 'lens' or schema and that therefore one's perception is always inherently subjective (see, for example, the work of Nietzsche).

von Helmholtz, a scientist in the field of visual perception was heavily influenced by Kant. Inspired by his philosophical arguments, he put forward scientific theories on how depth, colour, and motion perception could originate within the mind (von Helmholtz, 1897). He defined the word 'psychophysics' to differentiate between a physical change (e.g. the wavelength of light) and the resulting percept (colour). In 1867, Helmholtz formally proposed that perception occurs as a result of unconscious inference from sensory input and experience (von Helmholtz, 1924). To give an example, the sensory input from 3-dimensional objects is two dimensional, with the third dimension existing purely in the mind on the basis of prior experience and reasoning. Thus, von Helmholtz suggested that perception is a constructive process from several sources, not merely an acceptance of the sensory input.

Gestalt psychologists in the early 1900s raised questions around how perception is united into a cohesive 'Gestalt' rather than perceived as its divided sensory inputs (e.g. contours, changes in brightness, orientations). A whole Gestalt percept is somehow 'other' than the sum of its separate elements- our brains perceive a whole, not disparate parts (Koffka, 1922). The concept of a united Gestalt originated with von Ehrenfels (1890) but was made popular by Wertheimer's (1912) paper on gestalt phi motion, a special case of apparent motion where subjects experience 'pure' illusory motion without experiencing a moving object (see

Chapter 1.6.2. for more on apparent motion). From these inaugural works, the field divided between two lines. The Graz school of Gestalt psychology (led by Meinong, von Ehrenfels, and Benussi) separated input and perception, theorising that perception is produced on the basis of input. In contrast, the Berlin school (led by Wertheimer, Koffka, and Köhler) posit that Gestalt is a whole percept not necessarily founded on elements from sensory input. Perception in their view does not arise directly from input, but from dynamic physical processes in the brain (Kohler, 1920; Köhler, 1938). The two fields of Gestalt psychology therefore mirror older philosophical arguments.

Gestalt theory has significant implications for the subjective nature of some perception (such as context effects, illusions and bistability; discussed later in **chapter 1.6.**), as it emphasises how contextual processing in the cortex can modulate the perception of a stimulus. Gestalt theorists also introduced the ideal of an idealised or stable response to stimuli- proposing that for a stimulus, the resulting percept will be the most parsimonious option. This percept will encompass the optimal amount of the separate sensory inputs (Wertheimer, 1922). Gestaltists set out ‘rules’ which determine how sensory inputs are united into a coherent percept, such as similarity, proximity, common fate, direction, good continuation, uniform density, and symmetry (Wertheimer, 1922). Please note that these rules require integration of a context over areas not covered by the receptive field of any single visual cortical neuron, and therefore require communication laterally or through feedback from higher visual areas with larger receptive fields. Grouping factors in Gestalt psychological theories generally require bidirectional communication across multiple levels of a cortical visual hierarchy. Modern evaluations of Gestalt grouping principles suggest that initial grouping occurs at each cortical level, with feedback from higher to lower regions, until one coherent percept is reached (Wagemans et al., 2012).

Helmholtz’s and Gestalt theorists’ work heavily influenced more modern visual perception scientists such as Gregory and Rock. Gregory proposed that visual perception is dominated by top-down cortical feedback mechanisms i.e. perception arises mostly from internal brain computation and communication from higher visual areas down the cortical hierarchy, not from light input to the retina (Gregory, 1970). Many of these early theorists have noted that light input itself is so ambiguous that existing knowledge is required to make sense of the

stimulus. However, the resulting percept may not always be the correct interpretation of a sensory input. For Gregory perception was better considered as a ‘hypothesis’, which is based on prior knowledge and inference. The Gregorian human brain therefore constructs a hypothesis about reality based on the sensory input, the environment or context, and on pre-existing knowledge; then perceives this most likely hypothesis (Gregory, 1970). If the hypothesis is incorrect, then so is the percept (such as occurs in visual illusions). Rock’s (1997) Indirect Perception supports this notion of inferential perception, positing that perception is a form of ‘problem solving’; attempting to identify the source of a particular pattern of retinal stimulation.

1.4. The Bayesian Brain

One outstanding question is the mathematical realisation of such hypothesising and inference about the world. For this problem, researchers turned to Bayesian statistical theory (Thomas Bayes, 1701–1761). In inferential brain theories, any particular percept is only one of several possible hypotheses about the sensory input (in the case of visual perception, photons). These hypotheses have differing probabilities. With further input these hypotheses gain or lose evidence in their favour and therefore gain or lose probability. The aim of the brain is to create an internal model or hypothesis which best explains the sensory input from the outside world, and it is this model which dictates perception.

Bayes' theorem is stated as:

$$p(H|B) = \frac{p(B|H)p(H)}{p(B)}$$

The theorem calculates the probability of a hypothesis (H) based on knowledge about conditions related to the hypothesis (B). Probability in Bayesian theory is not an exact observed number; rather it is a quantification of belief or knowledge about a hypothesis. In the case of visual perception, it can be the probability of a certain percept. P(H) and P(B) are the *probabilities* of observing H and B, independent of one another. P(H|B), is a *conditional*

probability, describing the probability of observing hypothesis H when B is true i.e. the probability of a certain percept given a condition. $P(B|H)$ describes the probability of observing event or information B when hypothesis H is true i.e. the probability of a certain percept given the observed condition. Each probability and conditional probability is subject to a shift in value if the evidence for that hypothesis/information (or the evidence for a link between that hypothesis/information and another hypothesis/information) is increased or decreased. This statistical model allows the brain to reduce the number of possibilities for eventual visual perception.

Bayes theorem can be used to assess the *posterior probability* of an event given i) real data input, ii) a probability estimate based on prior probability, and iii) a likelihood function. The likelihood function arises from a statistical model of the observed data. In this formulation H is the hypothesis (the model for perception) that may be affected by data measured. B is the new measured data. So $P(H|B)$ is the *posterior probability* of the hypothesis (H), given the new data observed (B). $P(B|H)$ is the *likelihood* of the observed data given the hypothesis, based on the sampling distribution of the actual observed data. This indicates how consistent the new data observed is with the existing hypothesis. This is then multiplied by $P(H)$ the *prior probability* of the hypothesis before data was observed. This value is then divided by the *prior probability* of the new data observed. This happens iteratively, every time new evidence is observed. It is important to note that the prior probability, the sensory inputs, and the likelihood of a hypothesis (percept) are all subject to noise which widens their distributions. Stimuli in the natural world do not typically exactly replicate, and visual sensory input is inherently ambiguous and degraded. Therefore, both the learned associations between input and percepts (priors), and the sensory inputs, are associated with noise. In terms of the feedforward and feedback communication structure described previously, feedforward connections carry new data whilst feedback connections communicate the prior probabilities for the hypothesis and for the new sensory data.

Bayesian inference is one method for optimal reasoning that the brain could use to determine perception given ambiguous sensory inputs. For example it can be used to elucidate three-dimensional objects from two dimensional photon input, using priors that state that light comes from above (Scholl, 2005). Many aspects of human perceptual behaviour can be modelled using Bayesian statistics, for example Moreno-Bote, Knill, and Pouget (2011)

showed that in ambiguous bistable grating displays, the perceived depth order varies as would be expected under Bayesian sampling rules (for a review of perceptual results that support Bayesian brain theories see Kersten, Mamassian, & Yuille, 2004; Mamassian, Landy, & Maloney, 2002).

Bayesian priors in vision can be learnt or innate. If humans were born without any innate priors we would be unable to perceive anything under Bayesian brain theories. Therefore, there must be some innate priors in the system (Gregory, 2006). Natural scenes inherently have reliable, repeating statistics (Geisler & Perry, 2011; Rentschler, Jüttner, Unzicker, & Landis, 1999). However we also know that some reliable priors about the visual world, for example the prior that light comes from above, are malleable through learning (Adams, Graf, & Ernst, 2004). Scholl (2005, p 40) clarifies that the two need not be mutually exclusive; “it may be possible for the very same process to be both innately determined and yet to later change (even radically) in response to interaction with the environment”. He proposes the idea of the brain as having ‘factory default’ priors which are changed to a personalised specification for an individual through environmental learning. Interplay can exist between innate priors formed by genetics and resulting brain structures, and adaptive priors from functional learning (Kersten et al., 2004). Innate priors may also aid an organism by directing Bayesian learning. In human children, innate priors may make faces hold particular attention (although this is controversial; see Gauthier & Nelson, 2001; Kanwisher & Moscovitch, 2000), driving the brain to learn additional priors about faces through increased exposure. Orientation tuning in early visual cortex has innate structural basis, which then develops through visual experience (Weliky & Katz, 1997). In ferrets, spontaneous visual cortical activity becomes increasingly like the evoked response to natural stimuli through their developmental trajectory (Berkes, Orbán, Lengyel, & Fiser, 2011). There is therefore a ‘Bayesian like’ adaptation of internally generated activity to natural scene statistics.

Functionally for perception, Bayes theorem means that if we had very low belief in a particular hypothesis (percept) before any sensory input ($P(H)$), it remains quite unlikely even if evidence is highly compatible with that hypothesis. In contrast, if something was highly likely before, we may retain that probability even if the new data observed is quite incompatible with the hypothesis. The implementation of a Bayesian brain, where percepts have different prior probabilities, allows for perceptual stability and explains why many illusions we observe are extensions of existing likely observations. In the case of illusion,

researchers have suggested they reflect the optimal outcome of Bayesian inference - that they are sensible inferences based on the sensory input and priors available. Furthermore, this model for cortical function means that new evidence can be integrated constantly and iteratively. The priors, the posterior probability, and therefore percepts, are constantly revised. These probability functions can also mathematically be used to predict future data points over a posterior distribution, and again many proponents of Bayesian brain theories suggest that the cortex functions in a similar manner to predict upcoming stimuli.

1.5. Cortical Prediction

One modern Bayesian-type brain theory which stresses cortical prediction is hierarchical predictive coding (PC). PC theories hypothesise that the human cortex operates as a Bayesian prediction machine - its central purpose is to predict variance in incoming sensory information using top-down modelled expectations to avoid entropy in the system (Clark, 2013; Friston, 2010; Mumford, 1992; Rao & Ballard, 1999). An internal predictive model of the world is formed at higher cortical levels, which have large sensory receptive fields and include information about context and knowledge. This predictive model is fed back to lower sensory areas forming modal-specific probabilistic expectations about incoming stimuli (Clark, 2013; Rao & Ballard, 1999). The generative explanatory model is constructed from memory, analogy, and contextual associations (priors), and is consequently ever-evolving as an organism gains sensory experience throughout its lifetime (Bar, 2007). This predictive modelling is proposed to dominate cortical function. Muckli (2010), p.137, summarised this proposition as such:

“Sensory stimulation might be the minor task of the cortex... its major task is to ... predict upcoming stimulation as precisely as possible”.

Top-down modulation is economic as it allows minimal processing for any stimulus which is predicted- only the residual or non-explained sensory input must be processed, as only it is informative. This residual input is thought to propagate back up the cortical hierarchy through feedforward connectivity and is used to update the existing models (Friston, 2010; Hohwy, Roepstorff, & Friston, 2008; Huang & Rao, 2011; Jehee & Ballard, 2009; Lee & Mumford, 2003; Rao & Ballard, 1999). These ‘prediction errors’ communicate the difference between what was expected and what was received, therefore becoming a proxy for sensory

information itself (Feldman & Friston, 2010). In Predictive Coding models, increased neural activation is assigned to sensory input which is inconsistent with the predictive model (Muckli & Petro, 2013), whilst similar Adaptive Resonance theories suggest that unexpected stimuli should result in reduced activation (Carpenter & Grossberg, 2011; Grossberg, 2013), and other theorists such as Spratling suggest both should be possible in different cases (Spratling, 2008b). Some theorists propose that even action exists to remove prediction error and sources of entropy in the system (Friston, 2009, 2010). In these free-energy theories prediction errors are minimised by modulating the sensory inputs as well as the internal cortical models of upcoming stimuli. Prediction errors or ‘free energy’ in this theory is conceptualised as the difference between the prior distribution of beliefs (before data) and the posterior prior of these beliefs after sensory data has been assimilated.

To clarify, feedforward connections are hypothesised to carry residual error and representational stimulus content, whilst feedback connections are hypothesised to communicate predictions for incoming sensory input to the level below. This system is one of continuous recurrent processing throughout the cortex. Modelling and feedback predictions occur at every level of the hierarchy, and each level interacts with and influences the computation of adjacent levels (Friston, 2010). The precision and weightings of both feedback models and feedforward prediction errors and sensory input vary based on stimulus or model reliability and directed attention (Friston, 2009). Critically, feedback models and resulting prediction error modulate activation in the early sensory cortices, and correspondingly have a large influence on resulting perception. In these models the top-down feedback signal is more akin to our traditional conceptualisation of ‘perception’ than the bottom-up signal, which communicates largely the accuracy of the predictive causal model (Hohwy, 2007b).

The precisions and weightings of models and errors are dependent both on learning and on the levels of noise in these variables. Attention is one possible mechanism for balancing feedforward and feedback influence, through manipulating the precision of both predictions and of predictive errors (Bubic, Von Cramon, & Schubotz, 2010; Den Ouden, Kok, & De Lange, 2012; Feldman & Friston, 2010; Friston, 2009; Hohwy, 2010, 2012). Attention direction increases gain in error units, and therefore controls the influence of prediction errors and prior expectations at different levels (Friston, 2009), by providing increased gain i.e. attention gives weight and precision to error responses (Den Ouden et al., 2012; Feldman &

Friston, 2010; Friston, 2005, 2009; Friston, Daunizeau, Kilner, & Kiebel, 2010; Hohwy, 2012). This variance of precision and attention can explain why we can perceive things that are highly unusual in our environment, despite the cortex aiming to minimise error. Stimulus inputs are perceived when they are sufficiently reliable, and are made salient by error signal and attention. Such surprising stimuli can even modulate existing higher level models if they are reliable and salient enough (Clark, 2013). Additionally, precision may be one function of lateral interactions mediated by feedback (Clark, 2013; Erlhagen, 2003; Muckli & Petro, 2013).

1.6. Illusions Dissociate Perception from Stimulation

“Reality is not always probable, or likely.”

- *Jorge Luis Borges*

Thus far we have described how we receive feedforward sensory input from the eye, and information through intracortical feedback and lateral connections. We have considered historical and recent theories which characterise visual perception as a constructive and inferential process, predicting the visual environment based on these two sources of information (feedforward and feedback). The perceived visual sensory environment is a combination of sensory input and of prior knowledge, attention, perceptual task, expectations, memory, analogy, mood, reward, and numerous other cognitive factors; which are communicated to the visual cortex through cortical feedback (Gilbert & Li, 2013; Muckli & Petro, 2013).

As our experienced world is *constructed* as opposed to *veridical*, what we see can diverge radically from real-world stimulation and we can experience some dramatic instability in perception. For example, in classic bistable percepts such as the Necker cube, Rubin’s face/vase illusion, or binocular rivalry; conditions of high ambiguity cause perception to regularly switch between two mutually exclusive possibilities. These bistable percepts are associated with fluctuations in early visual cortex activity occurring with and prior to changes in perception (Haynes & Rees, 2005b; Parkkonen, Andersson, Hämäläinen, & Hari, 2008). These perceptual switches are driven by top-down modulation- motion area V5 and parietal

cortex indicate the perceived direction in bistable motion (Castelo-Branco et al., 2002; Dodd, Krug, Cumming, & Parker, 2001; Muckli et al., 2002; Williams, Elfar, Eskandar, Toth, & Assad, 2003) and connections from V5 to V1 dictate the resulting perception (Genç, Bergmann, Singer, & Kohler, 2011).

These top down effects on binocular rivalry can be modulated using TMS to disrupt feedback. TMS over right IPS prolongs the stability of a single stimulus in binocular rivalry (Zaretskaya, Thielscher, Logothetis, & Bartels, 2010). Top down influences on perception can be quite specific - TMS over the right anterior Superior parietal lobule (SPL) reduces stability i.e. increases perceptual switching (Carmel, Walsh, Lavie, & Rees, 2010; Kanai, Carmel, Bahrami, & Rees, 2011). When applied to posterior SPL, stability of the percept is increased (Kanai et al., 2011; Kanai, Paulus, & Walsh, 2010). Top down effects are information-specific, for example during binocular rivalry between a motion stimulus and a static stimulus disruptive TMS applied to V5 extends the period where the motion stimulus is not perceived (Zaretskaya & Bartels, 2013). Furthermore, visual cortices may represent the current percept during binocular rivalry, whilst higher temporal and frontal areas represent the switch in percept (Wang, Arteaga, & He, 2013).

Illusions are excellent examples of constructive perception. In illusions, we observe relatively stable deviations from veridical perception. Subjects with intact visual perception perceive a visual world which is not correct, based on a context which is ambiguous or which strongly implies an incorrect conclusion. Some authors have characterised illusions in terms of Bayesian statistical theory as ‘Bayes-optimal percepts’ - proposing that the illusion is the *most likely true* case in the sensory environment, given the stimulation input and prior expectations about the world. Others have characterised illusion in terms of predictive coding theory, as the most sensible predicted stimulus on the basis of the sensory input (see **Chapter 6.8** for a discussion of the illusions presented in this thesis and Bayes-optimal and predictive brain theories). Illusions can be interpreted as an effect of feedback modulation on the feedforward input- previous learning, expectation, or knowledge causes the brain to draw inaccurate inference from the input (Brown & Friston, 2012). This incorporates the assumption that the contexts which produce illusions would typically result in the correct perceptual conclusions

in the vast majority of sensory cases (Brown & Friston, 2012; Weiss, Simoncelli, & Adelson, 2002).

Illusions provide us with an ideal opportunity to study intracortical feedback. Previously, our group has isolated feedback by blocking feedforward input to sections of retinotopic visual cortex (Bennett et al., 2016; Morgan et al., 2015; Muckli et al., 2015; Petro, Smith, Zimmermann, De Martino, & Muckli, 2015; Revina, Petro, Denk-Florea, & Muckli, 2015; Revina, Petro, Rao, Smith, & Muckli, 2014; Smith & Muckli, 2010). Alternatively, illusions provide a unique opportunity to distinguish feedback and feedforward contributions (Muckli & Petro, 2013). They allow us to dissociate perception, which occurs as a combination of feedforward and feedback information, from actual feedforward stimulation (Petro, Vizioli, et al., 2015). In this manner we can examine the *confluence* of feedback and feedforward effects, as compared to segregated feedback effects.

1.6.1. Illusory Contours

Several common forms of illusion result from the interplay of feedforward and feedback effects. When we view a scene we finish objects in our visual world through amodal perceptual completion- even when objects are occluded by other objects, the visual system assumes that they exist as a whole behind the interruption (such as for the cat in Figure 1.2.a). There also exists a complimentary opposite, modal completion- the system infers the presence of an object from other objects that it appears to occlude in a form of figure-ground segregation (Seghier & Vuilleumier, 2006). Figure 1.2.b shows stimuli that induces both amodal and modal completion of triangles. In both cases the system extrapolates beyond what is actually received on the retina. However, only in modal completion is there illusory figure perception, in which the contextual cues trigger perceived contours of a non-existent object.

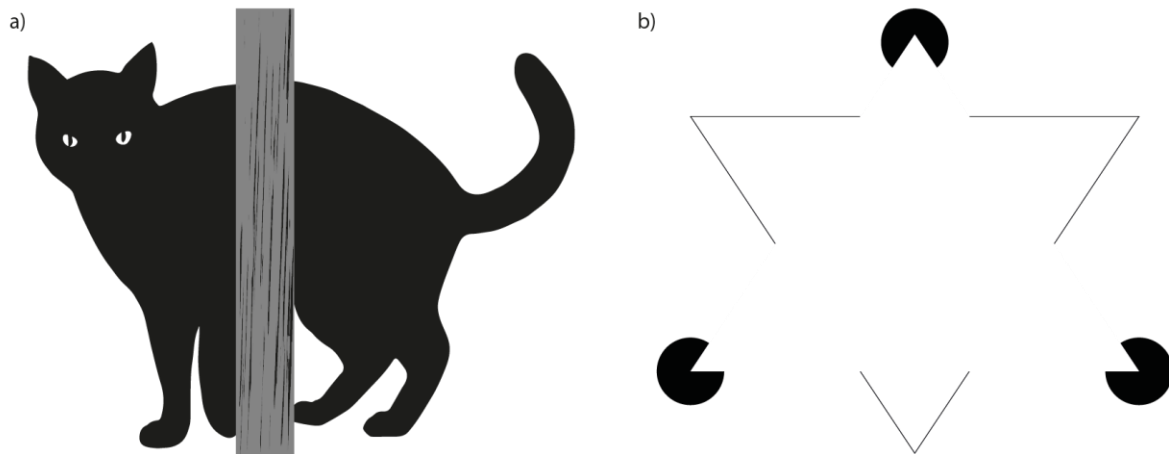


Figure 1.2. Amodal and modal completion. a) A cat behind a post, demonstrating amodal completion. Observers know that the cat continues behind the occluder but do not perceive the occluded section of the cat. b) Kanizsa triangle stimulus (Kanizsa, 1976), demonstrating modal completion- of an illusory white triangle; on top of two amodal completions- an outlined triangle and three black circles.

Illusory contour paradigms were popularised during the rise of Gestalt psychology (Kanizsa, 1976). The ‘Gestalt’ of a shape arises in concordance with several Gestalt principles: closure of an implied shape into a whole shape, even though the shape outline is broken; edge completion; and the overarching principle of *Pragnanz* – that the most simple explanation of input is correct and therefore becomes the resulting percept (Kohler, 1920). Like many Gestalt percepts, both modal and amodal completion seem to require feedback from higher visual areas such as the lateral occipital complex (LOC) and parietal cortex in order to be perceived as illusory whole images (Murray, Foxe, Javitt, & Foxe, 2004; Murray, Kersten, Olshausen, Schrater, & Woods, 2002). Furthermore, recurrent interactions between V1 and LOC are required for Kanizsa-type illusory figure perception – if this feedback is disturbed using TMS, contour completion does not occur (Wokke, Vandenbroucke, Scholte, & Lamme, 2012). Adaptation paradigms using illusory contours show that both higher (LOC and ventral occipitotemporal region (VOT)) and lower (V1 and V2) visual cortical regions are involved in inducing the perception of a united Gestalt (Altmann, Bühlhoff, & Kourtzi, 2003; Kourtzi, Tolia, Altmann, Augath, & Logothetis, 2003). Lee (2001) showed that V1 neurons respond to the illusory contours of Kanizsa figures. V1 reacts differently to amodal and modal contours, showing enhanced activity to illusory figures and reduced activity to surround objects with amodal completion (Lee, 2001). These differences likely occur as an effect of feedback modulation (Murray et al., 2004). Illusory contours have real-world effects-

Montaser-Kouhsari, Landy, Heeger, and Larsson (2007) observe orientation-selective adaptation to illusory contours in all retinotopic visual areas, and observe an increase in adaptation from lower to higher visual regions, again suggesting these contours are represented strongly throughout the hierarchy.

An interesting study by Kok and de Lange (2014) demonstrated the effect of such illusory contour and figure perception on neural activity in early visual cortex. V1 activity reflects the perception of illusory Kanizsa figures- increasing across the illusory figure itself and decreasing in the surround. The results observed were independent of attention. Several authors have suggested that feedback is involved in object perception and perceptual grouping (Roelfsema, 2006). When studied using high-field fMRI, across cortical layers, feedforward stimulus information was distributed across cortical layers whilst feedback related to the illusory Kanizsa shapes was found in deep layers of V1, although some subjects demonstrated feedback in the upper or even mid-layers (Kok, Bains, van Mourik, Norris, & de Lange, 2016). These data support results by (Self, van Kerkoerle, Super, & Roelfsema, 2013) who demonstrated that figure-ground discrimination in macaques is located in infragranular layer V and is consistent with the layer specificity of feedback and feedforward integration described in **Chapter 6.6**.

1.6.2. Apparent Motion

Motion is a crucial component of our visual world. When we observe motion, we do not merely perceive the moment-to-moment position of an object or scene. Instead, we extrapolate the motion speed and direction to predict where the object will appear next. When moving objects are presented with an identically located stationary flash, they are perceived as shifted forward in the direction of motion compared to the flash (flash lag effect; Whitney, 2002). Top-down feedback from V5 contributes to this motion misallocation and therefore may 'predict' motion (Maus, Fischer, & Whitney, 2013). In agreement with this, disruptive TMS delivered to V5 reduces the flash lag effect, bringing the moving bar perceptually closer to its true location. This reduction was most pronounced when pulses occurred just as the bar reached the flash position and at approximately 60 ms afterwards. These predictive

overshoots of motion are common in the psychophysical literature in low-contrast stimuli (Kanai, Sheth, & Shimojo, 2004) or for gradually fading objects in motion (Maus & Nijhawan, 2006). The effect is so strong that objects are perceived to be disappearing well into retinal blind spots, far past the spatial location at which stimulus input ceases (Maus & Nijhawan, 2008). In each of these cases the perception is not veridical- we perceive disappearances that are *inferred*. This extrapolation is accompanied by shifts in the neural signal, for example in data from cat V1 (Jancke, Chavane, Naaman, & Grinvald, 2004), and in shifts of the BOLD signal in humans (Whitney et al., 2003). Berry, Brivanlou, Jordan, and Meister (1999) also reported a predictive shift of motion information in the retina.

This extrapolation leads to several notable visual illusions. In the flash-lag effect, moving objects appear to have moved further than flashed objects even though they are presented at the same spatial location (Nijhawan, 2008). Maus, Weigelt, Nijhawan, and Muckli (2010) used stimuli which produced a motion-induced mislocalisation of the endpoint of fading objects. They found that the perceived final positions of the fading objects were predicted by an interaction of predictive position representations in V3a and offset transients in primary visual cortex. Geisler and Kersten (2002) found that the effects of luminance, contrast and shape on motion velocity illusions are consistent with Bayesian brain theories, suggesting that learning across visual experience allows contextual inference to inform the perception of motion.

The apparent motion illusion causes two alternately flashing token stimuli to be perceived as a singular object moving between these spaces in the visual field (Kolers, 1963; Shepard & Zare, 1983). The perceived trace of apparent motion is activated in V1 as if an object really passed across the visual field between the two token presentations, despite the cortex receiving no feedforward sensory input from the apparent motion trace (Larsen, Madsen, Ellegaard Lund, & Bundesen, 2006; Muckli et al., 2005). Multiple authors propose that the expectation of motion between the two locations creates this illusory trace. The effect is robust even without attention (Muckli et al., 2005). The top-down expectation and knowledge about how objects move between spaces is so strong that apparent motion and an accompanying activation trace can be produced on a curved illusory pathway (Akselrod, Herzog, & Ögmen, 2014). This trace reflects real neuronal activity in the area- Ahmed et al.

(2008) found that there is a wave of spiking in the area between the two token stimuli in ferret regions 17 and 18 (the homologue of human V1). This study used voltage-sensitive dyes which are sensitive to cortical feedback (Roland et al., 2006) and have been used to demonstrate feedback effects in other illusion studies (Jancke et al., 2004).

This illusory activation is likely formed by motion-related feedback from V5 (Akselrod et al., 2014; Kaas, Weigelt, Roebroek, Kohler, & Muckli, 2010; Muckli et al., 2005; see Figure 1.3.a and 1.3.b; Schwiedrzik, Alink, Kohler, Singer, & Muckli, 2007; Sterzer, Haynes, & Rees, 2006; Vetter, Grosbras, & Muckli, 2013; Wibralski, Bledowski, Kohler, Singer, & Muckli, 2009). The response in early visual cortex to the illusory trace does not start until 60ms post stimulus, after V5 activity (Wibralski et al., 2009). Additionally using dynamic causal modelling, Sterzer et al. (2006) demonstrated that feedback from V5 to V1 is engaged during illusory motion perception. The feedback motion trace affects behaviour, facilitating the detection of stimuli on the trace (Schwiedrzik et al., 2007). If probe targets are presented out of time with the predicted position of the illusory moving token they cause a signal increase, despite being less frequently detected than consistent targets (Alink, Schwiedrzik, Kohler, Singer, & Muckli, 2010). This has been interpreted as prediction error caused by the out of time targets being inconsistent with the predicted motion trace. Cortical feedback from V5 to V1 is required for apparent motion target prediction, if this feedback is disrupted using TMS, the detection advantage observed by Alink et al. is eliminated (Vetter et al., 2013). Hidaka, Nagai, and Gyoba (2009) induced apparent motion using bar stimuli, followed by either consistent or inconsistently moving bars. Subjects perceived consistent bar motion in both cases, demonstrating that apparent motion predictions are strong enough to completely overwrite feedforward perceptual information.

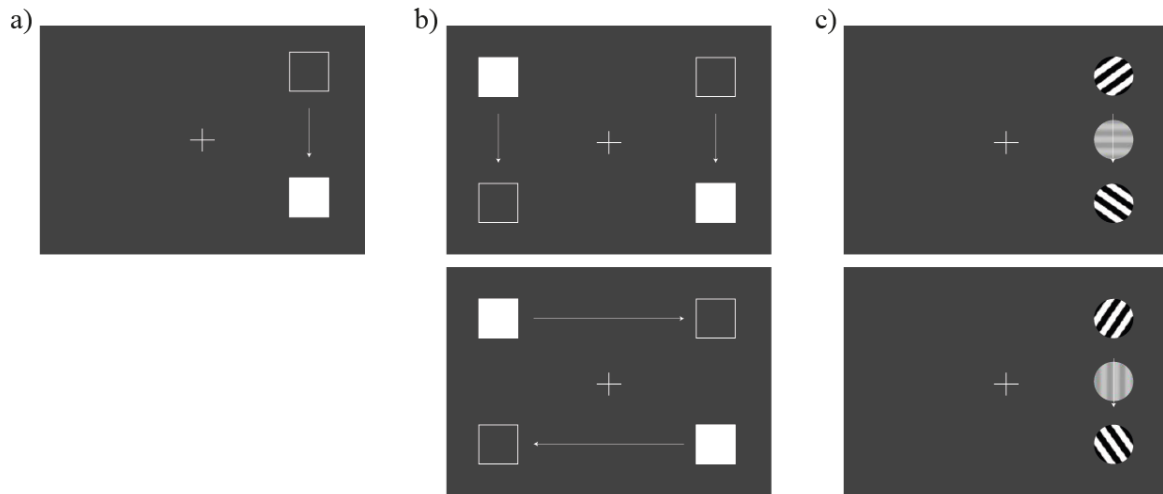


Figure 1.3. Apparent motion. a) Representation of stimuli used by Muckli et al. (2005). The upper stimulus with token presentation alternating between upper and lower visual field was used in Experiment 1. b) These ambiguous stimuli were used in Experiment 2 to demonstrate how the motion trace is affected by subject perception. Subjects can perceive targets moving horizontally or vertically with the same inducing stimulus. c) Representation of stimuli used by Chong, Familiar, and Shim (2015) with two oriented Gabor tokens as apparent motion inducers; greyscale circles show the inferred middle orientation decoded in V1 activity.

A recent variation on the apparent motion illusion, from Chong et al. (2015; see Figure 1.3.c); demonstrated the spatial, featural, and temporal specificity of feedback and prediction on the apparent motion trace. They used a set of orthogonal oriented Gabor tokens in place of apparent motion tokens and demonstrated that the centre of the motion trace in V1 represents an intermediate orientation, as if the stimulus rotated in space between the two tokens. Such a stimulus was never presented and subjects do not perceive the intermediate stimulus (apparent motion is not a form of imagery, although motion imagery can be decoded in V1 in other studies, see Kaas et al., 2010). Therefore this decodable feedback was constructed purely from higher level knowledge about stimulus rotation, orientation, and motion (Chong et al., 2015). Furthermore, previous behavioural results show that when using oriented Gabors as targets, orthogonal Gabor patches placed on the motion trace slow the perceived speed of the illusion, as if the interpolation is allowing time for rotation between the two points (Georges, Series, Frégnac, & Lorenceau, 2002). Some previous work has found that

object translations are extrapolated, but only at higher levels of the visual hierarchy (Weigelt, Kourtzi, Kohler, Singer, & Muckli, 2007).

Apparent motion provides us with a well-researched example of our constructive, bidirectional visual system in illusions. When our brain is presented with two quickly alternating tokens we unconsciously access higher level knowledge and experience which predicts that an object is in motion. Feedback from V5 to early visual cortex fills in the likely trace of the illusory object motion, promoting neuronal spiking on this trace and producing a BOLD signal increase. Consequently, we perceive an object bouncing back and forth.

1.6.3. Motion Silencing

In apparent motion, motion causes extra perception of a moving object trace that is not actually presented. Alternatively, the strong effects of motion stimuli can also cause stimuli that were presented to remain unseen. Suchow and Alvarez (2011) created a novel visual illusion using a circular array of coloured dots which changed in hue, luminance, size, and shape. They demonstrated that these properties appear to stop changing when the circle starts to rotate (Figure 1.4.a). This establishes that motion dominance can silence other forms of visual change. Similarly, in motion-induced blindness a salient target is perceptually silenced by the predictable motion of a moving distracter field (Bonneh et al., 2010; see Figure 1.4.b). Motion-induced blindness operates as a bistable percept- the target is either completely visible or completely extinguished. Like other bistable percepts, it may result from two possible predictive or explanatory models exerting a top-down influence over ambiguous stimuli (Hohwy et al., 2008). These results demonstrate a causal role for both the rPPC and V5/MT in MIB, and suggest that the rPPC is involved in shifting resources between competing functional areas, while V5/MT processing initiates and maintains MIB. Additionally, motion-induced blindness appears like a form of perceptual completion- the motion field appears to complete over the top of the target. We investigate the effects of feedback on early visual cortical activity during motion-induced blindness in **Chapter 4.2** using the stimulus depicted in Figure. 1.4.c. This chapter also includes a specific introduction to the illusion and potential contributing mechanisms.

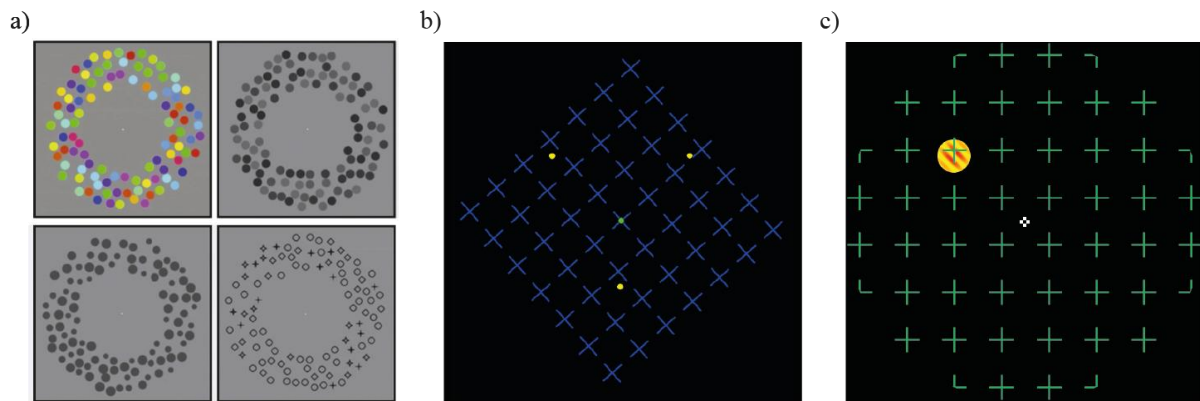


Figure 1.4. Motion illusions. a) Stimuli used by Suchow and Alvarez (2011) to examine silencing of (*clockwise from top left*) i) colour ii) luminance iii) shape and iv) size changes. b) Classic motion-induced blindness stimuli. c) Motion-induced blindness stimuli used in **chapter 4.1** and **4.2**.

1.6.4. Crossmodal Illusions

It is clear that illusory activity is often represented at the level of V1. What is unclear is the extent to which V1 represents illusory activity that is not primarily visual. Visual illusions dominate illusion research and other sensory illusions are often neglected. V1 can be driven purely by cross-modal stimuli, for example auditory stimuli activate early visual cortices (Martuzzi et al., 2007). Vetter et al. (2014) isolated feedback in V1 using categorical auditory stimulation delivered to blindfolded subjects. They found that cross-modal feedback created contextual information in V1 that could be used to decode the auditory stimulus the subject listened to. These properties are likely supported by direct connections from early auditory to early visual areas which target the periphery (Eckert et al., 2008), consistent with Vetter et al. (2014) who showed that decodable information about auditory scene was predominantly peripheral. Interestingly, the opposite is also true- visual stimuli that imply auditory stimuli can be decoded from early auditory cortices in the absence of actual sound (Meyer et al., 2010).

Importantly for the rubber hand illusion study that we present in **Chapter 3**, V1 is responsive to motor and tactile stimulation. Motor inputs in the mouse drive V1 activity during running in complete darkness in a manner similar to the spiking evoked by visual grating stimuli, demonstrating motion preparation in early visual cortex (Keller, Bonhoeffer, & Hübener, 2012). V1 can be rapidly and reversibly recruited by touch (Merabet et al., 2008). Additionally, action representations in the ventral stream have links to V1 (Kravitz et al., 2013). Feedback to early visual cortex may in fact be crucial for movement. Ban et al. (2013) showed that V1 represents occluded portions of objects and proposed that early visual cortex interacts with other modalities (haptic, tactile, motor) to facilitate action on objects or on the environment. Predictive signalling involved in action processing may originate in subcortical regions- cerebellar communication predicts the sensory consequences of actions (Wolpert & Kawato, 1998). However cerebellar feedback is implicated in many facets of perception (Roth, Synofzik, & Lindner, 2013), suggesting that this feedback information is domain-general not domain-specific (Petro, Vizioli, et al., 2015). Meyer and Olson (2011) found that this relationship between modalities is reciprocal- early somatosensory cortices are activated by viewing touch in the absence of tactile stimulation. To further the conceptualisation of illusions as an effect of cortical feedback, the rubber hand illusion provides an ideal opportunity to examine a multisensory illusion for which vision is only one key modality.

Crucially, illusions allow us to demonstrate the strength and flexibility of cortical feedback. These stimuli allow us to separate the effects of top-down information and veridical sensory stimulation; to understand how this feedback affects ongoing experience; and to examine what occurs when feedback and feedforward information interact. Furthermore, the effects of such confluence are observed all the way down at the traditionally low level of V1 in activation differences and multivariate representations of stimuli. We can therefore study these effects in a cortical region with well-defined response properties, which contains retinotopic field maps of stimulus representation; thus easing the process of discovering differences induced by cortical feedback.

1.7. Illusion, Hallucination, and Delusion

“A hallucination is a fact, not an error; what is erroneous is a judgment based upon it.”

- *Bertrand Russell*

One potential application of understanding cortical feedback is to understand neuropsychological disease. Deficits in cortical feedback and feedforward interactions may underlie disorders such as schizophrenia (Corlett, Taylor, Wang, Fletcher, & Krystal, 2010; Friston, 2005; Hohwy & Paton, 2010; Hohwy & Rajan, 2012; Sanders et al., 2012). Despite extensive research and application of pharmacological treatment, both the underlying pathophysiology and causal factors of schizophrenia remain unclear and existing treatment has limited efficacy (Insel, 2010). Perceptual deficits are highly prevalent across multiple domains including in auditory (Silverstein, Matteson, & Knight, 1996) and visual processing (Silverstein, Knight, et al., 1996); independent of cognitive dysfunction or recorded anatomical abnormalities (Uhlhaas & Mishara, 2007).

Many deficits in schizophrenia appear to stem from an inability to use top-down contextual or Gestalt information (Uhlhaas & Mishara, 2007). Matussek (in Cutting & Shepherd, 1987) described patients' visual world as being 'loosened' from its context; accompanied by a failure to grasp connectivity of objects, action and scene, and unusual allocation of attention to parts of a scene as opposed to the scene Gestalt. Multiple studies have demonstrated failures to combine perceptual elements into a united percept (Hemsley, 1994; Keri, Kiss, Kelemen, Benedek, & Janka, 2005; Uhlhaas & Mishara, 2007; Uhlhaas & Silverstein, 2003). Impaired contextual integration exists across spatial and temporal domains (Uhlhaas & Silverstein, 2005). Schizophrenic subjects appear typical in some paradigms, impaired in others, and advantaged in some cases; particularly when context is designed to be a distractor to lower the performance of typical participants (Uhlhaas & Silverstein, 2005). Positive (Keane, Silverstein, Wang, & Papatomas, 2013; Uhlhaas, Phillips, Mitchell, & Silverstein, 2006), negative (Koethe et al., 2009; Tadin et al., 2006), and cognitive symptoms (Uhlhaas et al., 2006) correlate with recorded perceptual dysfunctions. Perceptual deficits seem to be related to more chronic disorder (Silverstein et al., 2006) and are associated with poorer disorder prognosis, increased cognitive impairment, poor treatment prognosis, and lesser social function (Silverstein, Schenkel, Valone, & Nuernberger, 1998; Uhlhaas et al., 2006;

Uhlhaas & Silverstein, 2005). Importantly, perceptual fragmentation is correlated with psychosis severity (Matussek, from Cutting & Shepherd, 1987; Silverstein et al., 1998).

Such behavioural evidence has led to theories that schizophrenic subjects have a global processing deficit producing failures to link percepts into a coherent representation (Uhlhaas & Mishara, 2007). Crucially, they propose that symptoms of psychosis- hallucinations and delusions- do not arise purely from deficits in higher cognitive processing but from disrupted contextual feedback modulation of perception (Hemsley, 1994; Silverstein et al., 2006). Despite the salience of psychotic symptoms, many authors view perceptual deficits as the fundamental disorder, with psychotic symptoms as secondary reactions to unusual perceptual input.

1.7.1. Hallucinations and Delusions

In both hallucinations and illusions subjects can perceive an incorrect world-state from sensory information; including perceiving sensory stimulation that was not present, or misperceiving/not perceiving stimulation that was present. Illusion is robust in a typical population, whilst hallucination is common but not universal nor frequent. Importantly, the same inducing stimulus will promote similar illusions in most healthy subjects whilst hallucination demonstrates significant individual differences. Delusions appear more cognitive, demonstrating tenacious fixed false belief and resulting misperception of the world. However, many researchers propose that these beliefs are based on experience and interaction with the world (Corlett et al., 2010; Friston, 2010).

Dysfunctional top-down feedback may underlie hallucination and delusion in addition to perceptual deficits. Corlett, Frith, and Fletcher (2009) propose that the top-down modulation is over-exerted in schizophrenic subjects, causing false perception without feedforward input (hallucination, see also Fletcher & Frith, 2009). Some authors have suggested that hallucination occurs as a combination of an inability to unite sensory percepts, and dysfunction in categorising sensory stimuli generated by actions as self-generated.

Schizophrenic subjects show reduced ability to predict the sensory outcomes of their actions (Frith, Blakemore, & Wolpert, 2000; Shergill, Samson, Bays, Frith, & Wolpert, 2005; Voss et al., 2010). Alternatively, failed top-down perceptual inference could promote an increased reliance on bottom-up perception as opposed to higher level-driven strategies (Gilbert & Sigman, 2007). Without top-down influence the brain is unable to moderate perceptions and unable to integrate knowledge and sensory input (Corlett et al., 2010; Fletcher & Frith, 2009; Hemsley, 1994; John & Hemsley, 1992).

Delusions can also form under conditions of dysfunctional feedback. As top-down modulations direct attention, errant salience is given to non-relevant stimuli in an already-distorted sensory world (Heinz, 2002; Hemsley, 2005; Kapur, 2003). This salience promotes an incorrect focus on a feature of the external world, which then affects how the world is viewed and processed in future, eventually forming delusional thought (Adams, Stephan, Brown, Frith, & Friston, 2013; Corlett et al., 2010; Fletcher & Frith, 2009). This idea is not new; Maher (1974) originally suggested that delusions are rational responses to unusual experience. Hohwy and Rajan (2012) have proposed that delusions are similar to classical illusory experience, arising from faulty percepts. The difference is that illusions are an effect of otherwise facilitatory processing, whereas delusions arise from deficit processing. Delusions are highly tenacious once formed, which suggests that there is increased rather than reduced top-down signalling (Corlett et al., 2009 for a full review of common delusions and their link to neural network failures; Corlett et al., 2010). Many illusions share the delusional property of being irreversible, such as Muller-Lyer lines (in which measuring the lines objectively will not dispel the illusion that they are of different length), demonstrating a form of cognitive impenetrability specific to information from low level sensory processing (Hohwy & Rajan, 2012).

1.7.2. Visual Illusions in Schizophrenia

Schizophrenic subjects demonstrate distinct differences in illusion perception compared to typical subjects. As illusion can be considered an indicator of top-down contextual influence, these differences are also informative about underlying dysfunction (Notredame, Pins,

Deneve, & Jardri, 2015). In bistable percepts, typical subjects show perceptual stabilisation (the tendency to see the preceding percept after a bistable stimulus is removed then reinstated), whilst schizophrenic subjects do not (Schmack, Schnack, Priller, & Sterzer, 2015). The likelihood of stabilisation is also negatively correlated with delusional ideation in the schizophrenic (Schmack et al., 2015) and typical (Schmack et al., 2013) population. Schizophrenic subjects show a reduced effect of contextual surround in multiple studies (Chen, Norton, & Ongur, 2008; Dakin, Carlin, & Hemsley, 2005; Notredame et al., 2015; Tadin et al., 2006; Uhlhaas, Silverstein, Phillips, & Lovell, 2004). In the hollow mask illusion (Gregory & Gombrich, 1975) neurotypical subjects perceive a mask as constantly convex due to the strong top-down expectation that a face will be convex, whereas schizophrenic subjects can observe concave face stimuli (Dima et al., 2009; Keane et al., 2013; Schmeider, Leweke, Sternemann, Emrich, & Weber, 1996). During the illusion patients show a strengthened forward connection from V1 to LOC, whilst controls have a strengthening of the feedback connection (Dima et al., 2009). We behaviourally examine a face-space illusion in **Chapter 5** in neurotypical subjects.

Schizophrenic subjects are less susceptible to apparent or illusory motion (Crawford et al., 2010; Sanders, de Millas, Heinz, Kathmann, & Sterzer, 2013). Furthermore, increased delusion scores correlate with reduced apparent motion perception (Sanders et al., 2013). Previous studies by the same group showed that patient groups can predict the position of visual events on the apparent motion trace (Sanders et al., 2012). It therefore appears that they can predict the illusory target position but fail to integrate those top-down influences into a coherent motion percept the way that healthy subjects do. Tschacher, Schuler, and Junghan (2006) found that schizophrenic patients experienced reduced motion-induced blindness (MIB) effects if their symptoms were positive (hallucinations, thought disorder and delusions) and more decreased effects if their symptoms were negative (flattened affect for example), which suggests that different schizophrenic subtypes form different perceptual deficits. Positive symptoms are specifically associated with reduced illusion perception in schizophrenic groups (Keane et al., 2013; Sanders et al., 2013) but also in typical subjects (Bressan & Kramer, 2013). Importantly, most differences in illusion experience between schizophrenic and typical subjects suggest a reduced effect of top-down contextual integration through feedback. In theoretical terms, this is consistent with reduced cortical prediction or less precise Bayesian priors.

1.8. Summary and Thesis Purpose

We know that the cortex is not a passive receiver of sensory data and that perception is not a straight translation of the feedforward sensory input. Perception is the result of integration of intracortical contextual top-down feedback with feedforward sensory input. Cortical feedback modulates processing throughout the cortex, including at the earliest traditional sensory areas such as V1. Visual illusions are a valuable tool for probing cortical feedback, as they provide a clear case where feedforward input and the resulting percept differ as an effect of top-down modulation. However, we are still unaware to what extent illusory activity is represented in the cortex and early sensory cortex. If we can develop a full understanding of the neural underpinnings of illusions in a healthy population we can use them to investigate cortical processing in schizophrenia and other neuropsychological pathologies.

The described research has two associated aims. Firstly and most importantly, we aim to investigate how cortical feedback and feedforward mechanisms modulate perception in several visual illusions. We present two fMRI studies: the first study examines the role of crossmodal feedback to visual cortex during the rubber hand illusion (**Chapter 3**). In **Chapter 2** we investigate the same illusion behaviourally in healthy subjects who have scored highly on the Prodromal Questionnaire. The second examines whether the representation of a target in V1 is destroyed during motion-induced blindness perception across two fMRI datasets (**Chapter 4.2**). This is accompanied by a behavioural study which ascertained which target parameters (size, eccentricity) were possible when using oriented Gabors as motion-induced blindness targets (**Chapter 4.1**). We additionally present a behavioural study investigating a recently described illusion, flashed face distortion (Tangen, Murphy, & Thompson, 2011). We vary the timing of face presentations and modulate the race of the faces presented to determine whether this effect occurs due to face-specific or object-general predictive comparative encoding (**Chapter 5**).

We chose these illusions because they presented the opportunity to investigate novel properties of cortical feedback during illusory perception. The rubber hand illusion provides the opportunity to investigate an illusion that does not solely arise from visual input, but additionally from the influence of tactile and proprioceptive inputs. It is crucial to include influences from other senses to develop full picture of how feedback manipulates the visual system, particularly given previously reported effects of non-visual information in the visual cortex (Liang, Mouraux, Hu, & Iannetti, 2013; van Kemenade, Seymour, Wacker, et al., 2014; Vetter et al., 2014) and several illusions which rely on the co-occurrence of multisensory stimuli (Shams, Kamitani, & Shimojo, 2000). Additionally, sensory perception rarely occurs with only one sense in isolation and, although this thesis largely discusses the effects of feedback and theories of inference in vision, these theories are proposed to inform all senses and modulate how they interact. Thus it is important to begin considering the impact of sensory feedback on the primary cortices of other senses.

Our next illusion, Motion-Induced Blindness (MIB), shows a stunning modulation of perception in which a bright target completely disappears from conscious vision. Such a salient stimulus invokes a large response in early visual cortex. Nonetheless, internal processing blinds participants to seeing this target. This illusion presented us with the opportunity to study an illusion in which we could formulate a specific hypothesis for an effect on V1 multivariate activation without a change in stimulus. Lastly, flashed face distortion (FFD) allows us to examine a new illusion which has not yet been fully explored in terms of expectation and prediction. FFD provides a promising avenue for research due to the dramatic effects observed with typical stimuli in typical participants. Additionally, FFD is an ideal illusion with which to probe the timing specifications of feedback. The timing of different feedback effects and how these could possibly be integrated seamlessly is one particular concern for predictive coding theories of cortical function (see **chapter 6.6**).

Secondly, we aim to develop a theory of how these systems function in schizophrenic subjects and what neural outcomes would be expected in these illusory paradigms. With reliable illusory paradigms, we can form a link between feedback hypotheses and visual illusions, then between these visual illusions and the behavioural and neural outcomes in schizophrenic subjects. Our chosen illusions are largely well-documented in schizophrenic

populations. The rubber hand illusion has been extensively investigated in these subjects, as both a method to probe top-down effects and to probe self-perception in the disorder. This illusion is strengthened in schizophrenic subjects (Thakkar, Nichols, McIntosh, & Park, 2011). The MIB is also relatively well-established in Schizophrenic populations but, conversely, is either attenuated or strongly attenuated in schizophrenic subjects. See the discussion (**chapter 6.9.**) for theories on why the pattern of differences for each illusion may vary in these subject populations. Lastly, FFD has not been established in Schizophrenic population but it presents a very promising paradigm; as it allows us to probe both timing parameters in these clinical subjects, induces an illusory percept which seems hallucinatory, and may also be face-based. Schizophrenic participants have notable face processing deficits (Bortolon, Capdevielle, & Raffard, 2015; though these deficits may be caused by deficits in contextual integration); and do not experience illusions which depend on established priors regarding faces (for example the hollow mask illusion Dima et al., 2009). The causes and mechanisms of schizophrenia are poorly understood and interactive hierarchical models, such as the predictive coding hypothesis (see **Chapter 6.8**), could explain core symptoms of the disorder, help define its pathophysiology and create opportunities for novel therapy. Furthermore, feedback and feedforward mechanisms also underlie cortical processing in non-human mammals. Therefore animal models of feedback can be utilised to investigate cortical processing in schizophrenia.

2. CROSSMODAL BOUNDARIES OF THE RUBBER HAND ILLUSION IN SCHIZOTYPY

Fiona McGruer, Jennifer Murray, Peter J. Uhlhaas, and Lars Muckli.

University of Glasgow, Centre for Cognitive Neuroimaging, Institute of Neuroscience and Psychology, 58 Hillhead Street, G12 8QB, Glasgow, United Kingdom.

2.1. Abstract

In the Rubber Hand Illusion, subjects experience perceived ownership over a rubber limb following synchronous visuotactile stimulation to the subject's real hand and the rubber hand. Although the illusion is robust in a typical population, previous studies have shown that participants prone to psychosis experience more intense rubber hand ownership. We investigate whether the atypicalities involved in psychosis proneness are also involved in enhanced vulnerability to the rubber hand illusion, across varying visuotactile stimulation asynchronicity. We used the Prodromal Questionnaire (Loewy et al., 2011) to define two groups: subjects with a medium-high combined positive symptom and distress score (sub-clinical), and control subjects with a score of zero. We stimulated the real and rubber hands synchronously or asynchronously (200, 300, 400 or 600ms asynchronicity) and recorded subjective ratings of illusion strength. We found that as visuotactile asynchronicity increases, the strength of the illusory percept decreases (as shown by Shimada, Fukuda, & Hiraki, 2009). However, we did not find any effect of psychosis-proneness on rubber hand illusion perception.

2.2. Introduction

Predictive coding theories of cortical function suggest that the brain uses prior experience to inform perception (Bar, 2007; Clark, 2013; Friston, 2010; Muckli & Petro, 2013; see **Chapter 1.5**). The cortex is thought to infer the source of new sensory inputs in a manner akin to Bayesian mathematical theory, estimating the probability of a particular percept in light of prior knowledge about related sensory inputs and the likelihood of the percept (Friston, 2012; Knill & Pouget, 2004). These internal perceptual likelihoods are combined with sensory inputs to form conscious perception, thus creating a percept that is inferential not veridical (see **Chapter 1.4**). Bayesian learning and inference is proposed to underlie human body schema (Seth, 2013). A coherent body representation develops across a history of multisensory inputs consistent with the percept that the body belongs to oneself (Armel & Ramachandran, 2003; Körding & Wolpert, 2004). 'Body ownership' describes the understanding that one's body belongs uniquely to the perceiver and that one's bodily sensation is unique to oneself (Gallagher, 2000). Under typical conditions Bayesian learning

constantly reinforces correct body ownership e.g. you feel a touch to your limb, which is also seen, and heard. Thus evidence for the limb belonging to you is strengthened. Cortical body schema in this conceptualization is never static. Rather it is a result of several levels of integration of stimulus inputs from multiple senses and the source of these inputs, which allows us to delineate the difference between the self and other.

The rubber hand illusion (RHI) allows body ownership and schematic body representation to be manipulated under conditions of matching visual and tactile information originating from the rubber and real hands respectively (synchronous stimulation; Botvinick & Cohen, 1998; Ehrsson, Spence, & Passingham, 2004; Hohwy & Paton, 2010; Tsakiris & Haggard, 2005). In the RHI, this synchronous visuotactile stimulation produces the illusion that the rubber hand 'belongs' to the participant's body and is the source of their sensation (Botvinick & Cohen, 1998). Recent work has shown that the RHI can arise under a Bayesian mathematical model with both spatial and temporal inputs, and that under this model the illusion is stronger when synchronous stimulation is applied (Samad, Chung, & Shams, 2015). Proprioceptive rules must also be met for illusory ownership to occur- the rubber hand must be biologically plausible (within peripersonal space, anatomically congruent, and of realistic orientation; Costantini & Haggard, 2007; Guterstam, Gentile, & Ehrsson, 2013; Hohwy & Paton, 2010; Lloyd, 2007; Preston, 2013). Previous studies have typically used one asynchronous condition (~500ms asynchronicity), and generally report no RHI during such stimulation (Ehrsson, Holmes, & Passingham, 2005; Ehrsson et al., 2004; Tsakiris, Hesse, Boy, Haggard, & Fink, 2007).

Whilst the rubber hand illusion may seem to be an exceptional manipulation of body schema, in truth our internal body representation is so malleable as to allow subjects to perceive a whole-body virtual reality mannequin as their own body (Blanke & Metzinger, 2009; Ehrsson, 2007; Lenggenhager, Tadi, Metzinger, & Blanke, 2007). As long as visuotactile sensory input is consistent (i.e. coherent seen touch to the VR mannequin, felt touch to the subject's body, and proprioceptive similarity in posture), subject's feel as though the VR body is the source of their sensation. Subjects also experience proprioceptive drift towards the virtual reality mannequin - a shift in the perceived real body position towards the integrated limb, or mannequin.

Bodily ownership is further disrupted in some clinical conditions. Self-disturbances are a core symptom of Schizophrenia (Sass & Parnas, 2003; Voegeley, 2003), including distortions between the self and the external world (David et al., 2006). Such distortions in bodily ownership may correlate with psychosis symptom strength or coincide with psychosis onset (Nelson, Yung, Bechdolf, & McGorry, 2008). Body ownership has been studied empirically in schizophrenic and schizotypal populations using the RHI (Germine, Benson, Cohen, & Hooker, 2013; Thakkar et al., 2011). Schizophrenic subjects display significant disturbances in self-perception, which may be either reduced or increased, producing an enhanced distinction between the self and others (Thermenos et al., 2013). In schizophrenic subjects, the RHI is stronger, appears more rapidly following stimulation onset, and induces greater proprioceptive drift towards the fake hand (Peled, Ritsner, Hirschmann, Geva, & Modai, 2000; Thakkar et al., 2011). It is hypothesised that schizophrenic subjects either express a reduced top-down exertion of high level effects, or a stronger bottom-up influence of sensory input (Adams et al., 2013; Corlett et al., 2010). In the case of the RHI, either the strength of top-down body schema is reduced or the weighing of bottom-up visuotactile stimulation is increased. Such dysfunction may be a key mechanism in enhanced rubber hand illusion experience.

Schizophrenic symptoms can be expressed in the typical population to varying degrees, on a continuum of mental health known as schizotypy. Schizotypal subjects present symptoms associated with the disease whilst remaining sub-clinical, ranging from normal and imaginative states to psychosis (Bentall, Claridge, & Slade, 1989). Schizotypal traits interact with RHI susceptibility- Germine et al. (2013) found that positive schizotypal symptom presence in healthy subjects correlated with stronger illusion perception. Psychosis develops following a prodromal period, which may be a useful biomarker and a key target for intervention to control disease development (Addington et al., 2007). Bodily disturbance is evident in this prodromal stage and may form part of an existing vulnerability to psychosis (Lenzenweger, 2006, 2011; Nelson, Thompson, & Yung, 2012; Nelson et al., 2008; Sass & Parnas, 2003). Susceptibility to illusions such as the RHI therefore may be indicative of psychosis-proneness.

Shimada et al. (2009) examined illusion strength under varying visuotactile asynchronicities in a healthy population, finding that greater asynchronicities weakened the illusion. They demonstrated that the illusion percept is not significantly diminished until visuotactile asynchronicity is above 300ms, although some participants did experience the illusion at asynchronicities of 400 and 600ms. Whether schizophrenic patients would show a similar window of temporal integration is not clear. Schizophrenic participants demonstrate a wider temporal integration window in multiple multisensory studies and may therefore experience the RHI at greater asynchronicities (Parsons et al., 2013).

The current study examines the visuotactile boundaries of the RHI in a psychosis-prone group and in a control group. We recruited subjects who had responded to the Prodromal Questionnaire (Loewy et al., 2011), selecting one subset (control) from zero scorers and the experimental group from responders who scored highly, but were sub-clinical, in a combined measure of positive symptomology and symptom-based distress (Med-High Prodromal Group, MHPG). We presented RHI stimulation at 0, 200, 300, 400 and 600ms asynchronicity. Based on previous findings it was hypothesized firstly that the MHP group would experience the RHI more strongly during synchronous stimulation than controls (Germine et al., 2013), and that illusion response would decrease with increasing visuotactile asynchronicity in both groups (Shimada et al., 2009). We further hypothesised that the average illusion onset time would be shorter in the MHP group; that the MHP group would respond more strongly to ‘distracter’ statements about atypical experience; and that the MHP group would continue experiencing the illusion past the 300ms ‘cut-off’ that occurs in control subjects (Shimada et al., 2009).

2.3. Method

2.3.1. *Participants*

20 healthy subjects were recruited from a group of undergraduates who had completed the prodromal questionnaire (PQ; Loewy et al., 2011). 10 subjects were recruited from those who

2. CROSSMODAL BOUNDARIES OF THE RUBBER HAND ILLUSION IN SCHIZOTYPY

scored 0 on both positive psychotic symptoms and symptom-based distress (controls; 5 f); 10 subjects were recruited from subjects with medium to high scores on symptoms and associated distress (MHP group; 7 f). It is important to note that these scores were sub-clinical level. Subject groups were not matched; however both groups were recruited from a population of university undergraduates in their 20s. In each group, 2 subjects were ambidextrous; all other subjects were right-handed (as measured by the Edinburgh Handedness Questionnaire, Oldfield, 1971). All subjects had normal or corrected-to-normal vision. The experiment was approved by the ethics committee of the College of Science and Engineering, University of Glasgow.

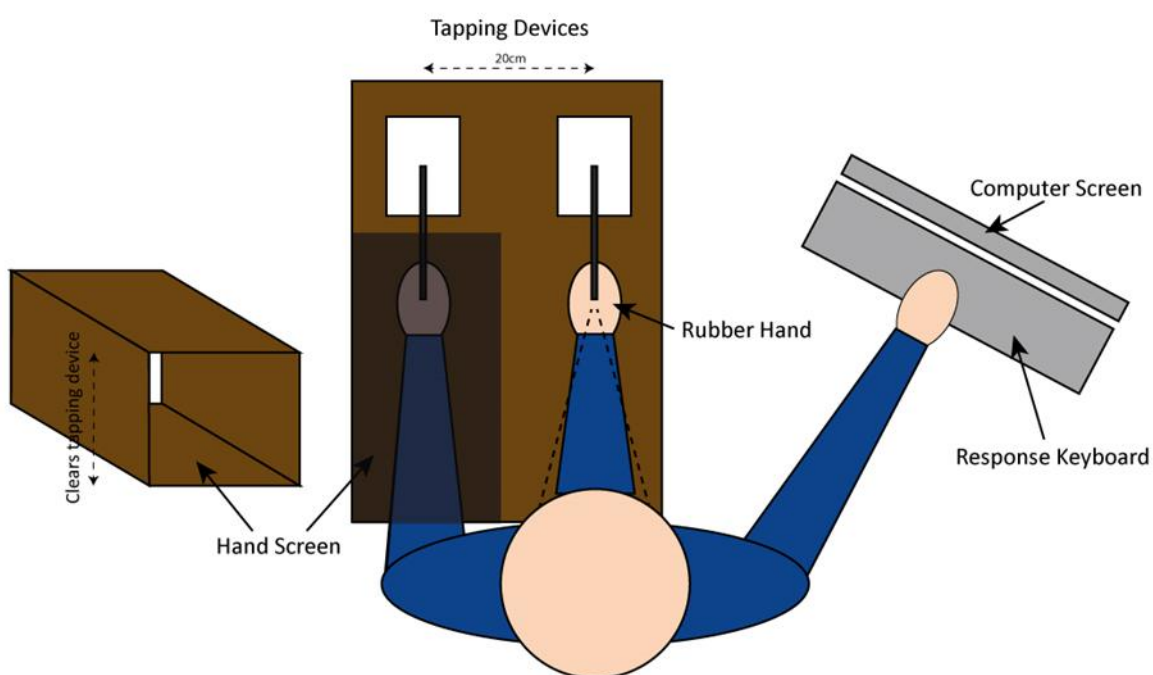


Figure 2.1. Stimulus set up. Subjects viewed a stimulated rubber hand whilst a second stimulation device was applied to the hidden real hand. There was 20 cm distance between both stimulation devices and the real and rubber hand. Subjects fixated on the rubber hand during stimulation, and then responded to Likert statements presented on the monitor using their right hand.

2.3.2. Apparatus:

An air-powered stimulation device was designed in the department of Psychology (shown in Figure. 2.1.). Hidden by a box screen, one stimulation rod was applied to the subject's real hand. In full view, the other device was applied to the fixated rubber hand. These devices were fixed 20cm apart, with the same distance between subject's real hand and the rubber hand. We applied stimulation to the same location on the rubber and real hand at a rate of 1Hz. Material similar to the subject's clothes covered the space between the rubber hand and subject's body. We presented instructions to the subject on a monitor. Subjects freely reported any illusion onset and rated their experience following each stimulation period using the keyboard on a 1-7 likert scale for 7 statements (Table.1.). The seven Likert statements probe the perception of the rubber hand. Statements 1-3 determine the extent to which the hand is integrated as part of the body where sensation originates. Statement 4 is a measure of the perceptual aspect of proprioceptive drift. Statements 5-7 determine unusual percepts subjects may have during the RHI. The choices were presented as a visual-analog scale on the screen. Subjects wore earplugs to avoid the tapping device providing an auditory cue of synchronicity.

Likert Statements:

1. It seemed as if I were feeling the touch of the rod in the location where I saw the rubber hand being touched.
2. It seemed as though the touch I felt was caused by the rod touching the rubber hand.
3. It felt as if the rubber hand were my hand.
4. It felt as if my real hand was drifting towards the rubber hand.
5. It seemed as if I might have more than one left hand or arm.
6. It felt as if my real hand were turning rubbery.
7. The rubber hand began to resemble my own hand (skin tone, features, shape).

Table 2.1. Likert statements. Subjects were prompted to respond to Likert statements following each stimulation block. Statements are taken from Botvinick and Cohen (1998). The statements 1-3 probe

illusory rubber hand ownership, the 4th statement probes proprioceptive drift, statements 5-7 probe unusual percepts.

2.3.3. *Design and Procedure*

Subjects provided written informed consent and completed the Edinburgh Handedness inventory (Oldfield, 1971). Subjects were provided with earplugs to remove auditory cues of stimulation asynchronicity. They sat at a table with their left hand placed in the box screen, palm facing down, with the tapping device hitting below the knuckle of the left middle finger. A life-sized rubber hand was fixed between the subject's left and right hand in clear view, with a second tapping device hitting the same location. Subjects were instructed not to move their left hand during the experiment and to fixate on the rubber hand. These instructions were repeated on screen throughout the experiment. Subjects first experienced a 5-minute block of synchronous stimulation. We then presented randomised blocks of varying visuotactile synchronicity (60s per block: 0ms, 200ms, 300ms, 400ms and 600ms asynchronicity). Each block synchronicity was repeated twice. During each stimulation period subjects freely reported a 'perceptual change' (illusion perception) using a key press. The details of the illusion were not provided so as not to mislead subjects. Following stimulation, subjects responded to statements about their illusory experience on a Likert scale (1 = very negative, not at all descriptive of perception, 7 = very positive, very descriptive of perception; statements taken from Botvinick & Cohen, 1998). Between each block there was a rest period determined by the subject, who pressed space to continue.

2.3.4. *Analysis*

Likert Statements

Of the Likert statements; items 1- 3 represent probes for illusion perception, item 4 probes proprioceptive drift, and items 5-7 judge alternative unusual phenomenon. Descriptive

statistics were calculated for the response to each Likert statement following each visuotactile asynchronicity condition, averaged across the two presentations of each asynchronicity. To ascertain if subject group had an impact on the statement responses following the 5-minute synchronous block we used Wilcoxon rank-sum tests for each statement response. We then used a three factor mixed ANOVA to test the main between-subject effects of subject group; within-subject effects of Likert statement (1-7), and visuotactile asynchronicity (0, 200, 300, 400, and 600ms); and their interactions on Likert statement responses. We used post-hoc Bonferroni-corrected t-tests to compare means between different levels of the main and interaction effects.

Online Responses

We produced descriptive statistics describing the response profile for the first online button-press response for each visuotactile asynchronicity and subject group.

2.4. Results

5-Minute Synchronous Stimulation Period

We examined the subjective Likert responses provided for statements 1-7 following the long synchronous stimulation period (Figure 2.2.)

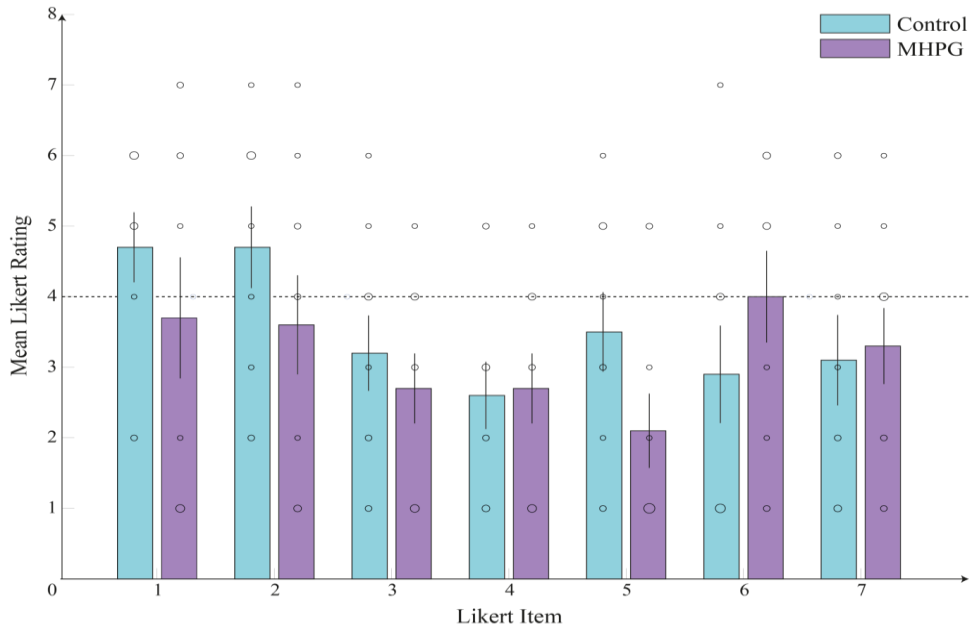


Figure 2.2. Long stimulation period. Mean Likert scale response to each statement item per group (control subjects in blue, MHPG subjects in purple). Points represent individual subject means, whilst point size denotes number of responses at that rating. Error bars represent standard error of the mean.

The control group provided descriptively higher responses to Likert statements 1-3 (#1 $m=4.7$ v 3.7 ; #2 $m=4.7$ v 3.6 ; #3 $m=3.2$ v 2.7). However, there was no significant difference between the two groups on statement #1 ($W(18) = 113.5$, $z=0.619$, $p=0.536$), #2 ($W(18) = 121.5$, $z=1.227$, $p=0.220$), or #3 ($W(18) = 101.50$, $z=-0.232$, $p=0.817$). Additionally, we found no significant difference between the control and MHP group for responses to statement #4 ($W(18)=103$, $z=-0.117$, $p= 0.907$), #5 ($W(18)=127.5$, $z=1.736$, $p=0.083$), #6 ($W(18)=87.5$, $z=-1.322$, $p=0.186$), or #7 ($W(18)=101.5$, $z=-0.232$, $p=0.817$).

Preliminary descriptive statistics, restricted to subjects who give a press response for illusion experience in the 5-minute stimulation block, suggest that there may be an effect of group in this subset, but we did not collect a large enough sample to statistically analyse this.

Parametric Variation of Visuotactile Synchrony (0, 200, 300, 400, 600ms)

2. CROSSMODAL BOUNDARIES OF THE RUBBER HAND ILLUSION IN SCHIZOTYPY

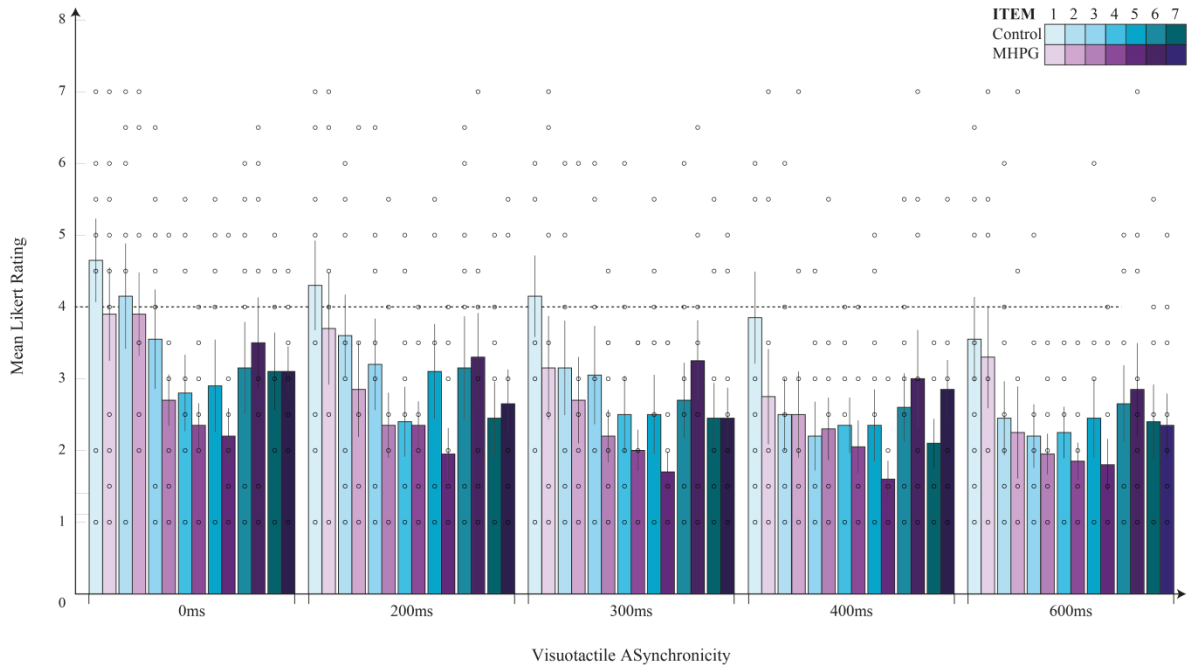


Figure 2.3. Short stimulation periods. Mean Likert scale response to each statement item per group (control subjects in blue, MHPG subjects in purple), and per visuotactile asynchronicity (colours indicated in legend). Points represent individual subject means. Error bars represent standard error of the mean.

Using a three-factor mixed ANOVA, we assessed the contributions of visuotactile synchronicity, Likert statement, and subject group on the Likert score provided (Figure 2.3.). We used Mauchly's test of sphericity to ensure equal variance for the differences between levels of our factors. Our data met the assumption of sphericity for the factor of visuotactile stimulation (Mauchly $df=9$, $p=0.38$) but did not meet this assumption for Likert statement ($df=20$, $p<0.0001$). Additionally, this test can fail to detect departures from sphericity in small samples such as ours. Therefore, we report Huynh-Feldt-corrected values throughout.

We found a main effect of visuotactile synchronicity ($F(3.6)=8.88$, $p<0.0001$, partial eta squared 0.33); in which Likert responses to the statements decrease as visuotactile asynchronicity increases. Like Shimada et al. (2009) we found significant differences between Likert statement responses at 0ms and 300ms asynchronicity (Mean difference=0.571, $p<0.038$) and 0ms and asynchronicities greater than 300ms. For the full list

of Bonferroni-corrected differences between visuotactile asynchronicities, see Table.A.2.1. in **Appendix 2**. We did not find a significant interaction between group and visuotactile synchronicity ($F(3.6)=0.352$, $p=0.82$, partial eta squared 0.019). We found a significant main effect of Likert statement ($F(3.6)=6.19$, $p<0.0001$, partial eta squared 0.26) but again did not find a significant interaction between group and Likert statement ($F(3.6)=1.1$, $p=0.36$, partial eta squared 0.058). The only significant difference observed was between Likert responses to statements 1 and 5 (Mean difference=1.475, $p<0.049$). For Bonferroni-corrected significant differences between Likert statements, see Table.A.2.2. in **Appendix 2**. We did find a significant interaction between visuotactile synchronicity and Likert statement ($F(17.2)=2.23$, $p=0.04$, partial eta squared 0.11). For Bonferroni-corrected significant differences between responses to visuotactile asynchronicity by Likert statements, see Table.A.2.3. in **Appendix 2**. We did not find an interaction between all three factors (group, visuotactile synchronicity, and Likert statement ($F(17.2)=1.23$; $p=0.24$, partial eta squared 0.064). It is important to note that in all cases our analyses are underpowered as our subject group is small.

Onset Latency of Rubber Hand Illusion between Groups

Figure 2.4.a displays the mean time into the stimulation period subjects responded with a button press to indicate ‘perceptual change’. During the long synchronous stimulation block, subjects in the MH group responded more slowly than subjects in the control group. During other stimulation blocks there is variation in the faster response group. Importantly, many subjects did not indicate a perceptual change and therefore these descriptive statistics are not representative of the group. Figure 2.4.b indicates the number of responses made by each group in each visuotactile asynchronicity. A greater number of MHPG subjects responded during the long synchronous stimulation block and in the 300ms and 400ms visuotactile stimulation blocks.

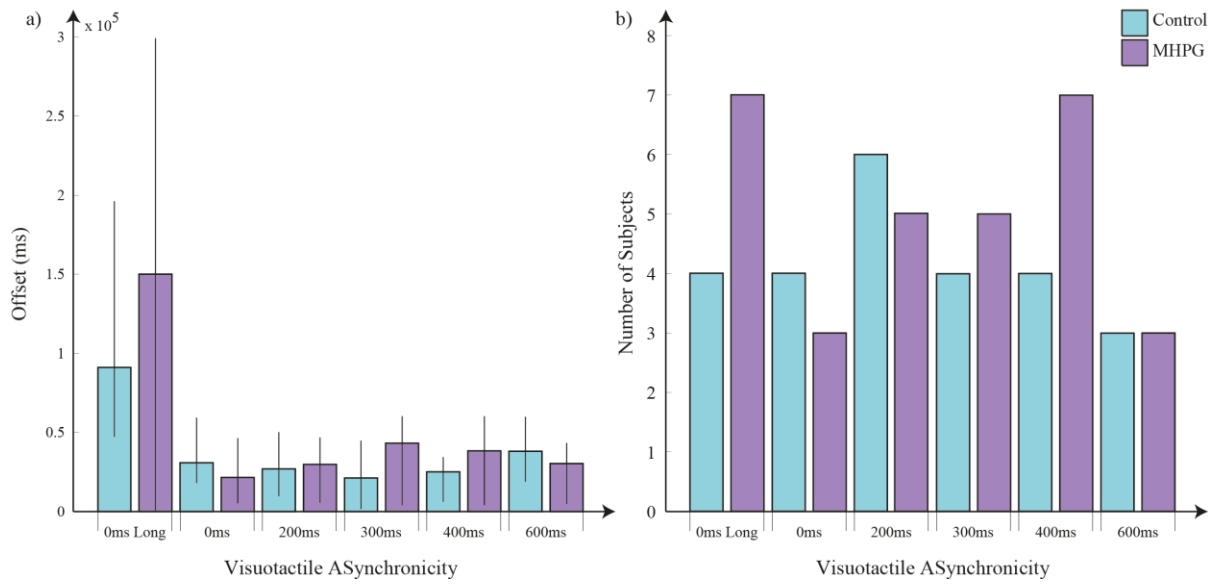


Figure 2.4. Button press responses to ‘perceptual change’. a) Mean onset latency of button presses indicating ‘perceptual change’ per group and per visuotactile asynchronicity. Bars indicate the range of responses (min to max value recorded). b) Number of subjects that reported ‘perceptual change’ per group and per visuotactile asynchronicity.

2.5. Discussion

Multimodal hierarchical interactions between three senses contribute to a Bayesian inference about the source of sensory inputs. This inference gives rise to illusory ownership of a rubber limb during the RHI (Apps & Tsakiris, 2014; Hohwy, 2007a, 2010; Seth, 2013). We suggest that the resulting perceptual illusion solves the mismatch between sensory input of visual localization outwith the body and existing internal high level body schema dictating that the hand is external; and tactile and proprioceptive inputs from the real hand to the sensory cortex signaling that the viewed hand is one’s own, (Hohwy & Paton, 2010). The internal body schema model reduces its likelihood so significantly in the face of visuotactile conflicts that prior body representation is ‘explained away’ by the illusion to include the rubber hand (Hohwy & Paton, 2010).

As visuotactile asynchronicity increases, the strength of the conflict between visuotactile stimulation and existing body schema decreases. Correspondingly, we found an interaction between visuotactile asynchronicity and Likert statement, and a significant main effect of

visuotactile asynchronicity on RHI experience in both control subjects and MHPQ subjects (as seen by Shimada et al., 2009 in typical subjects). In short stimulation blocks, we found that the response to illusion-probe statements (#1, 2, 3, 4) and the probe statements for atypical experience (#5, 6, 7) interacted with increasing asynchronicity in all subjects. The response to Likert statements also changed across Likert statements, but this effect is not linear.

Descriptively, we noted that the number of subjects who responded for illusory experience during the stimulation decreased as asynchronicity increased. Additionally, our paired comparisons showed that 300ms could be considered a ‘cut off’ after which perceptual responses significantly differ from synchronous stimulation (0ms asynchronicity). This suggests that the brain requires a temporal coherence of less than 300ms in order to bind visual and tactile inputs for self-processing. Shimada et al. (2009) found that at a temporal discrepancy of 600ms the RHI did not occur, and set 300ms as a ‘cut-off’, proposing that stimuli delayed by more than 300ms are not recognized to be self-generated. This is coherent with other work showing that if the tactile stimulation is delayed by over 300ms, subjects can tickle themselves (Blakemore, Frith, & Wolpert, 1999; Blakemore, Wolpert, & Frith, 2000). Beyond latencies of 200-300ms healthy subjects detect discrepancies between two multisensory stimuli presented together (Franck et al., 2001; Shimada, Hiraki, & Oda, 2005). Furthermore, Shimada, Suzuki, Yoda, and Hayashi (2014) repeated their RHI investigation with an accompanying visuotactile asynchrony detection experiment (stimuli also applied to the hand). Visuotactile asynchrony detection and the self-reported RHI experience were found to be related.

We found no significant differences in rubber hand illusion experience between groups for the long synchronous stimulation period and no significant difference between groups in illusory experience for any visuotactile synchronicity. Across visuotactile asynchronicities, we did not find a significant effect of subject group on RHI experience. These results were unexpected on two levels. Firstly, previous studies demonstrate higher illusion experience in schizophrenic groups (Peled et al., 2000; Thakkar et al., 2011) and schizotypal groups (Germine et al., 2013). It should be noted that Germine et al. (2013), found a significant relationship between psychosis proneness and RHI experience only during synchronous

stimulation. When asynchronous stimulation was introduced, they found the RHI diminished almost completely in all groups. Their schizotypal group did not respond on a heightened scale to statements regarding atypical experience, only to RHI probe statements. Peled et al. (2000) and Thakkar et al. (2011) also found that illusion strength correlated with positive symptomology only following synchronous stimulation. In support of our results, Naohiko and Shimada (2014) conducted a replication of the work of Shimada et al. (2009) with typical and schizotypal subjects and found no difference between high and low schizotypy groups across visuotactile asynchronicities.

As the RHI likely arises from an interaction of bottom-up (sensory input) and top-down (body schema and inference) computation, disturbances in merging these processing streams may lead to the exaggerated RHI witnessed in schizophrenia. Such dysfunction affects processing of the sensory world, including the interaction of the self and the external world (Mishara & Sterzer, 2015). Mayer-Gross (1932) suggested that reduced top-down perceptual expectation about the body contributes to ‘self-disturbances’ in the disorder (see also Mishara & Sterzer, 2015). More recently Asai, Mao, Sugimori, and Tanno (2011) suggested that during the RHI, schizophrenic subjects may replace their own ‘missing’ top-down bodily schema with external ownership of the rubber hand, facilitating more robust illusion experience. Peled et al. (2000) suggest that reduced top-down connectivity could drive this loosened body schema, allowing for the false binding of bottom-up stimuli (in this case visual and tactile) to dominate perception. Furthermore, visual information may be under-weighted in schizophrenia in influencing processing of other modalities (auditory and proprioceptive; De Gelder & Bertelson, 2003; Williams, Light, Braff, & Ramachandran, 2010).

Predictive coding models propose that the disturbances of the self that are observed in schizophrenia arise from imprecise predictions about the sensory consequences of actions (Adams et al., 2013; Blakemore & Frith, 2000; Frith, 1987; Synofzik, Thier, Leube, Schlotterbeck, & Lindner, 2010; Voss et al., 2010). In typical subjects there is successful suppression of internally generated sensation by top-down predictions (Seth, 2013). Other authors characterise this as a disturbance in corollary discharge mechanisms which allow typical subjects to recognize self-generated sensation (for example by action, Mathalon & Ford, 2008). Anomalous self-experience and RHI-experience in schizophrenia are likely

related to NMDA Glutamate dysfunction. Ketamine administration to healthy subjects increases RHI strength and proprioceptive drift during synchronous and asynchronous stimulation (Morgan et al., 2011).

Enhanced RH illusions can be linked to the formation of positive symptomology. Parnas and Sass (2001) suggested that schizophrenic delusions develop on the background of pre-existing anomalies of self-experience. Corlett, Honey, Krystal, and Fletcher (2011) suggest that in schizophrenia false interpretations of the sensory world create delusions and hallucinations on the basis of correct feedforward inputs (see also Fletcher & Frith, 2009). The RHI can be considered an example of this false belief in even healthy subjects. Others hypothesise that hallucinations and delusions are caused by self-misattribution in actions or body recognition (Arzy, Mohr, Michel, & Blanke, 2007; Asai et al., 2011; Platek & Gallup, 2002). Furthermore, the over-inclusive sense of ownership and agency observed in schizophrenia patients in RHI paradigms is similar to facets of common delusions (Frith et al., 2000). These theories both implicate aberrant prediction error as the cause of saliency or a surprise in response to normal sensory inputs (Hemsley, 2005). Delusions result when a maladaptive cognitive explanatory model is formed based on these prediction errors and feedforward stimulation, which is then applied to future sensory experiences (Adams et al., 2013; Corlett et al., 2011; Fletcher & Frith, 2009; Heinz, 2002; Kapur, 2003).

Prodromal phases of psychosis development are a key target for schizophrenia research in hope of identifying predictive aspects of high-risk subjects, developing early interventions, and preventing or slowing disease progression. Møller and Husby (2000) suggest that self-experiencing undergoes a core change during the prodromal phase. Retrospective studies of the prodrome support this theory (see Parnas, Jansson, Sass, & Handest, 1998; Parnas et al., 2005). In studies of first admission non-psychosis patients, self-disturbance is a strong predictor of future schizophrenia diagnosis (Parnas, 2003; Parnas & Handest, 2003; Parnas et al., 2005). Nelson et al. (2012) found that scores on the Examination of Anomalous Self-Experience scale predicted time to transition to schizophrenia in UHR subjects (EASE, (Parnas et al., 2005). Additionally, the same anomalies in prefrontal, lateral, temporal and parietal structures implicated in self-disturbances are hypothesized to be an early structural characteristic for premorbid risk of schizophrenia (Thermenos et al., 2013).

Schizophrenic groups typically present with a fundamental time perception deficit relevant to the RHI. This deficit is unaffected by stimuli duration (Carroll, Boggs, O'Donnell, Shekhar, & Hetrick, 2008; Elvevåg et al., 2003), and occurs independent of stimuli sensory modality (Davalos, Kisley, & Ross, 2003). Foucher, Lacambre, Pham, Giersch, and Elliott (2007) showed that schizophrenic patients perceive unimodal and bimodal visual and auditory stimuli as simultaneous over longer periods of time compared to control subjects. A similar effect was observed in studies of visual-only flicker fusion (Parsons et al., 2013). Dysfunction in perceptual binding in patients leads to erroneous causality judgements- for example Tschacher and Kupper (2006) demonstrated that increased perceived causality between stimuli was correlated with positive symptomology. We would therefore presume that schizotypal or prodromal subjects demonstrate a wider window of RHI integration.

However, other results suggest that prodromal subjects could show reduced binding as opposed to strengthened binding. Tschacher and Bergomi (2011) found that schizophrenic spectrum patients show attenuated type II binding (reduction in binding temporally delayed stimuli across different senses), proposing that this reduced neurocognitive binding is related to abnormalities in long-range neural synchronization (Meyer-Lindenberg, 2010; Uhlhaas et al., 2006). As psychosis is analogous to reduced multisensory integration rather than enhanced (Garcia, Sacks, & de Mamani, 2012), weaker somatosensory representation is a more characteristic theory for enhanced susceptibility to the RHI in people with schizophrenia (Peled, Pressman, Geva, & Modai, 2003). Schizophrenic patients also show abnormalities in oscillatory activity including reduced amplitude of evoked phase-locked oscillations. This deficit may prevent accurate coordination of cortical areas in order to integrate incoming sensory information (Javitt, 2009; Spencer et al., 2004; Uhlhaas et al., 2006).

Future Steps/Criticisms

Our two groups were recruited from subjects who had previously completed a mental health questionnaire which included the Prodromal Questionnaire. The score used to distinguish between the two groups was positive psychosis symptoms with related distress (subjects who

felt their symptoms also negatively impacted on their lives). Our control group was sampled from respondents who scored 0 on the combination of positive symptoms and distress (experiencing no positive symptoms and no distress). The MHPG was sampled from respondents which were medium-high scorers on these items, resulting in a group which was not at the top of the scale, and did not qualify for clinical evaluation. Such subjects are still members of the 'typical' response spectrum. Without a significant gap in positive symptoms and distress, significant differences were less likely to be observed between the two groups in our experiment. Future investigation should include subjects across an entire response profile to the Prodromal Questionnaire (from 0 scoring control subjects to subjects who respond at a clinical level). We could then examine whether there is an effect as psychosis tendency increases linearly, and determine if there are progressive differences in self-disturbance as the PQ score increases.

Furthermore, not all subjects included in the study perceived the illusion. There were a higher number of subjects who perceived the illusion in the control group than in the MHPQ group. Therefore mean statement responses are affected by non-responders. In a larger sample, analysis would be conducted only on subjects who experienced the illusion in the initial synchronous stimulation period. Analysis of the button press was further complicated by the deliberately vague instruction to report 'perceptual change' and several subjects who rated their illusion experience as strong on the Likert statements did not ever respond with a button press.

2.6. Conclusion

RHI experience demonstrates how malleable and impermanent body schema is, even in healthy subjects. Furthermore, the RHI shows that perceived reality is highly affected by sensory probability and integration (Hohwy & Paton, 2010). From the results of this study, we cannot support our hypothesis that as the proneness to psychosis increases the strength of the RHI also increases. There is preliminary evidence to suggest that with a larger subject pool and subjects from a higher psychosis proneness population, the results would have concurred with previous findings. However, we can agree with previous findings regarding

the effects of asynchronicity on the illusion - as the asynchronicity of visuotactile stimulation increases, the strength of the illusion perceived (as determined by the Likert scale) decreases (Shimada et al., 2009). From our results, we have additionally found that a temporal contiguity of less than 300ms is needed to elicit the RHI (Shimada et al., 2009).

3. VISUOTACTILE ILLUSION PERCEPTION IN EARLY VISUAL CORTEX

Fiona McGruer¹, Lucy S Petro¹, Luca Vizioli^{1,2}, Junpeng Lao³ & Lars Muckli¹

¹University of Glasgow, Centre for Cognitive Neuroimaging, Institute of Neuroscience and Psychology, 58 Hillhead Street, G12 8QB, Glasgow, United Kingdom.

²University of Minnesota, Center for Magnetic Resonance Research, 2021 6th Street SE Minneapolis, MN 55414, USA.

³Université de Fribourg, Department of Psychology, Rue P.A. de Faucigny 2, 1700 Fribourg, Switzerland.

We thank the European Research Council (ERC StG 2012_311751-'Brain reading of contextual feedback and predictions') for their generous support.

3.1. Abstract

During the rubber hand illusion, synchronous tactile stimulation to the subject's hidden real hand and to a visible rubber hand causes healthy subjects to perceive ownership of a fake limb. The illusion occurs as a result of coherent feedforward tactile and proprioceptive inputs to the sensory cortices, which then alter high level models of body schema. Whilst the ventral premotor cortex is traditionally considered to be the seat of the RHI, other diverse regions including visual motion area hMT+/V5 may be involved. We investigated how crossmodal and illusory feedback affects the response in motion sensitive area V5 and in early visual cortex (V1). In fMRI, participants viewed the rubber hand through a mirror whilst their hidden real hand was stimulated either synchronously or asynchronously. We used instant reports of subjects' experience to dissociate stimulation type and illusory experience. We found that stimulation and illusion experience interact to produce activation in V5 and V1, whilst BOLD activity in vPMC and the retinotopically specific rubber hand area of V1 increases when subjects experience the illusion. Multivariate pattern analyses demonstrated a coherent pattern during illusion perception in V1 and in the retinotopically specific subsection corresponding to the rubber hand (VHand). We therefore find effects of both multisensory stimulation and illusion perception in V5 and early visual cortex. These response properties do not result from retinal stimulation and thus occur through intracortical feedback.

3.2. Introduction

Predictive multimodal hierarchical interactions are proposed to underlie coherent body representation in sensory illusions such as the rubber hand illusion (RHI; Apps & Tsakiris, 2014; Hohwy, 2007a, 2010; Seth, Suzuki, & Critchley, 2011). The RHI is a visuotactile illusion in which subjects perceive ownership over a rubber hand. This occurs after synchronous tactile stimulation to the subject's own hand and visual stimulation to the rubber hand (Botvinick & Cohen, 1998; Ehrsson et al., 2004; Tsakiris & Haggard, 2005). Hohwy and Paton (2010) suggest the illusion is a perceptual solution to prediction error occurring between the sensory cortex coding real tactile stimulation and the visual system signalling

that the stimulation is to an external object. Prediction error occurs upon inconsistencies between modelled and incoming stimuli, and is transmitted up the cortical hierarchy to correct existing predictive models (Friston, 2010; Kok et al., 2012; Lee & Mumford, 2003; Rao & Ballard, 1999; Spratling, 2010). In the RHI the existing internal modelled body schema is inconsistent with the incoming tactile and proprioceptive signals. Illusory ownership arises when the sensory cortex succeeds in explaining away the discrepancy.

In light of this account, illusions like the RHI are a useful way to study how predictive feedback affects the visual response. Early visual cortex receives both feedforward input from the retina, and feedback input originating in higher cortical areas (Muckli & Petro, 2013). Feedback connections can modulate V1 in a spatio-temporal (Alink et al., 2010) and context-dependent manner (Smith & Muckli, 2010) and predictions can be both intra- and supra-modal (Erlhagen, 2003). Consequently, feedback allows V1 to represent non-visual information, including the categorical content of auditory stimulation in the absence of visual input (Vetter et al., 2014). In the apparent motion illusion, the perceived motion trace is activated in V1, by feedback from V5, despite no feedforward stimulation ((Muckli et al., 2005; Muckli et al., 2002; Sterzer et al., 2006; Vetter et al., 2014; Wibrall et al., 2009). Facilitated detection of targets on the illusory motion trace is destroyed when V5 is inhibited (Schwiedrzik et al., 2007; Vetter et al., 2014). V5 is proposed to play a primary role in the neural processing of the RHI (Bekrater-Bodmann et al., 2014; Schwiedrzik et al., 2007; Vetter et al., 2014). However, whether V5 responds only to visual motion during RHI induction (Kamitani & Tong, 2005; Seymour, Clifford, Logothetis, & Bartels, 2009) or to the tactile motion pattern of stimulation (Kamitani & Tong, 2005; Seymour et al., 2009; van Kemenade, Seymour, Christophel, Rothkirch, & Sterzer, 2014; van Kemenade, Seymour, Wacker, et al., 2014; Wacker, Spitzer, Lützkendorf, Bernarding, & Blankenburg, 2011) remains unclear.

We use the rubber hand illusion to test whether illusory perception and multisensory visuotactile stimulation affect cortical response in V5 and early visual cortex, in the absence of differential feedforward visual input. We employ a RHI setup where participants provide instant feedback of their perception, allowing us to dissociate illusory state and visuotactile stimulation. We investigate the univariate activity changes in visual cortex during different

tactile stimulation types and during the illusion; and multivariate activity patterns corresponding to tactile stimulation and the illusion. This is particularly crucial as most previous studies which have found non-visual information in early and higher visual cortex have found this is represented in the pattern of activation, not in overall activation (Albers et al., 2013; Harrison & Tong, 2009; Haynes & Rees, 2005b; Muckli, 2010; van Kemenade, Seymour, Wacker, et al., 2014; Vetter et al., 2014). Furthermore, we examine the multivariate pattern in regions of visual cortex across time; reasoning that the illusion develops across time, and that some regions may be involved in inciting the illusion but not in sustaining it. We also examine whether there is evidence for predictive error in the visual system during the RHI.

3.3. Method

3.3.1. *Participants*

29 healthy subjects (mean age 24, range 18-40; 19 female; normal or corrected-to-normal vision) were recruited through the University of Glasgow Psychology department subject pool. Subjects provided written informed consent, underwent MRI safety screening, and were paid for participation. The University of Glasgow ethics board approved the procedure (FIMS00747). Data from one subject was discarded due to technical issues.

3.3.2. *Apparatus*

We attached a custom-made tapping device driven by an air compressor to the scanner bed. This device tapped the subjects' left hand and a rubber left hand using plastic rods. Inside the MRI bore, the tapping device was calibrated for each subject to touch their hand and the rubber hand at the same location. Subjects' hands were hidden from their view under a screen. Subjects fixated on a board near the foot of the scanner bed (Figure 3.1.). The rubber hand was positioned at a biologically plausible angle and extension, and made visible in subjects' left visual field via a mirror mounted to the head coil. The rubber hand was Caucasian and wore a sleeve matching that worn by participants. Subjects held a response keypad in the non-stimulated, right hand.

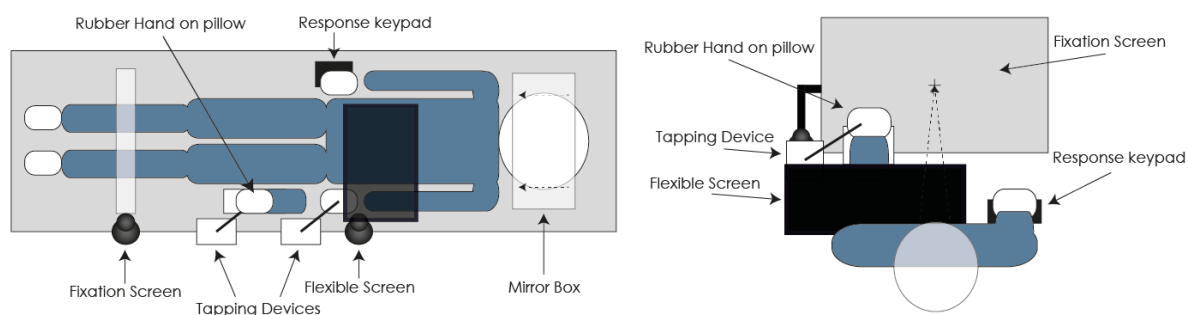


Figure 3.1. Rubber hand apparatus in the MRI scanner. a. The subject is prone, with an overhead mirror directing gaze towards the rubber hand and fixation screen. A flexible screen conceals the real hand and the first tapping device. The second device and rubber hand are visible. The fixation screen sits across the subject's lower body. The tapping devices are attached to the scanner table to optimally touch the real and rubber hand. The subject's right hand holds a response keypad. 1b. Elevation (subject) view: The subject views the fixation cross on a screen. The rubber hand and the rubber hand tapping device were visible in the lower left visual field.

3.3.3. Procedure

The experiment consisted of four runs of rubber hand stimulation. Each run lasted for 12 minutes and consisted of 6 randomly ordered blocks where tapping stimulation was either synchronous or asynchronous (3 of each). During synchronous tapping, the real hand and rubber hand were tapped at the same time. Each tap lasted 300ms with 700ms between taps. During asynchronous tapping, stimulation to the real and rubber hand was offset by 400ms. A block entailed 30s fixation, 60s stimulation (synchronous or asynchronous), rubber hand removal, and 30s of synchronous 'test tapping' with no rubber hand present. This test tapping condition functioned to provide a condition where visual movement of tapping devices was ongoing but the rubber hand was not present. Author FM replaced the rubber hand in time for the next fixation onset. Subjects were instructed to fixate and used the response keypad to freely report the onset (right index finger) and offset (right middle finger) of the illusion of rubber hand ownership.

23 of 29 subjects were also presented with retinotopic mapping sequences to locate early visual areas. Phase-encoded polar angle stimuli (Schira, Tyler, Breakspear, & Spehar, 2009) were projected onto a screen using E-Prime (version 2.0, Psychology Software Tools Inc.,

Sharpsburg, PA, USA; <http://www.pstnet.com>). Subjects reported central fixation colour change by button response. A flickering checkerboard wedge (22.5° polar angle) appeared at the right horizontal meridian and rotated clockwise, completing 12 full cycles of 360°, each of which lasted for 64s.

We localised lateral occipital cortex (LOC) in 16 subjects using Matlab for stimulation (R2012a, MathWorks, Natick, MA, USA). The LOC localiser was designed in the department (by J Lao, 2010). The stimuli were a fixation condition with a cross centred on blank grey screen, and greyscale images of objects, landscapes, and scrambled objects (the images used were from Kourtzi & Kanwisher, 2000, with permission). Images were presented at 23°x18° VA. In each run 7 blocks of each image type were presented in random order. Each block contained 20 images, presented for 450ms followed by 330ms inter-stimulus interval. Between blocks the fixation screen was presented for 12 s. LOC was defined by contrasting intact images > scrambled images. Subjects performed a one-back task while fixating centrally.

3.3.4. MRI Parameters

We measured blood oxygen level-dependent (BOLD) signals using an echo-planar imaging sequence on a 3T Siemens Tim Trio scanner with a 32 channel head coil. Four runs of 385 volumes were recorded for 20 subjects at voxel size of 1.5×1.5×1.9 mm (28 axial slices, TE: 30ms, TR: 2000ms, FA: 62° FOV: 192mm², inter-slice time: 71ms, gap thickness: 0.19mm). Resolution was dropped to 3mm³ (28 axial slices, TE: 30ms, TR: 2s, FA: 62° FOV: 210mm², inter-slice time: 71ms, gap thickness: 0.3mm, 5 retinotopically mapped) for the remaining subjects to allow for greater coverage. A high-resolution, 192-volume, 3D anatomical scan (3D MPRAGE, 1mm³ resolution) was also recorded. A short scout anatomical (128 vols) was recorded before each functional run. Polar angle retinotopic mapping (404 volumes) and LOC mapping (305 volumes) were run with identical parameters.

3.3.5. fMRI Pre-Processing

In Brainvoyager QX, anatomical images were normalised to Talairach space. Functional data for each subject and run (including retinotopic mapping and LOC localisation) were corrected for slice time with cubic spline interpolation and 3D motion using trilinear/sinc interpolation,

and were temporally filtered (high-pass filter with linear de-trending). The first 2 volumes per run were skipped to avoid saturation effects. No spatial smoothing was applied. Functional runs were aligned to each subject's T1-weighted structural image then spatially normalized into Talairach space. We examined subject motion over 6 parameters (3 translational and 3 rotational directions) and found motion never exceeded 1.5mm. We examined inter-subject alignment between functional data runs based on correlations of V1 spatial coverage. One subject showed alignment of $r < 0.90$ and this was driven by a single run which we excluded from analysis.

3.3.6. Behavioural Analysis

Four types of behavioural response were possible: Synchronous stimulation with rubber hand illusion perception (SI); synchronous stimulation but no rubber hand illusion (SN); asynchronous stimulation with illusion (AI); or asynchronous stimulation with no illusion (AN). We first calculated the amount of rubber hand illusion perception per stimulation condition (synchronous or asynchronous). Per subject, the length of time (in volumes) spent experiencing the illusion was summed per run and stimulation condition, and averaged across runs. We performed Wilcoxon signed rank tests to determine whether there was more illusion perception during synchronous or asynchronous tapping. We used a repeated-measures ANOVA to test for the interaction of stimulation condition (synchronous or asynchronous) and illusion perception (rubber hand perceived as own hand or not). To test if illusion experience occurs faster during synchronous stimulation, we averaged the time from stimulation onset either to illusion onset or report of no illusion. We performed Wilcoxon signed rank tests to determine if the onset of illusion perception was earlier during synchronous versus asynchronous stimulation. Matlab (R2012a, MathWorks, Natick, MA, USA) was used for behavioural analysis.

3.3.7. fMRI Analysis: Region of interest (ROI)

Primary visual cortex (V1) was defined in 24 (of 28) subjects using retinotopic polar angle mapping. Left and right V5 were defined in 28 subjects by contrasting all moving conditions (synchronous + asynchronous + test tapping) against fixation (regardless of perceptual experience). Lateral Occipital Complex (LOC) was defined in 12 subjects by contrasting hand present (synchronous + asynchronous) > hand absent (test tapping). In the remaining 16

subjects, LOC was defined using a localiser. A hand-specific patch ('VHand') within V1 was defined in 27 subjects with the contrast hand present (synchronous + asynchronous) > hand absent (test tapping). In subjects without retinotopic mapping, VHand patches were examined for their spatial relationship to the calcarine sulcus, to ensure they lay within V1. Ventral premotor cortex (vPMC) was defined anatomically in all subjects based on its relationship to sulcal architecture (Rizzolatti, Fogassi, & Gallese, 2002). For the TAL coordinates and number of voxels in each ROI, see Tables A.3.1. – A.3.6. in Appendix 3. Within these ROIs (V1, left and right V5, LOC, vPMC, VHand), we contrasted beta weights in four general linear models described below.

3.3.8. *fMRI Analysis: Univariate*

Functional data in regions of interest was examined using four multi-subject, multi-run (MSMR) general linear models (GLM). In the first random effects (RFX) GLM, we modelled synchronous, asynchronous, hand absent (test tapping) and fixation conditions (n=28). In the second GLM, we used a 2 (stimulation [synchronous or asynchronous]) by 2 (illusion [perceived or not]) factorial design. In the third GLM, we again used an FFX factorial design, modelling stimulation condition by illusion perception as in the second GLM. However, we additionally modelled the effects of tapping stimulation (synchronous, asynchronous and test tapping conditions, which were defined as predictors in the first GLM) in order to eliminate confound effects of tapping phase information and onset. The model therefore characterises both the basic tapping conditions and stimulation condition by illusion perception. We refer to this as a 'residuals analysis', as it is conducted on variance not explained by the tapping stimulation. The two factorial GLMs were confined to subjects with data for all stimulation/illusion percept pairings (n=21). Lastly we ran a 2 (stimulation [synchronous or asynchronous]) by 2 (illusion [perceived or not]) by 7 (ROI) factorial design to determine whether ROI had a significant impact on BOLD activation. We used contrasts to determine the effects of synchronous (S) versus asynchronous (A) stimulation, and of changes in stimulation, illusion perception, or the interaction of these factors in the predefined ROIs. GLM analysis and data visualisation was carried out in BrainVoyager QX (Version 2.4, Brain Innovation).

3.3.9. *fMRI Analysis: Representational Similarity*

We conducted multivariate analyses using a design which separated conditions of stimulation (synchronous or asynchronous) by illusion (rubber hand ownership or not). The multivariate activity patterns within a ROI can be considered a neural representation of a stimulus (Kriegeskorte, Mur, & Bandettini, 2008). For each ROI, we computed Representational Similarity Matrices (RSMs) on the pattern of beta weights (using iterative Pearson's correlates) for the four combinations of stimulation condition and illusion presence (SI, SN, AI, AN), across trials and subjects. We compared the multivariate representational pattern for each combination to all other combinations and trials, resulting in a correlation value reflecting similarity in multivariate pattern and a meaningful diagonal. The diagonal reflects the correlational similarity of all trials for each combination of stimulation condition and illusion presence for each subject. Off-diagonal values reflect correlation between trials of one combination of stimulation condition and illusion presence and another. Negative values are not possible in this measure of correlational similarity. To assess significance of the pattern similarity, we conducted permutation testing ($n=1000$) for each condition pairing and along the diagonal. In each permutation we randomly shuffled beta weights across trials and subjects and calculated a correlation value. We then calculated the occurrence of values higher than the true value and stated the p-value as the chance of obtaining a value as high as the true one in these random permutations. We performed Bonferroni adjustments on the p-values to account for multiple comparisons. We used Matlab (R2012a, MathWorks, Natick, MA, USA) for multivariate analyses.

3.3.10. fMRI Analysis: Representational Similarity across Time

Whilst representational similarity matrices allow us to examine our data without spatial averaging, they still require data to be average across the time course. As the RHI evolves and diminishes across time, we wished to examine these multivariate patterns at each time point. To this aim we examine the degree of similarity between neural representations elicited by each stimulation condition and illusory percept combination (synchronous stimulation with illusion, synchronous stimulation with no illusion, asynchronous stimulation with illusion, asynchronous stimulation with no illusion) at each time point prior to and following a change in percept (illusion or no illusion). For each ROI, we used a single time point/single trial approach to assess this evolution. We extracted the multi-voxel patterns within an ROI for each of the 10 TRs prior to and following each reported perceptual change. These epochs were aligned to the onset of the percept (report of illusion perception or none). In this case,

the report of no illusion could represent the offset of an illusory experience, or a report that a subject is not experiencing the illusion. For response-aligned multivariate BOLD time-courses, single trial representational similarity matrices (stRSMs) were computed on the BOLD percent signal change independently per subject, ROI and condition. Within each ROI and condition, we iteratively correlated (Pearson correlation) the values of the multivariate pattern of voxels at one time point with the multivariate pattern of voxels at each other possible time point. This procedure was repeated across all possible trial combinations (i.e. all other trials of that condition pair, and also against all other condition trials from that subject). The resulting matrices for each subject were averaged to obtain the final stRSM. Higher similarity (warm colours) reflects comparable multivoxel patterns of BOLD activation across time points.

To test for statistically significant differences between the stRSMs for each condition, we performed a 2 (illusion [perceived or not]) x 2 (stimulation [synchronous or asynchronous]) linear mixed model with an expanding sliding window approach. Independently per level, we centred a 2x2 TR window on the first point of the diagonal of both matrices and computed the mean of the values within the window (our TR was 2 seconds so 2x2 TRs is 4x4 seconds). We used the averaged values within the windows of our 4 levels (synchronous/illusion [SI]; asynchronous/illusion [AI]; synchronous/no illusion [SN]; asynchronous/no illusion [AN]) as inputs for our linear mixed model. The analysis was repeated on increasingly larger windows that expanded by 1 TR in each direction (when applicable), centred on each point of the diagonal. We performed Bonferroni adjustments on the p-values to account for multiple comparisons. This expanding sliding window approach allows us to investigate whether differences across stRSMs encompass a few time points or whether these are sustained over a larger time window.

3.4. Results

3.4.1. Behaviour

Time spent perceiving the illusion was significantly longer during synchronous stimulation than asynchronous ($z=2.9$, $p=0.0046$; averages of 56.2 TRs and 35.4 TRs over the entire

stimulation period for synchronous and asynchronous respectively, Figure 3.2). Subjects spent significantly more time not perceiving the illusion during asynchronous stimulation than during synchronous stimulation ($z=3.3277$, $p=0.0009$). During both synchronous and asynchronous stimulation, there was no significant difference in time spent perceiving the illusion versus not perceiving it ($z=-1.6$, $p=0.1011$ and $z=-1.9$, $p=0.06$ respectively). A repeated measures ANOVA of stimulation condition and illusion perception showed a significant interaction of condition and time spent perceiving the illusion ($F(27)=15.1$, $p<0.001$). The onset of illusion perception was not significantly different during synchronous versus asynchronous stimulation ($z=1.9416$, $p=0.06$).

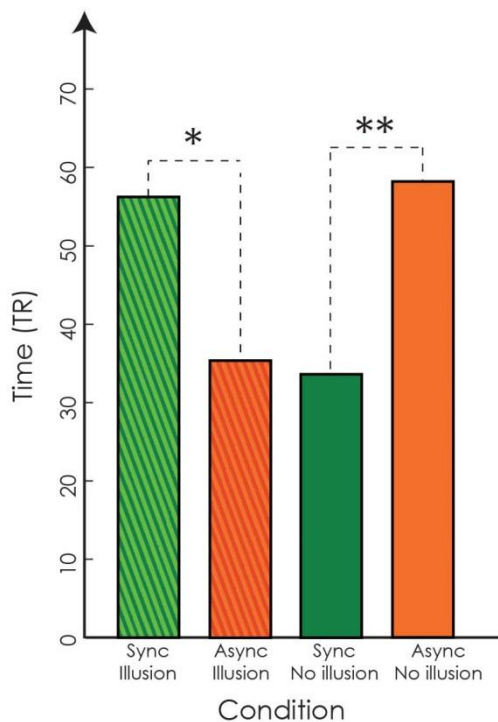


Figure 3.2. Behavioural responses. Amount of time spent experiencing the illusion or not, expressed as TRs (TR=2000ms); averaged across runs per subject and across subjects, per stimulation condition (1 TR = 2s, * $p<0.005$, ** $p<0.001$).

3.4.2. fMRI: Univariate Effects of Stimulation & Illusion Perception

We performed region of interest (ROI) analyses using a random effects general linear model of basic stimulation conditions. In V1 we found no significant effects of synchronous versus

asynchronous stimulation. In V1Hand, we found greater BOLD activation during synchronous stimulation than asynchronous stimulation ($t(\text{RFX})=2.177$, $p=0.039$). In a ROI analysis using this RFX GLM, we found no significant effects of synchronous versus asynchronous tap stimulation in left or right V5. In a ROI analysis using this RFX GLM, we found no significant effects of overall synchronous versus asynchronous tap stimulation in vPMC.

In a ROI analysis using the first factorial GLM (stimulation [synchronous or asynchronous] x illusion [perceived or not]), we found an interaction of stimulation and illusion perception in right V5 ($F=3.65$; $p=0.00026$); left V5 ($F=3.14$; $p=0.0017$); and V1 ($F=-3.79$; $p=0.00015$, Figure 3.3). As expected, V1 activation was lower with illusory experience during synchronous stimulation than with no illusory experience during synchronous stimulation or with illusory experience during asynchronous stimulation. Like V1, V5 activation was highest for incongruent stimulation and percept pairings. In right V5, activation was highest when there was synchronous stimulation with no illusion and lowest when there was illusion during synchronous stimulation. In left V5, activation was highest when there was illusory experience during asynchronous stimulation and lowest when there was no illusion under the same stimulation conditions. Using the first factorial FFX GLM (see Figure 3.3.), we observed separate main effects of stimulation and illusion in vPMC, in which synchronous stimulation contributed lower bold signal than asynchronous stimulation ($t(\text{FFX})=-2.068$; $p=0.039$) and illusion perception contributed higher bold signal than no illusion ($t(\text{FFX})=-4.068$; $p=0.000048$). In V1Hand we did not find significant effects of stimulation, illusion, or their interaction. No effects of stimulation, illusion, or their interaction were found in LOC.

In a ROI analysis using the factorial GLM on the residual data (stimulation [synchronous or asynchronous] x illusion [perceived or not]; conducted on variance not explained by the tapping stimulation), we found an interaction of stimulation and illusion perception in right V5 ($F=3.94$; $p=0.00008$), left V5 ($F=4.78$; $p=0.000002$), and V1 ($F=-3.91$; $p=0.000093$, Figure 3.3, dashed). Again, V1 activation was lower when there was illusory experience during synchronous stimulation than when there was illusory experience during asynchronous stimulation. In right V5, activation was highest when there was illusory experience during asynchronous stimulation and lowest when there was an illusion during synchronous stimulation. In left V5 activation was highest when there was illusory experience during asynchronous stimulation and lowest when there was no illusion under the same stimulation

conditions. Using the factorial GLM on the residuals data, we again observed a main effect of illusion in vPMC, in which illusion perception led to higher bold signal ($t(\text{FFX})=3.1$; $p=0.0019$). This effect appears to be driven by high activation for illusion perception during asynchronous stimulation. In V1Hand, we found a main effect of illusion, in which illusion perception contributed higher bold signal than no illusion ($t(\text{FFX})=-2.05$; $p=0.041$). We found no effects of stimulation, illusion, or their interaction in LOC.

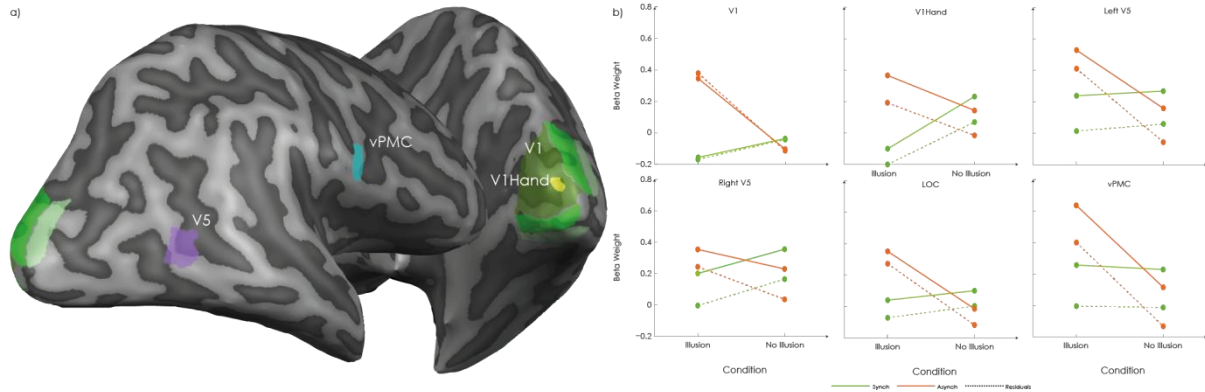


Figure 3.3. ROI definitions and Factorial GLMs in our regions of interest. Full data (solid lines) and data with the tapping stimulation pre-modelled and removed (residual data, dashed).

We chose not to use a three-way ANOVA with an additional factor of ROI as our main analysis as different subjects had different numbers of ROIs available for analysis (for example only $n=18$ subjects had a mapped V1). However, when checked there was not an effect of ROI ($F(3)=1, p=.415$; partial Eta squared = 0.143); an interaction between ROI and stimulation type ($F(3)=1, p=.416$; partial Eta squared = 0.143) or between ROI and illusion perception ($F(3)=1, p=.415$; partial Eta squared = 0.143)

3.4.3. fMRI: Multivariate Representation of Illusory Perception

Representational similarity matrices, computed between stimulation type and illusion perception pairings (SI, SN, AI, AN), show Pearson's r correlations between the representative multivariate patterns in each ROI (Figure 3.4). In V1 we observed significant positive correlations between and within the multivariate patterns created by the illusion conditions (SI $r=0.24$, AI $r=0.29$, SI and AI $r=0.27$; all $p(\text{Bonf}) < 0.05$). However, despite identical visual and tactile stimulation, we did not observe significant similarity within or

between illusion conditions and their corresponding non-illusion conditions (SN $r=0.13$, AN $r=0.19$, SI and SN $r=0.13$, AI and AN $r=0.14$).

A similar pattern of results was observed in VHand, with significant positive correlations in multivariate pattern between the two illusion conditions (SI and AI $r=0.28$; $p(\text{Bonf}) < 0.05$). In VHand there was greater variability in multivariate response to illusion during synchronous stimulation, but significant similarity in illusion during asynchronous stimulation (AI $r=0.26$; $p(\text{Bonf}) < 0.05$). Again we did not observe significant similarity within or between illusion conditions and their corresponding non-illusion stimulation conditions (SN $r=0.18$, AN $r=0.14$, SI and SN $r=0.14$, AI and AN $r=0.12$). These results suggest that in V1, and its subset VHand, illusion perception provokes a similar multivariate pattern across trials irrespective of stimulation type. This multivariate pattern is dissimilar to patterns observed when the illusion is not experienced.

We also found significant similarity during illusion perception across trials in vPMC (SI $r=0.29$, AI $r=0.28$; all $p(\text{Bonf}) < 0.05$) demonstrating that illusion-relevant patterns are found in vPMC, but that these patterns are not similar across stimulation types. The same similarity was not observed in non-illusion conditions. In right V5 significant similarity was only observed during no illusion perception in asynchronous stimulation (AN $r=0.41$, $p(\text{Bonf}) < 0.05$). In LOC there was significant similarity across trials of no illusion perception during synchronous stimulation (SN $r=0.26$, $p(\text{Bonf}) < 0.05$).

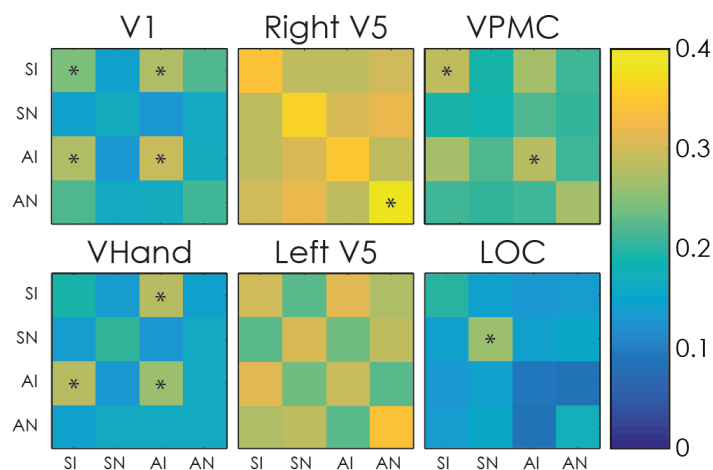


Figure 3.4. Representational similarity of stimulation and illusion condition pairings in each ROI. Gradient scale shows Pearson's r correlation strength. Stars indicate significance in a condition pairing (permutation tested, $n=1000$, to $p(\text{Bonf}) < 0.05$).

3.4.4. fMRI: Multivariate Representation of Illusory Perception across Time

Examination of representational similarity (Pearson's r correlations on the multivariate activation pattern) across time epochs revealed distinct temporal profiles in V5 and V1 for each percept during each stimulation condition (Figure 3.5). In right V5, we observed a significant effect of stimulation between 8 and 20s prior to perceptual onset ($p < 0.05$). This effect was driven by strong similarity in the neural pattern sustained prior to perceptual onset during asynchronous stimulation. Furthermore, we found significant effects of illusion perception from 10 to 14s prior to perceptual onset, and from 6 to 14s after perceptual onset ($p < 0.05$). Both of these temporal windows demonstrated higher neural pattern similarity centred on illusion perception compared to when the epoch was centred on a no illusion percept. Additionally, we found a significant interaction of these two factors between 6 and 20s prior to perceptual onset ($p < 0.05$). In left V5, we observed a significant effect of stimulation between 8 and 20s prior to perceptual onset ($p < 0.05$). We found comparatively greater similarity in the neural pattern prior to 'no illusion' percepts during asynchronous stimulation, which is likely to underlie this difference. We also found effects of illusion perception from 6 to 16s prior to perceptual onset ($p < 0.05$). This window showed higher neural pattern similarity prior to no illusion report. As no illusion reports are predominantly illusion offsets, this is likely to reflect pattern similarity during illusion perception. In vPMC we found a significant effect of illusion perception between 14 and 20s prior to perceptual onset ($p < 0.05$). In the other ROIs (V1, VHand, LOC), effects did not survive multiple comparison corrections.

3. VISUOTACTILE ILLUSION PERCEPTION IN EARLY VISUAL CORTEX

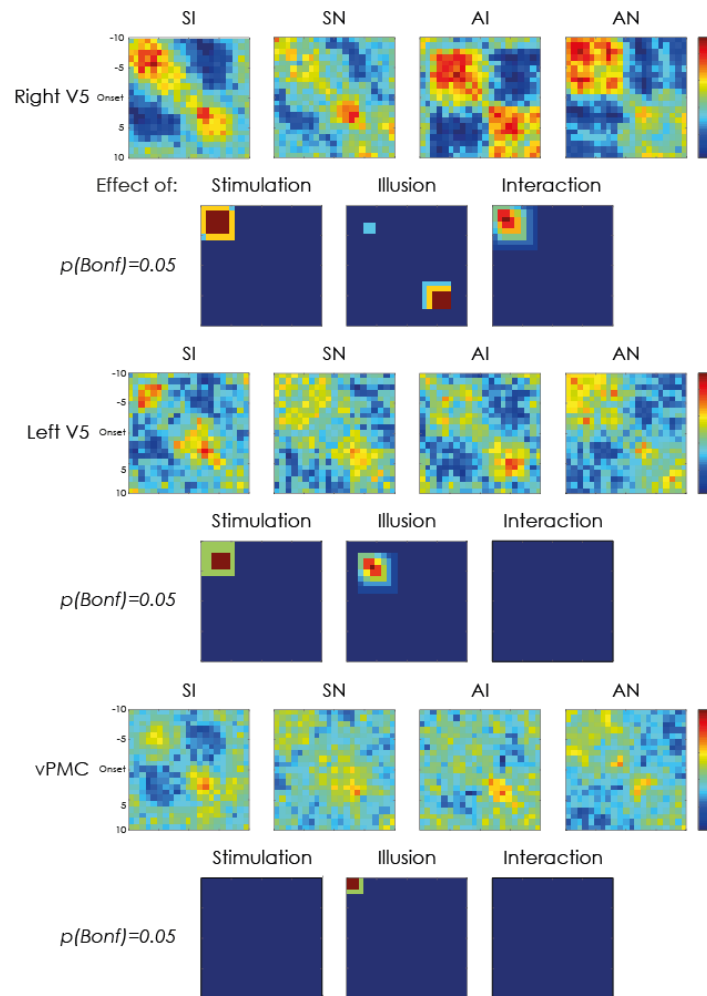


Figure 3.5. Single trial RSMs across time. Single trial RSMs on the BOLD % signal change across a 20 TR epoch centered on the perceptual onset. These figures demonstrate the evolution of similarity between the neural representation elicited by each stimulation and illusory percept combination, across time. Warm colours reflect higher similarity between multivoxel patterns of BOLD activation across time points. Bonferroni-adjusted significance masks (below stRSMs) display statistically significant effects of factors (stimulation type, illusion, or the interaction) on representational similarity. Colours on the significance masks indicate different sized windows of time in which there was a statistically significant effect of a factor, clarifying whether differences across stRSMs encompass a few time points or are sustained over a larger time window.

3.5. Discussion

We used the rubber hand illusion to demonstrate univariate and multivariate effects of illusory perception and multisensory (visuotactile) stimulation on cortical response in V1, V5, and vPMC. Participants provided instant feedback of their perception in a RHI

experiment, allowing us to fully study illusory state and visuotactile stimulation dissociated and when interacting.

V1 Demonstrates Interactive Effects of Stimulation and Illusory State

We found effects of stimulation type and illusory perception on early visual cortex, V1, in the absence of differential visual input. In support of Hohwy and Paton's (2010) proposal that the illusion resolves prediction error which arises during synchronous visual and tactile stimulation, V1 demonstrated a univariate interaction of stimulation type and illusion perception in ROI analysis. This illusion sensitivity and interaction could be indicative of a higher prediction error in specific conditions (Alink et al., 2010; Paton, Hohwy, & Enticott, 2012). As observed, the 'incongruent' stimulation and illusory perception pairings (no illusion during synchronous stimulation, illusion during asynchronous stimulation) should produce the highest activation/error, and induce the highest activation. Predictive errors have been demonstrated in retinotopically specific sub-regions of visual cortex and as a spatially diffuse effect, consistent with our findings (Alink et al., 2010; Muckli et al., 2005). In the subregion of V1 corresponding to the viewed rubber hand ('VHand'), we observe increased response to synchronous over asynchronous stimulation, and illusion perception produces more BOLD activity than no illusion perception.

Additionally, both V1 and VHand had significantly similar multivariate activation patterns between illusion conditions (SI and AI), across trials and subjects. This similarity was irrespective of stimulation and there was not significant similarity between illusion conditions and their matching stimulation non-illusion conditions, suggesting that early visual cortex holds a specific multivariate representation of the illusory state. Such response properties may seem to be out with the remit of V1 however, despite traditional conceptualisation of V1 as a feedforward orientation detector (Hubel & Wiesel, 1959), V1 receives feedback from numerous cortical areas (Bullier, 2001; Muckli & Petro, 2013). Activity in V1 is modulated by feedback information from other sensory modalities (Molholm et al., 2002; Morrell, 1972; Vetter et al., 2014), imagery (Albers et al., 2013), expectation (Kok et al., 2014), and higher cognitive processing (Muckli & Petro, 2013). Kok et al. (2012) showed that perceptual

expectation enhances representational content, increasing MVPA classification accuracy in V1 whilst suppressing V1 activation. Illusory multivariate similarity in our study therefore may reflect a form of representational sharpening upon the hand being coded as a body part. It is possible that V1 illusion representation occurs through feedback from V5. V5 has been shown to communicate illusory information to V1 (Seghier et al., 2000). This feedback has been demonstrated in the absence of feedforward stimulation in motion illusions such as apparent motion (Muckli et al., 2005; Muckli et al., 2002; Sterzer et al., 2006; Vetter et al., 2013; Wibral et al., 2009). Illusory feedback to V1 still occurs in the absence of visual attention (Muckli et al., 2005).

Another plausible cause of illusion-related univariate and multivariate activity in early visual cortex is the finding that multisensory interactions occur for own-body parts and objects in peripersonal space (Makin, Holmes, & Zohary, 2007). Feedback to early visual cortex may direct visual attention to such relevant items (Luck, Chelazzi, Hillyard, & Desimone, 1997; Ungerleider & Kastner, 2000) and, consistent with our finding of higher BOLD in illusion and synchronous conditions in VHand, attention increases BOLD signals in V1 (Gandhi, Heeger, & Boynton, 1999; Slotnick, Schwarzbach, & Yantis, 2003; Somers, Dale, Seiffert, & Tootell, 1999; Tootell et al., 1998; Watanabe, Harner, et al., 1998). Macaluso, Frith, and Driver (2000) demonstrated that touch enhances activity in early visual cortex if paired with a touch-relevant ipsilateral visual stimulus. This activation was driven by feedback from multimodal parietal regions and is likely to be a form of crossmodal attention direction.

Alternatively, the consistent representational pattern during illusion perception may be demonstrating that the rubber hand is coded as a body part which is available for action. Early visual cortex receives tactile and motor information, and V1 has demonstrated effects of action preparation (Ban et al., 2013). V1 also receives cerebellar feedback, which is implicated in predicting the consequence of actions (Blakemore, Frith, & Wolpert, 2001; Kawato & Wolpert, 1998) and in non-modal-specific prediction (Muckli & Petro, 2013; Roth et al., 2013). vPMC is also strongly functionally linked with the cerebellum (Dum & Strick, 2003).

V5 Demonstrates Interactive Effects of Stimulation and Illusory State

We find a univariate interaction for stimulation type and illusion perception in bilateral V5. An incongruent percept and stimulation pairing produces the highest activation (synchronous stimulation with no illusion). Hohwy and Paton (2010) suggested that the prediction error response during synchronous stimulation triggers the RHI to ‘explain away’ the error. We also demonstrate a differential response to tactile stimulation conditions, in the absence of differential visual input, supporting the proposal that V5 may be multi- or supra-modal (Alink et al., 2010; Chan, Simões-Franklin, Garavan, & Newell, 2010; Hagen et al., 2002; Lewis & Noppeney, 2010; Ricciardi et al., 2007; Sadaghiani, Maier, & Noppeney, 2009; Sani et al., 2010; Scheef et al., 2009; van Kemenade, Seymour, Wacker, et al., 2014; Wacker et al., 2011). In our study V5 demonstrated an interaction even in the residual data in which variance due to tapping stimulation was removed. This implies that information about stimulation type in V5 was either conceptual or based on congruence between stimulation type and illusory state. Unlike V1, V5 showed no coherent multivariate response for illusion perception across time.

The multivariate response in V5 supports suggestions that it is involved in the early development of the rubber hand illusion (Bekrater-Bodmann et al., 2014). In left V5, we find an effect of stimulation and illusion response on the multivariate pattern prior to perceptual response, particularly in no illusion perception during asynchronous stimulation, possibly due to high perceptual stability and predictability in this condition pairing (Kok et al., 2012). In right V5 there is an interaction in pattern inter-correlation prior to perceptual onset- coherent perceptual decisions and stimulation type (SI, AN) show greater correlation than other condition pairings. There are also effects of stimulation (greater similarity for asynchronous) and illusion (greater similarity for no illusion) perception separately pre-perceptual onset, and an effect of illusion perception on inter-correlation after perceptual onset. Lastly, in right V5 we find significant consistency in the multivariate pattern during asynchronous stimulation with no illusion, a condition which should not incite any prediction error.

It is particularly interesting that V5 shows a multivariate response related to stimulation and illusion perception, as the multivariate pattern in V5 has been shown to distinguish tactile stimulation previously (van Kemenade, Seymour, Wacker, et al., 2014; Wacker et al., 2011), coding different modalities in distinct populations (van Kemenade, Seymour, Wacker, et al., 2014). V5 is also heavily implicated in several visual illusions and in feeding information back to V1 to create perception (Muckli et al., 2005; Pascual-Leone & Walsh, 2001; Seghier et al., 2000; Silvanto et al., 2005). V5 shows involvement in hand-eye coordination (Beauchamp, LaConte, & Yasar, 2009), and therefore may be involved in recalibrating the body space after illusion induction (Tsakiris, 2010). V5 results are unlikely to be attentional (Treue & Maunsell, 1999), as if this was the case we would expect to observe an upregulation for all illusion presence, not the interaction we observe with stimulation type.

We used an unusual method to locate V5, and did not use an independent localiser separate from main experimental runs. There is significant overlap between V5 and the extrastriate body area (EBA), which may play a role in RHI perception (Costantini, Urgesi, Galati, Romani, & Aglioti, 2011; Limanowski, Lutti, & Blankenburg, 2014; Wold, Limanowski, Walter, & Blankenburg, 2014). As our study did not independently localise EBA and V5, we cannot be completely sure that sections of EBA did not contribute to our results. However, V5 was localised using conditions that both did and did not have a limb present and, contrary to previous EBA results (Limanowski et al., 2014), we find effects in bilateral not contralateral V5.

LOC Demonstrates Effects of Stimulation and Illusory State

In addition to the visual regions discussed previously, LOC reacted preferentially to synchronous stimulation. Additionally RSM analysis demonstrated that LOC shows more consistency in its multivariate pattern for synchronous conditions across different trials of that condition and subjects. Ehrsson et al. (2004) found that LOC demonstrates interactive effects of stimulation type and limb position congruence during the RHI. Whilst traditionally characterised as a high level shape processing area (Kourtzi & Kanwisher, 2001). LOC is sensitive to tactile and haptic stimulation when it is object- or limb- specific (Amedi,

Jacobson, Hendler, Malach, & Zohary, 2002; Amedi, Malach, Hendler, Peled, & Zohary, 2001; James et al., 2002; Stilla & Sathian, 2008). Additionally, LOC responds to objects in peripersonal space (Makin et al., 2007).

vPMC Demonstrates Effects of Stimulation and Illusory State

Consistent with previous research, we demonstrated a main effect of illusory state in contralateral ventral premotor cortex in which we observe higher BOLD signal during illusion perception (Ehrsson, 2007; Ehrsson et al., 2005; Ehrsson et al., 2004; Ehrsson, Wiech, Weiskopf, Dolan, & Passingham, 2007). Additionally, in vPMC we observed a particular multivariate pattern of activity related to illusion perception. This supports claims that vPMC activity is crucial to RHI perception. We also observe greater inter-correlation prior to a no illusion percept. We cannot separate effects of the previous percept so this may partially reflect greater inter-correlation late in illusion perception epochs. vPMC may function as a site for visual and somatosensory integration during the RHI (Bekrater-Bodmann et al., 2014; Nakashita et al., 2008). We did not find an effect of stimulation type, however previous findings suggest that vPMC discriminates sequential from non-sequential processing (Schubotz & von Cramon, 2003, 2004). As a potential effect of this discrimination, the multivariate pattern observed in vPMC during illusion perception was not similar between the two stimulation types.

3.6. Conclusion

Our results show that the effects of multisensory stimulation and illusory states are represented in cortical regions traditionally associated with solely visual processing including in very early visual areas. We found that perception of the rubber hand illusion interacts with tactile stimulation to change activation in V5, supporting this area's role in rubber hand illusion perception. We found this same interactive effect (of rubber hand illusion perception and stimulation type) on activation in V1. Furthermore the illusion produces a specific representative multivariate pattern in V1, and in a specific subregion of V1 corresponding to

3. VISUOTACTILE ILLUSION PERCEPTION IN EARLY VISUAL CORTEX

the rubber hand, irrespective of the tactile stimulation type. Such effects are not supported by the traditional response properties of V1 and thus are likely fed back from other sensory areas, or from higher cortical regions.

4. STIMULUS REPRESENTATIONS IN V1 FLUCTUATE WITH PERCEPTUAL VISIBILITY DURING MOTION-INDUCED BLINDNESS

4.1. EXPLORING THE PARAMETERS OF MOTION-INDUCED BLINDNESS USING ORIENTED GABOR PATCHES AS TARGETS

Fiona McGruer, Zoe Clay, Lucy S. Petro, and Lars Muckli.

University of Glasgow, Centre for Cognitive Neuroimaging, Institute of Neuroscience and
Psychology, 58 Hillhead Street, G12 8QB, Glasgow, United Kingdom.

4.1.1. Abstract

This study investigated the effect of using oriented Gabor patches as targets, at varying eccentricities, on perception of the motion-induced blindness illusion. We recruited 24 subjects over two experiments. Firstly, we ascertained that subjects experience MIB when viewing targets composed of oriented Gabor patches ($n=12$). We varied target eccentricity and, using repeated-measures ANOVA, found that MIB response rate and duration were greatly reduced at a target eccentricity of 4.2° compared to 5.8° and 7.1° ($n=12$). We discuss these results in context of a successive fMRI experiment (**Chapter 4.2**) and of the relationship between target eccentricity and cortical space. We conclude that oriented Gabor patches function as targets in motion-induced blindness stimuli, albeit with potentially reduced illusion perception. Furthermore, we found that when oriented Gabor patches are used as targets they are subject to the same effects of eccentricity as typical MIB targets.

4.1.2. Introduction

The visual world is constructed from the interplay of feedforward retinal input and intracortical processing. Visual illusions are a powerful way to distinguish visual sensory input (feedforward) from the resulting perception (a combination of feedforward and intracortical feedback). Several visual illusions specifically demonstrate the strong effects of motion feedback on visual experience. For example, in the apparent motion illusion observers perceive an illusory token moving across the screen when two separate flashing stimuli are presented sequentially. This illusion infers movement across a physically empty space on the retina, even though no stimulation is actually occurring (Muckli et al., 2002). Through motion feedback from V5, the relevant previously empty space in early visual cortex is activated (Vetter et al., 2013; Wibrall et al., 2009). Hidaka et al. (2009) showed that the motion prediction induced by apparent motion bars is so powerful as to silence awareness of motion moving in the opponent direction. Similar silencing has been demonstrated using rotational motion to stop awareness of large visual changes in size, shape and colour of objects presented on an annulus (Suchow & Alvarez, 2011).

Motion-induced blindness (MIB) is an illusion in which motion causes an object to completely disappear. A target surrounded by a coherent motion field becomes perceptually invisible even though the target remains physically present (Bonneh, Cooperman, & Sagi, 2001; Bonneh, Donner, Cooperman, Heeger, & Sagi, 2014). Motion-induced blindness may be an effect of active completion of the motion field over the target, as suggested by Schölvinck and Rees (2010) who found increased V1 and V5 BOLD activity during target invisibility consistent with prediction error (Alink et al., 2010, in apparent motion). Alternatively, MIB may represent a form of perceptual suppression of target awareness through feedback instead of overwriting. Target representation may therefore still be present in early visual cortex, as suggested by retention of orientation effects (Montaser-Kouhsari, Moradi, Zandvakili, & Esteky, 2004), and negative afterimages (Hofstoetter, Koch, & Kiper, 2004) of MIB targets. Top-down motion information from V5 may therefore affect the illusion either by filling in motion over the target or suppressing awareness of the target without affecting target representation.

These possibilities empower motion-induced blindness as an ideal tool to investigate and understand the underlying mechanisms of perception and the neural correlates of visual awareness (Bonneh et al., 2001; Mitroff & Scholl, 2005). This paper forms the basis of the fMRI study presented in **Chapter 4.2**, acting firstly as a pilot to screen individuals for the brain imaging experiment. Secondly, we investigate the effect of using oriented Gabor patches as targets on motion-induced blindness perception. Thirdly, we explore the effect of target retinal eccentricity on resulting MIB using oriented Gabor patches as targets. Additionally, we discuss the effects of such eccentricity on the successive fMRI study- as retinal eccentricity increases dedicated cortical space per stimulus size decreases (cortical magnification factor; Daniel & Whitteridge, 1961; Qiu et al., 2006; Wandell et al., 2007). We aim to maximise the cortical space of the target for fMRI by decreasing target orientation towards the fovea, whilst retaining MIB experience in a paradigm which uses oriented Gabor patches as targets. The fMRI study detailed in **Chapter 4.2** then investigates the representation of the target Gabor during perceptual blindness.

4.1.3. Method

4.1.3.1. *Participants*

The study sample consisted of 25 paid healthy volunteers (mean age 21.04 years, 19, female; normal vision) recruited from the subject pool of the University of Glasgow Psychology department ($n=12$ per experiment). One subject was excluded due to technical difficulties. Subjects provided written informed consent and answered a demographic questionnaire. Subjects were asked if they would be willing to return for later participation in an fMRI experiment. On completion of the study participants were debriefed.

4.1.3.2. *Design and Procedure*

For stimulus presentation and data collection we used NBS Presentation Programming (16.5, Neurobehavioral Systems, Berkeley, CA, USA). Our motion-induced blindness (MIB) stimulus consisted of a motion field and a target superimposed on a black background (Figure 4.1.1.). Subjects fixated on a central cross around which the motion field rotated. The motion field consisted of a grid array of green crosses (radius 12° VA, angular rotation speed 60 deg/sec). Whilst MIB displays typically include a protective zone around the target which the cross array does not enter, our cross array had no such exclusion zone and passed over the target. A target was presented in the upper left visual field (shown to produce most robust MIB; Bonnef et al., 2001; Hofstoetter et al., 2004). The target was a yellow circle (RGB 255 255 50) overlaid with a red Gabor (RGB 255 0 0; either 45° or 135° ; Gaussian envelope standard deviation 20px, frequency 0.05 cycles/pixel), and was displayed behind the rotating field. The target was scaled to 0.8° in diameter and appeared at 5.8° eccentricity for experiment 1 (3° left and 5° above the fixation cross), and at 4.2° (3° left and 3° above fixation) for one run and 7.1° (5° left and 5° above fixation) for the other in experiment 2. Run order was counterbalanced across subjects, all other parameters remained identical.

4.1. EXPLORING THE PARAMETERS OF MOTION-INDUCED BLINDNESS USING ORIENTED GABOR PATCHES AS TARGETS

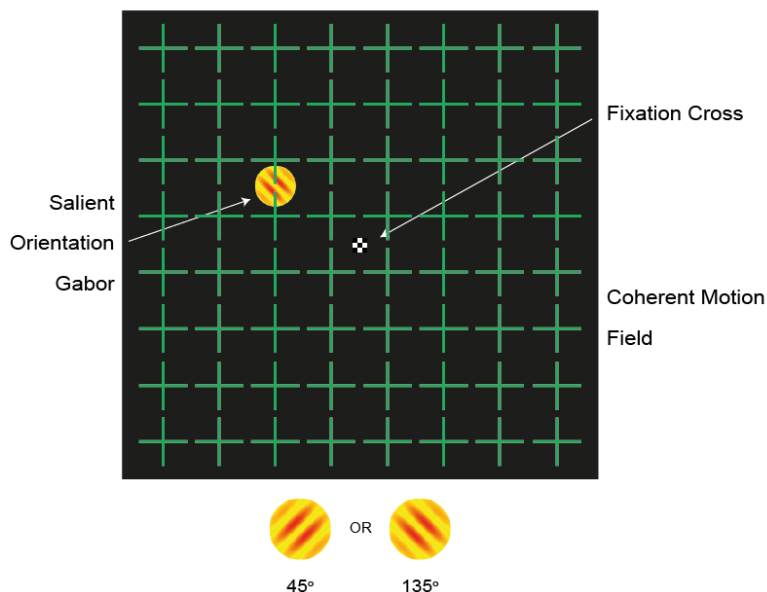


Figure 4.1.1. Motion-induced blindness stimuli. Red and yellow oriented Gabor targets were placed behind a rotating green cross array on a black background. Gabor targets are 0.8° with oriented Gabor of either 45° or 135° .

Subjects completed two runs of 6-8 minutes per run. In each run, subjects saw two blocks of ‘MIB’ stimuli each lasting 3 minutes. Each MIB block was preceded and succeeded by instructions and 10s of fixation (fixation cross and black screen). The cross array rotated clockwise in one block and counter-clockwise during the other block. The orientation of the target changed four times per block, pseudorandomly (45s for an orientation before change). The target was physically removed from the display 4 times during each the first MIB block, at random times for an interval lasting between 5-10s. Subjects were not informed that the target would be removed.

A chin rest was used for participant comfort and to ensure minimal head movement. The presentation screen was fixed 30cm from the observer at all times. Subjects fixated centrally throughout. Three times during each run, the fixation cross changed from white to red for 1s. Subjects were instructed to count colour changes and report this to the experimenter at the end of each run in an effort to reduce eye movement and distract attention away from the oriented Gabor patch target in order to minimise fluctuations in attention related to the

perceived target (Schölvinck & Rees, 2010). Subjects reported target invisibility with a button press (right index finger) and hold for the duration of invisibility (regardless of motion induced blindness or physical removal). We used Matlab (R2012a, MathWorks, Natick, MA, USA) to randomise fixation colour changes, target disappearance times, and the order of target presentation eccentricity.

4.1.3.3. Analysis

Matlab was used for behavioural analysis. The dependent variables were summed response rate (number of reported MIB experiences per run and block) and mean duration of MIB in milliseconds (total length of reported MIB experiences/number of MIB experienced in a run and block). For mean duration we used only MIB experiences that lasted over 500ms. Lastly, the mean reaction time to report 'MIB' after the physical removal of the target was assessed per subject per run. We performed a 2x2 repeated measures ANOVA to assess the contribution of run and block to MIB response rate and duration in experiment 1. We also conducted a 2x2 repeated measures ANOVA to assess the contributions of eccentricity and block to outcome duration and response rate in experiment 2. All ANOVA results were Bonferroni corrected. Wilcoxon Signed Rank tests were used to compare subject reaction time to the physically removed stimulus across runs (run 1 & run 2 in experiment 1) and eccentricity (runs of different eccentricity in experiment 2).

4.1.4. Results

Our data clearly indicates robust presence of the motion-induced blindness illusion when oriented Gabor patches are used as targets. In experiment 1, we observe MIB with reasonable duration and robust response rates (see Table 4.1.1.). For experiment 2, as the peripheral location of the target eccentricity of visual angle increases (to 7.1°) so too do the reported rates of MIB. On the other hand when the target is positioned closer to fovea, (4.24° of eccentricity) MIB response and durations are greatly reduced, particularly in response rates.

4.1. EXPLORING THE PARAMETERS OF MOTION-INDUCED BLINDNESS USING ORIENTED GABOR PATCHES AS TARGETS

	Expt. 1. (n=12)				Expt. 2. (n=12)			
	Mean		Std. Deviation		Mean		Std. Deviation	
Run	1	2	1	2	4.2°	7.1°	4.2°	7.1°
Duration	1652	1583	1087	1114	703	985	113	147
Rate	23.4	20.7	14.5	20.4	4.4	25	3.7	16.5
RT to Remove	661	720	561	506	622	667	111	187

Table 4.1.1. Behavioural outcomes. From each experiment and run we present mean and standard deviations for MIB duration, response rate and reaction time (RT) to the physically removed targets.

In experiment 1, we examined the effects of run and of the block of stimulation within a run. As the order of cross array rotation direction was randomised per subject, block refers to the first and second stimulus presentation, not to two defined rotation directions. We found no significant effect of run ($F(1,11) = 0.14$, $p = 0.71.$), of block ($F(1,11) = 0.37$, $p = 0.56.$), or of the interaction between run and block ($F(1,11) = 3.39$, $p = 0.09.$) on MIB duration (Figure 4.1.2.a). Additionally, we found no effects of run, block, nor any interaction, on response rates ($F(1,11) = 0.57$, $p = 0.47$; $F(1,11) = 0.74$, $p = 0.41$; $F(1,11) = 0$, $p = 0.99$; figure 4.1.2.b). We found no differences across runs for reaction times to the physically removed target ($t = 61$, $z = 1.72$, $p = 0.84$; figure 4.1.2.c).

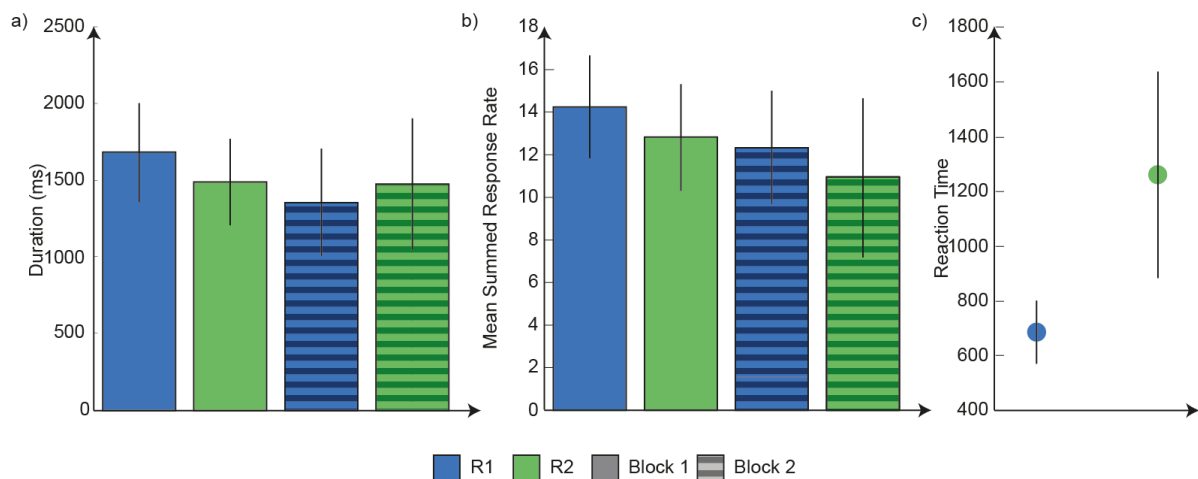


Figure 4.1.2. Results per run and block in Experiment 1. a) Mean duration and b) mean response rate; both of motion-induced blindness. In both graphs colours denote runs, and texture denotes block. c) Mean reaction time to physical removals per run. In all cases bars represent standard error of the mean.

In experiment 2, we examined the effects of target eccentricity and of the stimulus block. We found an effect of eccentricity ($F(1,11) = 42.6, p \leq 0.001$), a significant effect of block ($F(1,11) = 7.8, p = 0.017$), and small but significant effect of interaction between eccentricity and block ($F(1,11) = 5.3, p = 0.041$) on mean duration of MIB (Figure. 4.1.3.a). When the target is positioned closer to the fovea, (4.2° eccentricity) mean MIB duration is greatly reduced. MIB duration was reduced in block 2 for 4.2° but only marginally decreased in block 2 for 7.1° (see Figure 4.1.3.a).

Furthermore, we found a main effect of eccentricity ($F(1,11) = 14.3, p = 0.003$), on response rates of MIB (see figure 4.1.3.b). Response rate was much higher for 7.1° eccentricity than 4.2° . We found no main effect of block ($F(1,11) = 0.24, p = 0.63$), nor for the interaction between eccentricity and block ($F(1,11) = 2.8, p = 0.12$). Lastly, we ran a Wilcoxon Signed Rank test to compare the mean reaction times between eccentricities, the results were non-significant ($F(1,11) = 30, z = -706, p = 0.48$; figure 4.1.3.c) showing that eccentricity does not affect reaction time to physical removal of the target.

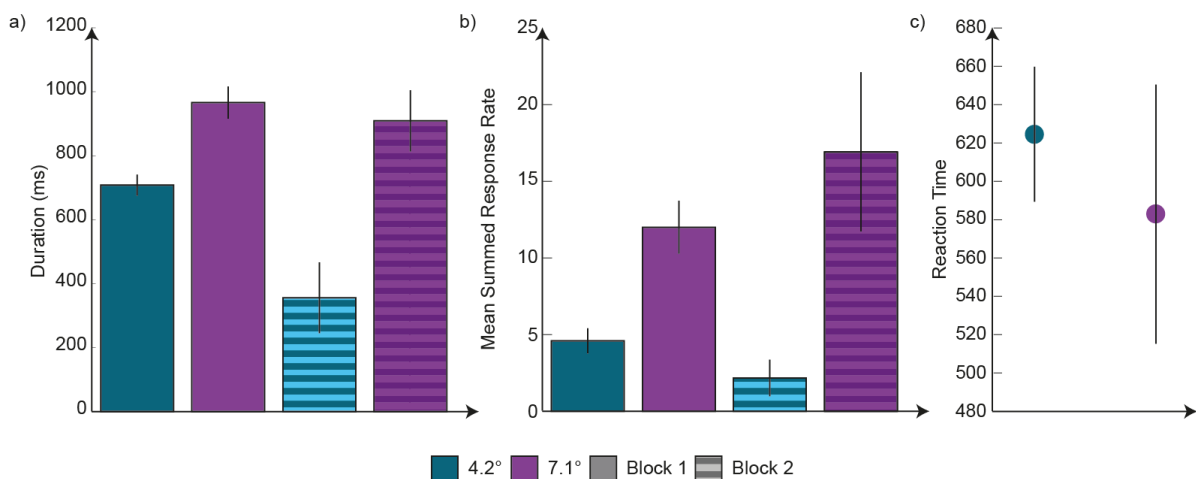


Figure 4.1.3. Results per eccentricity and block in Experiment 2. a) Mean duration and b) mean response rate; both of motion-induced blindness. In both graphs colours denote eccentricity, and texture denotes block. c) Mean reaction time to physical removals per eccentricity. In all cases bars represent standard error of the mean.

4.1.5. Discussion

The presented study investigated whether oriented Gabor patches can function as motion-induced blindness targets. Furthermore, we examined the relationship between retinal eccentricity and MIB perception when using such target variants. In experiment 1, we found that MIB experience is robust in measures of both duration and response rate when oriented Gabor patches are used as targets at 5.8° of radial visual angle. This was unaffected by run or block (and therefore unaffected by rotation direction as this varied by block). Subjects were able to respond correctly to physically removed targets in both runs.

It is crucial to note that, despite using very similar parameters, we observed lower mean durations of MIB than those reported by Schölvinck and Rees (2010). Using oriented Gabor patches as targets stimuli may therefore reduce overall MIB perception. To fully examine this effect, a direct comparison of plain and oriented Gabor patch targets must be made in future behavioural experiments with other parameters strictly controlled. Bonnefante et al. (2001) rigorously tested the parameters effecting motion-induced blindness, reporting 30% invisibility across time for a 0.2° target. Our target is much larger, allowing for cortical mapping in early visual cortex. Whilst our eccentricity was higher, greater target size greatly reduces MIB- there is a degraded illusion response that correlates with target size increase from $0.1-1^\circ$; when presented at an eccentricity of 1° (Bonnefante et al., 2001). However, others have found MIB experience using similar target size, at a smaller eccentricity, than the parameters we present here (Mitroff & Scholl, 2005). Interestingly, both Mitroff and Scholl (2005) and Bonnefante et al.'s (2001) stimuli include distractor targets, which may facilitate competition between the field and the targets and therefore facilitate MIB.

In experiment 2 we found that MIB duration and rate were greatly decreased from 7.1° target to 4.2° target presentation eccentricity. In duration we observed an interaction, in which the second block produced longer MIB duration for 7.1° but reduced duration for 4.2° . Lastly, we show that target eccentricity does not affect reaction time to physical removal of the target. These results were expected given the robust decreasing effect of reduced target stimulus eccentricity on MIB perception (Bonnefante et al., 2001). Whilst these observations are not

directly comparable, results in experiment 1 showed longer MIB durations but slightly lesser MIB response rates than the 7.1° condition in experiment 2. The target was only physically removed in block 1 of each eccentricity, which may affect the block by eccentricity interaction observed. However, we would expect the exclusion of physical removals to increase MIB at either eccentricity, not decrease the illusion at specific eccentricities.

Target/field contrast heavily influences MIB perception. Stronger target saliency, and stronger contrast between target and field, increases the amount of MIB perception in a block of stimulation (Bonneh et al., 2001). These parameters may interact with our oriented Gabor patch target, which may be less salient. We used red and yellow banded oriented Gabor patches as opposed to black and grey specifically to retain target/field contrast and target saliency. Two of our subjects did report perceived leftover ‘haze’ after the target disappearance. This is a novel effect, as MIB is said to operate on an ‘all or nothing’ principle (Bonneh et al., 2001). One potential mechanism is that the yellow bands are being silenced by the motion field, with red bands experiencing only perceptual fading effects, which tend towards higher eccentricities and happen more in cases of low contrast (Francis & Kim, 2012). In this case the yellow lines may function as separate ‘line’ targets, as used in other studies (Donner, Sagi, Bonneh, & Heeger, 2008). Other studies have successfully used black and grey oriented Gabor patches as targets and maintained target illusory disappearance (Bonneh et al., 2010). However, Bonneh et al. (2010) used higher frequency Gabors than those used in our study. In the future we may incorporate a rapidly flickering target to reduce adaptation or fading effects and retain target saliency (Schölvink & Rees, 2010). Flicker speed has a U-shaped effect on MIB perception- no flicker and high flicker speed enables increased target disappearance (Bonneh et al., 2001).

As in our study, targets presented to the left visual field facilitate illusion perception, with an increased rate of 18% disappearance for a left hemifield target as opposed to 13% for right hemifield (Hofstoetter et al., 2004). Our paradigm used a rotating cross array as the coherent motion field. Cross arrays have been used to generate disappearance in classic MIB stimuli by Bonneh et al. (2010) and Harris, Barack, McMahon, Mitroff, and Woldorff (2013); and were used in an MIB dumbbell paradigm by Mitroff and Scholl (2005). All authors used crosses in dark colours or greyscale, and our cross array was dark green. Other authors have

used random dot motion fields- Bonneh et al. (2001) used dots to robust effect; as did Hofstoetter et al. (2004). Motion induced blindness literature demonstrates a massive variation in the rotational speed of the background motion field across paradigms. The rotational speed of our motion field was 60 deg/s. Other papers have used much slower field speeds- Schölvinc and Rees (2010) used 5.5 deg/sec. Whereas Mitroff and Scholl (2005) used rotational speeds as fast as 470 deg/s. This could be an avenue for further investigation.

As in this study and the following fMRI study (**Chapter 4.2.**), the vast majority of motion-induced blindness paradigms use self-report to determine a subject's perception of the target. Such paradigms typically have subjects press or press and hold a response key to denote when the target is perceptually invisible (examples include Bonneh et al., 2001; Bonneh et al., 2014; Donner et al., 2008; Donner, Sagi, Bonneh, & Heeger, 2013; Hsieh & Peter, 2009; Kloosterman, Meindertsma, Hillebrand, et al., 2015; Kloosterman, Meindertsma, Loon, et al., 2015; Mitroff & Scholl, 2005; Schölvinc & Rees, 2009; Wallis & Arnold, 2009 and many others). Some authors have additionally had subjects report the features of the target with a button press, removing the press when the target disappears (colour; Jaworska & Lages, 2014). These paradigms produce a large amount of useable data, but have some obvious limitations. Responses will be subject to a lag related to the amount of time it takes to make a button response after the onset of a conscious percept. To correct for this, a paradigm could establish the response time for each subject to physical removal of a target, and correct the MIB onset by this mean value. Furthermore, this design means that resulting data (for example fMRI recordings or EEG) is confounded by activity related to the button press. Button presses can be decoded in fMRI (Liang et al., 2013). Furthermore, in these paradigms, subjects are forced to attend to the target to monitor it for disappearance and reappearance. Direct attention affects MIB duration – both increasing the likelihood of target disappearance but reducing the length of time it disappears for (Schölvinc & Rees, 2009).

Other authors have probed MIB more objectively by physically removing the target and measuring the reaction time until it is noted, reasoning that if the target is perceptually invisible subjects will not notice the removal (Kramer, Massaccesi, Semenzato, Cecchetto, & Bressan, 2013). Dieter, Tadin, and Pearson (2015) allowed the MIB inducing stimulus to break through continuous flash suppression and measured the reaction time until the target

was seen, reasoning that if the target is perceptually invisible subjects will not see its reappearance. These paradigms still raise concerns around the speed of subject motor response after a perceptual change. Attention is also still directed to the target and subjects still have to physically respond with a button press, albeit at a different time point. These paradigms also dramatically reduce the MIB data one has to work with as the target may for example be perceptually invisible many more times than the probe occurs, which will go unnoticed. Kramer et al. (2013) also suggest that such a method is only successful with a reduced target to background contrast, which reduces MIB perception (Bonneh et al., 2001), and with a more eccentric target (which will be given less cortical space in visual cortex).

Eye tracking could be a promising avenue to objectively determine MIB perception. Kloosterman, Meindertsma, Loon, et al. (2015) found that the pupil dilates when the percept changes during MIB stimulation, and that this dilation is larger for target disappearance than target reappearance. This change was independent of the length of a percept and independent of subject's overt report of a change. Pupillary dilation was 61% predictive of the reported percept. Eye tracking may be informative of perception as microsaccades reduce just prior to MIB disappearance and increase prior to reappearance (Bonneh et al., 2010; Hsieh & Peter, 2009). More investigation is needed to determine whether these variations are significantly predictive of the subject's percept. We decided to use a subject self-report button press to maximise our data (subjects press and hold for the duration of target invisibility). This allows all time points where a stimulus is presented to be allocated to 'target visible' or 'target invisible'. We use a central fixation task to partially control attention. Additionally, in our fMRI experiment (see **chapter 4.2.**) all decoding is conducted *within* a perceptual condition and therefore does not reflect a difference in button presses.

As we intend to use a similar stimulus in fMRI, we aimed to maximise visual cortical target representation. Cortical space varies as a function of eccentricity and visual field position by the cortical magnification factor (measured in mm of cortex per degrees of visual angle; Daniel & Whitteridge, 1961; Wandell et al., 2007). As eccentricity is reduced towards the fovea, or target size is increased, greater cortical space is devoted to a target (Qiu et al., 2006). There are also decreases in performance and visual acuity as eccentricity increases into the periphery (Qiu et al., 2006). These choices about stimulus parameters must be

balanced against their effects on MIB perception. MIB is reduced as a target becomes increasingly foveal (Bonneh et al., 2001). Larger targets also lead to reduced MIB at fixed eccentricities (Lages & Jaworska, 2011). In the interest of maximal cortical space we therefore intend to use this mid-range eccentricity of 5.8° in the following fMRI experiments.

4.1.6. Conclusion

In summary, oriented Gabor patches function as MIB targets; although darker band colours may effect complete disappearance. As with typical MIB targets, greater presentation eccentricity increases Motion-Induced Blindness of the oriented Gabor target. In **Chapter 4.2** we go on to use oriented Gabor patches of 45° and 135° as targets, presented at 5.8° radial visual angle to the upper left visual field. We investigate whether motion-induced blindness is an effect of active completion of the motion field over the target representation in V1, or if it represents a form of perceptual suppression with maintained target representation.

4.2. STIMULUS REPRESENTATIONS IN V1 FLUCTUATE WITH PERCEPTUAL VISIBILITY DURING MOTION-INDUCED BLINDNESS

Fiona McGruer, Lucy S. Petro, Lars Muckli

Institute of Neuroscience and Psychology, Centre for Cognitive Neuroimaging,
University of Glasgow 58 Hillhead Street, G12 8QB, Glasgow, United Kingdom

Acknowledgements

We thank the European Research Council (ERC StG 2012_311751-’Brain reading of contextual feedback and predictions’) and the Human Brain Project (EU Grant 604102 ‘Context-sensitive Multisensory Object Recognition: A Deep Network Model Constrained by Multi-Level, Multi-Species Data’) for their generous support. We thank Frances Crabbe for technical assistance and Matthew Bennett for insightful discussion.

4.2.1. Abstract

When viewing visual illusions and bistable stimuli our perception deviates from what was presented. In motion-induced blindness (MIB) a target surrounded by a motion field switches between perceptually visible and invisible, even though the target remains physically present. These switches in perceptual awareness may be related to fluctuations in the pattern of V1 activity representing the stimulus. To address whether this is the case we recorded functional magnetic resonance imaging data from subjects viewing an MIB stimulus with oriented Gabor patches ($45^\circ/135^\circ$) as target stimuli. We used multivariate pattern analyses to clarify whether the target representation in V1 is or is not preserved during perceived target disappearance. Our results showed that target properties are present in V1 when the target is visible but are not present during periods of perceived invisibility. Therefore we suggest that the V1 target stimulus representation fluctuates with perceptual visibility during motion-induced blindness. We propose that this fluctuation arises from completion of the motion field through feedback from V5, overwriting target representation in V1.

4.2.2. Introduction

Motion-induced blindness (MIB) is a bistable visual illusion in which a salient target stimulus surrounded by a coherent motion field alternates between perceptually visible and invisible, even though the target remains physically present (Bonneh et al., 2001; Bonneh et al., 2014). Dieter et al. (2015) recently proposed that motion-induced blindness occurs due to fluctuations in the pattern of activity in V1 representing the target stimulus. Such fluctuations in the V1 ‘stimulus representation’ would provide neural evidence that internal cortical processing can overwrite sensory stimulation (which remains constant in MIB). However, no study has explored how the target stimulus is encoded in patterns of neural activity during states of perceptual awareness and blindness in MIB. This is essential for understanding whether the target stimulus representation fluctuates, and if this

correlates with perceptual outcomes. During MIB the target is either overwritten or is still represented in V1. Overwriting could occur either through local interactions within V1 or through feedback from other cortical areas.

Neurophysiology and brain imaging (fMRI) findings suggest that, although higher-level interactions in the visual system contribute to motion-induced blindness, the target representation might be interrupted as early as primary visual cortex during perceptual disappearance. Using human fMRI, Schölvinc and Rees (2010) showed increased BOLD activity during target invisibility in the cortical representation of the target stimulus in V1 and also in V5. They suggest this BOLD increase is consistent with local ‘overwriting’ of the target from regions of V1 representing the motion field. One potential mechanism for this ‘overwriting’ is filling-in by boundary or contrast adaptation at the intersection of the target and field (Hsu, Yeh, & Kramer, 2004, 2006). Surface completion of the motion field stimulus may also occur within early visual cortex (Graf, Adams, & Lages, 2002). 3D objects, contours, and edges can all complete within V1 (Bakin, Nakayama, & Gilbert, 2000; Lee, 2001) and the independent effect of motion-induced blindness on multiple target objects suggests that the disappearance mechanism occurs at relatively fine spatial detail (Graf et al., 2002).

The target could also be overwritten by top-down effects. Schölvinc and Rees (2010) comment that cortical feedback is causally implicated in dictating bistable percepts. In other motion illusions feedback from V5 ‘writes’ illusory trace information into V1 (Akselrod et al., 2014; Chong et al., 2015; Muckli et al., 2005; Sterzer et al., 2006). Feedback therefore could also overwrite target information in V1 during MIB. This feedback may originate in V5 - Donner et al. (2008) found that V5 activation increases during target invisibility, whilst target visibility upregulates areas of dorsal extrastriate cortex. Local overwriting, surface completion, and top-down overwriting all suggest that target representation will be altered or even erased at early cortical levels; however no study has demonstrated this.

Alternatively, other studies suggest that target properties could be preserved in early visual cortex if illusory target disappearance emerges exclusively at higher cortical levels. For example, the illusion may arise from competition between cortical representations of the target and the motion field, from which only one percept can prevail (Bonneh et al., 2001; Donner et al., 2008; Keysers & Perrett, 2002), at multiple levels of the visual system (Donner et al., 2008). High level neural competition could result in perceptual blindness even whilst V1 continues to represent properties of the target. In support of this hypothesis, behavioural evidence suggests that the target representation in early visual cortex is preserved by feedforward processing during MIB. Perceptual invisibility of oriented Gabor patch targets does not reduce orientation adaptation, suggesting that neurons responsive to target orientation remain active (Montaser-Kouhsari et al., 2004). Invisible targets also induce negative afterimages as intense and long-lived as those created by perceived stimuli, again suggesting that adapting neurons are not affected by the illusion (Hofstoetter et al., 2004).

It is not currently known whether the cortical representation of the target is disrupted during motion-induced blindness, even though fluctuations in stimulus strength are suggested to underlie the illusion. Furthermore, it is not known at what stage of the visual hierarchy the target stimulus representation is disrupted. If target properties are present in V1 during MIB, then top-down signals do not ‘overwrite’ the feedforward processing of the target, and target invisibility originates at higher levels of the visual hierarchy. If properties of the target stimulus are not present in V1, this would suggest that completion of the motion field distorts the representation of the target, via cortical feedback or through lateral interactions within V1. Using functional magnetic resonance imaging, we measured human observers presented with the motion-induced blindness illusion. We used oriented Gabor patches ($45^\circ/135^\circ$) as the target stimuli, and employed multivariate pattern analyses to clarify whether target representation in V1 is preserved or distorted by overwriting during perceived target disappearance. We specifically examine how features of the target are represented during MIB, as opposed to examining a change in the associated BOLD signal (Donner et al., 2008; Schölvinc & Rees, 2010), or in a secondary perceptual effect (Hofstoetter et al., 2004; Montaser-Kouhsari et al., 2004). We

provide evidence for feedforward processing of target orientation during target visibility but not during motion-induced blindness, even though the target remains present. Our data suggest that fluctuations in the strength of the feedforward target stimulus representation are correlated to perceptual outcome. This may be caused by cortical feedback from motion-sensitive area V5 overwriting feedforward processing in V1, consistent with the idea that feedback causes perceptual switches during bistable percepts (Blake & Logothetis, 2002; Hohwy et al., 2008).

4.2.3. Method

4.2.3.1. Participants

We recruited 18 subjects for experiment 1 (mean age 23.05, range 18-30; 11 female) and 3 subjects for experiment 2 (mean age 24.6, range 23-26; 2 female). Subjects had normal vision and were right-handed. One subject completed both experiments. We recruited subjects through the University of Glasgow Psychology department subject pool. Subjects provided written informed consent, underwent MRI safety screening and were paid for participation. The University of Glasgow ethics board approved the procedure (#300140042).

4.2.3.2. Stimuli

During ‘motion-induced blindness’ (MIB) stimulation subjects fixated on a central cross around which a circular full-field array of green crosses rotated radially (radius 9.5° VA; angular rotation speed 60 deg/sec in experiment 1 and 120 deg/sec in experiment 2.). A target was presented in the upper left visual field, which is the location shown to produce most robust MIB (Bonneh et al., 2001). The target was a yellow circle overlaid with a red Gabor (either 45° or 135°; Gaussian envelope standard deviation 20px, frequency 0.05 cycles/pixel), and was displayed behind the

4.2. STIMULUS REPRESENTATIONS IN V1 FLUCTUATE WITH PERCEPTUAL VISIBILITY DURING MOTION-INDUCED BLINDNESS

rotating field. The target flickered at 15Hz for two subjects in experiment 1 (subjects 12 and 13). This change was implemented as our preliminary results showed that there was large hemodynamic onset when the target was physically removed from the image. We reasoned that this may occur because LGN and V1 respond not only to stimulus onsets but also to the offsets of stimuli that have been present for long intervals. We thus wanted to record data where the target presence was in constant fluctuation. As anticipated, this hemodynamic onset was not present when the target constantly flickered. The target was 1° visual angle in diameter and appeared at 5.8° eccentricity (3° left and 5° above the fixation cross).

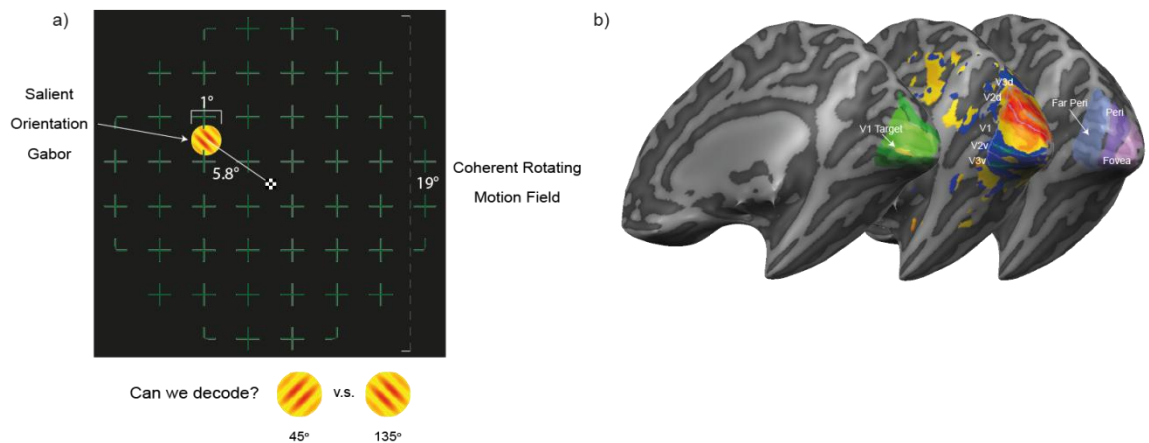


Figure 4.2.1. Stimulus, retinotopic mapping and target mapping. a) Motion-induced blindness stimuli with target in upper left, central fixation cross, and rotating circular array of crosses. We ask if we can decode the orientation of the Gabor presented on the target during motion-induced blindness. b) From left to right – inflated cortical mesh showing retinotopic and target mapping (yellow target region, light green V1, darker green V2v and V2d, darkest green V3v and V3d); retinotopic mapping (showing phase-encoded colour bands at the boundaries of early visual cortical lines V1, V2, V3); and eccentricity mapping (pink fovea, purple periphery, blue far periphery).

4.2.3.3. Procedure

Prior to fMRI participation, subjects completed two runs of a behavioural experiment to ensure they perceived the motion-induced blindness illusion (see **Chapter 4.1**). In

4.2. STIMULUS REPRESENTATIONS IN V1 FLUCTUATE WITH PERCEPTUAL VISIBILITY DURING MOTION-INDUCED BLINDNESS

each run, they observed two 3 minute blocks of MIB stimuli, each followed by a fixation block of 12s. The MIB stimulation was presented at 30cm viewing distance, but otherwise had identical parameters to the stimuli used in the fMRI experiments. We confirmed that they regularly perceived MIB for over 1 second prior to the fMRI experiments.

In two fMRI experiments, we presented visual stimulation via a head-coil-mounted mirror which allowed subjects to view stimuli projected to a screen at the end of the MRI bore. Visual stimulation was presented using Presentation software (Neurobehavioural Systems). In Experiment 1 subjects completed five 8 minute runs. During a run subjects viewed two blocks of 'MIB' stimuli, each lasting 3 minutes, and two blocks of 'target mapping' each lasting 12s. In Experiment 2 subjects completed twelve 14 minute runs across three days (4 runs per session). Each run contained four blocks of 3 minute 'MIB' stimuli, and two blocks of 'target mapping'. 'Target mapping' blocks were presented at the beginning and end of each run, and consisted of contrast-reversing checkerboards shown for 12s each at the same location that the target appeared during MIB stimulation. In both experiments, all blocks were preceded and succeeded by 12s of fixation (white fixation cross and black screen).

The orientation of the target switched between 45° and 135° four times per block in experiment 1 and eight times per block in experiment 2. Subjects were instructed to report the disappearance of the target by holding a right index finger button for the duration of disappearance. The task served to draw attention away from the target orientation, as we did not want subjects to focus on or notice the changes in orientation of the Gabor patch. Task can influence V1 activity, and higher task demands can make visual stimulation harder to decode (Woolgar, Williams, & Rich, 2015). Furthermore, we did not want a subject response to differentiate the oriented Gabors presented as tactile stimuli such as button presses can be decoded in visual cortex (Liang et al., 2013). The target disappeared from perceptual awareness either because subjects perceived motion-induced blindness, or because we removed the target. During experiment 1, the target was removed 4 times per MIB block, for an

interval of between 5-10s. Subjects were not informed that target removal would occur. The targets were never removed in Experiment 2 so target disappearance here was always attributed to motion-induced blindness. There were 3 possible resulting perceptual conditions for the target: No Target (not present, not visible; Experiment 1 only), Target (present and visible), and MIB (present, not visible). We required subjects to maintain central fixation so the fixation cross changed from white to red for 1s, four times during each run. Subjects responded to this colour change with a right middle finger button press.

We recorded polar angle and eccentricity retinotopic mapping (Figure 4.2.1.b). We used wedge-shaped, phase-encoded polar angle stimuli and radial phase-encoded eccentricity stimuli. During polar angle stimulation, a flickering checkerboard wedge (0.42 rad) appeared at the right horizontal meridian and rotated counter-clockwise, completing 12 full cycles of 360°. Each cycle lasted 28 TRs. During eccentricity stimulation, a flickering checkerboard annulus appeared at the centre field and moved outwards in eccentricity, for 12 full cycles. Each cycle lasted 64 TRs. Retinotopic mapping stimulation was presented using custom-made Matlab code (version R2012a, MathWorks, Natick, MA, USA; <http://www.mathworks.co.uk>). Two subjects in experiment 1 and all three subjects in experiment 2 completed retinotopic mapping in a separate session to their experimental runs. During the retinotopic mapping runs, subjects reported fixation colour changes with a button press (right index finger).

4.2.3.4. fMRI Parameters

We measured blood oxygen level-dependent (BOLD) signals using an echo-planar imaging sequence on a 3T Siemens Tim Trio scanner with a 32-channel head coil. In experiment 1, five runs of 500 volumes were recorded at voxel size of 2×2×2.5mm (15 axial slices, TE: 30ms, TR: 1000ms, FA: 62°, FOV: 192mm², inter-slice time: 66ms, gap thickness: 0.25mm). In experiment 2, twelve runs of 828 volumes were recorded at identical parameters. A high-resolution, 192-volume, 3D anatomical scan

4.2. STIMULUS REPRESENTATIONS IN V1 FLUCTUATE WITH PERCEPTUAL VISIBILITY DURING MOTION-INDUCED BLINDNESS

(T1 ADNI, 1mm³ voxel size; TE: 2.96ms, TR: 2300ms, TI: 900ms, FA: 9°, matrix: 256 x 256) was also recorded for each subject. This T1 is similar to an MPRAGE sequence but with sharpened grey/white matter contrast, improving its suitability for cortical segmentation (Jack et al., 2008). Polar angle retinotopic mapping (792 volumes) and eccentricity mapping (536 volumes) were recorded using the same parameters.

4.2.3.5. fMRI Pre-Processing

In Brainvoyager QX, anatomical images were normalised to Talairach space. Functional data for each subject and run (including retinotopic mapping) were corrected for slice time with cubic spline interpolation and were temporally filtered (high-pass filter with linear de-trending). The first 2 volumes were skipped to avoid saturation effects. Experimental runs were 3D motion-corrected to the first functional volume of the first run using trilinear/sinc interpolation then aligned to each subject's T1-weighted structural image and spatially normalized into Talairach space (VTCs). Retinotopic mapping runs were separately aligned to the anatomical. We examined inter-subject alignment between functional data runs based on correlations of pixel intensity in early visual cortex. In experiment 1, the average alignment across runs was $r=0.9502$ and never fell below $r=0.9193$. In experiment 2, the mean alignment score of functional runs across subjects was $r=0.9361$, with a minimum value of $r=0.9092$.

4.2.3.6. Behavioural Analysis

To characterise each subjects' illusion perception we calculated the mean length of MIB perception in milliseconds per run. For each subject, we extracted the data for the condition of MIB, computed the length of time each percept occurred for, counted the number of instances of MIB, calculated the mean length within the run, and then averaged across runs. We bootstrapped a 95% confidence interval for the

group mean length of MIB experience. First we calculated the mean length of MIB for each subject, and then sampled the mean of this group 1000 times with replacement. The 1000 resulting sample means were sorted. An overall mean and the upper and lower values of the 95% confidence interval were calculated. To learn how frequently subjects perceived the illusion, we counted the number of MIB occurrences for each subject in each run and calculated a mean across runs. We bootstrapped ($n=1000$) a 95% confidence interval for the group mean number of MIB experiences in the same manner used to sample the mean length. Behavioural analysis was performed individually per subject prior to scanning to ensure that they perceived the illusion. The same analysis was used for behavioural and fMRI experiments, using Matlab (R2012a, MathWorks, Natick, MA, USA).

Each fMRI volume was allocated to whichever perceptual state was the dominant percept during each TR (i.e. Target, MIB, or No Target). This was accomplished by comparing the millisecond-resolution perceptual response data to the 1000ms period corresponding to each TR, and allocating the recorded volume to whichever percept occupied the majority of that 1000ms (e.g. if the subject perceived the illusion for 800ms of that TR, the TR was allocated to the illusion condition). In experiment 1, three subjects had less than 5 volumes of illusion perception (for an orientation of the Gabor patch) and were discarded from further MIB analyses. In Experiment 2 we recruited three high-experiencing subjects who reported illusion presence of over 25% of time in a behavioural experiment prior to scanning. For each subject and run we calculated the percentage of volumes within a run that belonged to each perceptual state.

4.2.3.7. fMRI Analysis

fMRI Analysis: Univariate

General Linear Model (GLM) analysis and data preparation was carried out in BrainVoyager QX (Version 2.8.4, Brain Innovation, Maastricht, Netherlands, <http://www.brainvoyager.com>). We used two general linear models (GLM) in the univariate analysis. The first GLM modelled the 45° and 135° target MIB stimuli, fixation, and mapping blocks for each run and subject. This GLM was used to identify voxels that respond to the target (Figure 4.2.1.b). The second multi-subject ($n=15$ in Exp.1., $n=3$ in exp.2.), multi-run (MSMR) Random Effects (RFX) GLM modelled the subjects' percept: Target, MIB, or No Target-, fixation, and mapping blocks. For the flicker paradigm, we used two fixed effects GLMs, one per subject.

fMRI Analysis: Region of interest (ROI)

We defined two regions of interest (ROI) in each subject: motion-sensitive area V5 in the right hemisphere, and the region of V1 that responded to the target stimulus. We located right V5 by comparing BOLD activity during conditions that contained the motion field (regardless of target orientation and perceptual experience) against the condition of fixation (using a GLM contrast of 'motion field' > 'fixation'). This V5 ROI was visually inspected on each subject's folded cortical mesh to ensure that the chosen ROI was on the medial temporal gyrus, posterior to the lower bank of the dorsal superior temporal sulcus (consistent with its definition in the literature; Tootell et al., 1995; Tootell & Taylor, 1995; Watson et al., 1993; Zeki et al., 1991). We identified the region of V1 that responded to the target stimulus (henceforth the Target ROI) by measuring increased activity to the target mapping stimulus compared to fixation (using a GLM contrast of 'target mapping > fixation'). Target ROIs were visually inspected using the boundaries of early visual cortical areas and their eccentricity bands (figure 4.2.1.b), to ensure they were within right peripheral ventral V1. See Appendix 4.2. for TAL coordinates and voxel numbers for all ROIs. We entered the voxels from V5 and the target ROIs into a Multi-Subject, Multi-Run GLM to study the univariate responses to each perceptual condition (Target, MIB, or No Target).

fMRI Analysis: Multivariate Pattern Classification

In this fMRI study we used linear SVM classification to assess the information about the oriented Gabor target contained in the multivariate activation pattern. Linear SVM classification is a well-established multivariate analysis method (Haxby et al., 2001), which is highly popular for use in fMRI. In the region of V1 that responded to the target location, for each subject and run, we transformed each voxel's raw time course to percent signal change. The perceptual conditions (Target, MIB, and No Target) were used to index volumes corresponding to these conditions from the time course, with a time shift to account for the lag in the hemodynamic response function. We trained a linear support vector machine (SVM) to learn the multivariate activity patterns associated with the presentation of 45° and 135° oriented Gabor patches within each perceptual condition. To account for the unequal data available for each orientation during each percept (for example during times the target was visible, it may have more often been the 45° rather than 135° oriented Gabor), we extracted the orientation with the least volumes in that percept (MIB or target visible) and run, then randomly sampled an equal subset of volumes from the other orientation. Classification between 45° and 135° was performed on this equal subset. This was repeated 10 times, providing us with 10 sets of classification results based on the iterated comparison datasets of the same size.

Each of the 10 iterated samples was compared to the subset from the other orientation. For average trial classification, the classifier was trained to discriminate target orientation on the labelled activity patterns from trials in n-1 runs (the training dataset), and the resulting model was tested on the average activity patterns of the remaining run (the testing dataset which did not contribute to training the classifier). For single trial classification, the classifier was trained to discriminate target orientation on the labelled activity patterns from n-1 trials available, and the resulting model was tested on the remaining trial. This was repeated until each possible run, and each possible trial had been the testing dataset. Using this 'leave-one-run/trial-out' method, the classifier is always generalising its learnt discrimination of the two orientation conditions to a dataset not used to constructed

the discriminant function. Final classification results for average analysis and single trial analysis were created by averaging across all the accuracies from train-test iterations of that type. The two different types of classification training reflect slightly different aspects of the multivariate pattern, which is why both are reported.

An additional control classification was run which trained and tested on target mapping stimulation versus oriented Gabor patch (45° orientation), using iterative samples to match the number of volumes of the oriented Gabor patch to those of mapping stimulation (as this condition always had less volumes). We then completed leave-one-run/trial-out classification, as above.

In both fMRI experiments, subjects reported the target to be visible more frequently than they reported the target to have disappeared. In experiment 1, subjects perceived motion-induced blindness for an average of 16.3 volumes per run (range 3 - 44.6), and perceived the target to be visible for an average of 122.3 volumes per run (range 92.6 – 143.1). The longer experiment 2 had an average 137.2 volumes in which subjects reported target disappearance (range 67 - 224) and 222.8 volumes in which the target was visible (range 156 – 307). This was a concern, as linear SVM classifiers typically show enhanced performance with larger training and testing datasets. Thus, if we found that we could not classify during MIB but could classify when the target was visible, we would be concerned that this was only an effect of a smaller training dataset for MIB not an effect of the perceptual condition. To examine the effects of the smaller dataset, we sampled a subset of volumes from the ‘target visible’ data for each Gabor patch orientation equal to the maximal number of volumes available in the condition of MIB. We sampled 10 times per subject and across runs, providing us with 10 comparison datasets for each orientation of the same size. We could then enter this data into a classifier analysis, repeating the orientation discrimination classification as above, and obtaining results for when the target was visible but with the training dataset size of the MIB classification.

To determine statistical significance at the group level for each classifier (target visible, target invisible (MIB), target removed, target visible (restricted dataset)) a bootstrapped ($n=1000$) 95% confidence interval was calculated for each comparison by sampling with replacement from individual subject means. This was performed across all subjects for a visible target; however 3 subjects were excluded from the MIB analysis in experiment 1. Classification during perceptual states (Target, MIB, and No Target) was considered significantly above chance if the 95% CI did not include 50%. To determine statistical significance at individual subject level, a condition-label permutation ($n=1000$) was performed on classification values for each iteration and comparison. P-values were calculated as the probability of observing a value as large as the true performance in the distribution of permuted observations.

Despite its popularity, classification has several drawbacks as an analysis technique for assessing pattern information. Although linear SVM uses distance measures to assess which condition the testing dataset belongs to (linear SVM estimates the support vectors by maximizing the minimum distance to the boundaries of the training examples), the result of classification is a binary value (successful or unsuccessful). On each classification, for each set of training and testing data, the model either correctly guessed the condition label of the novel dataset or it did not. Thus the outcome dataset is an accuracy value (% of attempts correct) based on binary not continuous data. Relationships between successful percentages of classification are therefore not meaningful. In this study, for example, we cannot state whether classification during one perceptual condition performs more highly than during another, we can only say whether or not the classifier could decode. Other groups have used representational similarity analysis (RSA, Kriegeskorte et al., 2008), such as that used in Chapter 3. This method examines activation patterns in terms of their similarity, typically using Pearson's correlations. In RSA, similarity can be measured by the percentage of correct pairwise classifications (accuracy), but also by Pearson correlational distance, Euclidean distance, and Mahalanobis distance. Distances provide advantages over classification accuracy as they are continuous data and thus directly comparable. Additionally, they have a meaningful zero, allowing researchers to draw conclusions about proportional relationships (for

example that activation patterns during condition A are twice as similar as in condition B, Kriegeskorte, 2015). Kriegeskorte favours Euclidean and Mahalanobis distance as the outcome of these analyses is clearer to understand, and is not affected by outliers in small datasets as correlation is. Classifiers are additionally subject to ceiling and floor effects and run-specific shifts in activation patterns due to alignment of fMRI data.

With classifier data it is possible to use the shape of a receiving operator curve (ROC), and the empirical area under the curve (eAUC) to determine the success and accuracy of the model. ROC curves typically plot model sensitivity against 1-specificity, or true positive classifications against false positive classifications, whilst the classifier discrimination threshold is varied. The area under a curve can be of any value between 0 and 1, with higher values describing greater probability of successful classification and fit of the classification model. Chance is an AUC of 0.5. The initial problem with this is that the binary values that a classifier with two choices outputs does not provide false positive rates. As our classifier only ever chooses one of two options it cannot falsely positively identify a condition, only falsely allocate the activation pattern it to the other condition. Thus, instead the classifier can be asked to output distance of each outcome to the model hyperplane and this can be transformed into a predicted probability by using a binary logistic model (Platt, 1999). Probability can then be plotted for each model of the train/test data and area under a probability curve can be examined. eAUC is typically used with Linear Discriminant Analysis (LDA) classifiers and often assume a parametric distribution. Thus, the analysis is often unsuitable for use with SVM outputs as SVM output does not follow a parametric binomial distribution. However, it is possible to use non-parametric estimates of eAUC.

4.2.4. Results

4.2.4.1. Behavioural Analysis

4.2. STIMULUS REPRESENTATIONS IN V1 FLUCTUATE WITH PERCEPTUAL VISIBILITY DURING MOTION-INDUCED BLINDNESS

Experiment 1

The mean length of an MIB experience was 1.3 seconds (bootstrapped 95% confidence interval, CI, [1.04 , 1.62s], figure 4.2.2.a.). The mean number of MIB experiences per run was 14.68 (95% CI, [10.8, 19.9], figure 4.2.2.b.). Subjects experienced the illusion for a bootstrapped mean of 8.5% of run time (95% CI, [6.3, 11.4], figure 4.2.2.c.) as compared to 67.9% visible time (95% CI, [65, 70.6]) and 23.4% removed (95% CI, [22.4, 24]).

Experiment 2

The mean length of an MIB experience was 1.9 seconds (bootstrapped 95% confidence interval, CI, [1.3 , 2.4], figure 4.2.2.b.). The mean number of MIB experiences per run was 159.1 (95% CI, [145.8, 172.5], figure 4.2.2.b.). Subjects experienced the illusion for a bootstrapped mean of 38.1% of run time (95% CI, [30, 46.3], figure 4.2.2.c.) as compared to 61.9% visible time (95% CI, [53.7, 70]).

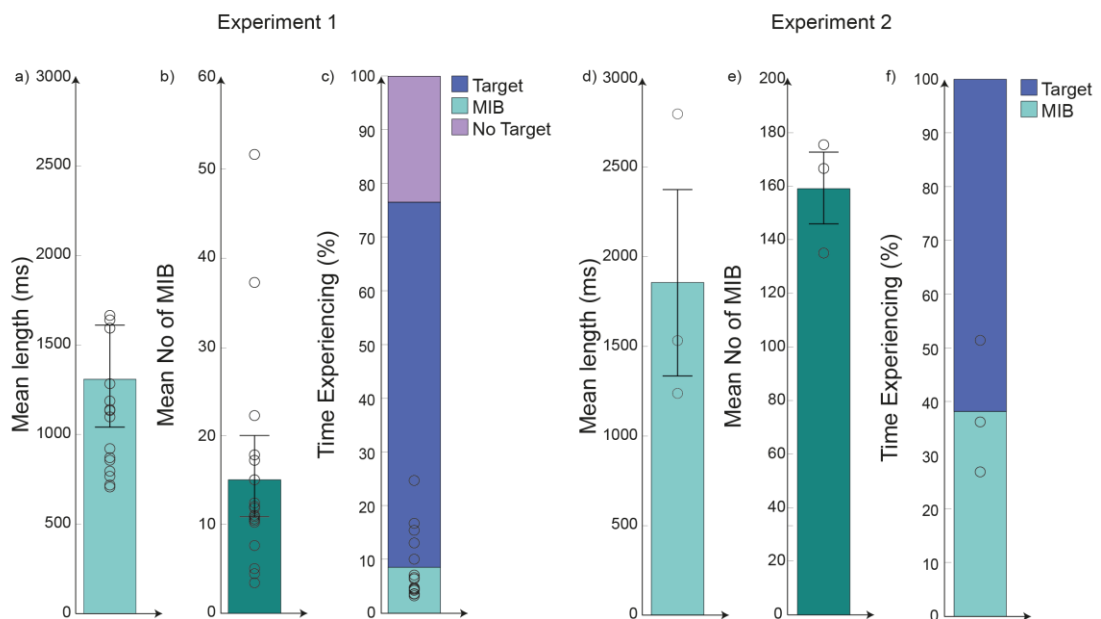


Figure 4.2.2. Behavioural results. Experiment 1: a) Mean length of MIB experience. b) Mean number of MIB experiences per run. c) Mean percent of overall time per run spent experiencing MIB against other percepts. Experiment 2: d) Mean length of MIB experience. e) Mean number of MIB experiences per run. f) Mean percent of overall time per run spent experiencing MIB against other percepts. In all cases circles represent single subjects and bars indicate bootstrapped ($n=1000$) 95% confidence interval.

4.2.4.2. ROI GLM Analysis

Experiment 1

In the group of 15 subjects who were presented with the static target, we investigated if BOLD activity in the region of V1 responding to the target differed across the perceptual conditions. We found no univariate difference in the Target ROI between perceptual experiences (MIB vs. Target, $t(\text{RFX})=0.233$, $p=0.8$; MIB vs. No Target, $t(\text{RFX})=0.69$, $p=0.5$; Visible vs. No Target, $t(\text{RFX})=1.26$, $p=0.23$). V5 was significantly more activated when subjects perceived motion-induced blindness than when the target was visible ($t(\text{RFX})=2.32$, $p=0.038$). Additionally in V5, activation during MIB and when the target was visible was significantly greater than when the target was removed ($t(\text{RFX})=5.564$, $p=0.00012$; $t(\text{RFX})=5.179$, $p=0.0002$ respectively).

Two subjects were presented with a flickering target to more accurately replicate Schölvink and Rees (2010). In the V1Target ROIs there were no significant differences between visible target and MIB activation (S1 $t(\text{FFX})=0.5$, $p=0.61$; S2 $t(\text{FFX})=0.24$, $p=0.81$). One of these subjects showed no significant activation differences between conditions in V1Target (Visible vs No Target $t(\text{FFX})=1.13$, $p=0.26$; MIB vs No Target $t(\text{FFX})=0.73$, $p=0.47$). In the other subject, V1Target was significantly more activated during MIB ($t(\text{FFX})=3.79$, $p=0.00015$) and when the target was visible ($t(\text{FFX})=12.43$, $p<0.000001$) than when the target was removed. In

4.2. STIMULUS REPRESENTATIONS IN V1 FLUCTUATE WITH PERCEPTUAL VISIBILITY DURING MOTION-INDUCED BLINDNESS

the V5 ROIs there were no significant differences between visible target and MIB activation (S1 $t(\text{FFX})=0.07$, $p=0.94$; S2 $t(\text{FFX})=1.34$, $p=0.18$). For both subjects V5 was significantly more activated when the target was visible (S1 $t(\text{FFX})=2.5$, $p<0.01$; S2 $t(\text{FFX})=17.1$, $p<0.000001$) than when the target was removed. For the second subject V5 was also more activated during MIB than when the target was removed (S1 $t(\text{FFX})=0.4$, $p=0.69$; S2 $t(\text{FFX})=6.93$, $p<0.000001$).

Experiment 2

No univariate difference was found between perceptual experiences in V1Target (MIB vs. Target, $t(\text{RFX})=0.198$, $p=0.96$) or in V5 ($t(\text{RFX})= -0.065$, $p=0.95$). In 2/3 individual subjects MIB produced significantly less signal in V5 than visible targets (S1 $t(\text{FFX})= 13.4$, $p<0.00001$; S3 $t(\text{FFX})= 7.4$, $p<0.00001$), and 1/3 subjects had more signal for MIB (S2 $t(\text{FFX})= 12.1$, $p<0.00001$). In V1 Target 2/3 individual subjects showed significantly more activation for MIB than visible targets (S2 $t(\text{FFX})= 10.1$, $p<0.00001$; S3 $t(\text{FFX})= 6.5$, $p<0.00001$), and the opposite was true in 1/3 subjects (S1 $t(\text{FFX})= 20.3$, $p<0.00001$).

There is a notable difference in activation between the two experiments. In the target region of V1, no group analysis found a significant difference between activation when the target was visible and activation during MIB. However, the activation is descriptively higher for MIB in experiment 1 and for visible targets in experiment 2. In V5 in experiment 1 there is significantly higher activation during MIB than when the target is visible. In experiment 2 there is no significant difference and the descriptive beta weights for the two conditions are reversed. More interestingly, the activation for all conditions in the target region of V1 is lower in experiment 2 than experiment 1, but the activation for all conditions in V5 is higher in experiment 2. The stimuli were identical in both experiments, but experiment 2 had longer runs with additional stimulation blocks. We would expect this to improve the estimation model for beta weights. We would also expect increased repetitions to reduce activation due to adaptation. However, subjects recruited for experiment 2 were all

4.2. STIMULUS REPRESENTATIONS IN V1 FLUCTUATE WITH PERCEPTUAL VISIBILITY DURING MOTION-INDUCED BLINDNESS

highly experienced fMRI participants and therefore may have superior attention, upregulating their BOLD activation.

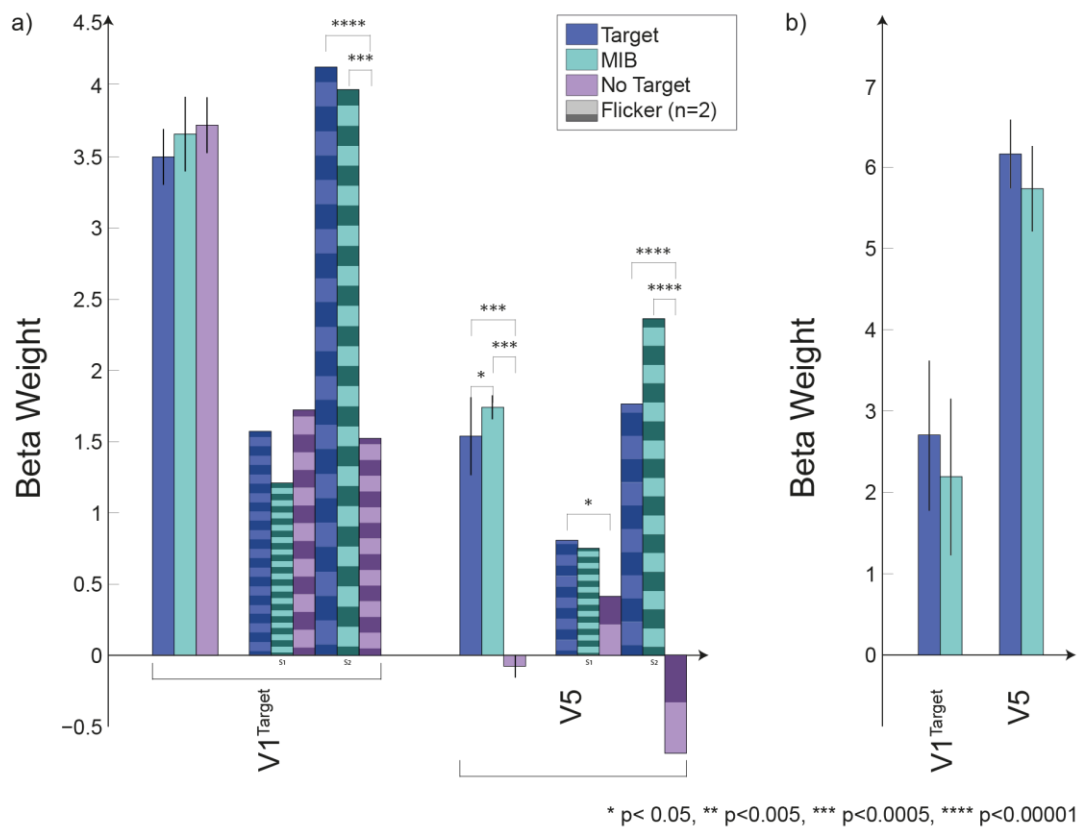


Figure 4.2.3. GLM results in our ROIs. a) Experiment 1: Univariate response in V1 Target space and V5 to each perceptual state (Target, MIB, No Target) during motion-induced blindness stimuli. Horizontal striped bars show each subject's result for the 'flicker paradigm'. b) Experiment 2: Univariate response in V1 Target and V5 to each perceptual state (Target, MIB) during motion-induced blindness stimuli. In both cases stars indicate significant differences as determined by testing contrasts in Linear GLM. Black vertical lines indicate standard error of the beta means.

4.2.4.3. Multivariate Pattern Classification

Classification aimed to decode whether the 45° or 135° oriented Gabor patch target was presented during perceptual conditions of MIB, Target and No Target. This was conducted by training and testing the classifier either on averaged patterns of activity for a whole run of each orientation (average or AVG classification analysis) or by

training and testing the classifier on single trial patterns of activity for each orientation (single trial or ST).

Experiment 1

We could decode target orientation in at least one analysis when the target was visible to subjects in 12 of 18 subjects (bootstrapped mean accuracies when using single trial and average analyses were 53.3% and 70.9% respectively; Figure 4.2.4.a. shows single subjects data in blue- only those with MIB decoding). However, during MIB, we were only able to decode target orientation in 2 of 15 subjects (bootstrapped mean accuracies when using single trial and average accuracies were 51.3% and 57.2% respectively, Figure 4.2.4.a shows single subject data in green), although the targets remained onscreen. At the group level, we could decode orientation when the targets were visible (Group 95% CI [52.1 , 54.5] for single trial analyses and 95% CI [64.1 , 77.2] for the average, Figure 4.2.4.b.). Again, we could decode orientation at the group level during motion-induced blindness in only one analysis (Group 95% CI [48,54.9] for single trial, and 95% CI [51.7, 62.2] for average, Figure 4.2.4.b).

We conducted three control analyses. To check that we were decoding target information, we ascertained that we could not decode when there was no target (see Figure 4.2.4.b mean 50.1% ST, Group 95% CI [48.4, 51.7], 49.1% AVG, Group 95% CI [43.7 , 53.9]; we can significantly decode in 1/16 individual subjects, on ST only). We also tested a classification that should decode easily- asking the classifier to decode between the target and the checkerboard mapping condition (bootstrapped mean 71.2% ST, Group 95% CI [68.7 , 73.8], 97.3% AVG, Group 95% CI [95.7 , 98.8]; we can significantly decode in 18/18 individual subjects in both analyses; not shown on graph).

4.2. STIMULUS REPRESENTATIONS IN V1 FLUCTUATE WITH PERCEPTUAL VISIBILITY DURING MOTION-INDUCED BLINDNESS

Our third control analysis was to decode visible target orientation when we restricted train and test volumes to the number of volumes used to decode during MIB. This was crucial to ensure that our effects (able to decode when the target was visible but not during MIB) were not merely due to the restricted number of train and test volumes during MIB compared to when the target was visible. With these data restrictions we were able to decode the target orientation when the target was visible at the group level (bootstrapped mean 51.6 % ST, Group 95% CI [50.5 , 52.7], and 57.9% AVG, Group 95% CI [53.9 , 61.6]; Figure 4.2.6.a). However we could not decode the orientation in any single subject (0/18 subjects significant; Figure 4.2.6.a). We therefore could not truly ascertain whether the disrupted decoding observed during MIB is an effect of the illusion or of reduced train and test volumes. Experiment 2 aimed to solve this concern.

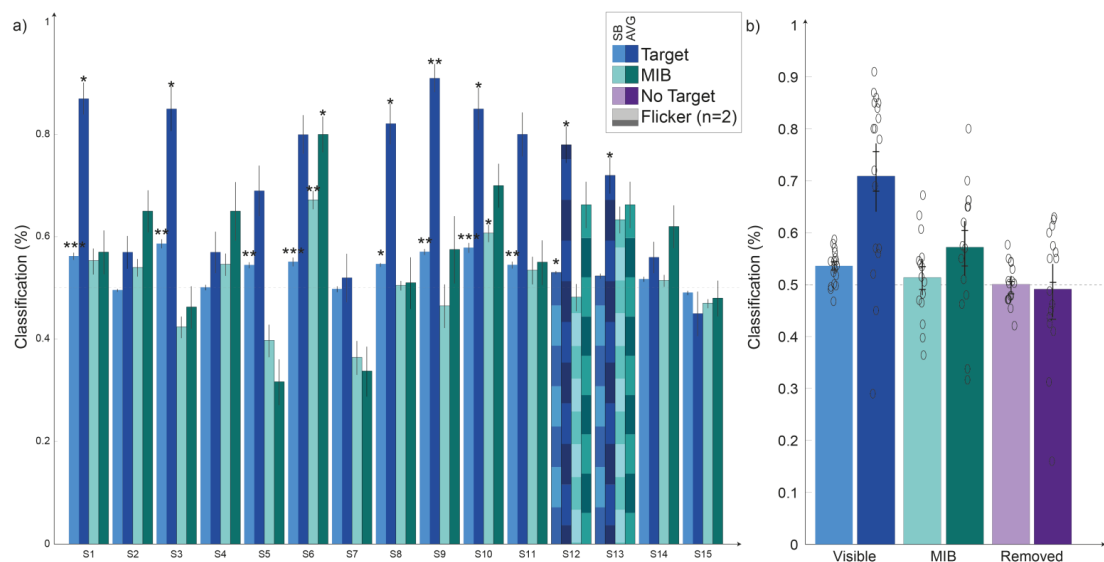


Figure 4.2.4. Multivariate classification results decoding 45° vs 135° Gabor patch orientation for Experiment 1. a) Single subject classification results when the target was visible (blue bars) and during MIB (green) demonstrate that we can decode orientation in most subjects when the target was visible to them but not when it was perceptually invisible. Vertical black lines indicate standard error of the single subject means. b) Group mean classification results when the target was visible (blue), during MIB (green), and when the target was physically removed (purple) demonstrate that at the group level we can decode orientation when the target was visible to subjects, when it was perceptually invisible, but cannot decode when it was physically removed from the image. Vertical lines indicate 95% bootstrapped ($n=1000$) confidence intervals on the group means. Horizontal lines indicate

4.2. STIMULUS REPRESENTATIONS IN V1 FLUCTUATE WITH PERCEPTUAL VISIBILITY DURING MOTION-INDUCED BLINDNESS

standard error of the group means. In both graphs) Chance classification performance is 0.5. Light colours indicate single trial classification method; dark colours indicate average classification method. Stars indicate single subject p-value * $p < 0.05$ ** $p < 0.01$ *** $p < 0.005$.

Experiment 2

In all three subjects we could decode target orientation when the target was visible (Figure 4.2.5., blue bars). Mean classification accuracy was 52.6% using single trial analysis (single subjects: 51.8%, $p=0.023$; 54.5%, $p=0.006$; 51.6%, $p=0.027$) and 81.3% using average trials (single subjects: 74.2%, $p=0.016$; 95.8%, $p=0.010$; 73.8%, $p=0.019$). In contrast, decoding was disrupted during MIB although the targets remained onscreen. Mean classification accuracy was 50.8% using single trial (single subjects: 50.4%, $p=0.30$; 50.6%, $p=0.32$; 51.3%, $p=0.12$) and 63.1% using average trials (67.5%, $p=0.037$; 61.7%, $p=0.16$; 60%, $p=0.15$). We were able to decode target orientation in 1 of 3 subjects, only using average trial decoding (Figure 4.2.5., green bars). As a control we could easily classify between the target checkerboard mapping condition and a present target with mean 83% ST (85.1%, $p=0.006$; 85.5%, $p=0.004$; 78.3%, $p=0.006$) and 99.7% AVG (100%, $p=0.01$; 100%, $p=0.01$; 99.2%, $p=0.008$). We can significantly decode in 3/3 individual subjects in all cases.

4.2. STIMULUS REPRESENTATIONS IN V1 FLUCTUATE WITH PERCEPTUAL VISIBILITY DURING MOTION-INDUCED BLINDNESS

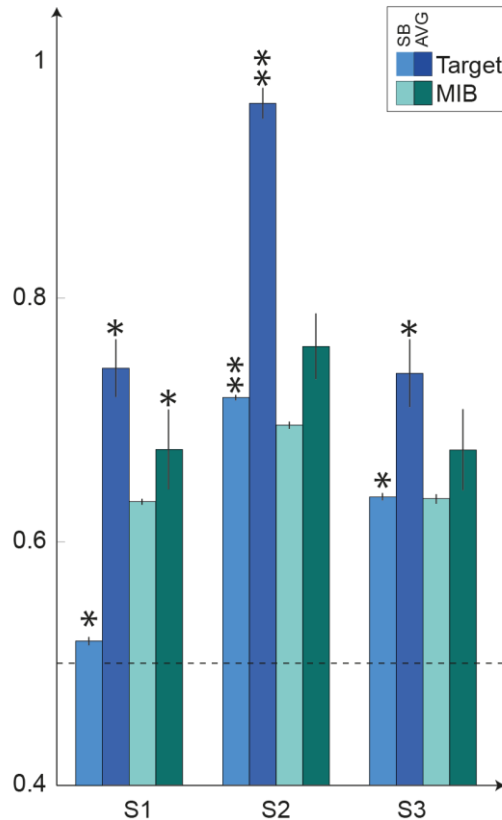


Figure 4.2.5. Multivariate classification results decoding 45° vs 135° Gabor patch orientation for Experiment 2. Single subject classification results when the target was visible (blue bars) and during MIB (green) demonstrate that for all subjects we can decode the orientation when the target was visible, however we could only decode when the target was perceptually invisible in one subject. Vertical lines indicate standard error of the single subject means. Chance classification performance is 0.5. Light colours indicate single block classification method; dark colours indicate average classification method. Stars indicate single subject p-value * $p < 0.05$ ** $p < 0.01$ *** $p < 0.005$.

Lastly, we ensured that visible target orientation could still be decoded when we restricted the train and test volumes to the number used to decode during MIB. We were able to significantly decode the visible target orientation. Mean accuracies when using single trial and average analyses were 52.6% (52.1%, $p=0.012$; 53.9%, $p=0.003$; 51.8%, $p=0.033$), and 75.7% (70.8%, $p=0.037$; 86.3%, $p=0.006$; 70%, $p=0.053$) respectively (see Figure 4.2.6.b).

4.2. STIMULUS REPRESENTATIONS IN V1 FLUCTUATE WITH PERCEPTUAL VISIBILITY DURING MOTION-INDUCED BLINDNESS

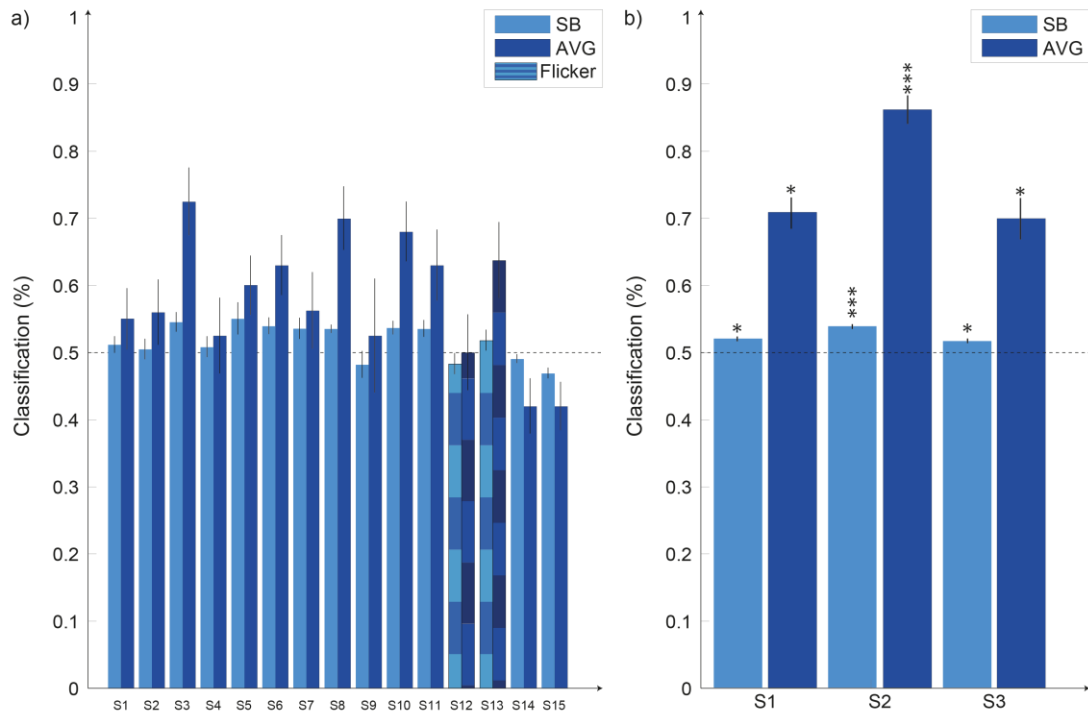


Figure 4.2.6. Control analysis equating volumes. Multivariate classification results decoding 45° vs 135° Gabor patch orientation when the target was visible. Analysis used only the number of volumes available for MIB decoding. a) In experiment 1- decoding is not possible in single subjects when only the number of volumes used for MIB classification is allowed. b) In experiment 2 classification is possible in single subjects using only the number of volumes available for MIB decoding. In both graphs) Vertical lines indicate standard error of the single subject means. Light colours indicate single trial analysis, dark colours indicate averaged analysis. Stars indicate single p-value * $p < 0.05$ ** $p < 0.01$ *** $p < 0.005$.

4.2.5. Discussion

Previously it was unclear whether targets were represented in V1 during perceptual blindness. We provide evidence that changes in conscious perception during a bistable visual illusion are paired with changes in the stimulus representation at the level of V1, in the absence of any change in the feedforward visual input. Using fMRI, we recorded subjects viewing MIB stimuli with targets which had orientation properties. We examined the representation of this feedforward target orientation

during perceived target visibility and invisibility. Our findings confirm that the target representation in early visual cortex is distorted when the target becomes invisible through motion-induced blindness, but not when the target remains visible.

Cortical Feedback during Motion-Induced Blindness

We propose that target representation during motion-induced blindness is distorted through cortical feedback from V5, as opposed to purely through lateral connectivity. Cortical feedback from diverse extrastriate areas is implicated in other illusions where effects are observed at the level of V1 (Fang, Boyaci, Kersten, & Murray, 2008; Jancke et al., 2004; Kok et al., 2014; Muckli et al., 2005; Murray, Boyaci, & Kersten, 2006). Extrastriate visual motion area MT/V5 is a likely candidate region for feedback to V1 during MIB- it is important in determining a global motion percept (Muckli et al., 2005), and is a causal feedback pathway in other motion illusions such as apparent motion (Akselrod et al., 2014; Chong et al., 2015; Muckli et al., 2005; Muckli et al., 2002; Sterzer et al., 2006; Vetter et al., 2013; Wibrall et al., 2009). V5 neuron receptive fields span dimensions far greater than the separation of our target and field stimuli, and back-projections from this region span the same dimensions or further, allowing V5 feedback to affect a wide region of early visual cortex (Stettler, Das, Bennett, & Gilbert, 2002). Crucially, V5 feedback is capable of ‘filling-in’ responses in V1, spurring V1 activation with particular features (Muckli et al., 2005). This includes information with specific temporal and orientation features (Chong et al., 2015). These properties would allow such feedback to ‘fill in’ information about the motion field in to V1, across the same space as the target representation, overwriting the feedforward signal.

We find increased activation in V5 during MIB in comparison to when the target is visible (also observed by Schölvinc & Rees, 2010). Nuruki, Oliver, Campana, Walsh, and Rothwell (2013) found that disrupting V5 using theta burst TMS stimulation reduces the frequency and duration of target disappearances; supporting a top-down role of V5 in inducing MIB. These findings are consistent with Donner

et al's (2008) results and accompanying proposal that top-down influence from ventral stream representations of the motion field cause target disappearance, whilst influence from target representations in the dorsal stream enable visibility. Additionally, Sterzer, Kleinschmidt, and Rees (2009) propose that MIB arises as the result of top-down feedback which dictates the 'winning' percept between the field and target, and suppresses feedforward information which is inconsistent with this percept. In this conceptualisation, top-down communication determines the perceptual outcome but also has neural effects in early visual cortex consistent with our observations. Previous neurophysiological results demonstrate that the presence of a motion field reduces neural responses to the physical removal and reinstatement of a target in macaque V1 (Libedinsky, Savage, & Livingstone, 2009). The authors propose that weakening of the bottom-up target response increases noise in the feedforward signal and therefore better enables disappearance to be imposed in a top-down manner. We demonstrate distortion of a still-present feedforward orientation stimulus during perceptual invisibility in MIB. We therefore support the proposition that MIB and other bistable percepts are driven by cortical competition between the neural representations of the static target and the moving mask at multiple levels of cortical visual processing (Blake & Logothetis, 2002; Bonneh et al., 2001; Donner et al., 2008; Graf et al., 2002).

Low level Mechanisms Cannot Adequately Explain MIB

Several investigations have suggested that target overwriting could occur entirely within early visual cortex through boundary or contrast adaptation (Hsu et al., 2004, 2006), or surface completion (Graf et al., 2002). Whilst MIB is subject to boundary adaptation and depth ordering, and occurs more at increasing eccentricities from fixation (Graf et al., 2002; Martinez-Conde, Macknik, Troncoso, & Dyar, 2006), MIB demonstrates some important behaviours which make low level overwriting an insufficient explanation (Hsu et al., 2006). MIB is perceived for greater percentages of time with higher contrast and higher saliency targets, whilst adaptations like perceptual fading occur predominantly at low contrast (Bonneh et al., 2001; Hsu et al., 2004). MIB persists with the target as close as 1° from central fixation, and MIB

targets protected by static masks do not disappear (Bonneh et al., 2001). Motion fields therefore appear to be necessary for MIB, whilst not necessary for boundary or contrast adaptation, or for surface completion (Graf et al., 2002). Additionally, MIB can occur with targets which slowly move, even across into the other visual hemifield (Bonneh et al., 2001). Thus the mechanism that causes MIB cannot be solely local. Multiple MIB targets disappear separately, or in a grouped manner depending on their higher-level properties- adaptations would predict that all targets disappear similarly (Bonneh et al., 2001). MIB also still occurs when the target is placed in front of the motion field, suggesting that surface completion alone is inadequate in explaining the effect (Graf et al., 2002). Hsieh and Peter (2009) demonstrated that microsaccades increase prior to target reappearance and decrease before disappearance, suggesting that MIB disappearance was an effect of adaptation and explainable solely by low level visual processes. However, Bonneh et al. (2010) demonstrated that microsaccadic change actually occurs in response to perceptual change during MIB, supported by a literature that demonstrates microsaccade rate and direction modulation in response to sensory and cognitive events (Engbert, 2006; Rolfs, 2009).

Motion-induced blindness can also be induced using illusory figure motion fields, therefore without any real feedforward stimulus (Graf et al., 2002). In this case lateral connectivity within V1 would contain no feedforward motion field information in the absence of feedback about the illusory figure (Kok et al., 2016; Kok & de Lange, 2014). Whilst it is still possible that our effects are partially driven by long-range lateral connections (Stettler et al., 2002), low level processing fails to provide a comprehensive explanation for the target distortion we observe. Furthermore, interactions of lateral connections are themselves driven partially by feedback (Ramalingam, McManus, Li, & Gilbert, 2013).

Retained Target Representations

We demonstrate distorted target representation in V1 in the majority of subjects during MIB; however we find that target orientation information is retained in a few subjects. Additionally, behavioural evidence suggests that target representation is preserved (Hofstoetter et al., 2004; Meital-Kfir, Bonnef, & Sagi, 2015; Mitroff & Scholl, 2005; Montaser-Kouhsari et al., 2004). Preserved target properties during invisibility suggest that MIB originates in extrastriate, not early, visual cortex. Cortical layer specificity may clarify why some preservation of target representation is seen in our, and others', data. The neocortex is sub-divided into six horizontal layers, which are distinct in their anatomy and connections to other sites. Feedback, feedforward, and lateral connections terminate in distinct layers of early visual cortex (Larkum, 2013; Markov et al., 2014; Sillito, Cudeiro, & Jones, 2006). Feedforward information is delivered to the mid-layers (Felleman & Van Essen, 1991). As feedforward information is always present during MIB stimulation, mid-layer representation of the target should be consistently present. Feedback terminates in the superficial (Muckli et al., 2015; Rockland & Pandya, 1979) and potentially in the deepest layers of V1 (Kok et al., 2016; Rockland & Pandya, 1979; Self et al., 2013). Feedback may terminate in deep layers when feedforward information is present and in superficial layers when it is not (Kok et al., 2016). Alternatively, long-range feedback from distal origins may arrive in deep layers (Markov et al., 2013). We hypothesise that feedback motion field information may be therefore present in superficial and/or deep cortical layers during MIB, disrupting decoding of the target representation. During target visibility these obscuring signals are not present. Our proposal therefore allows for a retained target representation in some cortical layers whilst other layers represent the motion field through feedback. Furthermore, the BOLD signal we recorded in 3T fMRI reflects the contribution of all cortical layers and thus our data will reflect both feedback and the preserved feedforward information in mid-layers (Uludağ, Müller-Bierl, & Uğurbil, 2009). Studies of motion-induced blindness using high-field fMRI would allow layer separation and permit us to clarify whether orientation representation is preserved in mid-layers during MIB.

V1 Activity Correlates with Perception

Our results contribute to a growing body of literature demonstrating that activity in early visual cortex can reflect conscious perception, as opposed to passively representing feedforward visual input (Rees, 2013; Rees, Kreiman, & Koch, 2002; Tong, 2003). In our paradigm we observe disruption of the target representation in V1 when it is invisible, despite ongoing feedforward stimulation. Activity in early visual cortical areas varies with perceptual awareness during other bistable percepts, for example in binocular rivalry (Lee, Blake, & Heeger, 2007; Polonsky, Blake, Braun, & Heeger, 2000; Tong, 2003; Tong & Engel, 2001), during figure/ground segregation (Lamme, 2003; Super, Spekreijse, & Lamme, 2003; Supèr, Spekreijse, & Lamme, 2001; Supèr, van der Togt, Spekreijse, & Lamme, 2003), and in the line-motion illusion (Jancke et al., 2004). However these changes in early visual cortex almost certainly occur in concert with feedback effects from higher level areas which may dictate the percept (Muckli et al., 2002; Murray et al., 2002; Sterzer, Russ, Preibisch, & Kleinschmidt, 2002). Crucially, several prominent theorists suggest that interactions between feedback and feedforward information dictate what reaches consciousness (Bachmann, 2015; Lamme, 2014; Rees, 2013) as fluctuations in early visual cortical areas can occur without accompanying perceptual change (Rees, 2013). Therefore in motion-induced blindness the fluctuation in feedforward stimulus representation may interact with alternating top-down representations of the motion field or target (Donner et al., 2008) to produce either target visibility or illusory blindness.

4.2.6. Conclusion

In conclusion, we present evidence that the cortical representation of the target is disrupted when the target is invisible during motion-induced blindness. Despite ongoing feedforward target input this disruption is apparent at the level of V1. Internal processing related to an illusory state therefore disturbs the feedforward processing of target properties. Our data additionally demonstrates a further link between V1 representation and resulting perception. We suggest that the observed

4.2. STIMULUS REPRESENTATIONS IN V1 FLUCTUATE WITH PERCEPTUAL VISIBILITY DURING MOTION-INDUCED BLINDNESS

low level distortion occurs through cortical feedback from extrastriate visual area V5. We propose that top-down motion field information from V5 overwrites feedforward target processing in V1, in line with propositions that top-down cortical competition drives motion-induced blindness and other bistable percepts.

5. OF MONSTERS AND MEN- THE FLASHED FACE DISTORTION ILLUSION AS A DEMONSTRATION OF OBJECT-GENERAL VISUAL PREDICTIVE CODING

Fiona McGruer^{1*} & Meike Ramon^{1,2*}.

¹*University of Glasgow, Centre for Cognitive Neuroimaging, Institute of Neuroscience and Psychology, 58 Hillhead Street, G12 8QB, Glasgow, United Kingdom*

²*University of Louvain, Psychological Science Research Institute, Institute of Neuroscience, 10, Place du Cardinal Mercier, 1348 Louvain-La-Neuve, Belgium*

* Both authors contributed equally to this work

Acknowledgements

FM is funded by the ESRC; MR is funded by the Belgian National Fund for Scientific Research (FNRS).

5.1. Abstract

The flashed face distortion (FFD, Tangen et al., 2011) is a new illusion in which faces presented briefly and sequentially in the visual periphery appear monstrously distorted. In this study, two experiments explored parameters of FFD which have yet to be systematically investigated: the effect of presentation timing on perceived distortion, and the reliance of the FFD effect on face-specific processing mechanisms. In the first experiment, subjects rated the magnitude of perceived distortion across different presentation durations and race of face stimuli (Western Caucasian, WC; Eastern Asian, EA). In the second experiment two groups of subjects (WC, EA) were required to judge on which side of the visual field the distortion was greater. Contrary to previous studies, the results of both experiments suggest that FFD is not strongly affected by the timing of successive stimuli presentations. Beyond this, perceived distortions did not vary as a function of subject/stimulus race, or visual field, indicating that the FFD illusion may not be mediated by face-specific mechanisms. We propose that the illusion is the result of a domain-general predictive network that compares successive objects when they rapidly replace one another in the same retinotopic space, emphasizing differences between successive stimuli.

5.2. Introduction

The human visual system has developed to rapidly form representations of the external sensory world. Adaptive behaviour relies on our ability to integrate novel incoming information to update these sensory representations and perceive our changing environment. Visual illusions can be utilized to study the mechanisms underlying this adaptive process, as they exploit the difference between perceived and actual visual stimulation. For example, during apparent motion observers perceive motion when individual stimuli are presented briefly at rapidly alternating locations. Illusions have been suggested to reflect the outcome of a constructive cortical system which perceives the most *likely* stimuli based on the sensory input it receives (Weiss et al., 2002). In the case of motion illusions, quick alternating inputs at two locations are most likely the effect of an item moving between two locations, and thus this is perceived.

One prominent explanatory model of visual perception, Predictive Coding theory (Clark, 2013; Friston, 2010; Lee & Mumford, 2003; Rao & Ballard, 1999) is founded in the idea of constructive perception. It posits that our brains form predictions about the sensory environment based on complex internal models. Such internal models are fed back down the cortical hierarchy, all the way to early sensory areas. Relative to the initially formed representation, differences in the actual incoming feedforward stimulation can be considered as ‘violations’ of expectations. These so-called prediction errors signal the need for an updated representation, and are fed forward up the hierarchy to inform higher models (Friston, 2010; Muckli & Petro, 2013). Representations are therefore continuously updated following comparison with new visual input (Friston, 2010). Feedback enables integration of these representations across greater distances of the visual field, and allows feedforward visual information to be combined with information from higher visual and non-visual cortical areas (Muckli & Petro, 2013).

Illusions are of particular interest in studying predictive feedback within the visual system, as they provide a unique opportunity to dissociate perceived (a combination of feedforward and feedback information) and actual (feedforward) stimulation. In this manner we can also examine the confluence of feedback and feedforward effects, as compared to purely feedforward effects. The aforementioned perception of apparent motion is considered to demonstrate the role of predictive coding as a general mechanism involved in perceptual processing. Under this conceptualization, prediction error arises due to the lack of feedforward stimulation in the parts of visual cortical space in which apparent motion is subjectively perceived. Motion feedback from V5 activates that space and thus reduces the prediction error (Muckli et al., 2005; Vetter et al., 2013; Wibrall et al., 2009). Predictive coding is also implicated in other illusory phenomena. Murray et al. (2006) established that retinotopic maps of proximally and distally located objects in V1 represent *perceived*, as opposed to *veridical* size in the visual field. Objects perceived to be further away were represented by larger proportions of V1 and V2 than the same objects perceived more closely, despite V1 and V2 typically representing the veridical size of an object in the retinotopic visual field. In the hollow mask illusion (Gregory, 1997; Króliczak, Heard, Goodale, & Gregory, 2006) strong prior expectations dictate that faces should be convex,

based on experience with human faces. These priors force viewers to always perceive the face as convex (Dima et al., 2009).

Recently, Tangen et al. (2011) reported the 'Flashed Face Distortion' (FFD) illusion. In this visual illusion faces presented rapidly in the visual periphery are perceived as monstrously distorted. The faces observed were eye-aligned Slavic faces, which were reported to become highly distorted after approximately one minute. The authors suggested that, "Relative encoding seems to drive the effect. That is, forcing the observer to encode each face in light of the others" (Tangen et al., 2011, p. 628). As the authors' aim was to describe a novel illusion, only few experimental details and no analyses were provided. Since this seminal report, only one other study has further investigated FFD (Wen & Kung, 2014). Focusing on the relationship between perceived distortion and neural activation within early visual cortex and two posterior face-preferential regions (occipital and fusiform face area, OFA and FFA), Wen and Kung (2014) reported that activation within these regions positively correlated with perceived distortion.

Given the scarcity of investigations of FFD, a number of questions remain unanswered. First, both Tangen et al. (2011) and Wen and Kung (2014) posit a relationship between the degree of perceived distortion and the timing at which faces are presented. Tangen et al. (2011) stated that a timing of 200-250ms per face presented was optimal, whilst Wen and Kung (2014) reported that 200-500ms was optimal, and Utz and Carbon (2015) reported preliminary results suggesting that the illusion decays at a presentation time of 100ms compared to 250ms. As the timing parameter was not varied parametrically in any study, the precise temporal limits of FFD remain currently unspecified.

A second question concerns the degree to which FFD relies on general object perception mechanisms, or those specific to faces. As mentioned above, Wen and Kung (2014) addressed the involvement of face-preferential areas in the FFD illusion. Given the use of faces as stimuli, at the surface the involvement of such regions may seem plausible. However, if the FFD effect arises due to a domain-general process, their approach and resulting conclusions may not be ideal. Tangen et al. (2011) reported that FFD is readily

perceived when stimuli are presented upright or inverted (although see Utz & Carbon, 2015, who suggest inversion lessens the illusion). In face processing literature, the dependency on canonical (i.e., upright) stimulus presentation is an indicator of the involvement of a face-specific mechanism—holistic processing (for reviews see Rossion, 2008, 2009). For instance, humans' ability to process facial information relevant for processing of identity is highly orientation-dependent, i.e., is reduced by stimulus inversion (Barton, Keenan, & Bass, 2001; Busigny & Rossion, 2010; Crookes & Hayward, 2012; Goffaux & Dakin, 2010; Pachai, Sekuler, & Bennett, 2013; Ramon, 2015; Sekunova & Barton, 2008; Tanaka & Gordon, 2011; Van Belle, De Graef, Verfaillie, Rossion, & Lefèvre, 2010; Yin, 1969). In stark contrast, processing of non-face objects of comparable inter-stimulus similarity is significantly less affected by changes in orientation (Haxby et al., 1999; Valentine, 1988).

We believe that the FFD illusion may represent a powerful tool to study the aforementioned predictive coding model on a behavioural and neural level. Under the assumptions of this theoretical model, FFD arises as internal representations of face stimuli are formed and compared to the continuously changing visual information as the stimuli are replaced by other faces. Given the likely atypical frequency with which different identities are perceived in the same retinotopic location, prediction error arises where there are comparative deviations between individual faces. These deviations are emphasized retinotopically by error signals and the internal model is updated with the details of the new face. Emphasis by retinotopically specific error is consistent with increases in activation observed by Wen and Kung (2014). This account of the illusion does not require the stimuli to be face-specific, as similar prediction error should occur for objects that occur in the same visual space.

We reasoned that prior to determining the neural correlates of FFD, the questions regarding time-dependency and face-specificity should first be systematically addressed. While the former can be tested through variations of presentation timing parameters, the question of face-specificity can be addressed in different ways. One approach is to test subjects' performance for faces and non-face objects under the same task constraints, (Hershler, Golan, Bentin, & Hochstein, 2010; McKone & Robbins, 2011; Rezlescu, Barton, Pitcher, & Duchaine, 2014; Sun et al., 2012). However, we suggest that for non-face objects it would be challenging—if not impossible—to elicit subjective impressions of grotesqueness (see

discussion). An alternative approach, adopted here, involves designing an experimental paradigm which incorporates well-established markers of face-specific processing mechanisms. In the present study we implemented two aspects to address face-specificity: race processing and visual field presentation.

Firstly, we used face stimuli derived from the same, or a different ethnic background relative to the observers'. Previous research suggests that the perceptual illusion that other-race faces 'all [...] look alike' (Anthony, Copper, & Mullen, 1992; Feingold, 1914; Hugenberg, Young, Sacco, & Bernstein, 2011; Malpass & Kravitz, 1969; Tanaka, Kiefer, & Bukach, 2004) is related to less efficient engagement of face-specific mechanisms for other-race faces (Michel, Corneille, & Rossion, 2007; Michel, Rossion, Han, Chung, & Caldara, 2006; Valentine, 1991; Vizioli, Rousselet, & Caldara, 2010). Therefore, we reasoned that, if FFD relies on face-specific mechanisms, it should be more pronounced for same, as compared to other-race faces. Secondly, we varied the location at which same- and other-race faces were presented. Previous research suggests that perceptual processing of faces is associated with left visual field (LVF) superiority (Ellis & Young, 1983; Levine, Banich, & Koch-Weser, 1988; Levy, Heller, Banich, & Burton, 1983; Rhodes, 1985; Sergent & Bindra, 1981; Yovel, Levy, Grabowecky, & Paller, 2003). We reasoned that face-specificity of FFD should therefore manifest in terms of more pronounced perceived grotesqueness for faces presented within the LVF.

To summarize, in the present study we sought to determine the temporal boundaries of the FFD illusion, as well as its face-specificity. To this end we parametrically varied the frequency with which face stimuli were replaced by the next face. Moreover, we used faces of same- and other-race individuals presented to groups of observers from two different ethnic backgrounds (Western Caucasian, WC; Eastern Asian, EA¹). Varying the duration of stimulus presentation, as well as stimulus race across visual fields, subjects indicated where faces were perceived as most grotesque. If face-specific mechanism(s) are at play, the observed FFD should be most pronounced for same-race faces presented at short durations

¹ Here, 'Western Caucasian' refers to white European subjects, while 'Eastern Asian' refers to subjects from the eastern subregion of the Asian continent (China, Macau, Japan, North Korea, South Korea, Mongolia, and Taiwan).

within the left visual field. Our findings indicate, however, that neither of these variables was associated with differences in perceived distortion magnitude, supporting the idea that a domain-general predictive coding account may best explain the FFD effect.

5.3. Method

5.3.1. *Participants*

Subjects with normal or corrected-to-normal vision were recruited through the University of Glasgow. All subjects received course credit or financial compensation for participation. Three independent groups of subjects were tested: the first ($n=10$, 7 female, mean age: 22.6 years, 9 right-handed) completed the first experiment. Two further groups of subjects from different ethnic backgrounds completed the second experiment (WC: $n=15$, 8 female, mean age: 21.7 years, 14 right-handed; EA: $n=15$, 8 female, mean age: 22.6 years, 15 right-handed). Subjects participated in only one of the experiments.

5.3.2. *Stimuli*

The stimuli used had been created for a previous study (Ramon et al., 2016), and contained individual identities belonging to two ethnic groups. Each stimulus set (WC, EA) consisted of faces of 25 young males and 25 young females (100 total identities). The stimuli represented full frontal 2D images rendered from 3D face models captured with 3D Studio Max (<http://www.autodesk.co.uk/>, 2008). The images were devoid of non-facial and external cues and were aligned for bilateral pupil position and mouth centre (warped so that all 3 landmarks were at the same position in subjects' visual field for every face). Sequences of stimuli were presented peripherally, offset by 5° of visual angle to either side of a central fixation cross (distance from fixation to the centre of the stimulus: 8° of visual angle). Face stimuli comprised 6° and 9° of visual angle in width and height, respectively. Figure 5.1.a illustrates examples of stimuli presented (consent for publication obtained for individuals depicted);

Figure 5.1.b illustrates the predicted observation of larger FFD under the assumption that the illusion reflects a face-specific mechanism.

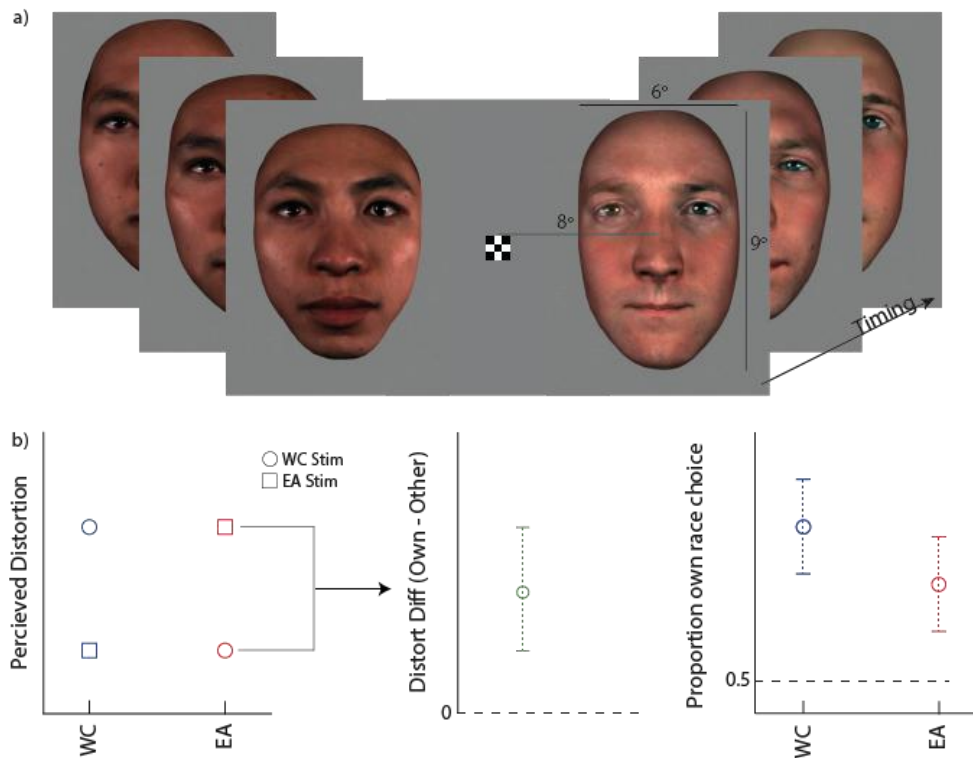


Figure 5.1. Experimental procedure and expected results. a. Examples of stimuli presented bilaterally to a central fixation. The number of faces presented per second was varied parametrically (see Methods). b. Expected outcome if FFD is face-specific: Perceived distortion and proportional distortion difference score (distortion score/total possible distortion score; for own-for other) should be greater for same- than for other-race faces (Experiment 1). Own-race faces should be perceived as more distorted than other-race faces in a forced choice decision paradigm, and thus proportional own-race choice (# of own race-choices/# of possible own-race choices) should be above 0.5 (Experiment 2).

5.3.3. Procedure

Prior to participation all subjects provided informed written consent. All subjects were tested on the same desktop computer screen (1920x1080 resolution); viewing distance (60cm) was kept constant using a chin rest. Subjects were instructed to maintain fixation and respond according to the instructions as provided by the experimenter.

Experiment 1. The first experiment served to establish whether timing had a significant effect on the perceived distortion of either own-race, or other-race face stimuli. The variables of interest in this experiment were presentation duration, and stimulus race. Subjects were presented with sets of faces displaying the same race across visual fields (WC/WC or EA/EA); presentation order for the 50 identities per race was randomised. Subjects saw 4 blocks of the experimental stimuli, with 16 trials per block and a break in between each block. Trials lasted between 6.25 and 25s depending on presentation timing of face stimuli (250ms, 500ms, 750ms, or 1000ms duration before replacement with next face). Each timing/stimulus race pairing was presented 8 times, in randomized order. Following each trial, subjects used the '1-7' number keys on the keyboard to indicate the perceived strength of the effect on a Likert scale shown on screen, 1 indicating 'no distortion' and 7 indicating 'extremely distorted'. Subjects completed a test trial of WC/EA faces at all four different timings to familiarise them with the experimental procedure, although two different race faces were never presented together in Experiment 1. The entire experiment lasted ~30min.

Experiment 2. The second experiment served to extend the findings of Experiment 1 to a scenario in which subjects performed forced-choice decisions, while manipulating observer race and visual field of stimulus presentation. The variables of interest in this experiment were visual field, presentation duration, as well as subject and stimulus race, respectively. In this experiment subjects were presented with sets of faces of the same or different races across both hemifields (WC/WC, EA/EA, WC/EA, or EA/WC); presentation order for the 50 identities per race was randomised. Each subject completed a total of 128 trials. Trial duration varied between 6.25s and 25s, depending on presentation duration (250ms, 500ms, 750ms and 1000ms), which varied in a quasi-randomized manner. Each of these visual field pairings (WC/WC, EA/EA, WC/EA, or EA/WC) as a given trial occurred eight times per presentation duration (250ms, 500ms, 750ms or 1000ms). At the end of each individual trial, subjects were instructed to indicate on which side the faces appeared to be more distorted, using a button press. Prior to the actual experiment, each subject completed one practice trial per timing (WC-WC pairing) to demonstrate the procedure. The entire experiment lasted ~45min.

5.3.4. Analysis

Experiment 1. For each subject, stimulus race, and presentation timing we calculated a proportionally-adjusted mean distortion score by averaging across trials for a given condition and dividing by the possible highest score (7). We then computed a difference score for each subject per timing as [own-race proportional distortion] – [other-race proportional distortion] (see also Figure 5.1.a); a difference score of zero therefore reflects no effect of stimulus race. For each presentation timing the difference scores were bootstrapped (number of bootstrap samples: 1000) to obtain 95% confidence intervals (btCIs) around the group mean. Differences were considered significant if btCIs did not include zero (no rated distortion difference between own- and other-race faces).

Experiment 2. For each subject, each visual field containing own-race stimulus, and presentation timing we calculated a score reflecting the proportional choice of own-race faces. This was calculated by extracting trials in which subjects had a choice of own- and other-race faces, and defining as [number of own-race choices]/[total possible number of own-race choices] to create a score reflecting the proportion of own-race choices. A proportional choice score of 0.5 therefore reflects own- and other-race faces being chosen equally. For each presentation timing and per visual field, proportional own-race choice values were bootstrapped (number of bootstrap samples: 1000) to obtain 95% confidence intervals (btCIs) around the group mean separately for each subject race group. Differences were considered significant if btCIs did not include 0.5 (an equal choice of own- and other-race faces).

5.4. Results

Experiment 1: Stimulus race and timing do not affect perceived distortion ratings

5. OF MONSTERS AND MEN- THE FLASHED FACE DISTORTION ILLUSION AS A DEMONSTRATION OF OBJECT-GENERAL VISUAL PREDICTIVE CODING

Mean distortion scores for WC and EA faces as a function of stimulus timing are provided in Table 5.1. These scores were similar across presentation timings, and differed slightly depending on stimulus race.

Timing	250ms		500ms		750ms		1000ms	
	WC	EA	WC	EA	WC	EA	WC	EA
Mean ±	5.41 ±	4.97 ±	5.83 ±	5.12 ±	5.58 ±	5.02 ±	5.59 ±	4.77 ±
SD	.84	.92	.86	1.11	.92	.89	1.16	1.15

Table 5.1. Distortion rating by stimulus race (SR) and presentation timing. Mean distortion ratings were extracted from a Likert scale of 1-7. Means are presented with standard deviations.

As illustrated in Figure 5.2. the bootstrapped 95% confidence intervals computed on the difference score of proportional distortion ratings between own- and other-race faces included zero at all stimulus timings. Therefore, subjects' ratings of perceived distortion did not significantly differ between own- and other-race face stimuli, regardless of presentation timing.

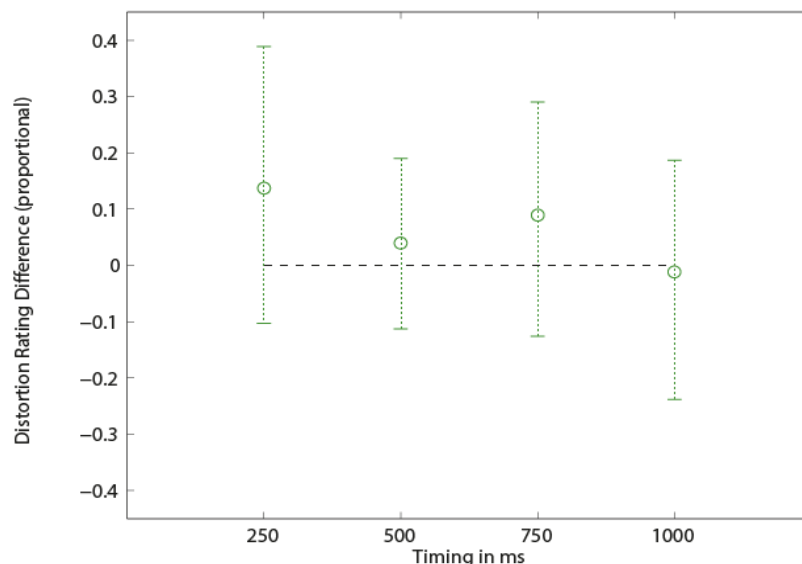


Figure 5.2. Proportional distortion difference between own- and other-race faces. 95% bootstrapped CIs around the proportional distortion rating (distortion rating/total possible distortion rating) for own-race - proportional distortion rating for other-race stimuli. All intervals include 0,

5. OF MONSTERS AND MEN- THE FLASHED FACE DISTORTION ILLUSION AS A DEMONSTRATION OF OBJECT-GENERAL VISUAL PREDICTIVE CODING

indicating no significant difference in perceived distortion due to stimulus race, at any presentation timing.

Experiment 2: Stimulus and subject race, presentation timing, and visual field do not affect distortion choice

Mean proportional own-race choices are provided in Table 2.; there were no obvious differences across presentation timings, visual field, or subjects' race.

Timing	<u>250ms</u>				<u>500ms</u>			
	<u>WC</u>		<u>EA</u>		<u>WC</u>		<u>EA</u>	
OwnSide	<u>Left</u>	<u>Right</u>	<u>Left</u>	<u>Right</u>	<u>Left</u>	<u>Right</u>	<u>Left</u>	<u>Right</u>
Mean ± SD	0.56 ± 0.26	0.58 ± 0.35	0.55 ± 0.3	0.43 ± 0.32	0.55 ± 0.37	0.58 ± 0.34	0.54 ± 0.24	0.53 ± 0.34
Timing	<u>750ms</u>				<u>1000ms</u>			
	<u>WC</u>		<u>EA</u>		<u>WC</u>		<u>EA</u>	
OwnSide	<u>Left</u>	<u>Right</u>	<u>Left</u>	<u>Right</u>	<u>Left</u>	<u>Right</u>	<u>Left</u>	<u>Right</u>
Mean ± SD	0.51 ± 0.35	0.54 ± 0.33	0.6 ± 0.27	0.54 ± 0.26	0.53 ± 0.35	0.55 ± 0.37	0.55 ± 0.3	0.59 ± 0.26

Table 5.2. Proportional own-race choice as a function of stimulus and subject race, visual field, and presentation timing.

The 95% confidence intervals computed on the proportional score of most distorted choices between own- and other-race faces included 0.5 (equal choice) at all stimulus timings for both groups of subjects (Figure 5.3.). This was true irrespective of the visual field within which own-race stimuli were presented. Therefore, in both groups of observers perceived distortion did not significantly differ between own- and other-race faces, at any stimulus timing or visual field.

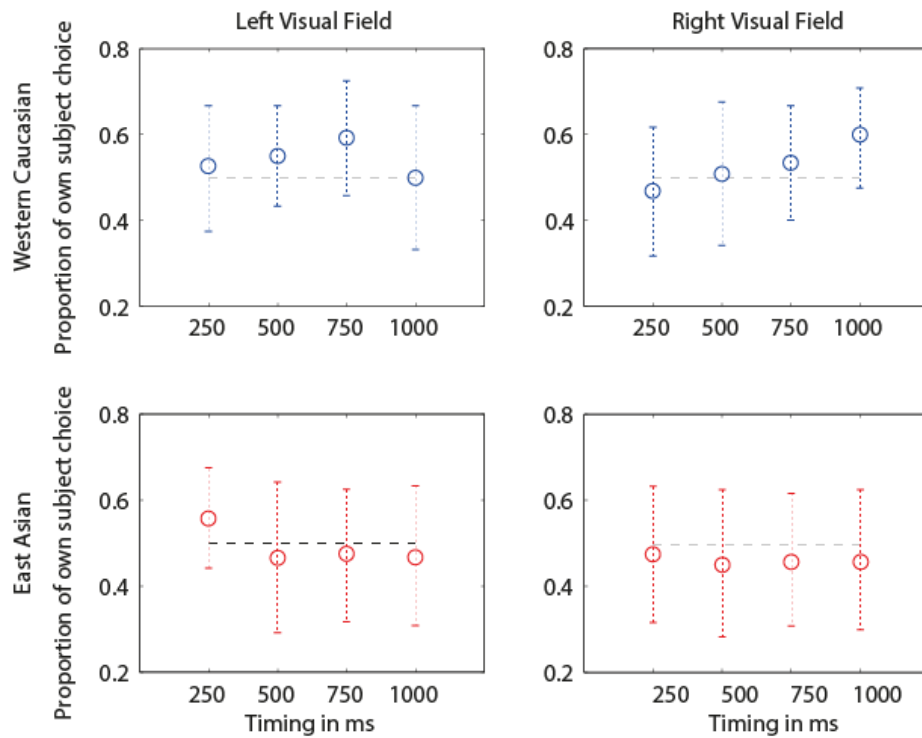


Figure 5.3. Proportional own-race choice as a function of stimulus and subject race, visual field, and presentation timing. 95% bootstrapped CIs around the mean proportion of own-race choices (*proportional own-race choice* = # of own-race choices/# of total possible own-race choices). Across both observer groups all intervals include 0.5, indicating no significant differences in choice of side due to stimulus race, in either visual field or at any presentation timing.

5.5. Discussion

In the present study we aimed to provide the first in-depth investigation into the temporal boundaries of the FFD effect, as well as the extent to which this illusion is driven by face-specific mechanisms. To this end, groups of observers from different ethnic backgrounds were presented with individual faces of same- or other-race faces that alternated with varying frequency. Following the initially reported presentation regime, the stimuli were presented bilaterally to both visual fields, and subjects indicated on which side FFD was perceived as most pronounced. Using a bootstrapping analysis technique with a 95% confidence interval, we found no significant effects of presentation duration, visual field presentation, or race of

subject/stimulus on the perceived distortion. In retrospect, a linear mixed effects model may have been more appropriately used to ensure our testing was adequately powered. However, we believe that our results are robust as they stand.

Presentation timing does not affect perceived distortion magnitude

Tangen et al. (2011) reported that presentation durations of 200-250ms per face gave rise to the strongest effects. Along the same line, Wen and Kung (2014) stated that presentation durations of between 250-500ms were optimal for eliciting FFD. Contrary to both studies, in independent groups of observers we discerned no effect of timing—irrespective of whether subjective distortion ratings were provided or subjects had to provide forced-choice decisions.

While further replication of this lack of time-dependency is required, two aspects regarding the previous reports of FFD should be considered. Firstly, the methodological details and rigor provided by Tangen et al. (2011) are limited—their goal was to provide a brief report of a novel visual illusion. Therefore, the presentation durations they state as being optimal are anecdotal not formally investigated. Secondly, Wen and Kung (2014) indicate that the perceived FFD strength was compromised when the number of faces was small. Wen and Kung's work demonstrates a conflation of the importance of many varied face stimuli and the importance of timing parameters—they varied number of faces presented and therefore can only imply that more individual faces produce greater distortion. Our work supports recent preliminary findings from Utz and Carbon (2015) that there is no significant difference in perceived distortion between presentation durations of 250ms and 1000ms. Additionally, Utz and Carbon (2015) found that perceived distortion does significantly decrease when faces are presented for only 100ms, suggesting that the presentation duration for each face cannot be too brief.

Other-race effects do not influence perceived distortion

Another issue concerns the stimuli used in the previously reported studies of the FFD illusion. Tangen et al. (2011) used a homogenous sample of Slovakian (Western Caucasian) faces presented to the Western Caucasian experimenters who acted as participants. Wen and Kung (2014) used the same set of faces in their study, and used a predominantly East Asian subject group ($n=13$ East Asian, 1 Central American; personal communication with Dr. Wen). Therefore, we assume that the effects are observed independently of the relationship between observer and stimulus race. However, it is possible that Wen and Kung's (2014) study contained an aspect of other-race processing that the original study did not. Interestingly, it is precisely the demonstration of increased encoding efficiency for, and subsequently discrimination between own-race faces along with the relative impairment for processing other-race faces that is considered an indication of face-specific mechanisms.

Therefore, we furthermore aimed to ascertain the extent to which FFD relies on face-specific mechanisms. Previous work observed that FFD is robust to orientation changes (i.e., it is also perceived when faces are presented in a non-canonical (inverted) orientation; Tangen et al., 2011). This provided preliminary evidence that face specific mechanisms may have only a partial role in the illusion. To address this question we manipulated the race of faces observed, i.e., both WC and EA observers judged FFD in same- and other-race faces. Under the assumption of reliance on a face-specific mechanism we reasoned that FFD should vary with the subjectively perceived similarity between individual faces, and therefore should be larger for own-, as compared to other-race faces. Other-race face similarity was suggested to be due to a smaller face-space model for other-race faces, based on reduced experience in differentiating other-race faces (Valentine, 1991). We found no indication that the FFD effect relies on face-specific mechanism(s), as perceived distortion did not vary as a function of stimulus/observer race. One other study has observed a reduction in FFD in other-race faces and also in ape faces (Utz & Carbon, 2015).

Visual Field Presentation does not Affect Perceived Distortion

Lastly, we investigated whether the FFD would differ across visual fields. Some illusions show a left visual field bias, including the Muller-Lyer illusion (Clem & Pollack, 1975; Houliard, Fraise, & Hecaen, 1976); the Opper-Kundt illusion (Rothwell & Zaidel, 1990); and the herringbone illusion (Rasmjou, Hausmann, & Güntürkün, 1999). Additionally, Michel et al. (2006) suggest that own-race faces are perceived more holistically than other-race faces, and Ramon and Rossion (2012) demonstrated that in early perceptual processing stages, holistic face processing is more prominent for stimuli presented in the left visual field. This is supported by the long standing left visual field bias (Gilbert & Bakan, 1973; Yovel, Tambini, & Brandman, 2008), which posits preferential and more efficient processing of visual information presented in the left as compared to the right visual field. Across subject groups, and independent of presentation timing, we found no difference in perceived distortion between left and right visual fields for own-, nor other-race faces.

Flashed face distortion is not face-specific

Based on the present and previous findings we argue that FFD depends on a general, i.e., non-face-specific mechanism. It bears similarities to both the Face Distortion After Effect (FDAE, Webster & Maclin, 1999) and shape-contrast effects. In the FDAE, prolonged adaptation to faces distorted on a single dimension creates perceived distortion in a successive normal face, in the opposite direction from the distortion of the training stimulus. There are three notable differences between the FDAE and FFD. Firstly, the FDAE only occurs with long adaptation periods (up to several minutes, Hills, Holland, & Lewis, 2010), whereas the FFD illusion is robust at 200ms per stimulus (100ms may be a lower limit, Utz & Carbon, 2015). Secondly, the FFD effect creates distortion in any contrasting dimension or feature, not a singular dimension. Lastly, the FDAE requires an unnaturally distorted adaptation image, whereas FFD occurs when all stimuli are non-distorted. A more relevant finding is that adaption to a normal face over 5 seconds biases subsequent face perception in the opposite direction (Leopold, O'Toole, Vetter, & Blanz, 2001). Later investigation by the same group found that the length of adaptation strengthens perceived distortion (Leopold, Rhodes, Müller, & Jeffery, 2005), whereas FFD occurs on a much shorter timescale. Suzuki and Cavanagh (1998) demonstrated shape contrast effects, in which rapidly presented shapes bias the perception of an existing shape. However, FFD operates when images are replaced

by one another, whereas in shape contrast effects interacting shapes are interspersed. Shape contrast effects also occur at much shorter latencies (for as little as 60ms presentation duration).

As stated before, a comparative illusion for non-face objects would be difficult to produce. It may be difficult to source objects in which all individual stimuli have diverse features that occupy similar retinotopic space in the manner that faces do, and that are aligned on a singular sensible dimension without recruiting artificial, and therefore unnatural objects (e.g., Greebles; Gauthier & Tarr, 1997). In such artificially-produced non-face objects distortions may be less obvious; i.e., potentially only Greeble experts could determine whether their dimensions appeared in any way distorted (Gauthier & Tarr, 1997; Tangen et al., 2011). We suggest that the perceived grotesqueness in FFD may be partially driven by the likelihood of noticing distortions in faces and saliency of these distortions even if the basic illusory effect originates from non-face-specific processing mechanisms.

Predictive coding in the flashed face distortion illusion

We suggest that cortical predictive coding mechanisms may underlie FFD. Specifically, based on our extensive experience through real-life scenarios, we create a model for perceiving objects or people in which they have constancy. An object or face must move, or be occluded, to be completely replaced by another. Our top-down prediction would therefore anticipate *temporal consistency* of the face or object identity occurring at a specific retinotopic location in the visual field. In the FFD paradigm, faces are quasi instantaneously and continuously replaced by others. Given a change of stimulus, the comparative differences between the new face and a prior one would create prediction error in early visual cortex (Alink et al., 2010). At locations of prediction error, the inconsistent new features are emphasized, creating the perceived distortion that represents the FFD illusion. Importantly, the conceptualization of FFD as a result of predictive coding introduces testable hypotheses- for example that faces which are more retinotopically similar should create less perceived distortion upon change. Secondly, we can hypothesize that learned face sequences should induce less perceived distortion than unlearned sequences.

Neural correlates of the flashed face distortion

Cortical prediction involvement in FFD is supported by Wen and Kung's (2014) findings. These authors reported a correlation between the magnitude of the perceived distortion and BOLD response in early visual cortex and posterior face selective regions (OFA, Gauthier & Tarr, 1997; and FFA, Kanwisher, McDermott, & Chun, 1997). We would suggest that on a neural level FFD results from feedback from higher visual areas to the early visual cortex. Leopold et al. (2001) note that the comparative face distortions they observe occur across different positioning and size of adapting and test stimuli, and are therefore unlikely to occur within early visual cortex. In the previously described FFD paradigms, the FFA and OFA may indeed be involved due to the use of face stimuli (Andrews et al., 2002; Haxby, Hoffman, & Gobbini, 2000; Kanwisher, Tong, & Nakayama, 1998). The lateral fusiform face area is particularly implicated in facial identity processing (George et al., 1999; Haxby et al., 2000; Hoffman & Haxby, 2000) and therefore may code when multiple facial identities replace one another at a single retinotopic location. However, FFA activation is reduced for inverted faces (Kanwisher et al., 1998), whilst FFD still occurs for inverted faces. FFA involvement alone cannot drive FFD. Therefore, we would suggest that effects comparable (if not larger) to those observed in the OFA and FFA may also be observed within object-preferential areas of the lateral occipital complex if objects were used (LOC, Grill-Spector, 2003; Malach, Levy, & Hasson, 2002). This region, as well as other extrastriate ventral occipito-temporal areas (e.g., Aguirre, Zarahn, & D'esposito, 1998; Epstein & Kanwisher, 1998; Ishai, Ungerleider, Martin, Schouten, & Haxby, 1999; Tanaka, 1993, 1996) represent objects across variations of luminance, motion, and texture and may therefore represent object 'gist' (Gilaie-Dotan, Ullman, Kushnir, & Malach, 2002; Grill-Spector et al., 1998; Ishai, Ungerleider, & Haxby, 2000; Kastner, De Weerd, & Ungerleider, 2000; Kourtzi & Kanwisher, 2000). Additionally, these regions show activation correlated with perception of an object and not low level feature attributes (Bar et al., 2001; Dolan et al., 1997; Doniger et al., 2000; Grill-Spector, Kushnir, Hendler, & Malach, 2000; Hasson et al., 2001; James, Humphrey, Gati, Menon, & Goodale, 2000; Kleinschmidt, Büchel, Zeki, & Frackowiak, 1998; Kleinschmidt et al., 2002; Kourtzi & Kanwisher, 2000; Moutoussis & Zeki, 2002; Tong, Nakayama, Vaughan, & Kanwisher, 1998; Vanni, Revonsuo, Saarinen, & Hari, 1996).

5.6. Conclusions

Our findings provide evidence that in the flashed face distortion illusion the presentation duration of successive stimuli does not significantly affect perceived distortion (when each stimulus is presented for a duration between 250 and 1000ms). Furthermore, the illusion does not appear to rely on face-specific processing mechanisms, as neither variations of stimulus race, nor visual field produced differences in the FFD. Based on our findings we propose that FFD is mediated by object-general predictive coding mechanisms, the neural basis of which will be addressed in the future.

6. DISCUSSION

This thesis investigated whether perceived reality, specifically during visual and multisensory illusions, is modulated by cortical feedback. Illusions present a valuable tool to probe the dissociation between sensory stimulation and resulting perception, and to understand the interactions between feedforward sensory input and feedback information. However, the effects of top-down and bottom-up information in illusion perception are not fully understood, and many illusions remain to be exploited to investigate cortical processing. In this thesis, we focused on how illusion-related feedback can modulate activity in early visual cortical area V1, either as a mechanism that induces the illusion or as an effect of the illusion at higher cortical levels. Secondly, we investigated the relationship between subject's scores on schizotypy scales and illusion perception. We discuss the potential for developing illusory paradigms in clinical subject groups as a method for exploring top-down feedback in schizophrenia. This thesis argues that feedback occupies a key role in illusion generation, contributes to illusory effects in V1, and is potentially important in understanding the schizophrenic response to illusory stimuli.

6.1. Chapter Summaries

We conducted four studies to investigate cortical feedback during visual illusions. In **Chapter 2** we investigated the crossmodal boundaries of the rubber hand illusion (RHI; Botvinick & Cohen, 1998) in subjects scoring more or less highly on the Prodromal Questionnaire (Loewy et al., 2011). We varied the synchronicity of visual and tactile stimulation to determine whether high-scoring subjects experienced different strengths of RHI perception than low scoring subjects. In **Chapter 3** we conducted an RHI fMRI study which used visuotactile stimulation to investigate tactile and proprioceptive crossmodal feedback to V1, and to examine the effects of illusory perception in V1. In **Chapter 4** we used the motion-induced blindness illusion (MIB; Bonnefante et al., 2001) to probe the role of feedback to V1 in illusions. We first determined with behavioural experiments whether oriented Gabor patches can act as MIB targets, and at which eccentricity and size (**Chapter 4.1**). We then presented an fMRI study which examined whether the features (orientation) of a target which is not perceived are still represented in V1, or whether this representation is overwritten by motion feedback (**Chapter 4.2**). In **Chapter 5** we tested whether a new visual

illusion, flashed face distortion (FFD; Tangen et al., 2011), relies on face-specific mechanisms, or can be explained by an object-general predictive coding framework. We now emphasize the key conclusions from each chapter, and then combine these findings to discuss their implications with respect to the current literature. Additionally, we discuss remaining challenges in the field, and potential for future studies.

Chapter 2: Crossmodal Boundaries of the RHI in Prodromal Subjects

In **Chapter 2** we performed a psychophysical experiment investigating rubber hand illusion perception in a group who obtained floor scores on the Prodromal Questionnaire (PQ; Loewy et al., 2011), and another who scored in the medium to high range. The PQ measures a subject's level of risk of psychosis. We varied the strength of the evidence for the illusory percept (that the hand was a body part) by changing the consistency of visual stimulation to the rubber hand and tactile stimulation to the real hand. Increased visuotactile asynchronicity has previously been shown to reduce illusion perception (Shimada et al., 2009). Following each stimulation period, subjects described their experiential outcomes using Likert scale statements. We anticipated that with increased visuotactile asynchronicity, the top-down evidence for the rubber hand as a body part would decrease and therefore illusion strength would decrease (Shimada et al., 2009). Additionally, we predicted that subjects scoring higher on the Prodromal Questionnaire would experience a stronger illusion, as previous evidence in schizophrenic subject groups would suggest (Germine et al., 2013; Peled et al., 2003; Thakkar et al., 2011). We expected the higher Prodromal scoring group to maintain illusion perception at higher asynchronicities (Parsons et al., 2013), whereas typical subjects experience illusion cessation at 300ms visuotactile asynchronicity (Shimada et al., 2009).

In both subject groups, increased visuotactile asynchronicity decreased the response to all Likert statements, replicating Shimada et al's (2009) finding in typical subjects. Above 300ms asynchronicity the illusion was significantly lessened. We propose that coherent visual and tactile feedforward information signalling a touch to one's own hand causes conflict between different multisensory inputs inferring the origin of sensation as part of the body or as the viewed rubber hand. The illusion arises to explain away this conflict. The sensation of body ownership is in this case top-down, and so the RHI demonstrates a case where high level information is affected by feedforward sensory inputs to form an illusion. When the visual and tactile touches are instead asynchronous, there is no modulation of the higher level

body schema. We did not find any effects of PQ scoring group on illusion perception, nor any interaction between PQ group and visuotactile synchronicity. This is in contrast to our expectation that higher PQ scorers would experience a stronger RHI and experience the illusion at higher visuotactile asynchronicities (Germine et al., 2013; Parsons et al., 2013). It is possible that the medium to high scoring group are simply not meaningfully different from the low scoring group. Alternatively, high-risk subjects as measured by the PQ may not show different effects during the RHI, and/or effects may not be observed until symptom onset. Importantly, the lack of a group difference in illusion perception suggests no difference in the change in top-down body schema. These results do not support a ‘spectrum’ of schizophrenia-proneness in illusion perception nor in effects on cortical feedback.

Chapter 3: Visuotactile Illusion Perception in Early Visual Cortex

Concurrent to the behavioural investigation of the rubber hand illusion, in **Chapter 3** we developed a fMRI paradigm for the rubber hand illusion in typical subjects. We investigated whether effects of the RHI are manifested in early visual cortices and/or affect neural processing in extrastriate cortex. Illusion-related feedback has been demonstrated in early visual cortex (Muckli et al., 2005; Seghier et al., 2000; Sterzer et al., 2006) but not in the case of multimodal illusions. The rubber hand illusion is traditionally associated with increased activation in the ventral premotor cortical areas and other motor and integration regions (Ehrsson et al., 2005; Ehrsson et al., 2004; Tsakiris & Haggard, 2005). However, several authors suggest that the illusion is also mediated by visual motion area V5 (Bekrater-Bodmann et al., 2014). In the RHI, vision appears to ‘win’ over existing body schema, suggesting that visual stimuli are influential enough to bring about high level cognitive changes in body schema. Subjects experienced two stimulation types (synchronous and asynchronous) and indicated their perception of illusion onset or absence. This allowed us to dissociate the effects of illusion perception and the stimulation condition. Importantly, visual input was consistent (regardless of stimulation or illusion perception), whilst tactile input and perceptual experience varied. We analysed the associated univariate and multivariate activity in vPMC, V5, LOC, V1 and the subregion of V1 corresponding to the retinotopic representation of the rubber hand.

We found that both tactile stimulation and illusion perception have effects on BOLD activation in multiple regions of visual cortex- V5, LOC and V1. We found V5 reacted in an

interactive manner to illusion presence and stimulation, as did global V1. We also found increased activation in vPMC and the rubber-hand-specific area in V1 for illusion perception irrespective of tactile stimulation type. Additionally we found a specific pattern of activation for illusory experience in early visual cortex (global V1 and hand-specific subregion of V1) irrespective of tactile stimulation type. Our results demonstrate firstly that tactile stimulation has effects even in the early sensory cortices of other modalities. We also observed that V5 and V1 react to the consistency between the current body schema and the stimulus inputs. That V5 and global V1 react most strongly to ‘inconsistent’ percept and stimulation pairings is consistent with ideas of ‘prediction error’ in reaction to unexpected stimuli (Alink et al., 2010, see discussion on cortical predictive coding theories in **chapters 1.5** and **6.8**) and demonstrates an interaction between the illusion-related feedback and tactile feedback to visual cortex. Furthermore, illusion perception induces a specific pattern in early visual cortex, irrespective of which stimulation condition was experienced. The pattern of activation is different when the illusion was not experienced, even when both tactile and visual stimulation were identical. The multisensory rubber hand illusion therefore seems to induce a unique representative pattern in V1.

Chapter 4: Orientation Decoding in Early Visual Cortex during Perceptual Blindness

In **Chapter 4** we probe whether changes in early visual cortex occur when an illusion erases awareness of visual stimuli. Previously Schölvink and Rees (2010) recorded increased activation in early visual cortex and V5 for blinded targets compared to visible or removed targets. This finding is consistent with a change in the target representation. We used motion-induced blindness stimuli with 45° or 135° oriented Gabor patches as targets to probe whether the multivariate target pattern is still represented in V1 during perceptual blindness. During apparent motion we know that motion feedback from V5 can ‘write’ information into V1 (Muckli et al., 2005; Sterzer et al., 2006). We therefore hypothesised that motion-induced blindness occurs when motion field information is fed back from V5 to early visual cortex, overwriting target pattern information in V1.

We observe increased activation in V5 during perceptual blindness, but not when the target is physically removed. Additionally, we find that orientation can no longer be decoded from V1 during motion-induced blindness, implying that target pattern representation is in some manner overwritten. We therefore present a case where identical feedforward input does not

produce an identical representation in early visual cortex. The representation is instead overwritten, likely by feedback from V5 regarding the surrounding motion field. Paired with the findings from **Chapter 3**, we also contribute to theories in which V1 activity is more closely related to perception than previously thought (Rees, 2013; Rees et al., 2002; Tong, 2003) – in this case disappearance of the target perceptually is paired with distortion of the target pattern representation in V1.

Chapter 5: Object-General Visual Predictive Coding

In **Chapter 5** we conducted a psychophysical experiment which probed a relatively newly discovered illusion- flashed face distortion (Tangen et al., 2011). We asked whether the illusion arises from face-specific mechanisms as previously speculated or object-general mechanisms. We proposed that the illusion could result from predictive comparisons within the same visual space, which are not necessarily face-specific. Subjects of two ethnicities observed 25 faces from two ethnic groups, of each gender, presented rapidly in the periphery of both visual hemifields. Subjects then reported their perception of distortion. In one experiment subjects were required to rate overall perceived distortion on a Likert scale, in the other they answered with a forced choice of which visual field presentation was more distorted. We varied race of the stimulus faces (same as subject or not) as the main item of interest, in addition to the visual field in which the same-race images appeared, and duration of each face presentation. Own-race and other-race effects are considered a marker of face-specific processing in psychophysical tasks (Michel et al., 2007; Michel et al., 2006; Vizioli et al., 2010). Additionally, face processing is associated with left visual field dominance (Yovel et al., 2003). These two variables therefore allowed us to test whether the illusion arises from face-specific mechanisms- if so, it should be enhanced for same-race faces and when presented to the left visual field.

We found that FFD is not sensitive to race differences, does not show a visual field bias, and does not show a timing difference. The illusion is therefore likely to reflect an object-general comparison process as opposed to a face-specific mechanism. These results reject the assumption in existing FFD studies that because the illusion involves faces it is necessarily face-specific. Additionally we propose this new illusion for consideration which may be an effect of top-down comparison processes. We propose opportunities for future research, including artificially manipulating the similarity between faces, or using objects as opposed

to faces to probe an object version of the illusion. If the distortions do arise from comparative processes, then perceived distortion should vary by how physically similar successive faces are (with less similar faces inducing greater distortion). Such a manipulation could also be used to confirm that FFD is not face-specific. If FFD is object-general then distortion should increase linearly with increased dissimilarity between successive faces. If however FFD induces some face-specific mechanisms one would expect significant increases in distortion when facial differences induce a new/different perceived identity across successive presented faces (Rhodes & Jeffery, 2006). Comparison during FFD may be underlined by a mechanism that says objects cannot rapidly replace one another in the same retinotopic space without movement. Thus another interesting variant on the illusion would be to study whether distortion arises if the next face stimulus moved into the space of the previous stimulus, instead of instantaneously replacing the previous face.

Through the four experimental chapters (**Chapters 2-5**) recurring themes have emerged- vision is constructive; the effects of illusions are observed at the level of early visual cortex; differences at low cortical levels are closely related to subjective perception, not merely to feedforward stimulus input; illusion effects may occur through predictive mechanisms in the cortex; and these paradigms may allow investigation into neural processing in schizophrenia. We now discuss these themes, the impact of our results on outstanding research questions, and the potential for future investigations in the field.

6.2. Vision is Constructive

Throughout the thesis we observe cases where subjective experience of the world does not match actual sensory input and does not reflect the veridical stimulus. In **Chapters 2 and 3** the rubber hand illusion induces false ownership of a rubber hand. Whilst tactile, visual, and proprioceptive inputs must be relatively similar between real and rubber hands in order to elicit the illusion, subjects are always aware that their own hand is merely hidden. Additionally, there are still tactile, proprioceptive and visual incongruities between real and rubber hands (for example the real hand being under the table, whilst a rubber hand sits on the table; rubber hand can be other-race; the illusion can be elicited with a non-hand object; subjects are still receiving tactile and proprioceptive information from their own hand). Nonetheless, the subject experience arising from multisensory inputs integrates the rubber

hand as a body part, replacing their real hand. In **Chapter 4** motion-induced blindness causes the complete disappearance of a target which is constantly present, even though the target is highly salient, and even if the target is flickering or moving slowly (Bonneh et al., 2001). In this illusion feedforward visual input (of the target) seems to be discarded from the resulting percept, whilst the motion field and other feedforward components (for example a fixation point) are always perceived. Lastly in **Chapter 5** flashed face distortion causes ‘monstrous’ alterations when perceiving normal face stimuli presented sequentially to the peripheral visual field. If visual perception resulted from a direct translation of feedforward sensory input, subjects should perceive only typical faces.

Illusions initially seem to reflect relatively unusual cases of perception, and therefore appear uninformative for typical visual processing. However, many authors consider illusions a demonstration of how the perceived world is constructed by the cortex (as opposed to sensory stimulation veridically reaching consciousness; Gregory, 1997). Perception arises as a result of recurrent cortical signalling at multiple levels (Bullier, 2001; Muckli & Petro, 2013). Feedback information from other senses, higher level sensory computation, knowledge, and context is combined with feedforward visual input at every level of the cortical hierarchy. Local visual information is typically ambiguous, and integration into a global sensory context through feedback greatly aids understanding and processing speed (Bullier, 2001; Olshausen & Field, 2005). Higher visual areas can also integrate stimuli across much larger physical spaces due to much larger receptive fields. Together feedback, feedforward, and lateral interactions dictate resulting visual awareness. Illusion perception can therefore allow researchers to elucidate the constructive mechanisms behind vision as we are aware of the true sensory input, and of the difference between veridical world state and resulting perception.

6.3. Illusory Effects are Observed at the Lowest Levels of the Traditional Cortical Hierarchy

Crucially, the fMRI studies detailed in **Chapters 3** and **4** demonstrate cases where, despite identical feedforward stimulation (visuotactile in **Chapter 3**, visual in **Chapter 4**), V1 activity is strikingly different during illusory experience. This evidence exists in contrast to traditional conceptions of early visual cortex which paint V1 as exclusively a feedforward

feature processor (Brewer et al., 2005; Wandell et al., 2007). Furthermore our data opposes models that propose solely higher-level origins of illusions and bistable percepts (Crick & Koch, 1995). In **Chapter 3** the pattern of activity in V1, and the retinotopically specific hand patch in V1, is similar when subjects perceive the rubber hand illusion, irrespective of the tactile stimulation. There is no corresponding coherent pattern for a lack of illusion perception suggesting that this is a top-down effect only during illusory perception and no similarity between stimulation types when the illusion was and was not perceived despite identical feedforward input. Illusory experience therefore affects the multivariate pattern in early visual cortex in a consistent way, whilst tactile stimulation does not. However tactile stimulation does affect activation in V1- early visual cortex was more active if the perception of illusion or no illusion was incoherent with the visuotactile stimulation (e.g. illusion during asynchronous stimulation), than if these were coherent (e.g. illusion during synchronous stimulation). During the RHI we therefore find that V1 represents information about the illusion, and about the coherence between the illusion and sensory inputs. As there is no differential visual stimulation, this nonvisual information likely arises from feedback pathways originating in far cortical regions. In primates, there are feedback connections between prefrontal cortex and the traditional ‘seat’ of the RHI- premotor cortex. Premotor cortex then has feedback connections to extrastriate dorsal visual regions, including V5; which then projects back to V1 (Gilbert & Li, 2013). Additionally, primary visual cortex is suggested to respond to sensorimotor expectations (Keller et al., 2012). One remaining research question is how exactly different feedback sources (in this illusion tactile and illusion information) are ‘integrated’ to produce increases or decreases in early visual cortex activation (see **Chapter 6.6** for further discussion of this).

In **Chapter 4** we observe distortion of specific features of the target pattern (orientation) in V1 during illusory target disappearance, despite constant and unchanging feedforward stimulation. This appears to be a strong demonstration of illusory perception distorting or destroying information representation in V1. Importantly, this likely reflects an addition of feedback motion information from V5, not necessarily reduction of the feedforward signal (Muckli et al., 2005; Sterzer et al., 2006; see also Chapter 4). Under this conceptualisation, the feedforward signal of both the target and the motion field are passed up the cortical hierarchy. In V5 the motion field is processed and is imposed down the hierarchy as the dominant percept (Sterzer et al., 2009). As receptive fields in this higher region are larger, the feedback motion field signal occludes the target in V1, perceptually blinding the target. It is

possible that feedback to early visual cortex occurs only whilst the target is blinded, or that the feedback is present during both target visibility and invisibility but is communicating different aspects of the stimulus (likely from different cortical areas; Donner et al., 2008).

MIB does not promote a change in spiking in target space compared to a visible target (Libedinsky et al., 2009; Maier et al., 2008; Wilke, Logothetis, & Leopold, 2006) but does promote a hemodynamic difference (Donner et al., 2008; Maier et al., 2008; Schölvinc & Rees, 2010). This suggests that MIB effects are partially fed back as fMRI reflects subthreshold activity far more than spiking activity (Logothetis, Pauls, Augath, Trinath, & Oeltermann, 2001). Additionally beta band modulation which is thought to carry feedback (Wang, 2010) occurs in V1 just prior to target disappearance, and the amplitude of this oscillatory activity correlates with target disappearance duration (Kloosterman, Meindertsma, Hillebrand, et al., 2015). Whilst Donner et al's (2008) data suggests V5 is causally involved in producing target disappearance; this could be better confirmed using dynamic causal modelling (in a similar manner to Sterzer et al., 2006). DCM is a widely-used analysis approach which infers effective connectivity between two regions i.e. infers one brain area's influence over the BOLD activity of another brain area. DCM analysis can only be successful with accurate knowledge about the coupling between neuronal activity and blood flow which forms the BOLD signal. The standard models, which have been used for over a decade (Friston, Harrison, & Penny, 2003; Stephan et al., 2008; Stephan, Weiskopf, Drysdale, Robinson, & Friston, 2007) are outdated and overly simplistic, with large unsupported inherent assumptions about neurovascular coupling (Havlicek et al., 2015). Havlicek et al. (2015) present a new model with increased complexity and updated assumptions. If one intends to use DCM at high field, it is also crucial that the underlying model is specialised for use in cortical layers. Heinzle, Koopmans, den Ouden, Raman, and Stephan (2016) have produced a DCM for layer data, which respects the influence of blood drain from lower to upper cortical layers (Friston et al., 2017).

It would also be informative to use our paradigm and analysis to investigate MIB's temporal evolution - does the cortical pattern representation of the target start to decay before the perceptual switch to target blindness, or afterwards? Investigations at higher field fMRI could elucidate feedback and feedforward contributions in MIB through high field fMRI recording

from distinct cortical layers, as feedback and feedforward are thought to arrive at different layers (see **Chapter 6.6**).

Whilst we did not investigate neural correlates of the flashed face distortion (FFD, **Chapter 5**), we can hypothesise about effects we may observe in V1. Firstly, we would expect an activation increase when the faces seem distorted, compared to when they do not (see Wen & Kung, 2014). We propose that FFD is driven by comparison between successive faces, and if so we would expect a graded increase in V1 activation in correspondence with perceived distortion (Alink et al., 2010; Kok et al., 2012; Petro, Smith, Schyns, & Muckli, 2013). Furthermore we would expect that specific feature distortion would be accompanied by activation in those sub-regions of V1, as contextual feedback effects can be retinotopically specific (Petro et al., 2013). Existing evidence supports our suggestion that V1 may react to perceived distortion despite normal feedforward stimuli- early visual cortex reacts to the subjective perception of faces, not to their low level features (Ayzenshtat, Gilad, Zurawel, & Slovin, 2012). Additionally, V1 contains information about visual expectation (Kastner, Pinsk, De Weerd, Desimone, & Ungerleider, 1999). During the FFD, V1 therefore likely reacts to the stimulus presented, anticipates information about the next face, and then also reacts with extra activation when a face is perceived as distorted. Feedback is a potential mechanism for comparing successive faces. Face-related feedback is sent from face areas in superior temporal sulcus to early visual cortex (Haxby et al., 2000; Rockland & Van Hoesen, 1994), both directly and via the occipital face areas (Gschwind, Pourtois, Schwartz, Van De Ville, & Vuilleumier, 2012). As the FFD is not necessarily face-specific, it may also be mediated by object related feedback from areas such as the lateral occipital complex. Additionally, the subjective emotional experience of monstrous faces may implicate pathways from the amygdala to V1 (Gschwind et al., 2012; Vuilleumier & Driver, 2007). This same pathway may not be implicated if FFD were extended to a paradigm using object stimuli as perceived object distortion seems unlikely to elicit a strong emotional response.

6.4. The Influence of Lateral Connectivity

Our fMRI results demonstrate illusion-induced effects in early visual cortex and extrastriate visual areas, particularly V5. V1 processing changes with perception, in the absence of any difference in feedforward visual stimulation. Lateral connectivity within early visual cortex is

not capable of explaining the tactile and illusory effects observed during the rubber hand illusion, as there was no feedforward visual difference between illusory and non-illusory time points (**Chapter 3**). However, in our motion-induced blindness paradigm (**Chapter 4**) lateral connections within V1 from areas representing the motion-field into areas representing the target may contribute to target invisibility (Jancke et al., 2004; Stettler et al., 2002).

During MIB we observe distortion of the feedforward oriented Gabor patch target stimulus when the target perceptually blinded but not when it is visible to subjects. We suggest that cortical feedback from V5 containing motion-field information ‘overwrites’ the target space in superficial cortical layers, thus distorting the feedforward target representation that remains present in mid-layers (see **Chapter 6.6**). We therefore are not implying that the representation necessarily disappears; only that it is distorted by additional information and cannot be decoded. Whilst low level explanations like adaptation (Gorea & Caetta, 2009), motion streak suppression (Wallis & Arnold, 2009), and filling-in (Hsu et al., 2006) may contribute to MIB, short range lateral connections in the retina or early visual cortex are unlikely to fully account for target disappearance. Targets still disappear when protected by a few visual degrees with no motion field (Bonneh & Donner, 2011). Common low level explanations such as adaptation or perceptual filling-in also provide no reason for the percept to alternate between visible and invisible.

It is possible that our effects are partially driven by long-range lateral connections such as those associated with contour integration (Stettler et al., 2002), however they fail to provide a comprehensive explanation for the target distortion we observe. If the illusion represented merely a low level lateral spread of information then the field should be equally effective whether it were moving or stationary (Graf et al., 2002). MIB can also be elicited using illusory motion fields that contain no feedforward stimulus (Graf et al., 2002). Additionally, slow-moving MIB targets can disappear through MIB and re-appear in opposite hemifields, demonstrating a motion-field dominance that exists across retinotopic space which lateral connections are not capable of covering (Bonneh & Donner, 2011). Additionally, if lateral connectivity is a primary causal mechanism, the highly salient orientation features of the target should also spread. Recent evidence also demonstrates that MIB continues under invisibility of both the target and motion field (through continuous flash suppression, Dieter et al., 2015) whilst lateral perceptual filling-in of contours does not (Meng, Ferneyhough, &

Tong, 2007). Continuous flash suppression does however allow for higher level processing to continue (Gayet, Van der Stigchel, & Paffen, 2014; Stein & Sterzer, 2014).

MIB is mediated by strong top-down effects such as higher order grouping (Bonneh et al., 2001). Targets also experience property updating during perceptual blindness, demonstrating that they are still being processed (Bonneh et al., 2001; Mitroff & Scholl, 2005). Perceptual alternation is therefore more likely to result from top-down switches in perceptual competition (Donner et al., 2008; Hohwy et al., 2008; Sterzer et al., 2009). That target salience increases disappearances (Bonneh et al., 2001) supports competition theories. However, the effects of top-down feedback may incite target disappearance partially through lateral connectivity - feedback can modulate lateral connections and the spread of information (Gilbert & Li, 2013). For example, feedback affects gain in V1 during contour integration, in a manner that is modulated by task dependency (Piëch, Li, Reeke, & Gilbert, 2013). Realistically, MIB is likely to reflect aspects of both top-down and lateral effects at the level of V1. Top-down motion field information is imposed onto the target space through feedback, combined with an influence of feedback on lateral connections into the target space, and potentially also fluctuations in the feedforward stimulus representation (Dieter et al., 2015; Donner et al., 2013).

6.5. Attention in Illusory Paradigms

Attention acts in a top-down manner to direct and drive visual processing through cortical feedback (Noesselt et al., 2002; Saalmann, Pigarev, & Vidyasagar, 2007). Attention increases local BOLD activation in V1 with or without a stimulus (Kastner et al., 1999; Slotnick et al., 2003; Tootell et al., 1998; Watanabe, Sasaki, et al., 1998), and strengthens the cortical representation of attended stimuli (Li et al., 2006). Additionally, feedback context and attention interact to enhance or suppress visual stimuli (Flevaris & Murray, 2015).

During the rubber hand illusion, attention may partially explain some of the neural effects we observe. Accounts of bodily processing suggest that stimuli in peripersonal space (space surrounding the body) engage a dedicated network (Makin et al., 2007; Rizzolatti, Fadiga, Fogassi, & Gallese, 1997; Rizzolatti, Scandolara, Matelli, & Gentilucci, 1981) and that greater visual processing is dedicated to objects in the peripersonal space (Makin, Holmes, & Ehrsson, 2008). Multisensory integration in the peripersonal space is required for RHI onset

(Ehrsson et al., 2004; Makin et al., 2008). Additionally, general attention to objects in the visual field, including the rubber hand in this case, increases BOLD activity in that retinotopic subsection of V1 (Macaluso et al., 2000; Tootell & Hadjikhani, 2000). This is consistent with BOLD increases we recorded during illusion perception in the hand-specific retinotopic space (Makin et al., 2008). The coherent pattern representation present in V1 during illusion perception is also consistent with attentional effects - when the rubber hand is perceived as a part of the body there is a strengthening of its cortical representation (Li et al., 2006). The interactive activation results in V1 and V5 are more difficult to interpret in relationship to attention.

Motion induced blindness is subject to some attentional effects. Directing attention to the target increases the tendency for perceptual disappearance (Geng, Song, Li, Xu, & Zhu, 2007; Schölvinck & Rees, 2010), however reduced attention to the stimulus also slows perceptual switching (thus increasing the length of disappearance periods, Schölvinck & Rees, 2010). Attention is not required for MIB to occur and it can occur out with awareness (Dieter et al., 2015). In our MIB paradigm (**Chapter 4**) major attentional components are controlled using a central fixation task. However, subjects must still attend to the target to report illusion on and offset. We cannot therefore completely disqualify covert attentional effects (for example subjects may monitor the space where they last saw the target in order to accurately report reappearances). These effects are unlikely to account for the V5 and V1 BOLD increases we observe during target disappearance, although they may mediate the top-down mechanisms of MIB. Neural competition accounts of MIB propose attention as one causal top-down factor, where the motion field and target compete for attention in a winner-takes-all manner (Bonneh et al., 2001; Donner et al., 2008). Since attention ought to be identical between the two target orientations, there is no impact on our decoding results as classification was always performed within a perceptual condition. Our experiment could be repeated with the addition of a distracter task to further reduce attentional effects, however this is likely to also reduce the time spent perceiving the illusion.

Whilst we did not study FFD in fMRI, attention is likely necessary for the illusion to occur. Perceived 'monstrousness' will also certainly attract attention to the face stimulus. This attention modulation may partially underlie the increased BOLD signal seen by other authors for increased distortion (Wen & Kung, 2014; although note that the authors increased the

number of facial identities to increase perceived distortion and therefore cannot separate effects of a larger stimulus set, attention, and perceived distortion).

6.6. Layer Specificity and Neurobiology

The neurobiological specificities of feedback modulation are only partially resolved. Feedforward and feedback integration, and resulting perception, may be organised and orchestrated through layer-specificity. The visual cortex is organised canonically in six distinct layers (although subdivisions are also apparent), each of which contains distinct cell types (Bastos et al., 2012; Douglas & Martin, 2007). Several investigations have shown that long-range feedback and feedforward information are projected to discrete layers in any given region of the human cortical hierarchy (see Figure 6.1.a.; Markov et al., 2013). This separation is similar to layer-specific contributions observed in the macaque, where feedback from V2 to V1 branches in supragranular layers I and II, and in infragranular layer V (Rockland & Virga, 1989). In rodents, long range cortical feedback connections terminate in supragranular layer I, and account for up to 90% of synaptic input to layer I with the remaining 10% originating locally (Larkum, 2013; Markov et al., 2014). In monkeys performing figure-ground segregation, feedback arrives to layers I and V (Self et al., 2013). In humans, feedback processing streams stem from deep pyramidal cells and arrive at superficial layer I and potentially at deep layer V, whilst feedforward signals originate in superficial pyramidal cells and arrive in the mid-layers (III/IV; Felleman & Van Essen, 1991; Shipp, 2007; see Figure. 6.1.a).

Muckli et al. (2015) used MVPA in 7T fMRI data to decode feedback information to an occluded quadrant of V1 whilst the other $\frac{3}{4}$ of V1 received feedforward natural scene information (for a similar investigation at 3T see Smith & Muckli, 2010). They demonstrated that contextual feedback in the occluded quadrant was projected specifically to superficial layers, whilst feedforward scene information in non-occluded V1 was also available in the mid layers (see Figure 6.1.c). Other authors have demonstrated feedback to the deepest layers (Kok et al., 2016). The same layer-specificity is also true of connections to the thalamus, which serves as a central relay for feedback communication between cortical regions (Llinás, Leznik, & Urbano, 2002; Muckli et al., 2015; Rubio-Garrido, Pérez-de-Manzo, Porrero, Galazo, & Clascá, 2009; Wimmer, Bruno, De Kock, Kuner, & Sakmann, 2010). Whilst we

describe only the basic layer architecture and connectivity, there are two types of feedforward and feedback connections sent to supragranular and infragranular cortical layers (Markov & Kennedy, 2013). It is unclear what the functional differences are between these two types, how they contribute to the complexities of feedback, and therefore how they contribute to feedforward and feedback integration.

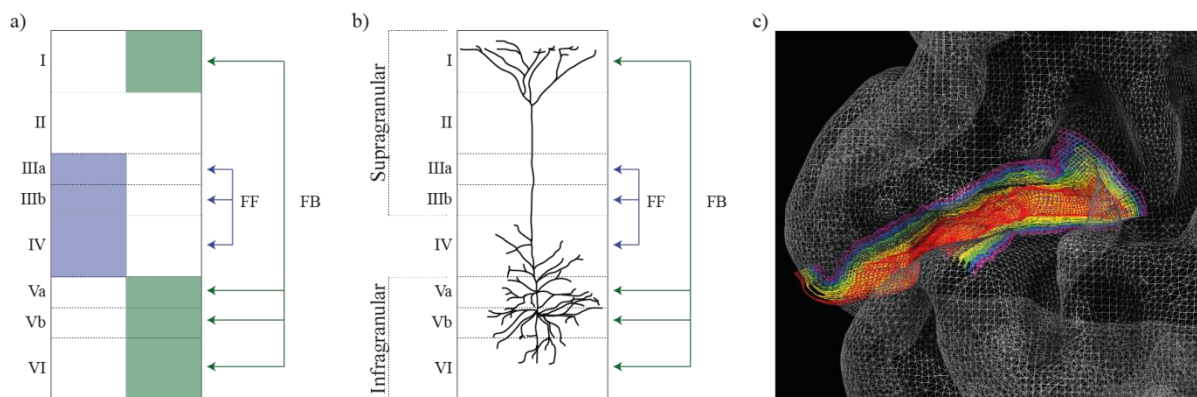


Figure 6.1. Layer specificity of feedback. a) Likely termination layers of feedforward and feedback connections in V1 showing feedback to outer and inner layers and feedforward to mid-layers, image created based on Felleman and Van Essen (1991) and Shipp (2007). b) Superimposition of a model layer V pyramidal neuron on the layer diagram, based on an illustration in Larkum (2013). c) Cortical layer separation in human fMRI in V1 displayed on the cortical mesh, from Muckli et al. (2015).

Critically, this layer specificity is consistent with the neuronal-scale architecture. At the neural level, pyramidal cells may be the crucial computational units in theories of bidirectional cortical function. These multipolar neurons have a pyramid-shaped cell body and long apical dendrites which extend through the cortical layers to layer I. Pyramidal cells dominate the human neocortex (Nieuwenhuys, 1994), which itself is ~80% of human brain mass (Geschwind & Rakic, 2013). An influential paper by Larkum (2013) proposed that in rodents feedback and feedforward inputs are integrated through back-propagation-activated calcium signalling (BAC) *within* L5 pyramidal neurons (see also Major, Larkum, & Schiller, 2013). Specifically, the proposal states that the dendritic trees of these pyramidal neurons link feedforward and feedback processing in an associative manner (Larkum, 2013; Larkum, Senn, & Lüscher, 2004; Larkum, Zhu, & Sakmann, 1999). Cortical feedback streams target inhibitory interneurons and the distal tufts of apical dendrites of layer V pyramidal neurons in layer I (Markram et al., 2004), whereas feedforward information arrives to the basal dendrites of level V pyramidal neurons (Chang, 1951; LaBerge & Kasevich, 2007; Larkum, 2013;

Llinás et al., 2002; Siegel, Körding, & König, 2000; Spratling, 2002). These pyramidal dendritic components are located in different layers of cortex (Douglas & Martin, 2007; see Figure 6.1.b. for a model LV pyramidal neuron; Larkum, 2013).

Cortical feedback does not only modulate feedforward activity, it can also drive cell firing (Bastos et al., 2012; De Pasquale & Sherman, 2011). As feedback input is proximal to a second spike initiation zone near the neurons' apical tufts (Larkum & Zhu, 2002), feedback is capable of creating robust action potentials through broad calcium spiking (Ca^{2+} spiking, secondary to the primary axonal initiation zone) if in conjunction with a sodium spike propagated from the soma (BAC; Larkum et al., 2004; Larkum et al., 1999). This trigger can actually drive more action potentials than direct feedforward input alone to the cell body (Larkum et al., 2004; Larkum & Zhu, 2002; Larkum, Zhu, & Sakmann, 2001). Distal apical tuft input is insufficient to drive neuronal firing alone (Larkum & Zhu, 2002; Williams & Stuart, 2002). However, feedforward inputs to the soma Na^+ initiation zone and feedback inputs to the secondary Ca^{2+} initiation zones interact (Larkum et al., 2004; Larkum et al., 1999). This allows feedforward and feedback activity to interact with one another as input to one initiation zone lowers the threshold for spiking at the other (Larkum, 2013). If inputs to the two initiation zones are temporally linked then the threshold for Ca^{2+} spiking is halved (Larkum et al., 1999). Feedforward input therefore leaves pyramidal cells very sensitive to feedback inputs at the apical dendrite, resulting in apical amplification of feedforward inputs when paired with feedback inputs (Larkum, 2013). Additionally, differing feedback input to the apical site can affect cell output, even with the same feedforward stimulus to the soma in each case (Phillips, Clark, & Silverstein, 2015; Phillips, 2015; Roelfsema, 2006). This intracellular integration mechanism therefore provides one way that illusions may result from modulations of the feedforward input. In this manner, 'inhibitory' feedback connections can also amplify feedforward inputs through intracellular NMDA receptor mechanisms (Larkum, 2013).

Contextual feedback modulations may also amplify pyramidal neuron responses through intercellular connections to other pyramidal neurons (Phillips et al., 2015). These ubiquitous modulatory connections are likely to be NMDA receptor-mediated (Phillips et al., 2015; Phillips & Singer, 1997; Self, Kooijmans, Supèr, Lamme, & Roelfsema, 2012). The calcium spiking central to apical amplification is also reliant on NMDA receptor activity (Larkum, 2013; Larkum, Nevian, Sandler, Polsky, & Schiller, 2009) therefore suggesting that NMDA

receptor function is crucial for contextual modulation (Phillips et al., 2015). NMDA receptors are associated with feedback processing, as they have a high concentration in supragranular layers (Rosier, Arckens, Orban, & Vandesande, 1993), are known cortical modulators (Collingridge & Bliss, 1987) and are crucial for the recurrent interactions involved in figure-ground segregation (Self et al., 2012).

What an individual perceives is formed by a combination of feedforward and feedback activity, arising as the result of not only intracellular integration, but also the activity of cortical microcircuits and of the interactions between cortical areas (Phillips et al., 2015). Computational biological models of feedback and feedforward interactions are constrained not only by the neural anatomy described above but also by the interactions of local GABAergic inhibitory interneurons, long-range glutamatergic excitatory neurons, and synaptic physiology (Larkum, 2013; Petro, Vizioli, et al., 2015). Oscillatory mechanisms also contribute to the integration of feedback and feedforward mechanisms (Engel, Fries, & Singer, 2001). Different frequency oscillations may also be restricted to different cortical layers and thus facilitate either feedback or feedforward processing (Maier, Aura, & Leopold, 2011; Roopun et al., 2008; Wang, 2010; Xing et al., 2012). Fully elucidating the computational biology is out with the remit of this thesis, however it is clear that the integration of feedforward and feedback activity occurs throughout the cortex and is a crucial mechanism for perception.

In the rubber hand illusion the effects we observe of illusion perception and tactile stimulation type must be feedback effects, as no differential feedforward visual stimulation is provided to subjects. We can therefore predict that these effects would predominantly be found in outer or inner cortical layers (Kok et al., 2012; Muckli et al., 2015), whilst midlayers would similarly represent mainly the feedforward visual stimulation. Interestingly, during illusion perception we find a univariate increase in the subregion of V1 retinotopically corresponding to the rubber hand. This could theoretically arise from apical amplification with feedback illusory information, in concordance with feedforward visual stimulation from the rubber hand. The activity in this region of V1, and in global V1, also becomes more coherent when there is illusion perception (across trials and subjects) suggesting that illusory feedback, coding the rubber hand as a body part or directing attention to the rubber hand, could act on many neurons across the population. As stated in **Chapter 6.3**, it is unclear how the combined effects of tactile and illusory feedback interact to produce different activation

in global V1 and V5. Either the two feedback sources are integrated across the population of pyramidal neurons in early visual cortex, or they are united at higher cortical levels (such as frontal regions) and fed back as a unified concept which characterises coherent or incoherent body schema and tactile input pairings.

The method we used in **Chapter 4** lacked the resolution to separate cortical layers, however we proposed that when the target is invisible it is still represented in midlayers of early visual cortex through feedforward (somatic) processing (Muckli et al., 2015). There is evidence for effects of feedforward activity even during target blindness (e.g. adaptation to orientation still occurs; Montaser-Kouhsari et al., 2004). The motion field feedback from V5 likely terminates in superficial layer I and/or inner layer VI during perceptual blindness (Kok et al., 2016; Muckli et al., 2015; Rockland & Knutson, 2000) and therefore causes the lack of decoding ability we observe during target invisibility in our 3T experiment (which records activity equally from all cortical layers). Therefore during MIB, decoding of target features should be possible in mid but not outer cortical layers. As driving feedforward inputs are always available to layer V pyramidal neurons in the target space, apical amplification may amplify the fed back ‘choice’ of percept delivered to the apical dendrite; depressing the alternative percept (Phillips, 2015; personal communication with W Phillips, 2016). The motion field dominates during target invisibility and the target features dominate during target visibility (**chapter 4**; Donner et al., 2008). There are no spiking differences recorded between visible and invisible targets in V1 (Maier et al., 2008), however if both perceptual states (visible and invisible targets) arise from a combination of feedforward and feedback activity then this is consistent with the effects of apical amplification.

Greater development of illusion studies into layer-specific recording using high field fMRI would help elucidate the integration of the feedforward stimulus with feedback and lateral contributions to produce perception. MIB presents a good candidate, as we have specific hypotheses for layer content during perceptual visibility and invisibility. Investigating layer specificity with illusions is of significant interest, as some previous studies (Muckli et al., 2015) have isolated feedback to investigate feedback layers, whereas MIB allows us to investigate a case where there is continuous feedforward input. In high-field fMRI, improved spatial resolution allows layer separation (Duyn, 2012). However this vastly superior voxel resolution (up to $\sim 0.8\text{mm}^3$ at 7T), comes with significant considerations in terms of acquisition, artefacts, and technological requirements. Head motion presents a much greater

problem at high field, causing greater distortion in the data. Subjects experience higher levels of muscle stimulation and heating through a higher specific absorption rate (SAR). Stronger artifacts, including greater inhomogeneity of the magnetic field, require more intensive preprocessing and more normalisation of the data. Data at 7T is difficult to align between runs, adding noise to the data that originates in the preprocessing in addition to the noise in the BOLD signal. Additionally, separation of the cortical layers is by hand and is time-intensive and is subject to human error. Whilst some groups have used automated software (Kok et al., 2016) these methods are not yet validated nor in universal use. Furthermore, fMRI resolution cannot be endlessly refined. Without significant improvements in gradient and detector technology, we cannot image at a higher resolution irrespective of the magnetic field strength (van der Kolk, Hendrikse, Zwanenburg, Visser, & Luijten, 2013). A parallel evolution of gradients, coils, and magnetic field strength is required. As fMRI is a measure of blood flow, imaging resolution is inherently limited to the point spread function of the BOLD signal; although micro-scale detail can nonetheless leave an imprint, for example in the use of adaptation paradigms to image orientation columns (Yacoub et al., 2008). This can be improved by using models of hemodynamic function specifically designed for use in laminar layers (Uludağ & Blinder, 2017).

6.7. Does Early Visual Cortex Represent Visual Awareness?

Our results are consistent with a growing body of literature demonstrating that visual cortex represents what subjects perceive, as opposed to acting as a passive receiver of exact feedforward retinal stimulation (Rees, 2013; Rees et al., 2002; Tong, 2003). Historically, electrophysiological results demonstrate little support for V1 involvement in visual awareness. fMRI results, however, confirm the role of V1 in perceptual suppression (Maier et al., 2008; Wilke et al., 2006). V1 activity co-varies with perceived stimuli during binocular rivalry (Haynes & Rees, 2005a, 2006; Lee et al., 2007; Norman, Polyn, Detre, & Haxby, 2006; Polonsky et al., 2000; Tong, 2003; Tong & Engel, 2001; Tong, Meng, & Blake, 2006). In bistable percepts, both higher extrastriate areas and early visual cortical regions can represent the perceived stimulus (Kleinschmidt et al., 1998; Muckli et al., 2002; Murray et al., 2002; Sterzer et al., 2002).

Although the concepts of consciousness and visual awareness remain controversial (Lamme, 2014; Rees et al., 2002), our fMRI data demonstrate two cases where changes in neural

processing at early sensory levels are related to changes in sensory awareness and the corresponding perceptual report, despite unchanging veridical feedforward input (**Chapters 3 and 4**). In the case of the multimodal rubber hand illusion (**Chapter 3**) this sensory awareness includes information about tactile stimuli and higher-level body schema, which are represented in V1. The RHI suggests that perceived reality is fragile, even when it pertains to one's own body. Additionally, during the RHI V1 even represents perceptions of non-visual realities. Body schema in this illusion occurs as a temporary result of coherent feedforward inputs, which is then easily modulated by new sensory inputs (Hohwy & Paton, 2010). The now-changed body schema representation at higher cortical levels, and the fed-back modulations that we observe within V1, may change how ongoing feedforward information is processed- after a successful RHI more extreme modulations of body schema become possible (such as perceiving a box as part of the body; Hohwy & Paton, 2010).

Multistable percepts provide an excellent opportunity to study the relationship between visual awareness and cortical representation (Crick & Koch, 1990). In the case of motion-induced blindness (**Chapter 4**), previous behavioural results suggest that the content of information in V1 did not reflect visual awareness, as target properties were retained (including orientation; Hofstoetter et al., 2004; Montaser-Kouhsari et al., 2004). Orientation aftereffects in general are not perceived despite their effects in V1 (Haynes & Rees, 2005a; He & MacLeod, 2001; Kamitani & Tong, 2005), showing some independence between awareness and V1 representation. However, in our study we find that visual cortical activity during the illusion reflects the subject's perception of the target- when it is invisible the target is not represented in V1, when it is visible it is represented. The target is therefore rendered subliminal during MIB- not merely unattended but also reduced in feedforward information (Dehaene, Changeux, Naccache, Sackur, & Sergent, 2006; Hesselmann, 2013).

We find mixed results of target activation in V1, although others find increases and decreases associated with illusory disappearance (Donner et al., 2008; Schölvinc & Rees, 2010). In our main experimental group we found higher BOLD activation in V5 during MIB compared to when the target was visible. However, we did not find significant differences between V1 activity during MIB and when the target was visible. Donner et al. (2008) found opposite activation effects during motion-induced blindness for subregions of visual cortex corresponding to the target and to the moving cross array. During MIB the activation of their target subregion in V4 decreased quickly after perceptual report. Conversely, mask sub-

regions in dorsal areas V3AB and pIPS, showed increased BOLD activity at this same time. Additionally, they demonstrated a general not spatially specific decrease in V1-V3 during MIB. This suggests that perhaps, in terms of studying BOLD activation, our analyses were too specific in their restriction to the target subregion of V1 and V5. Scholvinck and Rees (2010) also found an increase in V5 BOLD activity but in contrast with Donner et al (2008) they show an increase in V1 activity during MIB. This activation change has also been reported in early visual cortex during other bistable percepts (Lee et al., 2007; Polonsky et al., 2000; Tong & Engel, 2001). As described in chapter 4.1. our paradigm is based on their stimuli. Hsieh and Peter (2009) found that reappearance of the target on cessation of MIB induced BOLD increase in V1v and V2v, in contrast with the previously described results. They also demonstrate decreased BOLD activation in V5 when the target reappears. Unusually, target used by Hsieh and Peter (2009) was the same colour as the cross array surrounding it, and was very small at a relatively high eccentricity. Wells and Leber (2014) suggest that the discrepancy between Scholvinck and Rees (2010) and Donner et al's (2008) results could be accounted for by a difference in the coherence of the cross array. In one study this was a 2D mask (Schölvinck & Rees, 2010) and in the other a 3D a random dot cloud (Donner et al., 2008). This aligns our paradigm and results more closely with that of Schölvinck and Rees (2010).

One outstanding question, particularly in MIB, is the direction of the relationship between conscious perception and stimulus representation in early sensory cortices (Sterzer & Rees, 2006). Does top-down perception produce perceived target blindness and modulate V1 representation, or is disruption in V1 necessary for subjects to perceive target disappearance? Conscious access to stimuli varies as a function of expectation and prior information, suggesting that top-down modulations have a large effect on visual awareness (Melloni, 2014). Furthermore, V1 change alone is insufficient to cause consciousness changes (Lamme, 2006; Lamme, Supèr, Landman, Roelfsema, & Spekreijse, 2000; Rees et al., 2002; Tong, 2003). However representation in the early visual cortices may be a prerequisite for information to reach higher-level consciousness (Lamme & Roelfsema, 2000; Tong, 2003). Sensory percepts are influenced by top-down information before and after stimulus inputs (Rees, 2013), suggesting that a reciprocal relationship between top-down and bottom-up representations of the stimulus are required for stimulus awareness. Lamme (2014) also proposed that recurrent communication is important for differentiating conscious and unconscious perception (see also Bullier, 2001; Lamme & Roelfsema, 2000). At the level of

V1, it is also possible that during MIB dominant subpopulations of cells represent perceived stimuli, whilst other subpopulations represent alternative/feedforward input (as is the case during perceptual rivalry, Leopold & Logothetis, 1996). Lastly Bachmann and Hudetz (2015) suggest that apical amplification itself may determine whether content is conscious, further supporting that feedback to layer V pyramidal neurons in V1 may allow amplification of the target stimulus when it is visible and the field stimulus during target invisibility (see also Phillips et al., 2015). Layer specific recording could address questions about perceptual awareness by testing whether the representational layer profile of a stimulus in V1 is different for stimuli with and without awareness.

MIB can also arise completely out with visual awareness when the inducer stimulus is concealed by continuous flash suppression (CFS; Dieter et al., 2015). Whilst Dieter et al. (2015) suggest this is indicative of low level feedforward stimulus fluctuations underlying MIB, this finding does not mean that high level processing does not occur during MIB. Whilst MIB may not require consciousness awareness, lateral low level contour filling in does (Meng et al., 2007). High level computation can occur outside awareness (Lamme, 2014), contextual stimuli break through CFS faster than other stimuli (Stein, Hebart, & Sterzer, 2011; Stein & Sterzer, 2014; Wang, Weng, & He, 2012), and CFS breakthrough is modulated by expectation (Pinto, van Gaal, de Lange, Lamme, & Seth, 2015; e.g. during perceptual blindness there is nonetheless unconscious processing of higher level information). Motion integration also occurs during CFS (Faivre & Koch, 2014). This integration could be one mechanism by which motion-induced target blindness occurs during CFS. However, Kanizsa illusory figures do not complete when under CFS, therefore context illusions may require conscious awareness (Harris, Schwarzkopf, Song, Bahrami, & Rees, 2011). Crucially, recent evidence suggests that higher level processing may still occur due to significant limitations of the suppressive effects of CFS. Low level details may still be consciously perceived during CFS (for example location, Zadbood, Lee, & Blake, 2011). Recent work by Gelbard-Sagiv, Faivre, Mudrik, and Koch (2016) demonstrated that high level facial priming effects only happen during CFS if one low level feature is perceivable. Thus, here MIB features may still be visible even if they are not consciously perceived.

Our data cannot comment on V1 representation during FFD, however previous work has demonstrated increased activation with increased perceived distortion (Wen & Kung, 2014). Future studies using TMS could determine whether V1 upregulation promotes perceived

distortion and/or if V1 disruption reduces the perception of distortion, thus clarifying the causal contribution of V1 to distortion. Further work would be required using MVPA to determine whether facial identities are represented differently depending on perceived distortion, although the temporal dynamics required to elicit the illusion make FFD a poor choice for fMRI investigation into the link between representation and awareness.

It is important to note that we rely on correlations between fMRI data and behavioural report to study the effects of visual awareness in these illusions (Hesselmann, 2013; Overgaard, Rote, Mouridsen, & Ramsøy, 2006). The results we observe are therefore conflated with the effects of responding (Aru, Bachmann, Singer, & Melloni, 2012; De Graaf, Hsieh, & Sack, 2012) and do not allow us to separate conscious perception from a report of conscious perception (Fahrenfort & Lamme, 2012; Lamme, 2014). Additionally, we differentiate perceptual state through subjective, not objective, reports (Hesselmann, 2013). Future motion-induced blindness paradigms may better study the relationship between visual awareness and V1 representation if a single classifier model is applied at each time point. The decoding accuracy could then be correlated with the perceptual reports (Tsuchiya, Wilke, Frässle, & Lamme, 2015). Frässle, Sommer, Jansen, Naber, and Einhäuser (2014) note that a reliance on perceptual report as the only measure of perceptual state can be a crucial conceptual constraint when interpreting data. Whilst perceptual report matches objective measures like pupilometry in binocular rivalry, neural activity is affected by subjects reporting their perception (Frässle et al., 2014). Thus, we cannot ascertain whether asking participants to report changes in illusory percept has had an effect on the BOLD activation results we report in either **Chapter 3** or **Chapter 4.2**. This is of particular concern for **Chapter 3** as perceptual choice can be represented in the pattern of multivariate activity. Given the multitude of ways that feedback can impact on V1 activity (**chapter 1.2**) it is not unlikely that this would include perceptual choice. It is important to note that in **Chapter 4.2** we never decode between perceptual choices. As an alternative to perceptual report, the use of pupilometry in MIB is promising (Kloosterman, Meindertsma, Loon, et al., 2015; as described in **chapter 4.1**).

6.8. Illusions May be an Effect of Cortical Prediction

We have argued that the cortex produces perception from the interplay of feedforward sensory data, feedback context and lateral connectivity. However, this mechanistic approach

explains *how* but not *why* vision and other senses are constructed and not veridical. Why is feedback integrated into true sensory data to produce perception? One potential function of cortical feedback is hierarchical predictive coding. As described in chapter 1.5., hierarchical predictive coding theories hypothesise that the cortex aims to predict incoming sensory information using top-down modelled expectations, which are based on its history of learnt associations (Clark, 2013; Friston, 2010; Mumford, 1992; Rao & Ballard, 1999). It compares these to real incoming stimulation and updates the high level model using predictive errors which highlight the inconsistency between the model and actual incoming stimulation. The model for incoming stimulation is communicated through feedback connections, whilst the error and representation of the incoming stimulus is communicated through the feedforward processing stream. The comparison of these signals occurs at every cortical level, and the results of these computations inform neighbouring levels of the cortical hierarchy.

Whilst predictive coding offers an elegant theoretical proposal for global cortical function, and explanation for many pre-existing findings, we must also consider its biological realisation. The functional possibilities of feedback and feedforward interactions, described above, are relatively consistent with predictive coding hypotheses. In predictive coding terms, integrative properties and diverse anatomical connectivity of layer V pyramidal cells provide a mechanism for feedback predictive models of the world to be integrated with feedforward sensory information within the neuronal dendritic tree at each level of the cortical hierarchy (Larkum, 2013; Larkum et al., 2009; Larkum et al., 1999):

“the main function of the cortex – to associate external data with an internal representation of the world – could in theory be achieved without the need for complex circuitry, and instead use a single, essentially 2D sheet of vertically aligned pyramidal neurons”.

(Larkum, 2013, p 145).

Intracellular integration and apical amplification mean that the firing pattern formed by feedforward inputs (prediction errors in predictive coding theories) would be strongly mediated by feedback inputs to the dendrite (Bastos et al., 2012; Larkum, 2013). This allows the predictive brain to select the likely sensory interpretation given the top-down predictive model and sensory data (Douglas & Martin, 2007). The flexibility inherent in the system allows feedforward inputs that best match top-down predictions to have more influence as when a neuronal population is predicted by the top-down model, it will be easier to drive

spiking and therefore cortical representation (Bastos et al., 2012; Friston, 2002; Larkum, 2013). If the top-down prediction of selected input is strong enough, feedback can be influential enough to drive a response to stimuli that a cortical area is not selective for. For example, Egner, Monti, and Summerfield (2010) show that face areas will respond to houses under strong face expectations. Petro, Vizioli, et al. (2015) therefore term these pyramidal neurons ‘prediction units’. Predictive coding theories also predict the inhibitory effects of feedback connections (Bastos et al., 2012). Feedback to cortical microcircuits is largely inhibitory, consistent with a predictive brain which aims to suppress all which it has predicted (Bastos et al., 2012). Layer I, the target of feedback, is dominated by inhibitory cells (Chu, Galarreta, & Hestrin, 2003) which act upon computations in the midlayers (feedforward sensory information; Chu et al., 2003; Wozny & Williams, 2011).

One challenge for predictive coding accounts lies in how matches or mismatches between predictions and sensory data are realised. BAC signalling suggests that pyramidal neuron response will be amplified and spiking increased when the top-down prediction received at the apical tuft dendrite matches bottom-up sensory input to the basal dendrite (Larkum, 2013; Phillips, 2015). This supports theories such as Active Resonance (ART; Grossberg, 2013), however the central dogma of many predictive coding accounts is that activation should be *reduced* for predicted stimuli, thus justifying the economy of the system (Alink et al., 2010; Friston, 2009, 2010; Olsen, Bortone, Adesnik, & Scanziani, 2012; Petro, Vizioli, et al., 2015). One potential explanation for this contradiction is that BAC and apical amplification act within a single pyramidal neuron, whilst predictive coding may be implicated by the entire cortical column (Petro, Vizioli, et al., 2015; Phillips, 2015). The sum of a cortical column’s computation could silence predicted information, even if it is amplified at the level of an individual layer V neuron (Bastos et al., 2012; Petro, Vizioli, et al., 2015). Predicted stimuli could for example be disamplified through the inhibition of apical amplification (Phillips et al., 2015). It is therefore an outstanding question how amplification in Layer V could be coherent with inhibition in layers II/III. Although many details of intracellular and intercellular computation remain unknown, known properties of intracellular computation and the cortical microcircuit could allow predictive coding to function in the cortex.

Cortical prediction may play a role in the studies presented in this thesis. In the rubber hand illusion, the illusion may arise because the rubber hand belonging to the body is the most coherent explanation of inputs from vision, proprioception and tactile stimulation during

synchronous stimulation (Hohwy & Paton, 2010; Limanowski et al., 2014; Seth, 2013). In typical experience, consistent inputs from these senses would identify a correct limb, and that high level body schema model would be propagated down the cortical hierarchy. Several known variations of the RHI support this proposition, as if any of the inputs are reduced or incoherent then the illusion is reduced- asynchronous visuotactile stimulation reduces illusion perception (Botvinick & Cohen, 1998; Ehrsson et al., 2005; Ehrsson et al., 2004) and increased proprioceptive disparity leads to reduced illusion (Costantini & Haggard, 2007). Conversely adding a fourth piece of evidence in the form of agency dramatically increases the illusion strength (Kalckert & Ehrsson, 2012). The RHI paradigm challenges the idea of top-down body image as a robust phenomenon. Instead the illusion suggests that it results from ongoing computation, which bottom-up visuotactile and proprioceptive information can direct (Hohwy & Paton, 2010). Interestingly, making body image malleable leaves it open to more variation- after a successful illusion, one can easily generalise to even less likely cases of non-hand objects (Armel & Ramachandran, 2003; Hohwy & Paton, 2010). The top-down body image model is less reliable, so it is more easily updated by new feedforward input.

We observe univariate differences in activation between illusory conditions in **Chapter 3**. In concordance with prediction error theory the ‘inconsistent’ conditions- illusion perception during asynchronous stimulation and no illusion perception during synchronous stimulation- are those which elicit the most activation in visual cortical areas during RHI stimulation. We also observe significant representational similarity in V1 during illusion perception across trials and subjects. At each cortical level, error remains distinct from representational units (Clark, 2013). Representations can therefore be sharpened by feedback influences (producing less variability among representations of the same stimulus/condition), whilst feedforward activation is reduced as a result of lessened prediction error (Friston, 2005; Kok et al., 2012). Prediction in the brain is therefore consistent with both the sharpening of multivariate pattern and reduction of activation in early visual cortical response (Kok et al., 2012; Spratling, 2008b). This conceptualisation requires functional distinction in the neuroanatomy for subpopulations encoding perceptual causes (the predictive model) and prediction error (Friston, 2005). This may be realised through the separation of feedback to the apical dendrite and feedforward input to the basal dendrites of pyramidal neurons (Larkum, 2013; Phillips, 2015).

Predictive mechanisms may also apply during MIB. Target disappearance may occur partially because the target is unchanging, inconsistent with the moving object, and therefore uninformative about the motion of the field (Sterzer et al., 2009). The top-down model of the stimulus therefore becomes dominated by the motion field and the target disappears as motion feedback distorts its feedforward representation. Alternatively, when the target is invisible to subjects the observed distortion in feedforward stimulus representation could induce additional noise in the feedforward signal. This would give the feedforward information less weighting and therefore less influence on the perceptual outcome (Hohwy, 2012). However, this suggestion is in contrast to results showing that increased attention increases target disappearance, as attention also boosts the precision of sensory inputs. Future investigations could probe whether MIB relies on prediction mechanisms by altering the coherence ('precision' in predictive coding terms) of the motion field- less coherent motion fields should produce less robust illusion perception. In terms of neurobiology (see **Chapter 6.6**), MIB is a case where a driving signal is always present for modulatory activity to act upon. My intuition is that therefore the modulatory presynaptic (feedback or lateral) input in MIB represents a chosen percept and therefore dictates the resulting conscious percept. This suggests that any stimulus change would increase the likelihood of perceptual reappearance of the target, which has been demonstrated by Wu, Busch, Fabre-Thorpe, and VanRullen (2009) (a nearby flash causes target reappearance during MIB). In our study (**Chapter 4.2**) two subjects reported that the red fixation colour change caused target reappearance.

Hohwy et al. (2008) propose a predictive coding model for bistable stimuli with two representations in competition, which allows for switches between the perceptual options, as observed during MIB (Hohwy et al., 2008; Sterzer et al., 2009). Although perceptually invisible, the suppressed stimulus (for example the target) is still present and is unexplained by the top-down predictive model which suppresses it (the motion field). The prediction error associated with the unexplained stimulus increases (expressed as BOLD) and rises up the cortical hierarchy until the suppressed stimulus regains awareness. The same pattern of escalating error will then occur with the other competing perception. This conceptualisation may explain why MIB literature has shown both activation increases and decreases in V1 during MIB as the activation would start low then increase across time when the target is suppressed (Donner et al., 2008; Schölvinck & Rees, 2010). In support of this idea, MIB works

best under conditions of high perceptual competition- extremely salient targets surrounded by very coherently moving items drastically increase the length of target disappearance in the MIB illusion (Bonneh et al., 2001). Biased competition theories such as those proposed by Donner et al. are highly compatible with inferential brain theories such as Bayesian brain theories and predictive coding (Feldman & Friston, 2010). Prediction may also interact with attention during MIB. Attention is thought to adjust prediction error weightings (Kok et al., 2012) and reduced attention to the stimulus array slows perceptual switches for MIB (Schölvinck & Rees, 2009). However, attention directed away from the target also *reduces* disappearance whilst the effects of attention on prediction error weightings would predict *increased* disappearance (Geng et al., 2007; Schölvinck & Rees, 2009).

In **Chapter 5** we hypothesise that predictive mechanisms may underlie FFD. Under non-experimental stimulus conditions faces do not rapidly change in the same retinotopic space without moving. Therefore relatively quick changes between stimuli without interspersed masking causes distortion when the new face is compared to previous faces in retinotopic space. Wen and Kung (2014)'s demonstration of increased early visual cortical activation paired with increased perceived distortion is consistent with the idea that increased prediction error is related to distortion (Alink et al., 2010). This account of FFD makes some specific predictions for ongoing experiments; for example less low level visual differences between successive faces should induce less activation in V1 and less accompanying perceived distortion. It would therefore be highly informative to study the illusion using fMRI and face stimuli which are more or less dissimilar in their feedforward visual information.

Whilst it is tempting to accept that cortical prediction can explain our data, and many other existing results, predictive coding theories still attract significant controversy. In Clark's view (2013) action-oriented predictive coding models (Friston, 2009, 2010) come close to creating a unified theory of cortical function; encompassing perception, attention, and action. He praises their basis in previous theoretical work; including their relationship to Bayesian theories of inference, computational approaches to data, and their close correspondence with modern knowledge of neuronal behaviour. He additionally praises the breadth of predictive coding's applications.

However, it is this breadth that dilutes the impact of such theories. Predictive coding theories are currently so broad as to be unfalsifiable. Predictive coding is not concretely formulated, nor does it make precise predictions about data (Kogo & Trengove, 2015). The breadth of the theory also makes it difficult to test in a rational fashion. As cortical prediction is proposed to be embedded in all senses, a research paradigm that exemplified this theory and tested specific hypotheses would be impossible to design. Alternatively, one could review thousands of experiments across many years in order to determine their coherence with a fully realised pre-determined concept. However, simply reviewing existing phenomenological data using phrasing taken from outlines of predictive coding theory is not sufficient (Kogo & Trengove, 2015). Predictive coding theories therefore currently represent more a thematic framework from which to consider cortical processing behaviour than a specified and testable theory (Bubic et al., 2010).

Spratling's (2013) commentary on Clark (2013) raises an important concern; specific implementations of predictive coding theory are often mistaken for the overarching theory. The variance between implementations of predictive coding theories also leaves room for aspects to remain unspecified. As the term applies to a group of theories, not to a singular dogma, there is variation to allow for one implementation of the expansive theory to explain one result and another implementation to explain a contrasting result (for example the differing views on prediction error and resulting cortical activity espoused by Grossberg, 2013; Muckli & Petro, 2013; Spratling, 2010). For example, Rao and Ballard (1999) proposed that endstopping cells express prediction error about the discontinuation of an otherwise consistent line, whilst data demonstrated that this activation *increases* when there are collinear lines outside the receptive field of the cell (Kapadia et al., 1998; Kapadia, Westheimer, & Gilbert, 2000). This suggests that in fact feedback amplifies the activation, characterising this as a match to a prediction. This finding is consistent with theories by Grossberg (2013); Phillips (2015); or Spratling (2010), but not with existing theories arising from Muckli and Petro (2013); or Rao and Ballard (1999). Furthermore, the proposed mechanism for predictive coding within pyramidal neurons- in which the feedforward cascade carries error and representation and the feedback cascade carries predictions (above) is only one theoretical way that neuronal mechanisms can be grouped. The feedforward cascade could equally carry predictions (Spratling, 2008a; Spratling, 2013).

The complexity of predictions across temporal scales has not been clarified (Bubic et al., 2010). One could have long-term predictions based on a lifetime of experience and also short term predictions based on recent learning with near-immediate consequence (Schubotz, 2007). These are difficult to conceptualise and integrate in the current theory, which contains suggestions for spatially disparate as compared to spatially local predictions, but not for temporally disparate as compared to temporally local predictions. Despite some attempt by Larkum (2013), predictive coding theory is not well reconciled with neuronal computation at varying scales. As mentioned, there is significant ongoing debate about whether unexpected stimuli and prediction error should incur activation or deactivation in fMRI or electrophysiological recordings. Controversy also surrounds whether activation implies only error or also representational updating (Kogo & Trengove, 2015). This query makes the interpretation of data difficult. We previously mentioned data from Kok et al. (2016) showing that in Kanizsa triangles (Kanizsa, 1976) BOLD activity is upregulated for the illusory shapes. Is this BOLD activity indicative of prediction error or does it denote modification of the representation to match predictions of a shape? All fMRI data demonstrating error for unexpected stimuli shares this concern- is this representational updating or predictive error? Can the two be distinguished? Additionally, even the clearest propositions of Bayesian and predictive coding theories illuminate only the most well-defined cases of visual perception and action and fail to fully conceptualise highly cognitive processes such as imagination (Bubic et al., 2010).

Even if the neuronal mechanisms of predictive coding were completely clarified, testing methods are not currently advanced enough to examine these hypotheses. Current theories of neural computation specify that prediction, error, and representation occur interactively within the same cortical microcircuit (Larkum, 2013; Phillips, 2015). These neurons would be impossible to differentiate with coarser spatial methods like fMRI and EEG, and highly difficult even with single unit recording (Kogo & Trengove, 2015), particularly as feedback is thought to be better revealed by energy use at the synapse, blood flow, and therefore through fMRI (Logothetis, 2003, 2008).

Although much human psychophysical and neural data approximates the computation proposed in Bayesian brain theories and predictive coding theories, this does not serve as proof that this is what the cortex is doing. It is possible that cortical processing merely resembles Bayesian inference and prediction (Kogo & Trengove, 2015). The massive generalisability of cortical predictive coding means that few current theories of cortical function specifically challenge the overarching theory; that the brain uses priors to infer the state of the world. Furthermore, it is important to note that inferential processing has been a dominant idea in considerations of the human mind for centuries (see **Chapter 1.3**). Hawkins and Ahmad (2016) have recently expanded predictive and inferential brain theories to integrate the function of memory as a basis for prediction, spread across layers of neurons in the neocortex. This theory first appears in Hawkins 2004 book, *On Intelligence* (Hawkins & Blakeslee, 2004). As mentioned in Chapter 1.5. Grossberg has proposed a similar theory in Adaptive Resonance Theory (ART) – suggesting that feedback directs attention to expected stimuli, providing resonant similarity to learned expectations, which drive learning (Grossberg, 2013). As attention is directed to expected stimuli, this theory does not support the concept of predictive error. In adaptive resonance theory, unexpected stimuli (not predicted by top down modelling) force the brain to conduct hypotheses and learn how to predict the world better. Given the similarities between predictive coding and ART, the neuronal architecture described in **chapter 6.6** is also entirely consistent with ART as insofar known.

We currently still do not know how the brain reacts to specific illusions like those covered in this thesis. Whilst it is important to consider overarching theory, it is premature to assign the results regarding BOLD activity and the pattern of BOLD activity described in this thesis to any aspects of predictive coding theory. Whilst these theories are seductive in their ubiquity, we must be cautious in fully endorsing them. It is clear that the brain communicates in several different directions – feedforward, feedback, and laterally within cortical areas. However, until the mathematical theory is translated into highly specific neurophysiological predictions for the data, and until we are equipped with the method to study these exact predictions, there remains a gulf between theory and concrete neural mechanisms. There is a theoretical possibility that Bayesian brain theories and predictive coding theories could be one day be specified concretely and precisely enough that they would be directly testable. However, cognitive neuroscience is not currently in that place.

6.9. Illusion Studies may Elucidate Deficits in Schizophrenia

Several illusory phenomenon, including the illusions presented in this thesis, are prime tools for investigation into clinical populations (Notredame et al., 2015; White & Shergill, 2012). Normal constructive perception, illusions, and hallucinations share a notable similarity- they are visual (or other sensory) experiences which are only partially constrained by actual sensory input. However, hallucinations are dissimilar in one important aspect. Visual perception and visual illusions always have inducing stimuli, whereas hallucinations can be entirely internally generated. As discussed in **Chapter 1.3**, schizophrenic subjects demonstrate notable atypicalities in illusion perception. In typical subjects, illusions demonstrate a tendency towards perceiving what is dictated by feedback or top-down information, as opposed to veridical feedforward input (Notredame et al., 2015). Schizophrenic differences usually manifest as reduced illusory experience, particularly if the illusion is caused by the context or is an example of surround suppression e.g. there is less feedback influence (Chen et al., 2008; Dakin et al., 2005; Uhlhaas et al., 2004). Importantly, the deficits seen in illusion perception in schizophrenia often suggest that the affected systems are upstream regions, as illusions relying only on low level computations remain unaffected (Tibber et al., 2012; Yang et al., 2013).

The positive symptoms of schizophrenia- hallucinations and delusions- can be characterised as failures of feedback and feedforward interactions. Schizophrenic symptoms of psychosis have also been conceptualised in terms of predictive coding (Fletcher & Frith, 2009; Friston, 2005), with the disruption arising from feedforward and feedback signalling. Hallucinations are perceptions in the absence of inducing stimuli (or which surpass the inducing stimuli), considered to arise from the over exertion of top-down predictions over true input (Corlett et al., 2011; Corlett et al., 2010; Fletcher & Frith, 2009). In this manner, they are similar to our conceptualisation of illusions. In delusions, maladapted or absent top-down modulation was thought to allocate aberrant salience to stimuli, promoting learning and further disrupted feedback information (Corlett & Fletcher, 2012; Corlett et al., 2010; Fletcher & Frith, 2009; Friston & Kiebel, 2009; Kapur, 2003). A reduction in feedback predictions has also been used to explain reduced illusion perception in schizophrenic subjects (Silverstein & Keane, 2011). These propositions demonstrate a great conflict in schizophrenia research- differing results

and symptomology suggest both strong top-down effects on perception and also a stronger impact of feedforward information or veridical perception (Notredame et al., 2015).

Adams et al. (2013) suggest a resolution to this conflict may be that psychosis results from issues not with top-down prediction, but from a dysfunctional balance of the precision and weightings of fed forward sensory input and fed back predictions (Corlett et al., 2011; Friston, 2005; Schmack et al., 2013). They hypothesise that hallucinations result from enhanced top-down precision, allowing feedback to completely dominate sensory experience and falsely infer sensory stimulation (Schmack et al., 2013; Schmack et al., 2015). Delusions instead arise when precision and weightings of fed forward prediction error are increased, promoting attention to irrelevant stimuli and more updating of higher level predictive models on the basis of this inaccurate error information (Fletcher & Frith, 2009; Kapur, 2003). Delusions therefore develop across time. This explanation firstly does not require the conflict of top-down increase in one psychosis symptom but decrease in other. Secondly, this conceptualisation solves the tenacity problem - that if delusions arise purely from too much bottom-up influence of sensory data they should be easily changed (Corlett et al., 2010). This conceptualisation means that the dysfunction exists in the balance of influence of feedback and feedforward information (Jardri & Denève, 2013).

In terms of underlying neurobiology, greater precision is implemented in the brain by gain in the post-synaptic feedforward error signal (Feldman & Friston, 2010). This increase in gain heightens the weighting of the feedforward error signal. In line with the description of the neurobiology of feedforward and feedback described in **Chapter 6.6** and **6.8**; the pyramidal cell structures in superficial layers are thought to calculate these aberrant prediction errors. Importantly, glutamatergic NMDA receptor function modulates the post-synaptic gain of information and integration in the pyramidal neuron (Adams et al., 2013). This information can be integrated over long time periods, allowing feedback input to distal synapses to affect the output of the cell. NMDA receptor dysfunction is central to schizophrenia (Corlett et al., 2011). Dopaminergic activity also modulates synaptic gain, and again is dysfunctional in schizophrenia (Corlett et al., 2011; Friston, 2009, 2010). Consistent with the layer architecture of both feedback and feedforward processing, a review by Harrison and Weinberger (2005) showed that most recorded neuropathologies in schizophrenia were in the

midlayers and layer V (Adams et al., 2013). The majority of the obvious neuropathology is concentrated in high level prefrontal and temporal cortices, with particular deficits supragranular layers that contain superficial pyramidal cells.

Schizophrenic brains also demonstrate non-typical computations throughout the cortical microcircuit including deficits in inhibition (O'Donnell, 2011). If excitatory cortical loops are allowed to run riot with reduced inhibitory control, then both feedforward and feedback information will become stronger. Notredame et al. (2015) characterised this as a 'circular propagation' of issues- feedforward information is perpetuated up the hierarchy without inhibition where it affects high level representations, in turn feedback (affected by the feedforward input) can completely change the perception of feedforward activity when it is propagated down the hierarchy (Notredame et al., 2015). A reduction of inhibition therefore biases the system in two ways. Essentially the neuropathology observed in subject groups supports a hypothesis of dysfunction in pyramidal cell computation; mediated by issues with NMDA receptor function, and glutamatergic, GABAergic, and dopaminergic processing (particularly D1; Adams et al., 2013).

In the two illusions we investigate in fMRI, schizophrenic subjects experience a mixture of enhanced and reduced illusory effects. The rubber hand illusion (**Chapters 2 and 3**) is stronger in patient groups, quicker in onset, and induces greater distortion of perceived real hand position (Peled et al., 2003; Peled et al., 2000; Thakkar et al., 2011). Positive symptoms are related to increased illusion experience only during synchronous stimulation (Peled et al., 2003; Thakkar et al., 2011). The distinction between the self and other may be diminished in schizophrenia (Asai et al., 2011) and this is potentially related to their difficulty in separating self-generated from externally-generated actions (Blakemore et al., 2000; Synofzik et al., 2010; Voss et al., 2010). The rubber hand illusion may also be relevant for theories of how schizophrenic delusions arise- in this illusion psychiatrically healthy subjects accept unusual explanations for bottom-up sensory stimuli (that the rubber hand belongs to their body). This is in concordance with theories that propose that delusions are correct responses to atypical inputs (Fletcher & Frith, 2009). If feedforward input is dysfunctionally over weighted, then false beliefs will perpetuate (Hohwy & Paton, 2010).

These results have several potential explanations from bidirectional cortical processing. The combined feedforward inputs from visual, tactile, and proprioceptive senses must be coherent to incite the RHI (synchronous stimulation; Botvinick & Cohen, 1998; Hohwy & Paton, 2010; Paton et al., 2012). These feedforward signals are in contrast to internal, top-down body schema which models the existing hand as a body part. In typical subjects, coherent feedforward information from multiple modalities is sufficient to overcome and alter the existing body schema to incorporate the rubber hand. This new schema shows strong hallucination-like effects- subjects feel as if the rubber hand is the source of their sensation and even perceive the newly-integrated rubber hand as being more aesthetically similar to their existing limb. In schizophrenic subjects, either the multimodal bottom-up inputs are given more precision and weight in determining the resulting perception, or top-down body schema is weaker initially (Mishara & Sterzer, 2015). Given the broader research field, it seems likely that the gain of feedforward input is given more weight, resulting in strong feedforward influence in updating higher level body schema (Adams et al., 2013; Corlett et al., 2011). The new body schema is then fed back down the hierarchy, resulting in stronger RHI experience and faster illusion emergence (Thakkar et al., 2011). In our paradigm we would anticipate a stronger multivariate pattern for illusion perception in V1 in schizophrenic subject groups, indicative of the stronger illusion perception.

Conversely, motion-induced blindness is reduced in schizophrenic subjects, particularly in rate of illusory disappearance (Tschacher et al., 2006). MIB experience (rate and duration) within the patient group also positively correlates with positive symptoms (hallucinations and delusion), whilst negative symptoms were associated with reduced MIB experience. This suggests that the top-down motion information we observe in typical subjects is reduced in schizophrenic subjects, whilst the strength of the feedforward target presented is retained or enhanced. Early visual cortical GABA is correlated with fewer perceptual switches and lengthened duration of bistable percepts (van Loon et al., 2013). Schizophrenic subjects show reduced GABA in this region, related to more veridical perception in surround suppression paradigms (Yoon et al., 2010). The percept is biased to a visible target not to the motion field (invisible target). However, the mechanisms of MIB in schizophrenic groups do not precisely mimic those seen in other bistable stimuli. In bistable motion paradigms schizophrenic subjects show increased switching between two percepts, and do not show the ‘sticking’ to a percept seen in typical subjects (Schmack et al., 2015), whilst in MIB subjects stick to the veridical percept. Researches have suggested that MIB is not necessarily a case of true

bistability as it demonstrates different global and local effects (Jaworska & Lages, 2014). Unlike other bistable percepts MIB has one percept which is veridical and one which is inferred, whereas during other bistable percepts both percepts are equally veridical. One possibility is that top-down feedback influences only apply during target invisibility, against Donner et al. (2008) findings, which suggest that there are top-down effects from different sources during both target visibility and invisibility.

The different response profile of MIB seen in schizophrenia is consistent with Adams' proposals that precision may be affected in the pyramidal cells of schizophrenic subjects. We therefore may not observe the same extent of distortion of the target representation in V1 in such groups. Interestingly, schizophrenic subjects also experience less apparent motion (Crawford et al., 2010; Sanders et al., 2013). We suggest that MIB and apparent motion share a causal mechanism of feedback from V5 to V1 (Muckli et al., 2005; Muckli et al., 2002; Sterzer et al., 2006; see Chapter 4).

Due to its relative novelty, FFD has not been investigated in clinical groups. We would expect the FFD to be attenuated in schizophrenic populations, as they show attenuation of other context illusions (Notredame et al., 2015) and illusions which rely on expectations about faces (Dima et al., 2009). FFD may be interesting for use in a clinical population as it provides a case where completely typical feedforward face stimulation gives rise to a monstrous hallucination-like percept in typical observers. It therefore may also allow us to probe how such distortions are formed in healthy patients.

6.10. Conclusions

Visual perception is determined by the combination of feedforward retinal input to the eyes and feedback and lateral connections in the cortex which communicates context. This constructive mechanism results in highly adaptive perception. However, under certain conditions it can also give rise to incorrect percepts or even illusions. Illusions therefore have a special status as they can reveal the constructive powers of the visual cortex. This thesis aimed to elucidate feedback to early visual cortex during illusions. Furthermore, we aimed to develop the understanding of illusory paradigms in order to extend these into schizophrenic test groups. As illusions allow us to investigate constructive vision, they also allow us to elucidate the feedback and feedforward deficits in schizophrenia.

This thesis presented four experiments demonstrating the effects of constructive vision in illusions, and the illusion effect on early visual cortical activity. We employed a multimodal illusion to demonstrate that the congruency of multimodal feedforward inputs can change higher level models of body schema (**Chapter 2**). We then used fMRI to show that during this illusion there is information in early visual cortical activity about the illusory state and its congruence with the feedforward input (**Chapter 3**). In a second fMRI experiment we investigated an illusion in which motion causes visual stimuli to go unseen (**Chapter 4**). We demonstrate that illusory effects can interrupt the representation of a salient target in V1 despite constant feedforward input. This study also showed that V1 activity has a relationship with resulting visual awareness. Our data from both fMRI experiments is further evidence that top-down feedback has effects at the level of early visual cortex, even in the absence of differential feedforward input. In our last experimental chapter we explore a new visual illusion which causes perceived monstrous distortion in stimuli despite normal retinal input. The illusion appears to arise from object-general comparison mechanisms between successively presented stimuli.

Taken together, these chapters demonstrate several illusions that may arise from top-down feedback to the level of early visual cortex. We have discussed these results in the context of top-down feedback, considering whether lateral connections also contribute to the results we observe. We debate how attention may modulate the illusions we use and how it affects our data. Importantly we elucidate the biological realisation of feedback and feedforward integration in these illusions; proposing that layer-specific processing of feedback and feedforward information paired with integration of the two sources within layer V pyramidal neurons allows feedback to affect processing in visual cortex. We hypothesise on the neurobiological specifics in the illusions detailed in this thesis. We discuss the relationship between activity patterns in early visual cortex and the resulting perceptual awareness and suggest how our paradigms could be used to investigate consciousness. We propose that the predictive coding hypothesis of cortical function could explain the results we and others observe, is consistent with the underlying neurobiology, and discuss how our paradigms could be adapted to better probe cortical prediction.

Lastly, we present evidence that cortical feedback and feedforward contributions are dysfunctional in schizophrenia. We consider how this could produce the wide range of perceptual deficits observed and the positive symptoms of the disorder- hallucinations and delusions. We explore how the neuronal architecture underlying feedback and feedforward integration could be at fault in schizophrenia and characterise these deficits in terms of predictive coding theory. We discuss the schizophrenic response to illusory stimuli and explore the possibilities for using illusion studies like those we detail to elucidate feedback and feedforward integration problems in the disorder. If we can elucidate the mechanisms underlying these illusions, we can use them to investigate cortical processing in non-neurotypical populations in future.

Throughout the discussion we propose further avenues for research; specifically in using layer-specific high field fMRI to clarify how these illusions are manifested in cortical layers, utilising different analysis techniques to better investigate whether feedback is a causal mechanism in these illusions, as opposed to a secondary effect, and in applying these illusions to schizophrenia research. In terms of the application of these illusions to schizophrenia research, motion-induced blindness is a promising research avenue. Whilst the mechanisms of the illusion are not yet completely clear, there are recorded behavioural differences between schizophrenic and typical populations in the illusion which can be linked to the potential theoretical and neural underpinnings. We therefore have clear hypotheses for the feedforward and feedback integration differences that may be observed. Future investigation using more invasive techniques, such as optogenetic fMRI will be required to clarify the relationship between layer-specific BOLD response and neuronal contributions to feedback and the integration of feedback and feedforward (Lee et al., 2010).

7. REFERENCES

- Adams, R. A., Stephan, K. E., Brown, H. R., Frith, C. D., & Friston, K. J. (2013). The computational anatomy of psychosis. *Frontiers in Psychiatry*, 4.
- Adams, W. J., Graf, E. W., & Ernst, M. O. (2004). Experience can change the 'light-from-above' prior. *Nature neuroscience*, 7(10), 1057-1058.
- Addington, J., Cadenhead, K. S., Cannon, T. D., Cornblatt, B., McGlashan, T. H., Perkins, D. O., . . . Woods, S. W. (2007). North American Prodrome Longitudinal Study: a collaborative multisite approach to prodromal schizophrenia research. *Schizophrenia Bulletin*, 33(3), 665-672.
- Aguirre, G. K., Zarahn, E., & D'esposito, M. (1998). An area within human ventral cortex sensitive to "building" stimuli: evidence and implications. *Neuron*, 21(2), 373-383.
- Ahmed, B., Hanazawa, A., Undeman, C., Eriksson, D., Valentiniene, S., & Roland, P. E. (2008). Cortical dynamics subserving visual apparent motion. *Cerebral Cortex*, 18(12), 2796-2810.
- Akselrod, M., Herzog, M. H., & Ögmen, H. (2014). Tracing path-guided apparent motion in human primary visual cortex V1. *Scientific reports*, 4, 6063.
- Albers, A. M., Kok, P., Toni, I., Dijkerman, H. C., & de Lange, F. P. (2013). Shared representations for working memory and mental imagery in early visual cortex. *Current Biology*, 23(15), 1427-1431.
- Alink, A., Schwiedrzik, C. M., Kohler, A., Singer, W., & Muckli, L. (2010). Stimulus predictability reduces responses in primary visual cortex. *The Journal of neuroscience*, 30(8), 2960-2966.
- Altmann, C. F., Bühlhoff, H. H., & Kourtzi, Z. (2003). Perceptual organization of local elements into global shapes in the human visual cortex. *Current Biology*, 13(4), 342-349.
- Amedi, A., Floel, A., Knecht, S., Zohary, E., & Cohen, L. G. (2004). Transcranial magnetic stimulation of the occipital pole interferes with verbal processing in blind subjects. *Nature neuroscience*, 7(11), 1266-1270.
- Amedi, A., Jacobson, G., Hendler, T., Malach, R., & Zohary, E. (2002). Convergence of visual and tactile shape processing in the human lateral occipital complex. *Cerebral Cortex*, 12(11), 1202-1212.
- Amedi, A., Malach, R., Hendler, T., Peled, S., & Zohary, E. (2001). Visuo-haptic object-related activation in the ventral visual pathway. *Nature neuroscience*, 4(3), 324-330.
- Amedi, A., Malach, R., & Pascual-Leone, A. (2005). Negative BOLD differentiates visual imagery and perception. *Neuron*, 48(5), 859-872.
- Andrews, T. J., Schluppeck, D., Homfray, D., Matthews, P., & Blakemore, C. (2002). Activity in the fusiform gyrus predicts conscious perception of Rubin's vase-face illusion. *Neuroimage*, 17(2), 890-901.
- Angelucci, A., & Bressloff, P. C. (2006). Contribution of feedforward, lateral and feedback connections to the classical receptive field center and extra-classical receptive field surround of primate V1 neurons. *Progress in brain research*, 154, 93-120.
- Angelucci, A., & Bullier, J. (2003). Reaching beyond the classical receptive field of V1 neurons: horizontal or feedback axons? *The Journal of physiology*, 97(2), 141-154.
- Angelucci, A., Levitt, J. B., Walton, E. J., Hupe, J.-M., Bullier, J., & Lund, J. S. (2002). Circuits for local and global signal integration in primary visual cortex. *The Journal of neuroscience*, 22(19), 8633-8646.
- Anthony, T., Copper, C., & Mullen, B. (1992). Cross-racial facial identification: A social cognitive integration. *Personality and Social Psychology Bulletin*, 18(3), 296-301.
- Apps, M. A., & Tsakiris, M. (2014). The free-energy self: a predictive coding account of self-recognition. *Neuroscience & Biobehavioral Reviews*, 41, 85-97.
- Armel, K., & Ramachandran, V. S. (2003). Projecting sensations to external objects: evidence from skin conductance response. *Proceedings of the Royal Society of London B: Biological Sciences*, 270(1523), 1499-1506.
- Aru, J., Bachmann, T., Singer, W., & Melloni, L. (2012). Distilling the neural correlates of consciousness. *Neuroscience & Biobehavioral Reviews*, 36(2), 737-746.

- Arzy, S., Mohr, C., Michel, C. M., & Blanke, O. (2007). Duration and not strength of activation in temporo-parietal cortex positively correlates with schizotypy. *Neuroimage*, *35*(1), 326-333.
- Asai, T., Mao, Z., Sugimori, E., & Tanno, Y. (2011). Rubber hand illusion, empathy, and schizotypal experiences in terms of self-other representations. *Consciousness and cognition*, *20*(4), 1744-1750.
- Ayzenshtat, I., Gilad, A., Zurawel, G., & Slovin, H. (2012). Population response to natural images in the primary visual cortex encodes local stimulus attributes and perceptual processing. *The Journal of neuroscience*, *32*(40), 13971-13986.
- Bachmann, T. (2015). On the brain-imaging markers of neural correlates of consciousness. *Frontiers in Psychology*, *6*, 868.
- Bachmann, T., & Hudetz, A. G. (2015). It is time to combine the two main traditions in the research on the neural correlates of consciousness: $C = L \times D$. *Frontiers in Psychology*, *5*, 940.
- Bakin, J. S., Nakayama, K., & Gilbert, C. D. (2000). Visual responses in monkey areas V1 and V2 to three-dimensional surface configurations. *The Journal of neuroscience*, *20*(21), 8188-8198.
- Ban, H., Yamamoto, H., Hanakawa, T., Urayama, S.-i., Aso, T., Fukuyama, H., & Ejima, Y. (2013). Topographic representation of an occluded object and the effects of spatiotemporal context in human early visual areas. *The Journal of neuroscience*, *33*(43), 16992-17007.
- Bannert, M. M., & Bartels, A. (2013). Decoding the yellow of a gray banana. *Current Biology*, *23*(22), 2268-2272.
- Bar, M. (2007). The proactive brain: using analogies and associations to generate predictions. *Trends in cognitive sciences*, *11*(7), 280-289.
- Bar, M., Tootell, R. B., Schacter, D. L., Greve, D. N., Fischl, B., Mendola, J. D., . . . Dale, A. M. (2001). Cortical mechanisms specific to explicit visual object recognition. *Neuron*, *29*(2), 529-535.
- Barton, J. J., Keenan, J. P., & Bass, T. (2001). Discrimination of spatial relations and features in faces: Effects of inversion and viewing duration. *British Journal of Psychology*, *92*(3), 527-549.
- Bastos, A. M., Usrey, W. M., Adams, R. A., Mangun, G. R., Fries, P., & Friston, K. J. (2012). Canonical microcircuits for predictive coding. *Neuron*, *76*(4), 695-711.
- Bastos, A. M., Vezoli, J., Bosman, C. A., Schoffelen, J.-M., Oostenveld, R., Dowdall, J. R., . . . Fries, P. (2015). Visual areas exert feedforward and feedback influences through distinct frequency channels. *Neuron*, *85*(2), 390-401.
- Beauchamp, M. S., LaConte, S., & Yasar, N. (2009). Distributed representation of single touches in somatosensory and visual cortex. *Human brain mapping*, *30*(10), 3163-3171.
- Beck, D. M., & Kastner, S. (2009). Top-down and bottom-up mechanisms in biasing competition in the human brain. *Vision research*, *49*(10), 1154-1165.
- Bekrater-Bodmann, R., Foell, J., Diers, M., Kamping, S., Rance, M., Kirsch, P., . . . Çakmak, H. K. (2014). The Importance of Synchrony and Temporal Order of Visual and Tactile Input for Illusory Limb Ownership Experiences—An fMRI Study Applying Virtual Reality. *PLoS One*, *9*(1), e87013.
- Bennett, M., Petro, L., & Muckli, L. (2016). *Investigating cortical feedback of background scene and embedded objects to foveal and peripheral V1 using fMRI*. Paper presented at the Vision Sciences Society, Florida, USA.
- Bentall, R. P., Claridge, G., & Slade, P. D. (1989). The multidimensional nature of schizotypal traits: A factor analytic study with normal subjects. *British Journal of clinical psychology*, *28*(4), 363-375.
- Berkeley, G. (1709). *An Essay Towards a New Theory of Vision*. . Dublin, Ireland: Aaron Rhames, for Jeremy Pepyat.
- Berkes, P., Orbán, G., Lengyel, M., & Fiser, J. (2011). Spontaneous cortical activity reveals hallmarks of an optimal internal model of the environment. *Science*, *331*(6013), 83-87.
- Berry, M. J., Brivanlou, I. H., Jordan, T. A., & Meister, M. (1999). Anticipation of moving stimuli by the retina. *Nature*, *398*(6725), 334-338.
- Blake, R., & Logothetis, N. K. (2002). Visual competition. *Nature Reviews Neuroscience*, *3*(1), 13-21.

- Blakemore, S.-J., Frith, C. D., & Wolpert, D. M. (1999). Spatio-temporal prediction modulates the perception of self-produced stimuli. *Journal of cognitive neuroscience*, *11*(5), 551-559.
- Blakemore, S.-J., Frith, C. D., & Wolpert, D. M. (2001). The cerebellum is involved in predicting the sensory consequences of action. *Neuroreport*, *12*(9), 1879-1884.
- Blakemore, S.-J., Wolpert, D., & Frith, C. (2000). Why can't you tickle yourself? *Neuroreport*, *11*(11), R11-R16.
- Blakemore, S., & Frith, C. (2000). Functional neuroimaging studies of schizophrenia. In J. Mazziotta, A. Toga, & R. Frackowiak (Eds.), *Brain Mapping: the Disorders* (pp. 523-544). London, UK: Academic Press.
- Blanke, O., & Metzinger, T. (2009). Full-body illusions and minimal phenomenal selfhood. *Trends in cognitive sciences*, *13*(1), 7-13.
- Bonneh, Y., & Donner, T. (2011). Motion induced blindness. *Scholarpedia*, *6*(6), 3321.
- Bonneh, Y. S., Cooperman, A., & Sagi, D. (2001). Motion-induced blindness in normal observers. *Nature*, *411*(6839), 798-801.
- Bonneh, Y. S., Donner, T. H., Cooperman, A., Heeger, D. J., & Sagi, D. (2014). Motion-induced blindness and troxler fading: common and different mechanisms. *PLoS One*, *9*(3), e92894.
- Bonneh, Y. S., Donner, T. H., Sagi, D., Fried, M., Cooperman, A., Heeger, D. J., & Arieli, A. (2010). Motion-induced blindness and microsaccades: cause and effect. *Journal of vision*, *10*(14), 22-22.
- Bortolon, C., Capdevielle, D., & Raffard, S. (2015). Face recognition in schizophrenia disorder: A comprehensive review of behavioral, neuroimaging and neurophysiological studies. *Neuroscience & Biobehavioral Reviews*, *53*, 79-107.
- Botvinick, M., & Cohen, J. (1998). Rubber hands' feel' touch that eyes see. *Nature*, *391*(6669), 756-756.
- Bressan, P., & Kramer, P. (2013). The relation between cognitive-perceptual schizotypal traits and the Ebbinghaus size-illusion is mediated by judgment time. *Frontiers in Psychology*, *4*, 343.
- Bressler, S. L., Tang, W., Sylvester, C. M., Shulman, G. L., & Corbetta, M. (2008). Top-down control of human visual cortex by frontal and parietal cortex in anticipatory visual spatial attention. *The Journal of neuroscience*, *28*(40), 10056-10061.
- Brewer, A. A., Liu, J., Wade, A. R., & Wandell, B. A. (2005). Visual field maps and stimulus selectivity in human ventral occipital cortex. *Nature neuroscience*, *8*(8), 1102-1109.
- Brown, H., & Friston, K. J. (2012). Free-energy and illusions: the cornsweet effect. *Frontiers in Psychology*, *3*(43), 10.3389.
- Bubic, A., Von Cramon, D. Y., & Schubotz, R. I. (2010). Prediction, cognition and the brain. *Frontiers in human neuroscience*, *4*, 25.
- Budd, J. M. (1998). Extrastriate feedback to primary visual cortex in primates: a quantitative analysis of connectivity. *Proceedings of the Royal Society of London B: Biological Sciences*, *265*(1400), 1037-1044.
- Bullier, J. (2001). Integrated model of visual processing. *Brain Research Reviews*, *36*(2), 96-107.
- Busigny, T., & Rossion, B. (2010). Acquired prosopagnosia abolishes the face inversion effect. *Cortex*, *46*(8), 965-981.
- Carmel, D., Walsh, V., Lavie, N., & Rees, G. (2010). Right parietal TMS shortens dominance durations in binocular rivalry. *Current Biology*, *20*(18), R799-R800.
- Carpenter, G. A., & Grossberg, S. (2011). *Adaptive Resonance Theory*. New York, USA: Springer.
- Carroll, C. A., Boggs, J., O'Donnell, B. F., Shekhar, A., & Hetrick, W. P. (2008). Temporal processing dysfunction in schizophrenia. *Brain and cognition*, *67*(2), 150-161.
- Castelo-Branco, M., Formisano, E., Backes, W., Zanella, F., Neuenschwander, S., Singer, W., & Goebel, R. (2002). Activity patterns in human motion-sensitive areas depend on the interpretation of global motion. *Proceedings of the National Academy of Sciences*, *99*(21), 13914-13919.
- Chambers, C. D., Allen, C. P., Maizey, L., & Williams, M. A. (2013). Is delayed foveal feedback critical for extra-foveal perception? *Cortex*, *49*(1), 327-335.
- Chan, J. S., Simões-Franklin, C., Garavan, H., & Newell, F. N. (2010). Static images of novel, moveable objects learned through touch activate visual area hMT+. *Neuroimage*, *49*(2), 1708-1716.

- Chang, H.-T. (1951). Dendritic potential of cortical neurons produced by direct electrical stimulation of the cerebral cortex. *Journal of neurophysiology*, 14(1), 1-21.
- Chen, Y., Norton, D., & Ongur, D. (2008). Altered center-surround motion inhibition in schizophrenia. *Biological psychiatry*, 64(1), 74-77.
- Chong, E., Familiar, A. M., & Shim, W. M. (2015). Reconstructing representations of dynamic visual objects in early visual cortex. *Proceedings of the National Academy of Sciences*, 13(5), 1453-1458.
- Chu, Z., Galarreta, M., & Hestrin, S. (2003). Synaptic interactions of late-spiking neocortical neurons in layer 1. *The Journal of neuroscience*, 23(1), 96-102.
- Clark, A. (2013). Whatever next? Predictive brains, situated agents, and the future of cognitive science. *Behavioral and Brain Sciences*, 36(3), 181-204.
- Clem, R. K., & Pollack, R. H. (1975). Illusion magnitude as a function of visual field exposure. *Perception & Psychophysics*, 17(5), 450-454.
- Collingridge, G., & Bliss, T. (1987). NMDA receptors-their role in long-term potentiation. *Trends in neurosciences*, 10(7), 288-293.
- Corlett, P., & Fletcher, P. (2012). The neurobiology of schizotypy: fronto-striatal prediction error signal correlates with delusion-like beliefs in healthy people. *Neuropsychologia*, 50(14), 3612-3620.
- Corlett, P., Frith, C. D., & Fletcher, P. (2009). From drugs to deprivation: a Bayesian framework for understanding models of psychosis. *Psychopharmacology*, 206(4), 515-530.
- Corlett, P. R., Honey, G. D., Krystal, J. H., & Fletcher, P. C. (2011). Glutamatergic model psychoses: prediction error, learning, and inference. *Neuropsychopharmacology*, 36(1), 294-315.
- Corlett, P. R., Taylor, J., Wang, X.-J., Fletcher, P., & Krystal, J. (2010). Toward a neurobiology of delusions. *Progress in neurobiology*, 92(3), 345-369.
- Costantini, M., & Haggard, P. (2007). The rubber hand illusion: sensitivity and reference frame for body ownership. *Consciousness and cognition*, 16(2), 229-240.
- Costantini, M., Urgesi, C., Galati, G., Romani, G. L., & Aglioti, S. M. (2011). Haptic perception and body representation in lateral and medial occipito-temporal cortices. *Neuropsychologia*, 49(5), 821-829.
- Crawford, T., Hamm, J., Kean, M., Schmechtig, A., Kumari, V., Anilkumar, A., & Ettinger, U. (2010). The perception of real and illusory motion in schizophrenia. *Neuropsychologia*, 48(10), 3121-3127.
- Crick, F., & Koch, C. (1990). Towards a neurobiological theory of consciousness. *Seminars in the Neurosciences*, 2, 263-275.
- Crick, F., & Koch, C. (1995). Are we aware of neural activity in primary visual cortex? *Nature*, 375(6527), 121-123.
- Crookes, K., & Hayward, W. G. (2012). Face inversion disproportionately disrupts sensitivity to vertical over horizontal changes in eye position. *Journal of Experimental Psychology: Human Perception and Performance*, 38(6), 1428.
- Cutting, J., & Shepherd, M. (1987). *The Clinical Roots of the Schizophrenia Concept: Translations of Seminal European Contributions on Schizophrenia*. Cambridge, UK: Cambridge University Press.
- Dakin, S., Carlin, P., & Hemsley, D. (2005). Weak suppression of visual context in chronic schizophrenia. *Current Biology*, 15(20), R822-R824.
- Daniel, P., & Whitteridge, D. (1961). The representation of the visual field on the cerebral cortex in monkeys. *The Journal of physiology*, 159(2), 203-221.
- Das, A., & Gilbert, C. (1995). Receptive field expansion in adult visual cortex is linked to dynamic changes in strength of cortical connections. *Journal of neurophysiology*, 74(2), 779-792.
- Davalos, D. B., Kisley, M. A., & Ross, R. G. (2003). Effects of interval duration on temporal processing in schizophrenia. *Brain and cognition*, 52(3), 295-301.
- David, N., Bewernick, B. H., Cohen, M. S., Newen, A., Lux, S., Fink, G. R., . . . Vogeley, K. (2006). Neural representations of self versus other: visual-spatial perspective taking and agency in a virtual ball-tossing game. *Journal of cognitive neuroscience*, 18(6), 898-910.
- De Gelder, B., & Bertelson, P. (2003). Multisensory integration, perception and ecological validity. *Trends in cognitive sciences*, 7(10), 460-467.

- De Graaf, T. A., Hsieh, P.-J., & Sack, A. T. (2012). The ‘correlates’ in neural correlates of consciousness. *Neuroscience & Biobehavioral Reviews*, *36*(1), 191-197.
- De Pasquale, R., & Sherman, S. M. (2011). Synaptic properties of corticocortical connections between the primary and secondary visual cortical areas in the mouse. *The Journal of neuroscience*, *31*(46), 16494-16506.
- Dehaene, S., Changeux, J.-P., Naccache, L., Sackur, J., & Sergent, C. (2006). Conscious, preconscious, and subliminal processing: a testable taxonomy. *Trends in cognitive sciences*, *10*(5), 204-211.
- Den Ouden, H. E., Kok, P., & De Lange, F. P. (2012). How prediction errors shape perception, attention, and motivation. *Frontiers in Psychology*, *3*, 548.
- Desimone, R., & Duncan, J. (1995). Neural mechanisms of selective visual attention. *Annual review of neuroscience*, *18*(1), 193-222.
- DeYoe, E. A., Carman, G. J., Bandettini, P., Glickman, S., Wieser, J., Cox, R., . . . Neitz, J. (1996). Mapping striate and extrastriate visual areas in human cerebral cortex. *Proceedings of the National Academy of Sciences*, *93*(6), 2382-2386.
- DeYoe, E. A., & Van Essen, D. C. (1988). Concurrent processing streams in monkey visual cortex. *Trends in neurosciences*, *11*(5), 219-226.
- Dieter, K. C., Tadin, D., & Pearson, J. (2015). Motion-induced blindness continues outside visual awareness and without attention. *Scientific reports*, *5*.
- Dima, D., Roiser, J. P., Dietrich, D. E., Bonnemann, C., Lanfermann, H., Emrich, H. M., & Dillo, W. (2009). Understanding why patients with schizophrenia do not perceive the hollow-mask illusion using dynamic causal modelling. *Neuroimage*, *46*(4), 1180-1186.
- Dodd, J. V., Krug, K., Cumming, B. G., & Parker, A. J. (2001). Perceptually bistable three-dimensional figures evoke high choice probabilities in cortical area MT. *The Journal of neuroscience*, *21*(13), 4809-4821.
- Dolan, R., Fink, G., Rolls, E., Booth, M., Holmes, A., Frackowiak, R., & Friston, K. (1997). How the brain learns to see objects and faces in an impoverished context. *Nature*, *389*(6651), 596-599.
- Doniger, G. M., Foxe, J. J., Murray, M. M., Higgins, B. A., Snodgrass, J. G., Schroeder, C. E., & Javitt, D. C. (2000). Activation timecourse of ventral visual stream object-recognition areas: high density electrical mapping of perceptual closure processes. *Journal of cognitive neuroscience*, *12*(4), 615-621.
- Donner, T. H., Sagi, D., Bonneh, Y. S., & Heeger, D. J. (2008). Opposite neural signatures of motion-induced blindness in human dorsal and ventral visual cortex. *The Journal of neuroscience*, *28*(41), 10298-10310.
- Donner, T. H., Sagi, D., Bonneh, Y. S., & Heeger, D. J. (2013). Retinotopic patterns of correlated fluctuations in visual cortex reflect the dynamics of spontaneous perceptual suppression. *The Journal of neuroscience*, *33*(5), 2188-2198.
- Douglas, R. J., & Martin, K. A. (2007). Recurrent neuronal circuits in the neocortex. *Current Biology*, *17*(13), R496-R500.
- Driver, J., & Frackowiak, R. S. (2001). Neurobiological measures of human selective attention. *Neuropsychologia*, *39*(12), 1257-1262.
- Dum, R. P., & Strick, P. L. (2003). An unfolded map of the cerebellar dentate nucleus and its projections to the cerebral cortex. *Journal of neurophysiology*, *89*(1), 634-639.
- Duncan, R. O., & Boynton, G. M. (2003). Cortical magnification within human primary visual cortex correlates with acuity thresholds. *Neuron*, *38*(4), 659-671.
- Duyn, J. H. (2012). The future of ultra-high field MRI and fMRI for study of the human brain. *Neuroimage*, *62*(2), 1241-1248.
- Eckert, M. A., Kamdar, N. V., Chang, C. E., Beckmann, C. F., Greicius, M. D., & Menon, V. (2008). A cross-modal system linking primary auditory and visual cortices: Evidence from intrinsic fMRI connectivity analysis. *Human brain mapping*, *29*(7), 848-857.
- Egner, T., Monti, J. M., & Summerfield, C. (2010). Expectation and surprise determine neural population responses in the ventral visual stream. *The Journal of neuroscience*, *30*(49), 16601-16608.
- Ehrsson, H. H. (2007). The experimental induction of out-of-body experiences. *Science*, *317*(5841), 1048-1048.

- Ehrsson, H. H., Holmes, N. P., & Passingham, R. E. (2005). Touching a rubber hand: feeling of body ownership is associated with activity in multisensory brain areas. *The Journal of neuroscience*, 25(45), 10564-10573.
- Ehrsson, H. H., Spence, C., & Passingham, R. E. (2004). That's my hand! Activity in premotor cortex reflects feeling of ownership of a limb. *Science*, 305(5685), 875-877.
- Ehrsson, H. H., Wiech, K., Weiskopf, N., Dolan, R. J., & Passingham, R. E. (2007). Threatening a rubber hand that you feel is yours elicits a cortical anxiety response. *Proceedings of the National Academy of Sciences*, 104(23), 9828-9833.
- Ellis, H. D., & Young, A. (1983). The role of the right hemisphere in face perception. In A. Young (Ed.), *Functions of the right cerebral hemisphere* (pp. 33-64). London, UK: Academic Press.
- Elvevåg, B., McCormack, T., Gilbert, A., Brown, G. D., Weinberger, D. R., & Goldberg, T. E. (2003). Duration judgements in patients with schizophrenia. *Psychological medicine*, 33(7), 1249-1261.
- Engbert, R. (2006). Microsaccades: A microcosm for research on oculomotor control, attention, and visual perception. *Progress in brain research*, 154, 177-192.
- Engel, A. K., Fries, P., & Singer, W. (2001). Dynamic predictions: oscillations and synchrony in top-down processing. *Nature Reviews Neuroscience*, 2(10), 704-716.
- Engel, S., Zhang, X., & Wandell, B. (1997). Colour tuning in human visual cortex measured with functional magnetic resonance imaging. *Nature*, 388(6637), 68-71.
- Engel, S. A., Glover, G. H., & Wandell, B. A. (1997). Retinotopic organization in human visual cortex and the spatial precision of functional MRI. *Cerebral Cortex*, 7(2), 181-192.
- Engel, S. A., Rumelhart, D. E., Wandell, B. A., Lee, A. T., Glover, G. H., Chichilnisky, E.-J., & Shadlen, M. N. (1994). fMRI of human visual cortex. *Nature*, 370(6485), 106.
- Enns, J. T., & Di Lollo, V. (2000). What's new in visual masking? *Trends in cognitive sciences*, 4(9), 345-352.
- Epstein, R., & Kanwisher, N. (1998). A cortical representation of the local visual environment. *Nature*, 392(6676), 598-601.
- Erlhagen, W. (2003). Internal models for visual perception. *Biological cybernetics*, 88(5), 409-417.
- Fahrenfort, J. J., & Lamme, V. A. (2012). A true science of consciousness explains phenomenology: comment on Cohen and Dennett. *Trends in cognitive sciences*, 16(3), 138.
- Faivre, N., & Koch, C. (2014). Inferring the direction of implied motion depends on visual awareness. *Journal of vision*, 14(4), 4-4.
- Fang, F., Boyaci, H., Kersten, D., & Murray, S. O. (2008). Attention-dependent representation of a size illusion in human V1. *Current Biology*, 18(21), 1707-1712.
- Feingold, G. A. (1914). Influence of environment on identification of persons and things. *Journal of Criminal Law and Criminology*, 5(1), 39.
- Feldman, H., & Friston, K. (2010). Attention, uncertainty, and free-energy. *Frontiers in human neuroscience*, 4, 215.
- Felleman, D. J., & Van Essen, D. C. (1991). Distributed hierarchical processing in the primate cerebral cortex. *Cerebral Cortex*, 1(1), 1-47.
- Fitzpatrick, D. (2000). Seeing beyond the receptive field in primary visual cortex. *Current Opinion in Neurobiology*, 10(4), 438-443.
- Fletcher, P. C., & Frith, C. D. (2009). Perceiving is believing: a Bayesian approach to explaining the positive symptoms of schizophrenia. *Nature Reviews Neuroscience*, 10(1), 48-58.
- Flevaris, A. V., & Murray, S. O. (2015). Feature-based attention modulates surround suppression. *Journal of vision*, 15(1), 29-29.
- Foucher, J., Lacambre, M., Pham, B.-T., Giersch, A., & Elliott, M. (2007). Low time resolution in schizophrenia: Lengthened windows of simultaneity for visual, auditory and bimodal stimuli. *Schizophrenia research*, 97(1), 118-127.
- Francis, G., & Kim, J. (2012). Simulations of induced visual scene fading with boundary offset and filling-in. *Vision research*, 62, 181-191.
- Franck, N., Farrer, C., Georgieff, N., Marie-Cardine, M., Daléry, J., d'Amato, T., & Jeannerod, M. (2001). Defective recognition of one's own actions in patients with schizophrenia. *American Journal of Psychiatry*, 158(3), 454-459.

- Frässle, S., Sommer, J., Jansen, A., Naber, M., & Einhäuser, W. (2014). Binocular rivalry: frontal activity relates to introspection and action but not to perception. *The Journal of neuroscience*, *34*(5), 1738-1747.
- Friston, K. (2002). Functional integration and inference in the brain. *Progress in neurobiology*, *68*(2), 113-143.
- Friston, K. (2005). A theory of cortical responses. *Philosophical Transactions of the Royal Society of London B: Biological Sciences*, *360*(1456), 815-836.
- Friston, K. (2009). The free-energy principle: a rough guide to the brain? *Trends in cognitive sciences*, *13*(7), 293-301.
- Friston, K. (2010). The free-energy principle: a unified brain theory? *Nature Reviews Neuroscience*, *11*(2), 127-138.
- Friston, K. (2012). The history of the future of the Bayesian brain. *Neuroimage*, *62*(2), 1230-1233.
- Friston, K., & Kiebel, S. (2009). Predictive coding under the free-energy principle. *Philosophical Transactions of the Royal Society of London B: Biological Sciences*, *364*(1521), 1211-1221.
- Friston, K., Preller, K. H., Mathys, C., Cagnan, H., Heinzle, J., Razi, A., & Zeidman, P. (2017). Dynamic causal modelling revisited. *Neuroimage*, *In Press*.
- Friston, K. J., Daunizeau, J., Kilner, J., & Kiebel, S. J. (2010). Action and behavior: a free-energy formulation. *Biological cybernetics*, *102*(3), 227-260.
- Friston, K. J., Harrison, L., & Penny, W. (2003). Dynamic causal modelling. *Neuroimage*, *19*(4), 1273-1302.
- Frith, C. D. (1987). The positive and negative symptoms of schizophrenia reflect impairments in the perception and initiation of action. *Psychological medicine*, *17*(3), 631-648.
- Frith, C. D., Blakemore, S.-J., & Wolpert, D. M. (2000). Explaining the symptoms of schizophrenia: abnormalities in the awareness of action. *Brain Research Reviews*, *31*(2), 357-363.
- Gallagher, S. (2000). Philosophical conceptions of the self: implications for cognitive science. *Trends in cognitive sciences*, *4*(1), 14-21.
- Gandhi, S. P., Heeger, D. J., & Boynton, G. M. (1999). Spatial attention affects brain activity in human primary visual cortex. *Proceedings of the National Academy of Sciences*, *96*(6), 3314-3319.
- Garcia, C. P., Sacks, S. A., & de Mamani, A. G. W. (2012). Neurocognition and cognitive biases in schizophrenia. *The Journal of nervous and mental disease*, *200*(8), 724-727.
- Gauthier, I., & Nelson, C. A. (2001). The development of face expertise. *Current Opinion in Neurobiology*, *11*(2), 219-224.
- Gauthier, I., & Tarr, M. J. (1997). Becoming a “Greeble” expert: Exploring mechanisms for face recognition. *Vision research*, *37*(12), 1673-1682.
- Gayet, S., Van der Stigchel, S., & Paffen, C. L. (2014). Breaking continuous flash suppression: competing for consciousness on the pre-semantic battlefield. *Frontiers in Psychology*, *5*, 460.
- Geisler, W. S., & Kersten, D. (2002). Illusions, perception and Bayes. *Nature neuroscience*, *5*(6), 508-510.
- Geisler, W. S., & Perry, J. S. (2011). Statistics for optimal point prediction in natural images. *Journal of vision*, *11*(12), 14-14.
- Gelbard-Sagiv, H., Faivre, N., Mudrik, L., & Koch, C. (2016). Low-level awareness accompanies “unconscious” high-level processing during continuous flash suppression. *Journal of vision*, *16*(1), 3-3.
- Genç, E., Bergmann, J., Singer, W., & Kohler, A. (2011). Interhemispheric connections shape subjective experience of bistable motion. *Current Biology*, *21*(17), 1494-1499.
- Geng, H., Song, Q., Li, Y., Xu, S., & Zhu, Y. (2007). Attentional modulation of motion-induced blindness. *Chinese Science Bulletin*, *52*(8), 1063-1070.
- George, N., Dolan, R. J., Fink, G. R., Baylis, G. C., Russell, C., & Driver, J. (1999). Contrast polarity and face recognition in the human fusiform gyrus. *Nature neuroscience*, *2*(6), 574-580.
- Georges, S., Series, P., Frégnac, Y., & Lorenceau, J. (2002). Orientation dependent modulation of apparent speed: psychophysical evidence. *Vision research*, *42*(25), 2757-2772.
- Germine, L., Benson, T. L., Cohen, F., & Hooker, C. I. L. (2013). Psychosis-proneness and the rubber hand illusion of body ownership. *Psychiatry Research*, *207*(1), 45-52.

- Geschwind, D. H., & Rakic, P. (2013). Cortical evolution: judge the brain by its cover. *Neuron*, 80(3), 633-647.
- Gilaie-Dotan, S., Ullman, S., Kushnir, T., & Malach, R. (2002). Shape-selective stereo processing in human object-related visual areas. *Human brain mapping*, 15(2), 67-79.
- Gilbert, C., & Bakan, P. (1973). Visual asymmetry in perception of faces. *Neuropsychologia*, 11(3), 355-362.
- Gilbert, C. D., & Li, W. (2013). Top-down influences on visual processing. *Nature Reviews Neuroscience*, 14(5), 350-363.
- Gilbert, C. D., & Sigman, M. (2007). Brain states: top-down influences in sensory processing. *Neuron*, 54(5), 677-696.
- Goffaux, V., & Dakin, S. (2010). Horizontal information drives the behavioral signatures of face processing. *Frontiers in Psychology*, 1, 143.
- Goodale, M. A., & Milner, A. D. (1991). A neurological dissociation between perceiving objects and grasping them. *Nature*, 349(6305), 154.
- Gorea, A., & Caetta, F. (2009). Adaptation and prolonged inhibition as a main cause of motion-induced blindness. *Journal of vision*, 9(6), 16-16.
- Graf, E. W., Adams, W. J., & Lages, M. (2002). Modulating motion-induced blindness with depth ordering and surface completion. *Vision research*, 42(25), 2731-2735.
- Gregory, R. L. (1970). *The Intelligent Eye*. London, UK: Weidenfeld & Nicolson.
- Gregory, R. L. (1997). Knowledge in perception and illusion. *Philosophical Transactions of the Royal Society of London B: Biological Sciences*, 352(1358), 1121-1127.
- Gregory, R. L. (2006). Bayes Window (3): Where do prior probabilities come from? *Perception*, 35(3), 289-290.
- Gregory, R. L., & Gombrich, E. H. (1975). *Illusion in Nature and Art*. London, UK: Gerald Duckworth & Co Ltd.
- Grill-Spector, K. (2003). The neural basis of object perception. *Current Opinion in Neurobiology*, 13(2), 159-166.
- Grill-Spector, K., Kourtzi, Z., & Kanwisher, N. (2001). The lateral occipital complex and its role in object recognition. *Vision research*, 41(10), 1409-1422.
- Grill-Spector, K., Kushnir, T., Hendler, T., Edelman, S., Itzchak, Y., & Malach, R. (1998). A sequence of object-processing stages revealed by fMRI in the human occipital lobe. *Human brain mapping*, 6(4), 316-328.
- Grill-Spector, K., Kushnir, T., Hendler, T., & Malach, R. (2000). The dynamics of object-selective activation correlate with recognition performance in humans. *Nature neuroscience*, 3(8), 837-843.
- Grill-Spector, K., & Malach, R. (2004). The human visual cortex. *Annual review of neuroscience*, 27, 649-677.
- Grossberg, S. (2013). Adaptive Resonance Theory: How a brain learns to consciously attend, learn, and recognize a changing world. *Neural Networks*, 37, 1-47.
- Gschwind, M., Pourtois, G., Schwartz, S., Van De Ville, D., & Vuilleumier, P. (2012). White-matter connectivity between face-responsive regions in the human brain. *Cerebral Cortex*, 22(7), 1564-1576.
- Guterstam, A., Gentile, G., & Ehrsson, H. H. (2013). The invisible hand illusion: multisensory integration leads to the embodiment of a discrete volume of empty space. *Journal of cognitive neuroscience*, 25(7), 1078-1099.
- Hagen, M. C., Franzén, O., McGlone, F., Essick, G., Dancer, C., & Pardo, J. V. (2002). Tactile motion activates the human middle temporal/V5 (MT/V5) complex. *European Journal of Neuroscience*, 16(5), 957-964.
- Harris, J. A., Barack, D. L., McMahan, A. R., Mitroff, S. R., & Woldorff, M. G. (2013). Object-Category Processing, Perceptual Awareness, and the Role of Attention during Motion-Induced Blindness. *Cognitive Electrophysiology of Attention: Signals of the Mind*, 97.
- Harris, J. J., Schwarzkopf, D. S., Song, C., Bahrami, B., & Rees, G. (2011). Contextual illusions reveal the limit of unconscious visual processing. *Psychological science*, 22(3), 399-405.
- Harrison, L., Stephan, K., Rees, G., & Friston, K. (2007). Extra-classical receptive field effects measured in striate cortex with fMRI. *Neuroimage*, 34(3), 1199-1208.

- Harrison, P. J., & Weinberger, D. R. (2005). Schizophrenia genes, gene expression, and neuropathology: on the matter of their convergence. *Molecular Psychiatry*, *10*(1), 40-68.
- Harrison, S. A., & Tong, F. (2009). Decoding reveals the contents of visual working memory in early visual areas. *Nature*, *458*(7238), 632-635.
- Hasson, U., Harel, M., Levy, I., & Malach, R. (2003). Large-scale mirror-symmetry organization of human occipito-temporal object areas. *Neuron*, *37*(6), 1027-1041.
- Hasson, U., Hendler, T., Bashat, D. B., & Malach, R. (2001). Vase or face? A neural correlate of shape-selective grouping processes in the human brain. *Journal of cognitive neuroscience*, *13*(6), 744-753.
- Havlicek, M., Roebroeck, A., Friston, K., Gardumi, A., Ivanov, D., & Uludag, K. (2015). Physiologically informed dynamic causal modeling of fMRI data. *Neuroimage*, *122*, 355-372.
- Hawkins, J., & Ahmad, S. (2016). Why neurons have thousands of synapses, a theory of sequence memory in neocortex. *Frontiers in neural circuits*, *10*.
- Hawkins, J., & Blakeslee, S. (2004). On Intelligence: How a New Understanding of the Brain will lead to Truly Intelligent Machines. New York, USA: Times Books.
- Haxby, J. V., Gobbini, M. I., Furey, M. L., Ishai, A., Schouten, J. L., & Pietrini, P. (2001). Distributed and overlapping representations of faces and objects in ventral temporal cortex. *Science*, *293*(5539), 2425-2430.
- Haxby, J. V., Hoffman, E. A., & Gobbini, M. I. (2000). The distributed human neural system for face perception. *Trends in cognitive sciences*, *4*(6), 223-233.
- Haxby, J. V., Ungerleider, L. G., Clark, V. P., Schouten, J. L., Hoffman, E. A., & Martin, A. (1999). The effect of face inversion on activity in human neural systems for face and object perception. *Neuron*, *22*(1), 189-199.
- Haynes, J.-D., & Rees, G. (2005a). Predicting the orientation of invisible stimuli from activity in human primary visual cortex. *Nature neuroscience*, *8*(5), 686-691.
- Haynes, J.-D., & Rees, G. (2005b). Predicting the stream of consciousness from activity in human visual cortex. *Current Biology*, *15*(14), 1301-1307.
- Haynes, J.-D., & Rees, G. (2006). Decoding mental states from brain activity in humans. *Nature Reviews Neuroscience*, *7*(7), 523-534.
- He, S., & MacLeod, D. I. (2001). Orientation-selective adaptation and tilt after-effect from invisible patterns. *Nature*, *411*(6836), 473-476.
- Heinz, A. (2002). Dopaminergic dysfunction in alcoholism and schizophrenia—psychopathological and behavioral correlates. *European Psychiatry*, *17*(1), 9-16.
- Heinzle, J., Koopmans, P. J., den Ouden, H. E., Raman, S., & Stephan, K. E. (2016). A hemodynamic model for layered BOLD signals. *Neuroimage*, *125*, 556-570.
- Hemsley, D. R. (1994). A cognitive model for schizophrenia and its possible neural basis. *Acta Psychiatrica Scandinavica*, *90*(s384), 80-86.
- Hemsley, D. R. (2005). The development of a cognitive model of schizophrenia: placing it in context. *Neuroscience & Biobehavioral Reviews*, *29*(6), 977-988.
- Hershler, O., Golan, T., Bentin, S., & Hochstein, S. (2010). The wide window of face detection. *Journal of vision*, *10*(10), 21-21.
- Hesselmann, G. (2013). Dissecting visual awareness with FMRI. *The Neuroscientist*, *19*(5), 495-508.
- Hidaka, S., Nagai, M., & Gyoba, J. (2009). Spatiotemporally coherent motion direction perception occurs even for spatiotemporal reversal of motion sequence. *Journal of vision*, *9*(13), 6-6.
- Hills, P. J., Holland, A. M., & Lewis, M. B. (2010). Aftereffects for face attributes with different natural variability: Children are more adaptable than adolescents. *Cognitive Development*, *25*(3), 278-289.
- Hoffman, E. A., & Haxby, J. V. (2000). Distinct representations of eye gaze and identity in the distributed human neural system for face perception. *Nature neuroscience*, *3*(1), 80-84.
- Hofstoetter, C., Koch, C., & Kiper, D. C. (2004). Motion-induced blindness does not affect the formation of negative afterimages. *Consciousness and cognition*, *13*(4), 691-708.
- Hohwy, J. (2007a). Functional Integration and the mind. *Synthese*, *159*(3), 315-328.
- Hohwy, J. (2007b). The sense of self in the phenomenology of agency and perception. *Psyche*, *13*(2), 1-20.

- Hohwy, J. (2010). *The hypothesis testing brain: some philosophical applications*. Paper presented at the Australian Society for Cognitive Science Conference, Sydney, Australia.
- Hohwy, J. (2012). Attention and conscious perception in the hypothesis testing brain. *Frontiers in Psychology*, 3, 96.
- Hohwy, J., & Paton, B. (2010). Explaining away the body: Experiences of supernaturally caused touch and touch on non-hand objects within the rubber hand illusion. *PLoS One*, 5(2), e9416.
- Hohwy, J., & Rajan, V. (2012). Delusions as forensically disturbing perceptual inferences. *Neuroethics*, 5(1), 5-11.
- Hohwy, J., Roepstorff, A., & Friston, K. (2008). Predictive coding explains binocular rivalry: An epistemological review. *Cognition*, 108(3), 687-701.
- Hougaard, N., Fraise, P., & Hecaen, H. (1976). Effects of unilateral hemispheric lesions on two types of optico-geometric illusions. *Cortex*, 12(3), 232-240.
- Hsieh, P.-J., & Peter, U. T. (2009). Microsaccade rate varies with subjective visibility during motion-induced blindness. *PLoS One*, 4(4), e5163.
- Hsu, L.-C., Yeh, S.-L., & Kramer, P. (2004). Linking motion-induced blindness to perceptual filling-in. *Vision research*, 44(24), 2857-2866.
- Hsu, L.-C., Yeh, S.-L., & Kramer, P. (2006). A common mechanism for perceptual filling-in and motion-induced blindness. *Vision research*, 46(12), 1973-1981.
- Huang, Y., & Rao, R. P. (2011). Predictive coding. *Wiley Interdisciplinary Reviews: Cognitive Science*, 2(5), 580-593.
- Hubel, D. H., & Wiesel, T. N. (1959). Receptive fields of single neurones in the cat's striate cortex. *The Journal of physiology*, 148(3), 574-591.
- Hubel, D. H., & Wiesel, T. N. (1974). Sequence regularity and geometry of orientation columns in the monkey striate cortex. *Journal of Comparative Neurology*, 158(3), 267-293.
- Hugenberg, K., Young, S. G., Sacco, D. F., & Bernstein, M. J. (2011). Social categorization influences face perception and face memory. In A. Calder, G. Rhodes, M. Johnson, & J. V. Haxby (Eds.), *The Oxford handbook of face perception* (pp. 245). Oxford, UK: Oxford University Press.
- Hupe, J.-M., James, A. C., Girard, P., Lomber, S. G., Payne, B. R., & Bullier, J. (2001). Feedback connections act on the early part of the responses in monkey visual cortex. *Journal of neurophysiology*, 85(1), 134-145.
- Insel, T. R. (2010). Rethinking schizophrenia. *Nature*, 468(7321), 187-193.
- Ishai, A., Ungerleider, L. G., & Haxby, J. V. (2000). Distributed neural systems for the generation of visual images. *Neuron*, 28(3), 979-990.
- Ishai, A., Ungerleider, L. G., Martin, A., Schouten, J. L., & Haxby, J. V. (1999). Distributed representation of objects in the human ventral visual pathway. *Proceedings of the National Academy of Sciences*, 96(16), 9379-9384.
- Jack, C. R., Bernstein, M. A., Fox, N. C., Thompson, P., Alexander, G., Harvey, D., . . . Ward, C. (2008). The Alzheimer's disease neuroimaging initiative (ADNI): MRI methods. *Journal of magnetic resonance imaging*, 27(4), 685-691.
- James, T. W., Humphrey, G. K., Gati, J. S., Menon, R. S., & Goodale, M. A. (2000). The effects of visual object priming on brain activation before and after recognition. *Current Biology*, 10(17), 1017-1024.
- James, T. W., Humphrey, G. K., Gati, J. S., Servos, P., Menon, R. S., & Goodale, M. A. (2002). Haptic study of three-dimensional objects activates extrastriate visual areas. *Neuropsychologia*, 40(10), 1706-1714.
- Jancke, D., Chavane, F., Naaman, S., & Grinvald, A. (2004). Imaging cortical correlates of illusion in early visual cortex. *Nature*, 428(6981), 423-426.
- Jardri, R., & Denève, S. (2013). Circular inferences in schizophrenia. *Brain*, 136(11), 3227-3241.
- Javitt, D. C. (2009). Sensory processing in schizophrenia: neither simple nor intact. *Schizophrenia Bulletin*, 35(6), 1059-1064.
- Jaworska, K., & Lages, M. (2014). Fluctuations of visual awareness: Combining motion-induced blindness with binocular rivalry. *Journal of vision*, 14(11), 11-11.
- Jehee, J. F., & Ballard, D. H. (2009). Predictive feedback can account for biphasic responses in the lateral geniculate nucleus. *PLoS Computational Biology*, 5(5), e1000373.

- John, C. H., & Hemsley, D. R. (1992). Gestalt perception in schizophrenia. *European archives of psychiatry and clinical neuroscience*, 241(4), 215-221.
- Kaas, A., Weigelt, S., Roebroek, A., Kohler, A., & Muckli, L. (2010). Imagery of a moving object: the role of occipital cortex and human MT/V5+. *Neuroimage*, 49(1), 794-804.
- Kalckert, A., & Ehrsson, H. H. (2012). Moving a rubber hand that feels like your own: a dissociation of ownership and agency. *Frontiers in human neuroscience*, 6(40), 1-14.
- Kamitani, Y., & Tong, F. (2005). Decoding the visual and subjective contents of the human brain. *Nature neuroscience*, 8(5), 679-685.
- Kanai, R., Carmel, D., Bahrami, B., & Rees, G. (2011). Structural and functional fractionation of right superior parietal cortex in bistable perception. *Current Biology*, 21(3), R106-R107.
- Kanai, R., Paulus, W., & Walsh, V. (2010). Transcranial alternating current stimulation (tACS) modulates cortical excitability as assessed by TMS-induced phosphene thresholds. *Clinical Neurophysiology*, 121(9), 1551-1554.
- Kanai, R., Sheth, B. R., & Shimojo, S. (2004). Stopping the motion and sleuthing the flash-lag effect: spatial uncertainty is the key to perceptual mislocalization. *Vision research*, 44(22), 2605-2619.
- Kanizsa, G. (1976). Subjective contours. *Scientific American*, 234(4), 48-52.
- Kant, I. (1781). *Critique of Pure Reason*. London, UK: Penguin Classics.
- Kanwisher, N., McDermott, J., & Chun, M. M. (1997). The fusiform face area: a module in human extrastriate cortex specialized for face perception. *The Journal of neuroscience*, 17(11), 4302-4311.
- Kanwisher, N., & Moscovitch, M. (2000). The cognitive neuroscience of face processing: An introduction. *Cognitive Neuropsychology*, 17(1-3), 1-11.
- Kanwisher, N., Tong, F., & Nakayama, K. (1998). The effect of face inversion on the human fusiform face area. *Cognition*, 68(1), B1-B11.
- Kapadia, M., Westheimer, G., & Gilbert, C. (1998). *Spatial distribution and dynamics of contextual interactions in cortical area V1*. Paper presented at the Society for Neuroscience, Los Angeles, California.
- Kapadia, M. K., Westheimer, G., & Gilbert, C. D. (2000). Spatial distribution of contextual interactions in primary visual cortex and in visual perception. *Journal of neurophysiology*, 84(4), 2048-2062.
- Kapur, S. (2003). Psychosis as a state of aberrant salience: a framework linking biology, phenomenology, and pharmacology in schizophrenia. *American Journal of Psychiatry*, 160(1), 13-22.
- Kastner, S., De Weerd, P., & Ungerleider, L. G. (2000). Texture segregation in the human visual cortex: a functional MRI study. *Journal of neurophysiology*, 83(4), 2453-2457.
- Kastner, S., Pinsk, M. A., De Weerd, P., Desimone, R., & Ungerleider, L. G. (1999). Increased activity in human visual cortex during directed attention in the absence of visual stimulation. *Neuron*, 22(4), 751-761.
- Kawato, M., & Wolpert, D. (1998). Internal models for motor control. In B. G. R. & G. J. A. (Eds.), *Novartis Foundation Symposium 218 - Sensory Guidance of Movement* (pp. 291-307). Chichester, UK: John Wiley & Sons, Ltd.
- Kayser, C., Kim, M., Ugurbil, K., Kim, D.-S., & König, P. (2004). A comparison of hemodynamic and neural responses in cat visual cortex using complex stimuli. *Cerebral Cortex*, 14(8), 881-891.
- Keane, B. P., Silverstein, S. M., Wang, Y., & Papatomas, T. V. (2013). Reduced depth inversion illusions in schizophrenia are state-specific and occur for multiple object types and viewing conditions. *Journal of Abnormal Psychology*, 122(2), 506.
- Keller, G. B., Bonhoeffer, T., & Hübener, M. (2012). Sensorimotor mismatch signals in primary visual cortex of the behaving mouse. *Neuron*, 74(5), 809-815.
- Keri, S., Kiss, I., Kelemen, O., Benedek, G., & Janka, Z. (2005). Anomalous visual experiences, negative symptoms, perceptual organization and the magnocellular pathway in schizophrenia: a shared construct? *Psychological medicine*, 35(10), 1445-1455.
- Kersten, D., Mamassian, P., & Yuille, A. (2004). Object perception as Bayesian inference. *Annual Review of Psychology*, 55, 271-304.

- Keyser, C., & Perrett, D. I. (2002). Visual masking and RSVP reveal neural competition. *Trends in cognitive sciences*, 6(3), 120-125.
- Kleinschmidt, A., Büchel, C., Zeki, S., & Frackowiak, R. (1998). Human brain activity during spontaneously reversing perception of ambiguous figures. *Proceedings of the Royal Society of London B: Biological Sciences*, 265(1413), 2427-2433.
- Kleinschmidt, A., Thilo, K. V., Büchel, C., Gresty, M. A., Bronstein, A. M., & Frackowiak, R. S. (2002). Neural correlates of visual-motion perception as object-or self-motion. *Neuroimage*, 16(4), 873-882.
- Kloosterman, N. A., Meindertsma, T., Hillebrand, A., van Dijk, B. W., Lamme, V. A., & Donner, T. H. (2015). Top-down modulation in human visual cortex predicts the stability of a perceptual illusion. *Journal of neurophysiology*, 113(4), 1063-1076.
- Kloosterman, N. A., Meindertsma, T., Loon, A. M., Lamme, V. A., Bonnef, Y. S., & Donner, T. H. (2015). Pupil size tracks perceptual content and surprise. *European Journal of Neuroscience*, 41(8), 1068-1078.
- Knill, D. C., & Pouget, A. (2004). The Bayesian brain: the role of uncertainty in neural coding and computation. *Trends in neurosciences*, 27(12), 712-719.
- Koethe, D., Kranaster, L., Hoyer, C., Gross, S., Neatby, M. A., Schultze-Lutter, F., . . . Leweke, F. M. (2009). Binocular depth inversion as a paradigm of reduced visual information processing in prodromal state, antipsychotic-naïve and treated schizophrenia. *European archives of psychiatry and clinical neuroscience*, 259(4), 195-202.
- Koffka, K. (1922). Perception: An introduction to the Gestalt-theorie. *Psychological bulletin*, 19(10), 531-585.
- Kogo, N., & Trengove, C. (2015). Is predictive coding theory articulated enough to be testable? *Frontiers in Computational Neuroscience*, 9, 111.
- Kohler, W. (1920). *Die physischen Gestalten in Ruhe und im stationären Zustand*. Erlangen, Germany: Braunschweig: Friedr. Vieweg & Sohn.
- Köhler, W. (1938). Physical Gestalten. In W. D. Ellis (Ed.), *A Source Book of Gestalt Psychology*. Highland, US: Gestalt Journal Press.
- Koivisto, M., Railo, H., Revonsuo, A., Vanni, S., & Salminen-Vaparanta, N. (2011). Recurrent processing in V1/V2 contributes to categorization of natural scenes. *The Journal of neuroscience*, 31(7), 2488-2492.
- Kok, P., Bains, L. J., van Mourik, T., Norris, D. G., & de Lange, F. P. (2016). Selective activation of the deep layers of the human primary visual cortex by top-down feedback. *Current Biology*, 26(3), 371-376.
- Kok, P., & de Lange, F. P. (2014). Shape perception simultaneously up- and downregulates neural activity in the primary visual cortex. *Current Biology*, 24(13), 1531-1535.
- Kok, P., Failing, M. F., & de Lange, F. P. (2014). Prior expectations evoke stimulus templates in the primary visual cortex. *Journal of cognitive neuroscience*, 26(7), 1546-1554.
- Kok, P., Jehee, J. F., & de Lange, F. P. (2012). Less is more: expectation sharpens representations in the primary visual cortex. *Neuron*, 75(2), 265-270.
- Kolers, P. A. (1963). Some differences between real and apparent visual movement. *Vision research*, 3(5-6), 191-206.
- Körding, K. P., & Wolpert, D. M. (2004). Bayesian integration in sensorimotor learning. *Nature*, 427(6971), 244-247.
- Kourtzi, Z., & Kanwisher, N. (2000). Cortical regions involved in perceiving object shape. *The Journal of neuroscience*, 20(9), 3310-3318.
- Kourtzi, Z., & Kanwisher, N. (2001). Representation of perceived object shape by the human lateral occipital complex. *Science*, 293(5534), 1506-1509.
- Kourtzi, Z., Tolias, A. S., Altmann, C. F., Augath, M., & Logothetis, N. K. (2003). Integration of local features into global shapes: monkey and human fMRI studies. *Neuron*, 37(2), 333-346.
- Kramer, P., Massacesi, S., Semenzato, L., Cecchetto, S., & Bressan, P. (2013). Motion-induced blindness measured objectively. *Behavior research methods*, 45(1), 267-271.
- Kravitz, D. J., Saleem, K. S., Baker, C. I., Ungerleider, L. G., & Mishkin, M. (2013). The ventral visual pathway: an expanded neural framework for the processing of object quality. *Trends in cognitive sciences*, 17(1), 26-49.

- Kriegeskorte, N. (2015). Crossvalidation in brain imaging analysis. *bioRxiv*, 017418.
- Kriegeskorte, N., Mur, M., & Bandettini, P. A. (2008). Representational similarity analysis—connecting the branches of systems neuroscience. *Frontiers in systems neuroscience*, 2, 4.
- Króliczak, G., Heard, P., Goodale, M. A., & Gregory, R. L. (2006). Dissociation of perception and action unmasked by the hollow-face illusion. *Brain research*, 1080(1), 9-16.
- LaBerge, D., & Kasevich, R. (2007). The apical dendrite theory of consciousness. *Neural Networks*, 20(9), 1004-1020.
- Lages, M., & Jaworska, K. (2011). Fluctuations of visual awareness: Motion induced blindness and binocular rivalry. *Journal of vision*, 11(11), 318.
- Lamme, V. (2014). The Crack of Dawn: Perceptual Functions and Neural Mechanisms that Mark the Transition from Unconscious Processing to Conscious Vision. *Open MIND*, 22.
- Lamme, V. A. (2003). Why visual attention and awareness are different. *Trends in cognitive sciences*, 7(1), 12-18.
- Lamme, V. A. (2004). Separate neural definitions of visual consciousness and visual attention; a case for phenomenal awareness. *Neural Networks*, 17(5), 861-872.
- Lamme, V. A. (2006). Towards a true neural stance on consciousness. *Trends in cognitive sciences*, 10(11), 494-501.
- Lamme, V. A., & Roelfsema, P. R. (2000). The distinct modes of vision offered by feedforward and recurrent processing. *Trends in neurosciences*, 23(11), 571-579.
- Lamme, V. A., Supèr, H., Landman, R., Roelfsema, P. R., & Spekreijse, H. (2000). The role of primary visual cortex (V1) in visual awareness. *Vision research*, 40(10), 1507-1521.
- Larkum, M. (2013). A cellular mechanism for cortical associations: an organizing principle for the cerebral cortex. *Trends in neurosciences*, 36(3), 141-151.
- Larkum, M. E., Nevian, T., Sandler, M., Polsky, A., & Schiller, J. (2009). Synaptic integration in tuft dendrites of layer 5 pyramidal neurons: a new unifying principle. *Science*, 325(5941), 756-760.
- Larkum, M. E., Senn, W., & Lüscher, H.-R. (2004). Top-down dendritic input increases the gain of layer 5 pyramidal neurons. *Cerebral Cortex*, 14(10), 1059-1070.
- Larkum, M. E., & Zhu, J. J. (2002). Signaling of layer 1 and whisker-evoked Ca²⁺ and Na⁺ action potentials in distal and terminal dendrites of rat neocortical pyramidal neurons in vitro and in vivo. *The Journal of neuroscience*, 22(16), 6991-7005.
- Larkum, M. E., Zhu, J. J., & Sakmann, B. (1999). A new cellular mechanism for coupling inputs arriving at different cortical layers. *Nature*, 398(6725), 338-341.
- Larkum, M. E., Zhu, J. J., & Sakmann, B. (2001). Dendritic mechanisms underlying the coupling of the dendritic with the axonal action potential initiation zone of adult rat layer 5 pyramidal neurons. *The Journal of physiology*, 533(2), 447-466.
- Larsen, A., Madsen, K., Ellegaard Lund, T., & Bundesen, C. (2006). Images of illusory motion in primary visual cortex. *Journal of cognitive neuroscience*, 18(7), 1174-1180.
- Lee, J. H., Durand, R., Gradinaru, V., Zhang, F., Goshen, I., Kim, D.-S., . . . Deisseroth, K. (2010). Global and local fMRI signals driven by neurons defined optogenetically by type and wiring. *Nature*, 465(7299), 788-792.
- Lee, S.-H., Blake, R., & Heeger, D. J. (2007). Hierarchy of cortical responses underlying binocular rivalry. *Nature neuroscience*, 10(8), 1048-1054.
- Lee, T. S. (2001). Dynamics of subjective contour formation in the early visual cortex. *Proceedings of the National Academy of Sciences*, 98(4), 1907-1911.
- Lee, T. S., & Mumford, D. (2003). Hierarchical Bayesian inference in the visual cortex. *Journal of the Optical Society of America*, 20(7), 1434-1448.
- Lee, T. S., Mumford, D., Romero, R., & Lamme, V. A. (1998). The role of the primary visual cortex in higher level vision. *Vision research*, 38(15), 2429-2454.
- Lenggenhager, B., Tadi, T., Metzinger, T., & Blanke, O. (2007). Video ergo sum: manipulating bodily self-consciousness. *Science*, 317(5841), 1096-1099.
- Lenzenweger, M. F. (2006). Schizotaxia, schizotypy, and schizophrenia: Paul E. Meehl's blueprint for the experimental psychopathology and genetics of schizophrenia. *Journal of Abnormal Psychology*, 115(2), 195.

- Lenzenweger, M. F. (2011). *Schizotypy and Schizophrenia: The View from Experimental Psychopathology*. New York, USA: Guilford Press.
- Leopold, D. A., & Logothetis, N. K. (1996). Activity changes in early visual cortex reflect monkeys' percepts during binocular rivalry. *Nature*, *379*(6565), 549-553.
- Leopold, D. A., O'Toole, A. J., Vetter, T., & Blanz, V. (2001). Prototype-referenced shape encoding revealed by high-level aftereffects. *Nature neuroscience*, *4*(1), 89-94.
- Leopold, D. A., Rhodes, G., Müller, K.-M., & Jeffery, L. (2005). The dynamics of visual adaptation to faces. *Proceedings of the Royal Society of London B: Biological Sciences*, *272*(1566), 897-904.
- Levine, S. C., Banich, M. T., & Koch-Weser, M. P. (1988). Face recognition: a general or specific right hemisphere capacity? *Brain and cognition*, *8*(3), 303-325.
- Levy, J., Heller, W., Banich, M. T., & Burton, L. A. (1983). Asymmetry of perception in free viewing of chimeric faces. *Brain and cognition*, *2*(4), 404-419.
- Lewis, R., & Noppeney, U. (2010). Audiovisual synchrony improves motion discrimination via enhanced connectivity between early visual and auditory areas. *The Journal of neuroscience*, *30*(37), 12329-12339.
- Li, W., Piëch, V., & Gilbert, C. D. (2006). Contour saliency in primary visual cortex. *Neuron*, *50*(6), 951-962.
- Liang, M., Mouraux, A., Hu, L., & Iannetti, G. (2013). Primary sensory cortices contain distinguishable spatial patterns of activity for each sense. *Nature communications*, *4*.
- Libedinsky, C., Savage, T., & Livingstone, M. (2009). Perceptual and physiological evidence for a role for early visual areas in motion-induced blindness. *Journal of vision*, *9*(1), 14-14.
- Limanowski, J., Lutti, A., & Blankenburg, F. (2014). The extrastriate body area is involved in illusory limb ownership. *Neuroimage*, *86*, 514-524.
- Llinás, R. R., Leznik, E., & Urbano, F. J. (2002). Temporal binding via cortical coincidence detection of specific and nonspecific thalamocortical inputs: a voltage-dependent dye-imaging study in mouse brain slices. *Proceedings of the National Academy of Sciences*, *99*(1), 449-454.
- Lloyd, D. M. (2007). Spatial limits on referred touch to an alien limb may reflect boundaries of visuo-tactile peripersonal space surrounding the hand. *Brain and cognition*, *64*(1), 104-109.
- Loewy, R. L., Pearson, R., Vinogradov, S., Bearden, C. E., & Cannon, T. D. (2011). Psychosis risk screening with the Prodromal Questionnaire—brief version (PQ-B). *Schizophrenia research*, *129*(1), 42-46.
- Logothetis, N. K. (2003). The underpinnings of the BOLD functional magnetic resonance imaging signal. *The Journal of neuroscience*, *23*(10), 3963-3971.
- Logothetis, N. K. (2008). What we can do and what we cannot do with fMRI. *Nature*, *453*(7197), 869-878.
- Logothetis, N. K., Pauls, J., Augath, M., Trinath, T., & Oeltermann, A. (2001). Neurophysiological investigation of the basis of the fMRI signal. *Nature*, *412*(6843), 150-157.
- Luck, S. J., Chelazzi, L., Hillyard, S. A., & Desimone, R. (1997). Neural mechanisms of spatial selective attention in areas V1, V2, and V4 of macaque visual cortex. *Journal of neurophysiology*, *77*(1), 24-42.
- Macaluso, E., Frith, C. D., & Driver, J. (2000). Modulation of human visual cortex by crossmodal spatial attention. *Science*, *289*(5482), 1206-1208.
- Maher, B. A. (1974). Delusional thinking and perceptual disorder. *Journal of individual psychology*, *30*(1), 98.
- Maier, A., Aura, C. J., & Leopold, D. A. (2011). Infragranular sources of sustained local field potential responses in macaque primary visual cortex. *The Journal of neuroscience*, *31*(6), 1971-1980.
- Maier, A., Wilke, M., Aura, C., Zhu, C., Frank, Q. Y., & Leopold, D. A. (2008). Divergence of fMRI and neural signals in V1 during perceptual suppression in the awake monkey. *Nature neuroscience*, *11*(10), 1193-1200.
- Major, G., Larkum, M. E., & Schiller, J. (2013). Active properties of neocortical pyramidal neuron dendrites. *Annual review of neuroscience*, *36*, 1-24.
- Makin, T. R., Holmes, N. P., & Ehrsson, H. H. (2008). On the other hand: dummy hands and peripersonal space. *Behavioural brain research*, *191*(1), 1-10.

- Makin, T. R., Holmes, N. P., & Zohary, E. (2007). Is that near my hand? Multisensory representation of peripersonal space in human intraparietal sulcus. *The Journal of neuroscience*, 27(4), 731-740.
- Malach, R., Levy, I., & Hasson, U. (2002). The topography of high-order human object areas. *Trends in cognitive sciences*, 6(4), 176-184.
- Malach, R., Reppas, J., Benson, R., Kwong, K., Jiang, H., Kennedy, W., . . . Tootell, R. (1995). Object-related activity revealed by functional magnetic resonance imaging in human occipital cortex. *Proceedings of the National Academy of Sciences*, 92(18), 8135-8139.
- Malpass, R. S., & Kravitz, J. (1969). Recognition for faces of own and other race. *Journal of personality and social psychology*, 13(4), 330.
- Mamassian, P., Landy, M., & Maloney, L. T. (2002). Bayesian modelling of visual perception. In R. P. N. Rao, B. A. Olshausen, & M. S. Lewicki (Eds.), *Probabilistic models of the brain* (pp. 13-36). Cambridge, MA, USA: MIT Press.
- Markov, N. T., Ercsey-Ravasz, M., Van Essen, D. C., Knoblauch, K., Toroczkai, Z., & Kennedy, H. (2013). Cortical high-density counterstream architectures. *Science*, 342(6158), 1238406.
- Markov, N. T., & Kennedy, H. (2013). The importance of being hierarchical. *Current Opinion in Neurobiology*, 23(2), 187-194.
- Markov, N. T., Vezoli, J., Chameau, P., Falchier, A., Quilodran, R., Huissoud, C., . . . Ullman, S. (2014). Anatomy of hierarchy: feedforward and feedback pathways in macaque visual cortex. *Journal of Comparative Neurology*, 522(1), 225-259.
- Markram, H., Toledo-Rodriguez, M., Wang, Y., Gupta, A., Silberberg, G., & Wu, C. (2004). Interneurons of the neocortical inhibitory system. *Nature Reviews Neuroscience*, 5(10), 793-807.
- Martinez-Conde, S., Macknik, S. L., Troncoso, X. G., & Dyar, T. A. (2006). Microsaccades counteract visual fading during fixation. *Neuron*, 49(2), 297-305.
- Martuzzi, R., Murray, M. M., Michel, C. M., Thiran, J.-P., Maeder, P. P., Clarke, S., & Meuli, R. A. (2007). Multisensory interactions within human primary cortices revealed by BOLD dynamics. *Cerebral Cortex*, 17(7), 1672-1679.
- Mathalon, D. H., & Ford, J. M. (2008). Corollary discharge dysfunction in schizophrenia: evidence for an elemental deficit. *Clinical EEG and Neuroscience*, 39(2), 82-86.
- Maunsell, J. H., & Treue, S. (2006). Feature-based attention in visual cortex. *Trends in neurosciences*, 29(6), 317-322.
- Maus, G. W., Fischer, J., & Whitney, D. (2013). Motion-dependent representation of space in area MT+. *Neuron*, 78(3), 554-562.
- Maus, G. W., & Nijhawan, R. (2006). Forward displacements of fading objects in motion: the role of transient signals in perceiving position. *Vision research*, 46(26), 4375-4381.
- Maus, G. W., & Nijhawan, R. (2008). Motion extrapolation into the blind spot. *Psychological science*, 19(11), 1087-1091.
- Maus, G. W., Weigelt, S., Nijhawan, R., & Muckli, L. (2010). Does area V3A predict positions of moving objects. *Frontiers in Psychology*, 1(186), 1-11.
- Mayer-Gross, W. (1932). Die klinik. In O. Bumke (Ed.), *Handbuch der Geisteskrankheiten* (pp. 293-578). Berlin, Germany: Springer.
- Mazer, J. A., Vinje, W. E., McDermott, J., Schiller, P. H., & Gallant, J. L. (2002). Spatial frequency and orientation tuning dynamics in area V1. *Proceedings of the National Academy of Sciences*, 99(3), 1645-1650.
- McKone, E., & Robbins, R. (2011). Are faces special? In A. Calder, G. Rhodes, M. Johnson, & J. V. Haxby (Eds.), *The Oxford handbook of face perception* (pp. 149-176). Oxford, UK: Oxford University Press.
- Meital-Kfir, N., Bonne, Y., & Sagi, D. (2015). Visual representations in the absence of visual awareness. *Journal of vision*, 15(12), 1038-1038.
- Melloni, L. (2014). Consciousness as inference in time. *Open MIND*, 22(C).
- Meng, M., Ferneyhough, E., & Tong, F. (2007). Dynamics of perceptual filling-in of visual phantoms revealed by binocular rivalry. *Journal of vision*, 7(13), 8-8.

- Menon, R. S., Ogawa, S., Strupp, J. P., & Uğurbil, K. (1997). Ocular dominance in human V1 demonstrated by functional magnetic resonance imaging. *Journal of neurophysiology*, *77*(5), 2780-2787.
- Merabet, L. B., Hamilton, R., Schlaug, G., Swisher, J. D., Kiriakopoulos, E. T., Pitskel, N. B., . . . Pascual-Leone, A. (2008). Rapid and reversible recruitment of early visual cortex for touch. *PLoS One*, *3*(8), e3046.
- Meyer-Lindenberg, A. (2010). From maps to mechanisms through neuroimaging of schizophrenia. *Nature*, *468*(7321), 194-202.
- Meyer, K., Kaplan, J. T., Essex, R., Webber, C., Damasio, H., & Damasio, A. (2010). Predicting visual stimuli on the basis of activity in auditory cortices. *Nature neuroscience*, *13*(6), 667-668.
- Meyer, T., & Olson, C. R. (2011). Statistical learning of visual transitions in monkey inferotemporal cortex. *Proceedings of the National Academy of Sciences*, *108*(48), 19401-19406.
- Michalareas, G., Vezoli, J., Van Pelt, S., Schoffelen, J.-M., Kennedy, H., & Fries, P. (2016). Alpha-beta and gamma rhythms subserve feedback and feedforward influences among human visual cortical areas. *Neuron*, *89*(2), 384-397.
- Michel, C., Corneille, O., & Rossion, B. (2007). Race categorization modulates holistic face encoding. *Cognitive Science*, *31*(5), 911-924.
- Michel, C., Rossion, B., Han, J., Chung, C.-S., & Caldara, R. (2006). Holistic processing is finely tuned for faces of one's own race. *Psychological science*, *17*(7), 608-615.
- Mishara, A. L., & Sterzer, P. (2015). Phenomenology is Bayesian in its application to delusions. *World Psychiatry*, *14*(2), 185-186.
- Mishkin, M., Ungerleider, L. G., & Macko, K. A. (1983). Object vision and spatial vision: two cortical pathways. *Trends in neurosciences*, *6*, 414-417.
- Mitroff, S. R., & Scholl, B. J. (2005). Forming and updating object representations without awareness: Evidence from motion-induced blindness. *Vision research*, *45*(8), 961-967.
- Molholm, S., Ritter, W., Murray, M. M., Javitt, D. C., Schroeder, C. E., & Foxe, J. J. (2002). Multisensory auditory-visual interactions during early sensory processing in humans: a high-density electrical mapping study. *Cognitive brain research*, *14*(1), 115-128.
- Møller, P., & Husby, R. (2000). The initial prodrome in schizophrenia: searching for naturalistic core dimensions of experience and behavior. *Schizophrenia Bulletin*, *26*(1), 217.
- Montaser-Kouhsari, L., Landy, M. S., Heeger, D. J., & Larsson, J. (2007). Orientation-selective adaptation to illusory contours in human visual cortex. *The Journal of neuroscience*, *27*(9), 2186-2195.
- Montaser-Kouhsari, L., Moradi, F., Zandvakili, A., & Esteky, H. (2004). Orientation-selective adaptation during motion-induced blindness. *Perception*, *33*(2), 249-254.
- Moreno-Bote, R., Knill, D. C., & Pouget, A. (2011). Bayesian sampling in visual perception. *Proceedings of the National Academy of Sciences*, *108*(30), 12491-12496.
- Morgan, A., Petro, L., Vizioli, L., & Muckli, L. (2015). Retinotopically occluded subsections of early visual cortex contain contextual information about individual scenes, category and depth. *Journal of vision*, *15*(12), 516-516.
- Morgan, H. L., Turner, D. C., Corlett, P. R., Absalom, A. R., Adapa, R., Arana, F. S., . . . Haggard, P. (2011). Exploring the impact of ketamine on the experience of illusory body ownership. *Biological psychiatry*, *69*(1), 35-41.
- Morrell, F. (1972). Visual system's view of acoustic space. *Nature*, *238*, 44-46.
- Moutoussis, K., & Zeki, S. (2002). The relationship between cortical activation and perception investigated with invisible stimuli. *Proceedings of the National Academy of Sciences*, *99*(14), 9527-9532.
- Muckli, L. (2010). What are we missing here? Brain imaging evidence for higher cognitive functions in primary visual cortex V1. *International Journal of Imaging Systems and Technology*, *20*(2), 131-139.
- Muckli, L., De Martino, F., Vizioli, L., Petro, L. S., Smith, F. W., Ugurbil, K., . . . Yacoub, E. (2015). Contextual feedback to superficial layers of V1. *Current Biology*, *25*(20), 2690-2695.
- Muckli, L., Kohler, A., Kriegeskorte, N., & Singer, W. (2005). Primary visual cortex activity along the apparent-motion trace reflects illusory perception. *PLoS One Biology*, *3*(8), e265.

- Muckli, L., Kriegeskorte, N., Lanfermann, H., Zanella, F. E., Singer, W., & Goebel, R. (2002). Apparent motion: event-related functional magnetic resonance imaging of perceptual switches and states. *The Journal of neuroscience*, 22(9), 166.
- Muckli, L., & Petro, L. S. (2013). Network interactions: Non-geniculate input to V1. *Current Opinion in Neurobiology*, 23(2), 195-201.
- Mumford, D. (1992). On the computational architecture of the neocortex. *Biological cybernetics*, 66(3), 241-251.
- Murray, M. M., Foxe, D. M., Javitt, D. C., & Foxe, J. J. (2004). Setting boundaries: brain dynamics of modal and amodal illusory shape completion in humans. *The Journal of neuroscience*, 24(31), 6898-6903.
- Murray, S. O., Boyaci, H., & Kersten, D. (2006). The representation of perceived angular size in human primary visual cortex. *Nature neuroscience*, 9(3), 429-434.
- Murray, S. O., Kersten, D., Olshausen, B. A., Schrater, P., & Woods, D. L. (2002). Shape perception reduces activity in human primary visual cortex. *Proceedings of the National Academy of Sciences*, 99(23), 15164-15169.
- Nakashita, S., Saito, D. N., Kochiyama, T., Honda, M., Tanabe, H. C., & Sadato, N. (2008). Tactile-visual integration in the posterior parietal cortex: A functional magnetic resonance imaging study. *Brain research bulletin*, 75(5), 513-525.
- Nelson, B., Thompson, A., & Yung, A. R. (2012). Basic self-disturbance predicts psychosis onset in the ultra high risk for psychosis “prodromal” population. *Schizophrenia Bulletin*, 38(6), 1277-1287.
- Nelson, B., Yung, A. R., Bechdolf, A., & McGorry, P. D. (2008). The phenomenological critique and self-disturbance: implications for ultra-high risk (“prodrome”) research. *Schizophrenia Bulletin*, 34(2), 381-392.
- Nieuwenhuys, R. (1994). The neocortex. *Anatomy and embryology*, 190(4), 307-337.
- Nijhawan, R. (2008). Visual prediction: Psychophysics and neurophysiology of compensation for time delays. *Behavioral and Brain Sciences*, 31(02), 179-198.
- Noesselt, T., Hillyard, S. A., Woldorff, M. G., Schoenfeld, A., Hagner, T., Jäncke, L., . . . Heinze, H.-J. (2002). Delayed striate cortical activation during spatial attention. *Neuron*, 35(3), 575-587.
- Norman, K. A., Polyn, S. M., Detre, G. J., & Haxby, J. V. (2006). Beyond mind-reading: multi-voxel pattern analysis of fMRI data. *Trends in cognitive sciences*, 10(9), 424-430.
- Notredame, C.-E., Pins, D., Deneve, S., & Jardri, R. (2015). What visual illusions teach us about schizophrenia. *Frontiers in Integrative Neuroscience*, 8(64).
- Nuruki, A., Oliver, R., Campana, G., Walsh, V., & Rothwell, J. C. (2013). Opposing roles of sensory and parietal cortices in awareness in a bistable motion illusion. *Neuropsychologia*, 51(13), 2479-2484.
- O'Donnell, P. (2011). Adolescent onset of cortical disinhibition in schizophrenia: insights from animal models. *Schizophrenia Bulletin*, 37(3), 484-492.
- Oldfield, R. C. (1971). The assessment and analysis of handedness: the Edinburgh inventory. *Neuropsychologia*, 9(1), 97-113.
- Olsen, S. R., Bortone, D. S., Adesnik, H., & Scanziani, M. (2012). Gain control by layer six in cortical circuits of vision. *Nature*, 483(7387), 47-52.
- Olshausen, B. A., & Field, D. J. (2005). How close are we to understanding V1? *Neural computation*, 17(8), 1665-1699.
- Overgaard, M., Rote, J., Mouridsen, K., & Ramsøy, T. Z. (2006). Is conscious perception gradual or dichotomous? A comparison of report methodologies during a visual task. *Consciousness and cognition*, 15(4), 700-708.
- Pachai, M. V., Sekuler, A. B., & Bennett, P. J. (2013). Sensitivity to information conveyed by horizontal contours is correlated with face identification accuracy. *Frontiers in Psychology*, 4, 74.
- Parkkonen, L., Andersson, J., Hämäläinen, M., & Hari, R. (2008). Early visual brain areas reflect the percept of an ambiguous scene. *Proceedings of the National Academy of Sciences*, 105(51), 20500-20504.

- Parnas, J. (2003). Self and schizophrenia: a phenomenological perspective. In T. Kircher & A. S. David (Eds.), *The self in neuroscience and psychiatry* (pp. 217-241). Cambridge, MA, USA: Cambridge University Press.
- Parnas, J., & Handest, P. (2003). Phenomenology of anomalous self-experience in early schizophrenia. *Comprehensive psychiatry*, *44*(2), 121-134.
- Parnas, J., Jansson, L., Sass, L., & Handest, P. (1998). Self-experience in the prodromal phases of schizophrenia: A pilot study of first-admissions. *Neurology Psychiatry and Brain Research*, *6*(2), 97-106.
- Parnas, J., Møller, P., Kircher, T., Thalbitzer, J., Jansson, L., Handest, P., & Zahavi, D. (2005). EASE: examination of anomalous self-experience. *Psychopathology*, *38*(5), 236-258.
- Parnas, J., & Sass, L. A. (2001). Self, solipsism, and schizophrenic delusions. *Philosophy, Psychiatry, & Psychology*, *8*(2), 101-120.
- Parsons, B. D., Gandhi, S., Aurbach, E. L., Williams, N., Williams, M., Wassef, A., & Eagleman, D. M. (2013). Lengthened temporal integration in schizophrenia. *Neuropsychologia*, *51*(2), 372-376.
- Pascual-Leone, A., & Walsh, V. (2001). Fast backprojections from the motion to the primary visual area necessary for visual awareness. *Science*, *292*(5516), 510-512.
- Paton, B., Hohwy, J., & Enticott, P. G. (2012). The rubber hand illusion reveals proprioceptive and sensorimotor differences in autism spectrum disorders. *Journal of autism and developmental disorders*, *42*(9), 1870-1883.
- Peled, A., Pressman, A., Geva, A. B., & Modai, I. (2003). Somatosensory evoked potentials during a rubber-hand illusion in schizophrenia. *Schizophrenia research*, *64*(2), 157-163.
- Peled, A., Ritsner, M., Hirschmann, S., Geva, A. B., & Modai, I. (2000). Touch feel illusion in schizophrenic patients. *Biological psychiatry*, *48*(11), 1105-1108.
- Petro, L., Smith, F., Zimmermann, J., De Martino, F., & Muckli, L. (2015). Measuring the precision of feedback fields in V1 using 3T and 7T fMRI. *Journal of vision*, *15*(12), 517-517.
- Petro, L. S., Smith, F. W., Schyns, P. G., & Muckli, L. (2013). Decoding face categories in diagnostic subregions of primary visual cortex. *European Journal of Neuroscience*, *37*(7), 1130-1139.
- Petro, L. S., Vizioli, L., & Muckli, L. (2015). Contributions of cortical feedback to sensory processing in primary visual cortex. *Frontiers in Psychology*, *5*, 1223.
- Phillips, W., Clark, A., & Silverstein, S. M. (2015). On the functions, mechanisms, and malfunctions of intracortical contextual modulation. *Neuroscience & Biobehavioral Reviews*, *52*, 1-20.
- Phillips, W. A. (2015). Cognitive functions of intracellular mechanisms for contextual amplification. *Brain and cognition*, *112*, 39-53.
- Phillips, W. A., & Singer, W. (1997). In search of common foundations for cortical computation. *Behavioral and Brain Sciences*, *20*(04), 657-683.
- Piëch, V., Li, W., Reeke, G. N., & Gilbert, C. D. (2013). Network model of top-down influences on local gain and contextual interactions in visual cortex. *Proceedings of the National Academy of Sciences*, *110*(43), E4108-E4117.
- Pinto, Y., van Gaal, S., de Lange, F. P., Lamme, V. A., & Seth, A. K. (2015). Expectations accelerate entry of visual stimuli into awareness. *Journal of vision*, *15*(8), 13-13.
- Platek, S. M., & Gallup, G. G. (2002). Self-face recognition is affected by schizotypal personality traits. *Schizophrenia research*, *57*(1), 81-85.
- Plato. Theory of Forms.
- Plato. Theory of Ideas.
- Platt, J. (1999). Probabilistic outputs for support vector machines and comparisons to regularized likelihood methods. In A. J. Smola, P. Bartlett, B. Scholkopf, & D. Schuurmans (Eds.), *Advances in large margin classifiers* (pp. 61-74). Cambridge, MA, USA: MIT Press.
- Polonsky, A., Blake, R., Braun, J., & Heeger, D. J. (2000). Neuronal activity in human primary visual cortex correlates with perception during binocular rivalry. *Nature neuroscience*, *3*(11), 1153-1159.
- Preston, C. (2013). The role of distance from the body and distance from the real hand in ownership and disownership during the rubber hand illusion. *Acta psychologica*, *142*(2), 177-183.

- Qiu, A., Rosenau, B. J., Greenberg, A. S., Hurdal, M. K., Barta, P., Yantis, S., & Miller, M. I. (2006). Estimating linear cortical magnification in human primary visual cortex via dynamic programming. *Neuroimage*, *31*(1), 125-138.
- Raichle, M. E. (2011). The restless brain. *Brain connectivity*, *1*(1), 3-12.
- Raichle, M. E., & Mintun, M. A. (2006). Brain work and brain imaging. *Annual review of neuroscience*, *29*, 449-476.
- Ramalingam, N., McManus, J. N., Li, W., & Gilbert, C. D. (2013). Top-down modulation of lateral interactions in visual cortex. *The Journal of neuroscience*, *33*(5), 1773-1789.
- Ramon, M. (2015). Differential processing of vertical interfeature relations due to real-life experience with personally familiar faces. *Perception*, *44*(4), 368-382.
- Ramon, M., Miellet, S., Dzieciol, A. M., Konrad, B. N., Dresler, M., & Caldara, R. (2016). Super-Memorizers Are Not Super-Recognizers. *PLoS One*, *11*(3), e0150972.
- Ramon, M., & Rossion, B. (2012). Hemisphere-dependent holistic processing of familiar faces. *Brain and cognition*, *78*(1), 7-13.
- Rao, R. P., & Ballard, D. H. (1999). Predictive coding in the visual cortex: a functional interpretation of some extra-classical receptive-field effects. *Nature neuroscience*, *2*(1), 79-87.
- Rasmjou, S., Hausmann, M., & Güntürkün, O. (1999). Hemispheric dominance and gender in the perception of an illusion. *Neuropsychologia*, *37*(9), 1041-1047.
- Rees, G. (2013). Neural correlates of consciousness. *Annals of the New York Academy of Sciences*, *1296*(1), 4-10.
- Rees, G., Friston, K., & Koch, C. (2000). A direct quantitative relationship between the functional properties of human and macaque V5. *Nature neuroscience*, *3*(7), 716-723.
- Rees, G., Kreiman, G., & Koch, C. (2002). Neural correlates of consciousness in humans. *Nature Reviews Neuroscience*, *3*(4), 261-270.
- Rentschler, I., Jüttner, M., Unzicker, A., & Landis, T. (1999). Innate and learned components of human visual preference. *Current Biology*, *9*(13), 665-671.
- Revina, Y., Petro, L. S., Denk-Florea, C., & Muckli, L. (2015). *Increased stimulation of the non-classical receptive field region results in more information in occluded V1*. Paper presented at the European Conference of Visual Perception, Liverpool, UK.
- Revina, Y., Petro, L. S., Rao, I., Smith, F. W., & Muckli, L. (2014). *Cortical feedback: spatial frequency content and generalisation to feedforward signals*. Paper presented at the Human Brain Mapping: 20th Annual Meeting, Hamburg, Germany.
- Rezliescu, C., Barton, J. J., Pitcher, D., & Duchaine, B. (2014). Normal acquisition of expertise with greebles in two cases of acquired prosopagnosia. *Proceedings of the National Academy of Sciences*, *111*(14), 5123-5128.
- Rhodes, G. (1985). Lateralized processes in face recognition. *British Journal of Psychology*, *76*(2), 249-271.
- Rhodes, G., & Jeffery, L. (2006). Adaptive norm-based coding of facial identity. *Vision research*, *46*(18), 2977-2987.
- Ricciardi, E., Vanello, N., Sani, L., Gentili, C., Scilingo, E. P., Landini, L., . . . Pietrini, P. (2007). The effect of visual experience on the development of functional architecture in hMT+. *Cerebral Cortex*, *17*(12), 2933-2939.
- Rizzolatti, G., Fadiga, L., Fogassi, L., & Gallese, V. (1997). The space around us. *Science*, *277*(5323), 190.
- Rizzolatti, G., Fogassi, L., & Gallese, V. (2002). Motor and cognitive functions of the ventral premotor cortex. *Current Opinion in Neurobiology*, *12*(2), 149-154.
- Rizzolatti, G., Scandolara, C., Matelli, M., & Gentilucci, M. (1981). Afferent properties of periarculate neurons in macaque monkeys. II. Visual responses. *Behavioural brain research*, *2*(2), 147-163.
- Rock, I. (1997). *Indirect Perception*. Cambridge, MA, USA: MIT Press.
- Rockland, K. S., & Knutson, T. (2000). Feedback connections from area MT of the squirrel monkey to areas V1 and V2. *Journal of Comparative Neurology*, *425*(3), 345-368.
- Rockland, K. S., & Pandya, D. N. (1979). Laminar origins and terminations of cortical connections of the occipital lobe in the rhesus monkey. *Brain research*, *179*(1), 3-20.

- Rockland, K. S., & Van Hoesen, G. W. (1994). Direct temporal-occipital feedback connections to striate cortex (V1) in the macaque monkey. *Cerebral Cortex*, 4(3), 300-313.
- Rockland, K. S., & Virga, A. (1989). Terminal arbors of individual "Feedback" axons projecting from area V2 to V1 in the macaque monkey: A study using immunohistochemistry of anterogradely transported Phaseolus vulgaris-leucoagglutinin. *Journal of Comparative Neurology*, 285(1), 54-72.
- Roelfsema, P. R. (2006). Cortical algorithms for perceptual grouping. *Annual review of neuroscience*, 29, 203-227.
- Roland, P. E., Hanazawa, A., Undeman, C., Eriksson, D., Tompa, T., Nakamura, H., . . . Ahmed, B. (2006). Cortical feedback depolarization waves: a mechanism of top-down influence on early visual areas. *Proceedings of the National Academy of Sciences*, 103(33), 12586-12591.
- Rolfs, M. (2009). Microsaccades: small steps on a long way. *Vision research*, 49(20), 2415-2441.
- Roopun, A. K., Kramer, M. A., Carracedo, L. M., Kaiser, M., Davies, C. H., Traub, R. D., . . . Whittington, M. A. (2008). Temporal interactions between cortical rhythms. *Frontiers in neuroscience*, 2, 34.
- Rosier, A.-M., Arckens, L., Orban, G., & Vandesande, F. (1993). Laminar distribution of NMDA receptors in cat and monkey visual cortex visualized by [3H]-MK-801 binding. *Journal of Comparative Neurology*, 335(3), 369-380.
- Rossion, B. (2008). Picture-plane inversion leads to qualitative changes of face perception. *Acta psychologica*, 128(2), 274-289.
- Rossion, B. (2009). Distinguishing the cause and consequence of face inversion: The perceptual field hypothesis. *Acta psychologica*, 132(3), 300-312.
- Roth, M. J., Synofzik, M., & Lindner, A. (2013). The cerebellum optimizes perceptual predictions about external sensory events. *Current Biology*, 23(10), 930-935.
- Rothwell, B., & Zaidel, E. (1990). Visual field differences in the magnitude of the Oppel-Kundt illusion vary with processing time. *Perception & Psychophysics*, 47(2), 180-190.
- Rubio-Garrido, P., Pérez-de-Manzo, F., Porrero, C., Galazo, M. J., & Clascá, F. (2009). Thalamic input to distal apical dendrites in neocortical layer 1 is massive and highly convergent. *Cerebral Cortex*, 19(10), 2380-2395.
- Saalman, Y. B., Pigarev, I. N., & Vidyasagar, T. R. (2007). Neural mechanisms of visual attention: how top-down feedback highlights relevant locations. *Science*, 316(5831), 1612-1615.
- Sadaghiani, S., Maier, J. X., & Noppeney, U. (2009). Natural, metaphoric, and linguistic auditory direction signals have distinct influences on visual motion processing. *The Journal of neuroscience*, 29(20), 6490-6499.
- Samad, M., Chung, A. J., & Shams, L. (2015). Perception of body ownership is driven by Bayesian sensory inference. *PLoS One*, 10(2), e0117178.
- Sanders, L. L. O., de Millas, W., Heinz, A., Kathmann, N., & Sterzer, P. (2013). Apparent motion perception in patients with paranoid schizophrenia. *European archives of psychiatry and clinical neuroscience*, 263(3), 233-239.
- Sanders, L. L. O., Muckli, L., de Millas, W., Lautenschlager, M., Heinz, A., Kathmann, N., & Sterzer, P. (2012). Detection of visual events along the apparent motion trace in patients with paranoid schizophrenia. *Psychiatry Research*, 198(2), 216-223.
- Sani, L., Ricciardi, E., Gentili, C., Vanello, N., Haxby, J. V., & Pietrini, P. (2010). Effects of visual experience on the human MT+ functional connectivity networks: an fMRI study of motion perception in sighted and congenitally blind individuals. *Frontiers in systems neuroscience*, 4, 159.
- Sass, L. A., & Parnas, J. (2003). Schizophrenia, consciousness, and the self. *Schizophrenia Bulletin*, 29(3), 427-444.
- Scheef, L., Boecker, H., Daamen, M., Fehse, U., Landsberg, M. W., Granath, D.-O., . . . Effenberg, A. O. (2009). Multimodal motion processing in area V5/MT: evidence from an artificial class of audio-visual events. *Brain research*, 1252, 94-104.
- Schira, M. M., Tyler, C. W., Breakspear, M., & Spehar, B. (2009). The foveal confluence in human visual cortex. *The Journal of neuroscience*, 29(28), 9050-9058.

- Schmack, K., de Castro, A. G.-C., Rothkirch, M., Sekutowicz, M., Rössler, H., Haynes, J.-D., . . . Sterzer, P. (2013). Delusions and the role of beliefs in perceptual inference. *The Journal of neuroscience*, *33*(34), 13701-13712.
- Schmack, K., Schnack, A., Priller, J., & Sterzer, P. (2015). Perceptual instability in schizophrenia: Probing predictive coding accounts of delusions with ambiguous stimuli. *Schizophrenia Research: Cognition*, *2*(2), 72-77.
- Schmeider, U., Leweke, F., Sternemann, U., Emrich, H., & Weber, M. (1996). Visual 3D illusion: a systems-theoretical approach to psychosis. *European archives of psychiatry and clinical neuroscience*, *246*(5), 256-260.
- Scholl, B. J. (2005). Innateness and (Bayesian) visual perception. In P. Carruthers, S. Laurence, & S. Stich (Eds.), *The Structure of the Innate Mind* (pp. 34-52). Cambridge, UK: Cambridge University Press.
- Schölvinck, M. L., & Rees, G. (2009). Attentional influences on the dynamics of motion-induced blindness. *Journal of vision*, *9*(1), 38-38.
- Schölvinck, M. L., & Rees, G. (2010). Neural correlates of motion-induced blindness in the human brain. *Journal of cognitive neuroscience*, *22*(6), 1235-1243.
- Schubotz, R. I. (2007). Prediction of external events with our motor system: towards a new framework. *Trends in cognitive sciences*, *11*(5), 211-218.
- Schubotz, R. I., & von Cramon, D. Y. (2003). Functional-anatomical concepts of human premotor cortex: evidence from fMRI and PET studies. *Neuroimage*, *20*, S120-S131.
- Schubotz, R. I., & Von Cramon, D. Y. (2004). Sequences of abstract nonbiological stimuli share ventral premotor cortex with action observation and imagery. *The Journal of neuroscience*, *24*(24), 5467-5474.
- Schwiedrzik, C. M., Alink, A., Kohler, A., Singer, W., & Muckli, L. (2007). A spatio-temporal interaction on the apparent motion trace. *Vision research*, *47*(28), 3424-3433.
- Seghier, M., Dojat, M., Delon-Martin, C., Rubin, C., Warnking, J., Segebarth, C., & Bullier, J. (2000). Moving illusory contours activate primary visual cortex: an fMRI study. *Cerebral Cortex*, *10*(7), 663-670.
- Seghier, M., & Vuilleumier, P. (2006). Functional neuroimaging findings on the human perception of illusory contours. *Neuroscience & Biobehavioral Reviews*, *30*(5), 595-612.
- Sekunova, A., & Barton, J. J. (2008). The effects of face inversion on the perception of long-range and local spatial relations in eye and mouth configuration. *Journal of Experimental Psychology: Human Perception and Performance*, *34*(5), 1129.
- Self, M. W., Kooijmans, R. N., Supèr, H., Lamme, V. A., & Roelfsema, P. R. (2012). Different glutamate receptors convey feedforward and recurrent processing in macaque V1. *Proceedings of the National Academy of Sciences*, *109*(27), 11031-11036.
- Self, M. W., van Kerkoerle, T., Super, H., & Roelfsema, P. R. (2013). Distinct roles of the cortical layers of area V1 in figure-ground segregation. *Current Biology*, *23*(21), 2121-2129.
- Serences, J. T., & Saproo, S. (2010). Population response profiles in early visual cortex are biased in favor of more valuable stimuli. *Journal of neurophysiology*, *104*(1), 76-87.
- Sereno, M. I., Dale, A., Reppas, J., & Kwong, K. (1995). Borders of multiple visual areas in humans revealed by functional magnetic resonance imaging. *Science*, *268*(5212), 889.
- Sergent, J., & Bindra, D. (1981). Differential hemispheric processing of faces: methodological considerations and reinterpretation. *Psychological bulletin*, *89*(3), 541.
- Seth, A. K. (2013). Interoceptive inference, emotion, and the embodied self. *Trends in cognitive sciences*, *17*(11), 565-573.
- Seth, A. K., Suzuki, K., & Critchley, H. D. (2011). An interoceptive predictive coding model of conscious presence. *Frontiers in Psychology*, *2*.
- Seymour, K., Clifford, C. W., Logothetis, N. K., & Bartels, A. (2009). The coding of color, motion, and their conjunction in the human visual cortex. *Current Biology*, *19*(3), 177-183.
- Shams, L., Kamitani, Y., & Shimojo, S. (2000). Illusions: What you see is what you hear. *Nature*, *408*(6814), 788.
- Sharpee, T. O., & Victor, J. D. (2009). Contextual modulation of V1 receptive fields depends on their spatial symmetry. *Journal of computational neuroscience*, *26*(2), 203-218.
- Shepard, R. N., & Zare, S. L. (1983). Path-guided apparent motion. *Science*, *220*(4597), 632-634.

- Shergill, S. S., Samson, G., Bays, P. M., Frith, C. D., & Wolpert, D. M. (2005). Evidence for sensory prediction deficits in schizophrenia. *American Journal of Psychiatry*.
- Shimada, S., Fukuda, K., & Hiraki, K. (2009). Rubber hand illusion under delayed visual feedback. *PLoS One*, *4*(7), e6185.
- Shimada, S., Hiraki, K., & Oda, I. (2005). The parietal role in the sense of self-ownership with temporal discrepancy between visual and proprioceptive feedbacks. *Neuroimage*, *24*(4), 1225-1232.
- Shimada, S., Suzuki, T., Yoda, N., & Hayashi, T. (2014). Relationship between sensitivity to visuotactile temporal discrepancy and the rubber hand illusion. *Neuroscience research*, *85*, 33-38.
- Shipp, S. (2007). Structure and function of the cerebral cortex. *Current Biology*, *17*(12), R443-R449.
- Shuler, M. G., & Bear, M. F. (2006). Reward timing in the primary visual cortex. *Science*, *311*(5767), 1606-1609.
- Siegel, M., K rding, K. P., & K nig, P. (2000). Integrating top-down and bottom-up sensory processing by somato-dendritic interactions. *Journal of computational neuroscience*, *8*(2), 161-173.
- Sillito, A. M., Cudeiro, J., & Jones, H. E. (2006). Always returning: feedback and sensory processing in visual cortex and thalamus. *Trends in neurosciences*, *29*(6), 307-316.
- Silvanto, J., Cowey, A., Lavie, N., & Walsh, V. (2005). Striate cortex (V1) activity gates awareness of motion. *Nature neuroscience*, *8*(2), 143-144.
- Silverstein, S., Uhlhaas, P. J., Essex, B., Halpin, S., Schall, U., & Carr, V. (2006). Perceptual organization in first episode schizophrenia and ultra-high-risk states. *Schizophrenia research*, *83*(1), 41-52.
- Silverstein, S. M., & Keane, B. P. (2011). Perceptual organization impairment in schizophrenia and associated brain mechanisms: review of research from 2005 to 2010. *Schizophrenia Bulletin*, *37*(4), 690-699.
- Silverstein, S. M., Knight, R. A., Schwarzkopf, S. B., West, L. L., Osborn, L. M., & Kamin, D. (1996). Stimulus configuration and context effects in perceptual organization in schizophrenia. *Journal of Abnormal Psychology*, *105*(3), 410.
- Silverstein, S. M., Matteson, S., & Knight, R. A. (1996). Reduced top-down influence in auditory perceptual organization in schizophrenia. *Journal of Abnormal Psychology*, *105*(4), 663.
- Silverstein, S. M., Schenkel, L. S., Valone, C., & Nuernberger, S. W. (1998). Cognitive deficits and psychiatric rehabilitation outcomes in schizophrenia. *Psychiatric Quarterly*, *69*(3), 169-191.
- Sirotin, Y. B., & Das, A. (2009). Anticipatory haemodynamic signals in sensory cortex not predicted by local neuronal activity. *Nature*, *457*(7228), 475-479.
- Slotnick, S. D., Schwarzbach, J., & Yantis, S. (2003). Attentional inhibition of visual processing in human striate and extrastriate cortex. *Neuroimage*, *19*(4), 1602-1611.
- Slotnick, S. D., Thompson, W. L., & Kosslyn, S. M. (2005). Visual mental imagery induces retinotopically organized activation of early visual areas. *Cerebral Cortex*, *15*(10), 1570-1583.
- Smith, F. W., & Muckli, L. (2010). Nonstimulated early visual areas carry information about surrounding context. *Proceedings of the National Academy of Sciences*, *107*(46), 20099-20103.
- Somers, D. C., Dale, A. M., Seiffert, A. E., & Tootell, R. B. (1999). Functional MRI reveals spatially specific attentional modulation in human primary visual cortex. *Proceedings of the National Academy of Sciences*, *96*(4), 1663-1668.
- Spencer, K. M., Nestor, P. G., Perlmutter, R., Niznikiewicz, M. A., Klump, M. C., Frumin, M., . . . McCarley, R. W. (2004). Neural synchrony indexes disordered perception and cognition in schizophrenia. *Proceedings of the National Academy of Sciences of the United States of America*, *101*(49), 17288-17293.
- Spratling, M. (2002). Cortical region interactions and the functional role of apical dendrites. *Behavioral and cognitive neuroscience reviews*, *1*(3), 219-228.
- Spratling, M. (2008a). Reconciling predictive coding and biased competition models of cortical function. *Frontiers in Computational Neuroscience*, *2*(4).

- Spratling, M. W. (2008b). Predictive coding as a model of biased competition in visual attention. *Vision research*, 48(12), 1391-1408.
- Spratling, M. W. (2010). Predictive coding as a model of response properties in cortical area V1. *The Journal of neuroscience*, 30(9), 3531-3543.
- Spratling, M. W. (2013). Distinguishing theory from implementation in predictive coding accounts of brain function. *Behavioral and Brain Sciences*, 36(03), 231-232.
- Stein, T., Hebart, M. N., & Sterzer, P. (2011). Breaking continuous flash suppression: a new measure of unconscious processing during interocular suppression. *Frontiers in human neuroscience*, 5.
- Stein, T., & Sterzer, P. (2014). Unconscious processing under interocular suppression: getting the right measure. *Frontiers in Psychology*, 5, 387.
- Stephan, K. E., Kasper, L., Harrison, L. M., Daunizeau, J., den Ouden, H. E., Breakspear, M., & Friston, K. J. (2008). Nonlinear dynamic causal models for fMRI. *Neuroimage*, 42(2), 649-662.
- Stephan, K. E., Weiskopf, N., Drysdale, P. M., Robinson, P. A., & Friston, K. J. (2007). Comparing hemodynamic models with DCM. *Neuroimage*, 38(3), 387-401.
- Sterzer, P., Haynes, J.-D., & Rees, G. (2006). Primary visual cortex activation on the path of apparent motion is mediated by feedback from hMT+/V5. *Neuroimage*, 32(3), 1308-1316.
- Sterzer, P., Kleinschmidt, A., & Rees, G. (2009). The neural bases of multistable perception. *Trends in cognitive sciences*, 13(7), 310-318.
- Sterzer, P., & Rees, G. (2006). Perceived size matters. *Nature neuroscience*, 9(3), 302-302.
- Sterzer, P., Russ, M. O., Preibisch, C., & Kleinschmidt, A. (2002). Neural correlates of spontaneous direction reversals in ambiguous apparent visual motion. *Neuroimage*, 15(4), 908-916.
- Stettler, D. D., Das, A., Bennett, J., & Gilbert, C. D. (2002). Lateral connectivity and contextual interactions in macaque primary visual cortex. *Neuron*, 36(4), 739-750.
- Stilla, R., & Sathian, K. (2008). Selective visuo-haptic processing of shape and texture. *Human brain mapping*, 29(10), 1123-1138.
- Suchow, J. W., & Alvarez, G. A. (2011). Motion silences awareness of visual change. *Current Biology*, 21(2), 140-143.
- Sugita, Y. (1999). Grouping of image fragments in primary visual cortex. *Nature*, 401(6750), 269-272.
- Sun, Y.-H., Ge, L., Quinn, P. C., Wang, Z., Xiao, N. G., Pascalis, O., . . . Lee, K. (2012). A new “fat face” illusion. *Perception*, 41(1), 117-120.
- Super, H., Spekreijse, H., & Lamme, V. A. (2003). Figure-ground activity in primary visual cortex (V1) of the monkey matches the speed of behavioral response. *Neuroscience letters*, 344(2), 75-78.
- Supèr, H., Spekreijse, H., & Lamme, V. A. (2001). Two distinct modes of sensory processing observed in monkey primary visual cortex (V1). *Nature neuroscience*, 4(3), 304-310.
- Supèr, H., van der Togt, C., Spekreijse, H., & Lamme, V. A. (2003). Internal state of monkey primary visual cortex (V1) predicts figure-ground perception. *The Journal of neuroscience*, 23(8), 3407-3414.
- Suzuki, S., & Cavanagh, P. (1998). A shape-contrast effect for briefly presented stimuli. *Journal of Experimental Psychology: Human Perception and Performance*, 24(5), 1315.
- Synofzik, M., Thier, P., Leube, D. T., Schlotterbeck, P., & Lindner, A. (2010). Misattributions of agency in schizophrenia are based on imprecise predictions about the sensory consequences of one's actions. *Brain*, 133(1), 262-271.
- Tadin, D., Kim, J., Doop, M. L., Gibson, C., Lappin, J. S., Blake, R., & Park, S. (2006). Weakened center-surround interactions in visual motion processing in schizophrenia. *The Journal of neuroscience*, 26(44), 11403-11412.
- Tanaka, J. W., & Gordon, I. (2011). Features, configuration, and holistic face processing. In A. Calder, G. Rhodes, M. Johnson, & J. V. Haxby (Eds.), *The Oxford handbook of face perception* (pp. 177-194). Oxford, UK: Oxford University Press.
- Tanaka, J. W., Kiefer, M., & Bukach, C. M. (2004). A holistic account of the own-race effect in face recognition: Evidence from a cross-cultural study. *Cognition*, 93(1), B1-B9.
- Tanaka, K. (1993). Neuronal mechanisms of object recognition. *Science*, 262(5134), 685-685.

- Tanaka, K. (1996). Inferotemporal cortex and object vision. *Annual review of neuroscience*, 19(1), 109-139.
- Tangen, J. M., Murphy, S. C., & Thompson, M. B. (2011). Flashed face distortion effect: Grotesque faces from relative spaces. *Perception*, 40(5), 628-630.
- Thakkar, K. N., Nichols, H. S., McIntosh, L. G., & Park, S. (2011). Disturbances in body ownership in schizophrenia: evidence from the rubber hand illusion and case study of a spontaneous out-of-body experience. *PLoS One*, 6(10), e27089.
- Thermenos, H., Keshavan, M., Juelich, R., Molokotos, E., Whitfield-Gabrieli, S., Brent, B., . . . Seidman, L. (2013). A review of: Neuroimaging of young relatives of persons with schizophrenia: a developmental perspective from schizotaxia to schizophrenia. *American Journal of Medical Genetics Part B: Neuropsychiatric Genetics*, 162B(7), 604-635.
- Tibber, M. S., Anderson, E. J., Bobin, T., Antonova, E., Seabright, A., Wright, B., . . . Dakin, S. C. (2012). Visual surround suppression in schizophrenia. *Frontiers in Psychology*, 4, 88.
- Tong, F. (2003). Primary visual cortex and visual awareness. *Nature Reviews Neuroscience*, 4(3), 219-229.
- Tong, F., & Engel, S. A. (2001). Interocular rivalry revealed in the human cortical blind-spot representation. *Nature*, 411(6834), 195-199.
- Tong, F., Meng, M., & Blake, R. (2006). Neural bases of binocular rivalry. *Trends in cognitive sciences*, 10(11), 502-511.
- Tong, F., Nakayama, K., Vaughan, J. T., & Kanwisher, N. (1998). Binocular rivalry and visual awareness in human extrastriate cortex. *Neuron*, 21(4), 753-759.
- Tootell, R., & Hadjikhani, N. (2000). Attention-brains at work! *Nature neuroscience*, 3, 206-207.
- Tootell, R. B., Hadjikhani, N., Hall, E. K., Marrett, S., Vanduffel, W., Vaughan, J. T., & Dale, A. M. (1998). The retinotopy of visual spatial attention. *Neuron*, 21(6), 1409-1422.
- Tootell, R. B., Reppas, J. B., Dale, A. M., & Look, R. B. (1995). Visual motion aftereffect in human cortical area MT revealed by functional magnetic resonance imaging. *Nature*, 375(6527), 139.
- Tootell, R. B., & Taylor, J. B. (1995). Anatomical evidence for MT and additional cortical visual areas in humans. *Cerebral Cortex*, 5(1), 39-55.
- Treue, S., & Maunsell, J. H. (1999). Effects of attention on the processing of motion in macaque middle temporal and medial superior temporal visual cortical areas. *The Journal of neuroscience*, 19(17), 7591-7602.
- Tsakiris, M. (2010). My body in the brain: a neurocognitive model of body-ownership. *Neuropsychologia*, 48(3), 703-712.
- Tsakiris, M., & Haggard, P. (2005). The rubber hand illusion revisited: visuotactile integration and self-attribution. *Journal of Experimental Psychology: Human Perception and Performance*, 31(1), 80.
- Tsakiris, M., Hesse, M. D., Boy, C., Haggard, P., & Fink, G. R. (2007). Neural signatures of body ownership: a sensory network for bodily self-consciousness. *Cerebral Cortex*, 17(10), 2235-2244.
- Tschacher, W., & Bergomi, C. (2011). Cognitive binding in schizophrenia: weakened integration of temporal intersensory information. *Schizophrenia Bulletin*, 37(suppl 2), S13-S22.
- Tschacher, W., & Kupper, Z. (2006). Perception of causality in schizophrenia spectrum disorder. *Schizophrenia Bulletin*, 32(suppl 1), S106-S112.
- Tschacher, W., Schuler, D., & Junghan, U. (2006). Reduced perception of the motion-induced blindness illusion in schizophrenia. *Schizophrenia research*, 81(2), 261-267.
- Tsuchiya, N., Wilke, M., Frässle, S., & Lamme, V. A. (2015). No-report paradigms: extracting the true neural correlates of consciousness. *Trends in cognitive sciences*, 19(12), 757-770.
- Uhlhaas, P. J., & Mishara, A. L. (2007). Perceptual anomalies in schizophrenia: integrating phenomenology and cognitive neuroscience. *Schizophrenia Bulletin*, 33(1), 142-156.
- Uhlhaas, P. J., Phillips, W. A., Mitchell, G., & Silverstein, S. M. (2006). Perceptual grouping in disorganized schizophrenia. *Psychiatry Research*, 145(2), 105-117.
- Uhlhaas, P. J., & Silverstein, S. M. (2003). The continuing relevance of gestalt psychology for an understanding of schizophrenia. *Gestalt Theory*, 4, 256-270.

- Uhlhaas, P. J., & Silverstein, S. M. (2005). Perceptual organization in schizophrenia spectrum disorders: empirical research and theoretical implications. *Psychological bulletin*, *131*(4), 618.
- Uhlhaas, P. J., Silverstein, S. M., Phillips, W. A., & Lovell, P. G. (2004). Evidence for impaired visual context processing in schizotypy with thought disorder. *Schizophrenia research*, *68*(2), 249-260.
- Uludağ, K., & Blinder, P. (2017). Linking brain vascular physiology to hemodynamic response in ultra-high field MRI. *Neuroimage*(In press).
- Uludağ, K., Müller-Bierl, B., & Uğurbil, K. (2009). An integrative model for neuronal activity-induced signal changes for gradient and spin echo functional imaging. *Neuroimage*, *48*(1), 150-165.
- Ungerleider, S., & Kastner, L. G. (2000). Mechanisms of visual attention in the human cortex. *Annual review of neuroscience*, *23*(1), 315-341.
- Utz, S., & Carbon, C.-C. (2015). Is the Flashed Face Distortion Effect expertise-based?-a systematic experimental investigation. *Journal of vision*, *15*(12), 147-147.
- Valentine, T. (1988). Upside-down faces: A review of the effect of inversion upon face recognition. *British Journal of Psychology*, *79*(4), 471-491.
- Valentine, T. (1991). A unified account of the effects of distinctiveness, inversion, and race in face recognition. *The Quarterly Journal of Experimental Psychology*, *43*(2), 161-204.
- Van Belle, G., De Graef, P., Verfaillie, K., Rossion, B., & Lefèvre, P. (2010). Face inversion impairs holistic perception: Evidence from gaze-contingent stimulation. *Journal of vision*, *10*(5), 10-10.
- van der Kolk, A. G., Hendrikse, J., Zwanenburg, J. J., Visser, F., & Luijten, P. R. (2013). Clinical applications of 7T MRI in the brain. *European journal of radiology*, *82*(5), 708-718.
- van Kemenade, B. M., Seymour, K., Christophel, T. B., Rothkirch, M., & Sterzer, P. (2014). Decoding pattern motion information in V1. *Cortex*, *57*, 177-187.
- van Kemenade, B. M., Seymour, K., Wacker, E., Spitzer, B., Blankenburg, F., & Sterzer, P. (2014). Tactile and visual motion direction processing in hMT+/V5. *Neuroimage*, *84*, 420-427.
- van Loon, A. M., Knapen, T., Scholte, H. S., John-Saaltink, E. S., Donner, T. H., & Lamme, V. A. (2013). GABA shapes the dynamics of bistable perception. *Current Biology*, *23*(9), 823-827.
- Vanni, S., Revonsuo, A., Saarinen, J., & Hari, R. (1996). Visual awareness of objects correlates with activity of right occipital cortex. *Neuroreport*, *8*(1), 183-186.
- Vetter, P., Grosbras, M.-H., & Muckli, L. (2013). TMS over V5 disrupts motion prediction. *Cerebral Cortex*, *25*(4), 1052-1059.
- Vetter, P., Smith, F. W., & Muckli, L. (2014). Decoding sound and imagery content in early visual cortex. *Current Biology*, *24*(11), 1256-1262.
- Victor, J. D., Purpura, K., Katz, E., & Mao, B. (1994). Population encoding of spatial frequency, orientation, and color in macaque V1. *Journal of neurophysiology*, *72*(5), 2151-2166.
- Vizioli, L., Rousset, G. A., & Caldara, R. (2010). Neural repetition suppression to identity is abolished by other-race faces. *Proceedings of the National Academy of Sciences*, *107*(46), 20081-20086.
- Vogeley, K. (2003). Schizophrenia as disturbance of the self-construct. In T. Kircher & A. S. David (Eds.), *The Self in Neuroscience and Psychiatry*. (pp. 361-379). Cambridge, UK: Cambridge University Press.
- von Ehrenfels, C. (1890). Über gestaltqualitäten. *Vierteljahresschrift für wissenschaftliche Philosophie*, *14*(3), 249-292.
- von Helmholtz, H. (1924). *Treatise on Physiological Optics Vol. III*. Washington, DC, USA: The Optical Society of America.
- von Helmholtz, H. (1897). *Handbuch Der Physiologischen Optik (Handbook Of Physiological Optics)*. Leipzig, Germany: Allgemeine Encyklopädie der Physik.
- Voss, M., Moore, J., Hauser, M., Gallinat, J., Heinz, A., & Haggard, P. (2010). Altered awareness of action in schizophrenia: a specific deficit in predicting action consequences. *Brain*, *133*(10), 3104-3112.

- Vuilleumier, P., & Driver, J. (2007). Modulation of visual processing by attention and emotion: windows on causal interactions between human brain regions. *Philosophical Transactions of the Royal Society of London B: Biological Sciences*, 362(1481), 837-855.
- Wachtler, T., Sejnowski, T. J., & Albright, T. D. (2003). Representation of color stimuli in awake macaque primary visual cortex. *Neuron*, 37(4), 681-691.
- Wacker, E., Spitzer, B., Lützkendorf, R., Bernarding, J., & Blankenburg, F. (2011). Tactile motion and pattern processing assessed with high-field fMRI. *PLoS One*, 6(9), e24860.
- Wagemans, J., Elder, J. H., Kubovy, M., Palmer, S. E., Peterson, M. A., Singh, M., & von der Heydt, R. (2012). A century of Gestalt psychology in visual perception: I. Perceptual grouping and figure-ground organization. *Psychological bulletin*, 138(6), 1172.
- Wallis, T. S., & Arnold, D. H. (2009). Motion-induced blindness and motion streak suppression. *Current Biology*, 19(4), 325-329.
- Walsh, V., & Cowey, A. (1998). Magnetic stimulation studies of visual cognition. *Trends in cognitive sciences*, 2(3), 103-110.
- Wandell, B. A. (1999). Computational neuroimaging of human visual cortex. *Annual review of neuroscience*, 22(1), 145-173.
- Wandell, B. A., Dumoulin, S. O., & Brewer, A. A. (2007). Visual field maps in human cortex. *Neuron*, 56(2), 366-383.
- Wang, L., Weng, X., & He, S. (2012). Perceptual grouping without awareness: Superiority of Kanizsa triangle in breaking interocular suppression. *PLoS One*, 7(6), e40106.
- Wang, M., Arteaga, D., & He, B. J. (2013). Brain mechanisms for simple perception and bistable perception. *Proceedings of the National Academy of Sciences*, 110(35), E3350-E3359.
- Wang, X.-J. (2010). Neurophysiological and computational principles of cortical rhythms in cognition. *Physiological reviews*, 90(3), 1195-1268.
- Wässle, H. (2004). Parallel processing in the mammalian retina. *Nature Reviews Neuroscience*, 5(10), 747-757.
- Watanabe, M., Cheng, K., Murayama, Y., Ueno, K., Asamizuya, T., Tanaka, K., & Logothetis, N. (2011). Attention but not awareness modulates the BOLD signal in the human V1 during binocular suppression. *Science*, 334(6057), 829-831.
- Watanabe, T., Harner, A. M., Miyauchi, S., Sasaki, Y., Nielsen, M., Palomo, D., & Mukai, I. (1998). Task-dependent influences of attention on the activation of human primary visual cortex. *Proceedings of the National Academy of Sciences*, 95(19), 11489-11492.
- Watanabe, T., Sasaki, Y., Miyauchi, S., Putz, B., Fujimaki, N., Nielsen, M., . . . Miyakawa, S. (1998). Attention-regulated activity in human primary visual cortex. *Journal of neurophysiology*, 79(4), 2218-2221.
- Watson, J. D., Myers, R., Frackowiak, R. S., Hajnal, J. V., Woods, R. P., Mazziotta, J. C., . . . Zeki, S. (1993). Area V5 of the human brain: evidence from a combined study using positron emission tomography and magnetic resonance imaging. *Cerebral Cortex*, 3(2), 79-94.
- Webster, M. A., & Maclin, O. H. (1999). Figural aftereffects in the perception of faces. *Psychonomic bulletin & review*, 6(4), 647-653.
- Weigelt, S., Kourtzi, Z., Kohler, A., Singer, W., & Muckli, L. (2007). The cortical representation of objects rotating in depth. *The Journal of neuroscience*, 27(14), 3864-3874.
- Weiss, Y., Simoncelli, E. P., & Adelson, E. H. (2002). Motion illusions as optimal percepts. *Nature neuroscience*, 5(6), 598-604.
- Weliky, M., & Katz, L. C. (1997). Disruption of orientation tuning in visual cortex by artificially correlated neuronal activity. *Nature*, 386(6626), 680.
- Wells, E. T., & Leber, A. B. (2014). Motion-induced blindness is influenced by global properties of the moving mask. *Visual Cognition*, 22(1), 125-140.
- Wen, T., & Kung, C.-C. (2014). Using functional magnetic resonance imaging to explore the flashed face distortion effect. *Journal of vision*, 14(12), 29-29.
- Wertheimer, M. (1912). *Experimentelle studien über das sehen von bewegung*. Leipzig, Germany: JA Barth.
- Wertheimer, M. (1922). Untersuchungen zur Lehre von der Gestalt. *Psychologische Forschung*, 1(1), 47-58.

- White, T. P., & Shergill, S. S. (2012). Using illusions to understand delusions. *Frontiers in Psychology*, 3, 407.
- Whitney, D. (2002). The influence of visual motion on perceived position. *Trends in cognitive sciences*, 6(5), 211-216.
- Whitney, D., Goltz, H. C., Thomas, C. G., Gati, J. S., Menon, R. S., & Goodale, M. A. (2003). Flexible retinotopy: motion-dependent position coding in the visual cortex. *Science*, 302(5646), 878-881.
- Wibral, M., Bledowski, C., Kohler, A., Singer, W., & Muckli, L. (2009). The timing of feedback to early visual cortex in the perception of long-range apparent motion. *Cerebral Cortex*, 19(7), 1567-1582.
- Wilke, M., Logothetis, N. K., & Leopold, D. A. (2006). Local field potential reflects perceptual suppression in monkey visual cortex. *Proceedings of the National Academy of Sciences*, 103(46), 17507-17512.
- Williams, L. E., Light, G. A., Braff, D. L., & Ramachandran, V. S. (2010). Reduced multisensory integration in patients with schizophrenia on a target detection task. *Neuropsychologia*, 48(10), 3128-3136.
- Williams, M. A., Baker, C. I., de Beeck, H. P. O., Shim, W. M., Dang, S., Triantafyllou, C., & Kanwisher, N. (2008). Feedback of visual object information to foveal retinotopic cortex. *Nature neuroscience*, 11(12), 1439-1445.
- Williams, S. R., & Stuart, G. J. (2002). Dependence of EPSP efficacy on synapse location in neocortical pyramidal neurons. *Science*, 295(5561), 1907-1910.
- Williams, Z. M., Elfar, J. C., Eskandar, E. N., Toth, L. J., & Assad, J. A. (2003). Parietal activity and the perceived direction of ambiguous apparent motion. *Nature neuroscience*, 6(6), 616-623.
- Wimmer, V. C., Bruno, R. M., De Kock, C. P., Kuner, T., & Sakmann, B. (2010). Dimensions of a projection column and architecture of VPM and POm axons in rat vibrissal cortex. *Cerebral Cortex*, bhq068.
- Wokke, M. E., Vandenbroucke, A. R., Scholte, H. S., & Lamme, V. A. (2012). Confuse your illusion: feedback to early visual cortex contributes to perceptual completion. *Psychological science*, 24(1), 63-71.
- Wold, A., Limanowski, J., Walter, H., & Blankenburg, F. (2014). Proprioceptive drift in the rubber hand illusion is intensified following 1 Hz TMS of the left EBA. *Frontiers in human neuroscience*, 8, 390.
- Wolpert, D. M., & Kawato, M. (1998). Multiple paired forward and inverse models for motor control. *Neural Networks*, 11(7), 1317-1329.
- Woolgar, A., Williams, M. A., & Rich, A. N. (2015). Attention enhances multi-voxel representation of novel objects in frontal, parietal and visual cortices. *Neuroimage*, 109, 429-437.
- Wozny, C., & Williams, S. R. (2011). Specificity of synaptic connectivity between layer 1 inhibitory interneurons and layer 2/3 pyramidal neurons in the rat neocortex. *Cerebral Cortex*, 21(8), 1818-1826.
- Wu, C.-T., Busch, N. A., Fabre-Thorpe, M., & VanRullen, R. (2009). The temporal interplay between conscious and unconscious perceptual streams. *Current Biology*, 19(23), 2003-2007.
- Xing, D., Shen, Y., Burns, S., Yeh, C.-I., Shapley, R., & Li, W. (2012). Stochastic generation of gamma-band activity in primary visual cortex of awake and anesthetized monkeys. *The Journal of neuroscience*, 32(40), 13873-13880a.
- Yacoub, E., Harel, N., & Ugurbil, K. (2008). High-field fMRI unveils orientation columns in humans. *Proceedings of the National Academy of Sciences*, 105(30), 10607-10612.
- Yang, E., Tadin, D., Glasser, D. M., Hong, S. W., Blake, R., & Park, S. (2013). Visual context processing in schizophrenia. *Clinical Psychological Science*, 1(1), 5-15.
- Yin, R. K. (1969). Looking at upside-down faces. *Journal of experimental psychology*, 81(1), 141.
- Yoon, J. H., Maddock, R. J., Rokem, A., Silver, M. A., Minzenberg, M. J., Ragland, J. D., & Carter, C. S. (2010). GABA concentration is reduced in visual cortex in schizophrenia and correlates with orientation-specific surround suppression. *The Journal of neuroscience*, 30(10), 3777-3781.

- Yovel, G., Levy, J., Grabowecky, M., & Paller, K. A. (2003). Neural correlates of the left-visual-field superiority in face perception appear at multiple stages of face processing. *Journal of cognitive neuroscience*, *15*(3), 462-474.
- Yovel, G., Tambini, A., & Brandman, T. (2008). The asymmetry of the fusiform face area is a stable individual characteristic that underlies the left-visual-field superiority for faces. *Neuropsychologia*, *46*(13), 3061-3068.
- Zadbood, A., Lee, S.-H., & Blake, R. (2011). Stimulus fractionation by interocular suppression. *Frontiers in human neuroscience*, *5*(135).
- Zaretskaya, N., & Bartels, A. (2013). Perceptual effects of stimulating V5/hMT+ during binocular rivalry are state specific. *Current Biology*, *23*(20), R919-R920.
- Zaretskaya, N., Thielscher, A., Logothetis, N. K., & Bartels, A. (2010). Disrupting parietal function prolongs dominance durations in binocular rivalry. *Current Biology*, *20*(23), 2106-2111.
- Zeki, S., Watson, J., Lueck, C., Friston, K. J., Kennard, C., & Frackowiak, R. (1991). A direct demonstration of functional specialization in human visual cortex. *The Journal of neuroscience*, *11*(3), 641-649.

8. APPENDICES

Appendix 2

A.2.1. Pairwise comparisons for the main effect of visuotactile synchronicity on Likert statement responses.

Pairwise Comparisons - Visuotactile Asynchronicity						
Visuotactile Condition		Mean Difference (I-J)	Std. Error	Sig.	95% Confidence Interval	
					Lower Bound	Upper Bound
0ms	200ms	0.329	0.134	0.249	-0.101	0.758
	300ms	.571*	0.172	0.038	0.022	1.121
	400ms	.782*	0.189	0.006	0.179	1.385
	600ms	.832*	0.195	0.005	0.209	1.455
200ms	0ms	-0.329	0.134	0.249	-0.758	0.101
	300ms	0.243	0.116	0.509	-0.128	0.614
	400ms	0.454	0.153	0.083	-0.036	0.943
	600ms	0.504	0.181	0.124	-0.076	1.083
300ms	0ms	-.571*	0.172	0.038	-1.121	-0.022
	200ms	-0.243	0.116	0.509	-0.614	0.128
	400ms	0.211	0.181	1.000	-0.369	0.790
	600ms	0.261	0.171	1.000	-0.287	0.808
400ms	0ms	-.782*	0.189	0.006	-1.385	-0.179
	200ms	-0.454	0.153	0.083	-0.943	0.036
	300ms	-0.211	0.181	1.000	-0.790	0.369
	600ms	0.050	0.118	1.000	-0.329	0.429
600ms	0ms	-.832*	0.195	0.005	-1.455	-0.209
	200ms	-0.504	0.181	0.124	-1.083	0.076
	300ms	-0.261	0.171	1.000	-0.808	0.287
	600ms	-0.050	0.118	1.000	-0.429	0.329

Table A.2.1. Comparisons between Likert responses for visuotactile asynchronicities. Blue highlights demonstrate those which are significant. Significance measurements are Bonferroni corrected.

A.2.2. Pairwise comparisons for the main effect of Likert statement on Likert statement responses.

Pairwise Comparisons - Likert Statement						
Likert Statement	Mean Difference (I-J)	Std. Error	Sig.	95% Confidence Interval		
				Lower Bound	Upper Bound	
1	2	0.725	0.312	0.674	-0.377	1.827
	3	1.160	0.384	0.154	-0.196	2.516
	4	1.440	0.433	0.079	-0.090	2.970
	5	1.475*	0.416	0.049	0.005	2.945
	6	0.715	0.415	1.000	-0.752	2.182
	7	1.140	0.367	0.129	-0.157	2.437
	2	1	-0.725	0.312	0.674	-1.827
3		0.435	0.260	1.000	-0.482	1.352
4		0.715	0.334	0.965	-0.463	1.893
5		0.750	0.312	0.573	-0.353	1.853
6		-0.010	0.239	1.000	-0.853	0.833
7		0.415	0.278	1.000	-0.568	1.398
3		1	-1.160	0.384	0.154	-2.516
	2	-0.435	0.260	1.000	-1.352	0.482
	4	0.280	0.202	1.000	-0.433	0.993
	5	0.315	0.147	0.973	-0.205	0.835
	6	-0.445	0.303	1.000	-1.513	0.623
	7	-0.020	0.128	1.000	-0.472	0.432
	4	1	-1.440	0.433	0.079	-2.970
2		-0.715	0.334	0.965	-1.893	0.463
3		-0.280	0.202	1.000	-0.993	0.433
5		0.035	0.175	1.000	-0.582	0.652
6		-0.725	0.295	0.512	-1.767	0.317
7		-0.300	0.157	1.000	-0.855	0.255
5		1	-1.475*	0.416	0.049	-2.945
	2	-0.750	0.312	0.573	-1.853	0.353
	3	-0.315	0.147	0.973	-0.835	0.205
	4	-0.035	0.175	1.000	-0.652	0.582
	6	-0.760	0.277	0.279	-1.737	0.217
	7	-0.335	0.157	0.996	-0.891	0.221
	6	1	-0.715	0.415	1.000	-2.182
2		0.010	0.239	1.000	-0.833	0.853
3		0.445	0.303	1.000	-0.623	1.513
4		0.725	0.295	0.512	-0.317	1.767
5		0.760	0.277	0.279	-0.217	1.737
7		0.425	0.274	1.000	-0.544	1.394
7		1	-1.140	0.367	0.129	-2.437
	2	-0.415	0.278	1.000	-1.398	0.568
	3	0.020	0.128	1.000	-0.432	0.472
	4	0.300	0.157	1.000	-0.255	0.855
	5	0.335	0.157	0.996	-0.221	0.891
	6	-0.425	0.274	1.000	-1.394	0.544

Table A.2.2. Comparisons between Likert responses for Likert statements. Blue highlights demonstrate those which are significant. Significance measurements are Bonferroni corrected.

A.2.3. 95% Confidence intervals on the mean for the interactive effects of visuotactile synchronicity and Likert statement on Likert statement responses.

Pairwise Comparisons - Visuotactile Condition x Statement					
Visuotactile Condition		Mean	Std. Error	95% Confidence Interval	
				Lower Bound	Upper Bound
0ms	1	4.275	0.436	3.359	5.191
	2	4.025	0.468	3.041	5.009
	3	3.125	0.390	2.305	3.945
	4	2.575	0.308	1.928	3.222
	5	2.550	0.376	1.759	3.341
	6	3.325	0.450	2.379	4.271
	7	3.100	0.322	2.424	3.776
200ms	1	4.000	0.501	2.948	5.052
	2	3.225	0.438	2.306	4.144
	3	2.775	0.391	1.953	3.597
	4	2.375	0.295	1.754	2.996
	5	2.525	0.377	1.733	3.317
	6	3.225	0.473	2.231	4.219
	7	2.550	0.349	1.818	3.282
300ms	1	3.650	0.460	2.684	4.616
	2	2.925	0.446	1.988	3.862
	3	2.625	0.388	1.809	3.441
	4	2.250	0.305	1.609	2.891
	5	2.100	0.310	1.449	2.751
	6	2.975	0.385	2.167	3.783
	7	2.450	0.325	1.768	3.132
400ms	1	3.300	0.461	2.331	4.269
	2	2.500	0.393	1.675	3.325
	3	2.250	0.324	1.570	2.930
	4	2.200	0.267	1.638	2.762
	5	1.975	0.281	1.385	2.565
	6	2.800	0.415	1.929	3.671
	7	2.475	0.266	1.917	3.033
600ms	1	3.425	0.462	2.454	4.396
	2	2.350	0.411	1.486	3.214
	3	2.075	0.263	1.523	2.627
	4	2.050	0.221	1.585	2.515
	5	2.125	0.326	1.440	2.810
	6	2.750	0.420	1.867	3.633
	7	2.375	0.341	1.658	3.092

Table A.2.3. 95% Confidence intervals for Likert responses for the interaction between visuotactile asynchronicities and Likert statements.

Appendix 3

Appendix 3.1. V1 TAL Coordinates and Number of Voxels

V1	mean x	mean y	mean z	std dev x	std dev y	std dev z	n voxels
S1	7.86	-80.15	9.66	3.73	8.84	5.74	5926
S2	5.71	-82.84	-3.28	3.77	8.55	9.92	7713
S3	12.48	-86.67	6.14	4.25	8.76	7.58	6402
S4	8.33	-89.5	3.89	3.97	6.04	10.57	6830
S5	12.07	-83	3.42	5.79	8.19	5.75	6258
S6	5.07	-82.28	-6.88	4.78	7.6	8.61	6089
S7	11.47	-88.01	0.6	8.23	6.95	9.8	8683
S8	9.89	-78.61	-7.79	6.2	7.41	5.07	5307
S9	8.78	-85.57	8.19	3.84	8.11	8.1	7858
S10	9.31	-79.98	-9.39	5.34	10.03	9.76	8187
S11	8.91	-81.3	-0.55	5.91	9.63	8.42	8680
S12	0.05	-85.73	-12.98	5.07	8.71	6.96	5332
S13	6.78	-83.34	2.17	5.78	9.25	9.05	8016
S14	8.55	-82.83	4.47	4.32	8.17	7.12	7571
S15	12.63	-80.78	7.26	7.02	10.76	7.54	10115
S16	6.94	-78.86	1.09	4.1	8.71	7.3	5489
S17	8.12	-80.3	-3.39	4.7	8	8.34	5586
S18	8.64	-85.18	-2.42	5.08	9.24	6.43	6803
S19	8.6	-87.95	2.04	7.37	7.87	6.45	6593
S20	12.22	-89.24	-0.19	7.44	8.06	5.54	7150
S21	9.41	-86.04	2.78	6.13	10.36	5.08	6755
S22	6.69	-86.96	10.14	3.98	8.02	6.04	5526
S23	5.54	-88.04	-6.38	4.28	8.58	9.92	7458
Mean TAL Location	8.436956522	-84.05043478	0.373913043	5.264347826	8.514782609	7.612608696	6970.73913

Table A.3.1. Mean TAL coordinates, TAL coordinate standard deviations, and number of voxels for the V1 ROI of each subject.

Appendix 3.2. Left V5 TAL Coordinates and Number of Voxels

Left V5	mean x	mean y	mean z	std dev x	std dev y	std dev z	n voxels
S1	-41.86	-65.67	0.21	3.14	2.39	1.23	312
S2	-58.16	-34.77	14.27	4.49	4.38	3.17	1239
S3	-54.26	-40.37	4.24	1.96	1.54	1.42	114
S4	-51.75	-68.29	9.76	3.06	3.32	2.65	421
S5	-60.88	-47.53	10.71	3.94	3.04	4.81	1012
S6	-44.13	-45.33	8.45	1.78	2.75	1.52	181
S7	-53.98	-65.02	13.1	4.27	3.83	3.28	1267
S8	-42.52	-64.86	4.72	3.01	2.21	2.09	321
S9	-44.54	-50.12	-2.12	3.1	2.18	2.46	687
S10	-49.85	-49.22	0.97	3.86	2.76	1.81	596
S11	-37.63	-70.97	6.52	2.63	3.98	2.59	739
S12	-55.6	-49.42	7.02	1.35	1.27	1.39	99
S13	-50.97	-60.55	9.24	2.67	4.1	1.61	432
S14	-53.96	-57.27	4.11	3.2	3.66	2.81	1193
S15	-48.48	-64.35	3.34	2.67	2.85	3.67	939
S16	-45.53	-62.81	10.66	3.61	2.47	2.76	742
S17	-45.96	-67.65	-3.51	4.19	2.56	2.97	1051
S18	-38.72	-58.6	5.09	1.5	2.08	3.24	229
S19	-47.4	-49.23	10.29	3.53	4.39	2.23	619
S20	-55.38	-59.76	2.92	2.7	1.27	2.06	107
S21	-43.49	-65.12	-1.28	4.19	3.7	2.35	546
S22	-37.49	-70.34	5.94	2.26	3.59	2.04	484
S23	-58.04	-55.21	-2.83	3.87	3.95	2.91	1188
S24	-38.38	-74.08	7.07	2.27	2.69	1.75	295
S25	-45.85	-58.92	4.33	2.48	2.01	2.94	377
S26	-52.96	-54.36	9.72	3.9	2.9	2.99	924
S27	-48.68	-67.11	14.78	1.83	1.99	4.23	345
S28	-53.26	-60.72	9.02	2.75	1.69	2.02	395
Mean TAL Location	-48.56107143	-58.4875	5.955	3.0075	2.841071429	2.535714286	601.9285714

Table A.3.2. Mean TAL coordinates, TAL coordinate standard deviations, and number of voxels for the left V5 ROI of each subject.

Appendix 3.3. Right V5 TAL Coordinates and Number of Voxels

Right V5	mean x	mean y	mean z	std dev x	std dev y	std dev z	n voxels
S1	41.53	-62.71	4.59	2.38	2.67	3.09	733
S2	37.13	-62.15	5.17	2.79	3.11	3.37	929
S3	41.02	-61.42	7.26	2.47	1.94	4.27	699
S4	44.44	-55.48	6.61	4.15	3.73	2.1	1046
S5	41.98	-76.57	-0.07	3.2	3.27	2.77	756
S6	43.21	-57.29	1.51	5.91	2.73	4.01	941
S7	41.27	-60.23	5.85	3.22	4.95	1.92	1060
S8	41.52	-58.91	-3.86	1.56	2.47	2.42	292
S9	36.16	-68.12	-0.27	2.16	4.39	2.2	617
S10	47.86	-52.49	-5.07	4.48	3.46	2.34	1283
S11	47.59	-66.2	-0.47	3.83	2.37	3.11	966
S12	49.43	-68.94	-9.87	3.27	3.07	2.81	853
S13	37.55	-59.57	9.05	2.72	3.95	2.4	779
S14	45.16	-65.18	-5.18	6.21	2.82	2.54	1405
S15	45.25	-59.32	5.16	3.44	2.61	2.81	876
S16	42.31	-57.77	6.77	3.75	2.21	3.08	701
S17	43.08	-68.38	0.36	3.43	3.7	2.43	860
S18	43.89	-56.82	5.03	2.7	4.41	2.25	792
S19	41.88	-51.41	7.71	2.87	2.89	3.3	813
S20	44.74	-56.37	0.77	3.02	1.66	1.98	353
S21	39.82	-62.17	5.08	2.58	2.9	2.81	771
S22	45.23	-55.95	0.59	4.15	2.28	2.31	685
S23	36.5	-63.47	-1.48	2.23	5.97	5.96	1172
S24	39.65	-72.19	7.3	1.91	3.25	2.52	384
S25	39.15	-56.64	5.7	2.28	3.44	2.19	657
S26	42.83	-60.02	1.75	2.16	3.5	3.28	824
S27	40.82	-58.31	13.64	2.79	2.72	2.98	716
S28	44.19	-72.43	-1.19	3.93	3.55	3.5	1436
Mean TAL Location	42.32821429	-61.66107143	2.587142857	3.199642857	3.215	2.883928571	835.6785714

Table A.3.3. Mean TAL coordinates, TAL coordinate standard deviations, and number of voxels for the right V5 ROI of each subject.

Appendix 3.4. Lateral Occipital Complex TAL Coordinates and Number of Voxels

LOC	mean x	mean y	mean z	std dev x	std dev y	std dev z	n voxels
S1	38.8	-72.84	0.97	3.01	1.62	3.36	518
S2	38.97	-68.02	-4.24	2.55	2.12	3.1	585
S3	43.04	-62.25	-7.02	2.96	5.22	2.13	912
S4	41.09	-68.75	-1.56	3.43	4.93	2.82	1117
S5	28.34	-81.71	-9.2	2.02	2.98	2.93	531
S6	45.09	-72.91	-4.8	2.1	5.43	3.53	614
S7	42.66	-76.34	7.02	2.61	2.59	3.4	792
S8	43.89	-77.25	-8.39	3.22	1.33	0.88	104
S9	36.75	-69.82	-0.99	2.69	2.79	2.16	593
S10	41.39	-72.7	-5.87	3.15	2.25	3.53	755
S11	38.77	-79.5	-4.16	2.62	4.1	2.11	738
S12	44.23	-70.69	-10.47	2.8	3.89	2.31	690
S13	47.22	-74.91	-5.1	2.43	3.36	5.03	1243
S14	41.72	-67.81	-15.19	3.15	3.63	3.34	1282
S15	39.36	-79.28	-3.27	1.96	2.14	1.51	272
S16	39.64	-72.79	4.36	3.53	2.91	2.63	810
S17	43.67	-63.92	-6	2.74	2.56	3.75	884
S18	47.81	-60.82	-9.02	2.96	5.06	3.34	1269
S19	45.95	-72.19	3.79	1.76	2.89	1.73	368
S20	38.1	-67.98	-12.67	1.98	2.56	2.01	381
S21	42.3	-74.64	-6.11	2.89	3.39	2.78	729
S22	43.81	-74.4	-9.76	2.27	3.16	3.33	853
S23	43.06	-73.67	-5.67	3.67	3.09	3.15	895
S24	41.96	-81.63	-0.54	2.06	2.04	2.5	404
S25	45.45	-65.76	-6.2	2.8	3.55	2.21	671
S26	46.98	-72.86	-10.27	2.5	3.88	3.11	803
S27	44.47	-68.05	0.9	2.41	2.26	2.54	508
S28	43.36	-70.69	-16.88	3.15	3.02	3.95	1070
Mean TAL Location	42.06714286	-71.935	-5.226428571	2.693571429	3.169642857	2.8275	728.25

Table A.3.4. Mean TAL coordinates, TAL coordinate standard deviations, and number of voxels for the LOC ROI of each subject.

Appendix 3.5. VHand TAL Coordinates and Number of Voxels

VHand	mean x	mean y	mean z	std dev x	std dev y	std dev z	n voxels
S1	10.17	-80.26	7.03	3.02	2.25	2.16	544
S2	1.3	-84.19	-0.65	1.48	2.28	1.63	219
S3	7.62	-74.06	-2.59	1.38	1.27	1.46	106
S4	13.39	-85.16	-1.48	2.64	1.82	2.44	228
S5	1.81	-84.86	-3.48	2.74	1.78	2.01	418
S6	5.98	-76.2	1.58	1.5	1.39	1.39	105
S7	3.8	-89.63	-13.45	2.2	2.39	3.65	596
S8	0.42	-85.77	-10.66	1.75	2.73	2.39	420
S9	17.95	-84.15	-7.41	1.38	1.74	1.86	153
S10	14.4	-88.06	9.52	3.13	2.09	2.71	461
S11	9.41	-73.97	5.54	3.04	1.71	1.69	344
S12	2.33	-83.59	-15.04	1.54	1.77	1.59	190
S13	6.04	-85.82	2.14	2.78	2.62	2.89	517
S14	0.29	-84.24	0.23	1.5	2.11	1.91	242
S15	3.64	-85.77	-5.07	1.53	2.59	1.77	286
S16	14.26	-94.61	5.07	1.52	2.44	2.36	246
S17	12.62	-84.18	1.64	5.21	3.73	3.4	443
S18	11.01	-85.78	2.2	1.25	2.08	1.35	143
S19	6.14	-74.28	0.52	2.48	3.07	2.1	471
S20	18.24	-94.81	-10.98	1.98	2.72	2.33	213
S21	9.15	-92.15	0.42	1.37	1.72	1.58	165
S22	15.57	-95.86	-5.1	1.58	1.78	1.53	100
S23	24.23	-94.88	-9.53	3.9	2.05	3.12	533
S24	23.71	-95.3	1.37	2.51	2.42	2.62	420
S25	1.41	-75.24	5.24	1.15	1.32	1.41	80
S26	4.18	-79.66	-6.81	3.33	2.57	2.59	668
Mean TAL Location	9.195	-85.09538462	-1.913461538	2.226538462	2.170769231	2.151538462	319.6538462

Table A.3.5. Mean TAL coordinates, TAL coordinate standard deviations, and number of voxels for the VHand ROI of each subject.

Appendix 3.6. VHand TAL Coordinates and Number of Voxels

vPMC	mean x	mean y	mean z	std dev x	std dev y	std dev z	n voxels
S1	55.67	0.56	16.66	3.26	1.95	3.65	829
S2	49.87	2.45	15.13	2.9	2.02	4.16	857
S3	55.41	2.17	21.5	2.56	1.7	4.26	670
S4	51.39	8.23	17.43	3.74	1.9	3.25	820
S5	53.26	10.67	17.15	3.74	2.73	3.76	1083
S6	54.82	-4.03	23.06	2.67	1.75	3.03	480
S7	53.89	4.91	15.51	2.9	2.48	4.5	1028
S8	55.08	4.38	23.37	3.32	2.79	2.46	711
S9	56.27	2.76	18.19	2.58	1.7	3.79	656
S10	52.89	0.95	19.54	2.93	1.57	4.28	758
S11	54.59	5.3	12.7	3.04	1.49	3.51	530
S12	49.82	4.11	18.19	2.53	2.42	4.16	856
S13	54.16	4.3	14.13	3.09	1.98	5.28	800
S14	55.59	-2	21.57	5.28	1.91	5.55	1611
S15	48.83	3.43	16.94	2.84	1.99	4.36	809
S16	54.1	-1.09	20.87	4.95	2.32	2.96	901
S17	48.86	-0.56	23.35	2.91	1.61	4.13	581
S18	57.08	-3.04	18.44	3.05	2.26	2.93	649
S19	54.26	8.54	16.22	2.99	2.23	4.64	976
S20	54.97	4.91	17.38	2.52	1.65	4.93	771
S21	56.01	0.1	17.76	2.53	2.41	2.67	446
S22	50.77	8.99	17.7	3.99	2.04	4.01	1047
S23	55.33	5.8	18.08	2.97	2.6	4.48	958
S24	56.36	-0.21	19.13	2.2	1.58	4.33	574
S25	54.38	-1.87	20.15	2.75	1.65	3.28	582
S26	55.74	5.58	16.77	3.36	3.07	3.5	871
S27	48.56	10.14	4.11	2.06	1.7	2.38	259
S28	54.59	-2.03	25.51	4.03	1.81	4.05	969
Mean TAL Location	53.6625	2.980357143	18.091	3.131785714	2.046785714	3.8675	788.643

Table A.3.6. Mean TAL coordinates, TAL coordinate standard deviations, and number of voxels for the VHand ROI of each subject.

Appendix 4.2.

Appendix 4.2.1. Experiment 1: V1 Target Region TAL Coordinates and Number of Voxels

Experiment 1							
V1 Target Region	mean x	mean y	mean z	std dev x	std dev y	std dev z	n voxels
S1	3.12	-74.65	0.91	2.51	3.16	3.02	406
S2	-0.51	-74	-9.07	1.52	2.56	2.69	441
S3	4.12	-81.58	-9.16	2.54	3.94	2.69	853
S4	3.1	-77.76	-14.77	1.85	3.19	1.89	358
S5	1.79	-78.92	-9.82	1.24	2.06	2.35	226
S6	5.45	-72.53	-1.98	2	2.34	3	529
S7	-1.58	-78.52	-17.23	1.49	2.21	2.45	324
S8	1.78	-76.85	-16.11	2.22	2.74	2.93	594
S9	2.49	-78.12	-6.34	2.68	5.01	2.2	837
S10	1.45	-77.59	-8.85	2.18	4.74	3.26	1272
S11	0.23	-82.14	-12.28	1.67	4.03	4.15	1051
S12	5.39	-79.51	-13.17	1.53	2.45	1.89	284
S13	3.01	-73.62	-8.49	2.19	3.12	3.9	1026
S14	1.06	-74.34	0.56	1.3	1.77	2	180
S15	0.85	-69.09	-9.09	1.42	1.85	1.44	141
S16	2.96	-68.91	-12.69	2.2	1.03	2.01	146
S17	2.81	-71.02	-6.75	0.61	1.79	1.49	64
S18	5.22	-71.16	0.86	1.52	2.43	2.26	292
Mean TAL Location	2.3744	-75.573	-8.526	1.815	2.801111	2.534444	501.333

Table A.4.2.1. Mean TAL coordinates, TAL coordinate standard deviations, and number of voxels for the target ROI of each subject. Blue denotes subject who saw a flickering target.

Appendix 4.2.2. Experiment 2: V1 Target Region TAL Coordinates and Number of Voxels

Experiment 2							
V1 Target Region	mean x	mean y	mean z	std dev x	std dev y	std dev z	n voxels
S1	2.11	-78.43	-4.69	2.03	3.22	5.23	1125
S2	5.1	-83.6	-11.61	2.62	2.24	3.9	736
S3	2.63	-70.93	1.84	2.69	2.83	3.07	791
Mean TAL Location	3.28	-77.653	-4.82	2.446667	2.763333	4.066667	884

Table A.4.2.2. Mean TAL coordinates, TAL coordinate standard deviations, and number of voxels for the target ROI of each subject.

Appendix 4.2.3. Experiment 1: V5 Target Region TAL Coordinates and Number of Voxels

Experiment 1							
V5	mean x	mean y	mean z	std dev x	std dev y	std dev z	n voxels
S1	46.63	-67.32	3.19	3.25	2.24	1.98	501
S2	43.12	-57.57	1.64	5.29	3.58	2.32	904
S3	38.43	-58.72	12.62	3.73	2.72	4.34	1464
S4	47.4	-61.86	3.65	3.92	2.18	1.76	362
S5	44.83	-61.25	3.35	4.23	2.39	2.52	626
S6	38.19	-54.54	11.3	1.8	2.61	2.68	302
S7	35.61	-68.1	1.49	2.77	2.44	4.51	778
S8	36.23	-61.7	0.22	2.26	1.77	1.69	221
S9	38.53	-68.39	7.13	3.18	3.15	1.8	389
S10	38.14	-62.35	6.45	3.29	1.53	3.05	392
S11	33.2	-67.44	12.69	2.01	3.6	1.89	296
S12	43.33	-63.91	-0.4	2.59	2.89	1.93	323
S13	44.63	-53.53	1.67	2.21	1.49	1.87	130
S14	48.99	-57.53	9.27	1.82	1.57	2.77	237
S15	39.07	-68.92	1.31	2.32	2.75	1.57	300
S16	36.7	-64.99	-9.7	1.94	1.59	1.84	210
S17	40.55	-56.99	-0.64	2.09	2.63	2.11	330
S18	47.87	-65.82	-5.75	3.28	2.14	2.3	422
Mean TAL Location	41.192	-62.274	3.305	2.887778	2.403889	2.385	454.833

Table A.4.2.3. Mean TAL coordinates, TAL coordinate standard deviations, and number of voxels for the V5 ROI of each subject. Blue denotes subject who saw a flickering target.

Appendix 4.2.4. Experiment 2: V5 Target Region TAL Coordinates and Number of Voxels

Experiment 2							
V5	mean x	mean y	mean z	std dev x	std dev y	std dev z	n voxels
S1	46.96	-66.53	0.32	2.9	2.38	4.4	569
S2	32.44	-68.56	9.96	2.05	4.01	1.94	508
S3	38.28	-69.37	2.8	3.33	3.76	4.4	1062
Mean TAL Location	39.227	-68.153	4.36	2.76	3.383333	3.58	713

Table A.4.2.4. Mean TAL coordinates, TAL coordinate standard deviations, and number of voxels for the V5 ROI of each subject.